TU/e EINDHOVEN UNIVERSITY OF TECHNOLOGY

Quantitative electron probe microanalysis of nitrogen

Citation for published version (APA):
Bastin, G. F., & Heijligers, H. J. M. (1988). *Quantitative electron probe microanalysis of nitrogen*. Eindhoven University of Technology.

Document status and date:
Published: 01/01/1988

Document Version:
Publisher's PDF, also known as Version of Record (includes final page, issue and volume numbers)

Please check the document version of this publication:

• A submitted manuscript is the version of the article upon submission and before peer-review. There can be important differences between the submitted version and the official published version of record. People interested in the research are advised to contact the author for the final version of the publication, or visit the DOI to the publisher's website.
• The final author version and the galley proof are versions of the publication after peer review.
• The final published version features the final layout of the paper including the volume, issue and page numbers.

Link to publication

General rights
Copyright and moral rights for the publications made accessible in the public portal are retained by the authors and/or other copyright owners and it is a condition of accessing publications that users recognise and abide by the legal requirements associated with these rights.

- Users may download and print one copy of any publication from the public portal for the purpose of private study or research.
- You may not further distribute the material or use it for any profit-making activity or commercial gain
- You may freely distribute the URL identifying the publication in the public portal.

If the publication is distributed under the terms of Article 25fa of the Dutch Copyright Act, indicated by the "Taverne" license above, please follow below link for the End User Agreement:

www.tue.nl/taverne

Take down policy
If you believe that this document breaches copyright please contact us at:

openaccess@tue.nl

providing details and we will investigate your claim.

Download date: 04. Oct. 2023

G J K
8 8
B A S

... / of Solid State Chemistry
... ial Science

tue

University of Technology Eindhoven
The Netherlands

Quantitative Electron Probe Microanalysis of Nitrogen

ISBN 90-6819-010-5 CIP

Dr.Ir. G.F. Bastin and Ir. H.J.M Heijligers

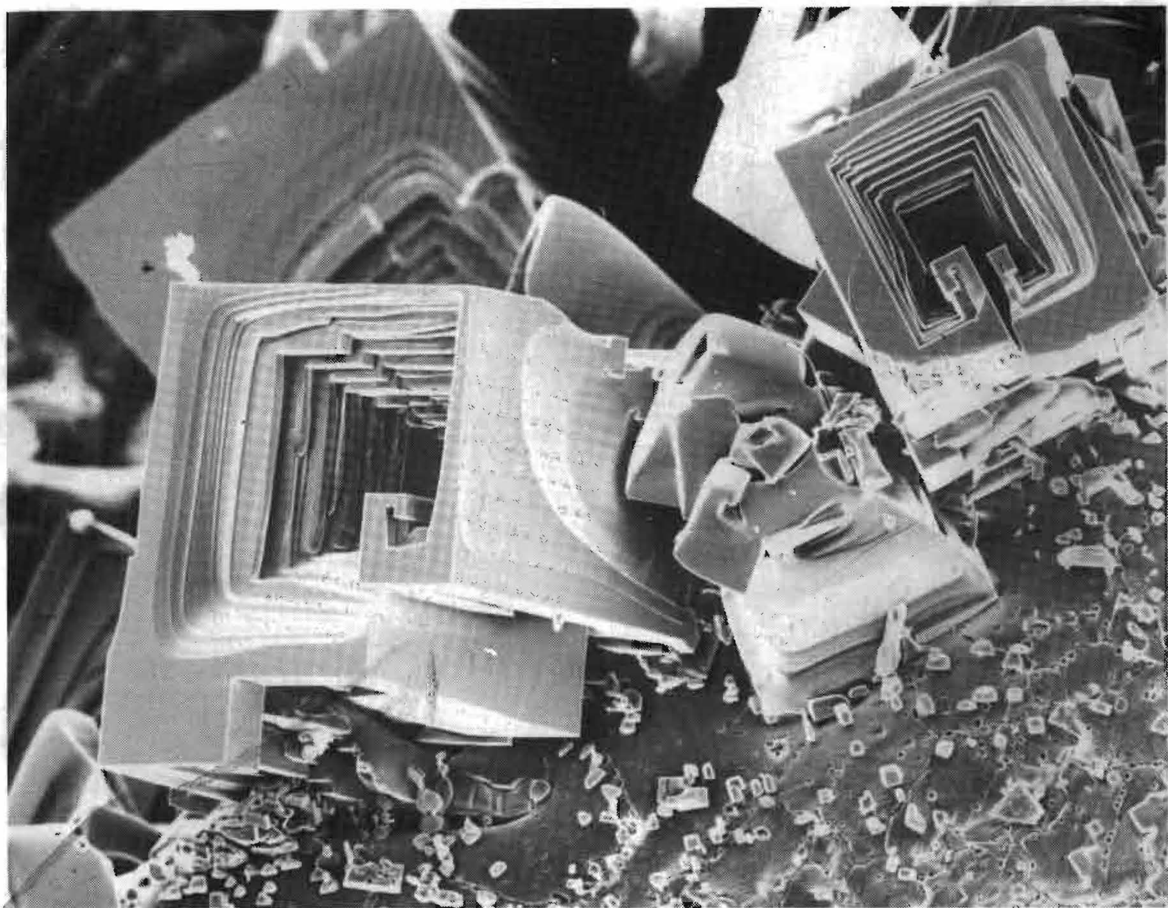

QUANTITATIVE ELECTRON PROBE MICROANALYSIS OF NITROGEN

LABORATORY of SOLID STATE CHEMISTRY
and MATERIALS SCIENCE

UNIVERSITY OF TECHNOLOGY EINDHOVEN
THE NETHERLANDS

University of Technology
Laboratory of Solid State Chemistry and Materials Science
P.O.Box 513, NL-5600 MB EINDHOVEN
The Netherlands

ISBN 90-6819-010-5 CIP
Dr.Ir.G.F.Bastin and Ir.H.J.M.Heijligers

QUANTITATIVE ELECTRON PROBE MICROANALYSIS OF NITROGEN

Dr.Ir.G.F.Bastin and Ir.H.J.M.Heijligers
Laboratory of Solid State Chemistry
and Materials Science
University of Technology
P.O.Box 513, NL-5600 MB Eindhoven
The Netherlands

Work performed in the period:February 1985-September 1988

September 1st 1988

CIP-DATA KONINKLIJKE BIBLIOTHEEK, DEN HAAG

Bastin, G.F.

Quantitative electron probe microanalysis of nitrogen /
G.F.Bastin and H.J.M.Heijligers. - Eindhoven :
University of Technology, Laboratory of Solid State
Chemistry and Materials Science. - Ill.
With ref.
IBSN 90-6819-010-5
SISO 542 UDC 543.5:546.17
Subject heading: nitrogen ;electron probe microanalysis.

© University of Technology, Eindhoven
Laboratory of Solid State Chemistry and Materials Science.
P.O.Box 513, Nl-5600 MB EINDHOVEN
The Netherlands

IBSN 90-6819-010-5 CIP

Cover photographs :
Scanning Electron Micrographs of TiN crystals grown by heating Titanium in a Nitrogen atmosphere at 2000 °C in an R.F. furnace

CONTENTS

page

SUMMARY 1

I INTRODUCTION 3

II PRACTICAL PROBLEMS IN THE ANALYSIS OF ULTRA-LIGHT ELEMENTS 5

III EXPERIMENTAL PROCEDURES 18
III.1 Preparation of Nitrides 18
III.2 Characterization of Nitride specimens 20
III.3 Mounting, polishing and examination procedures 24
III.4 Technical details of the microprobe used 25
III.5 Measurements of Area-Peak Factors 26
III.6 Measurements of Integral k-ratios between 4 and 30 kV 28

IV RESULTS 29
IV.1 Oxygen contamination in the microprobe 29
IV.2 New procedures for the analysis of Nitrogen in the presence of Titanium 34
IV.2.1 Analysis of existing methods 34
IV.2.2 The new method 36
IV.2.3 Quantitative analysis of low Nitrogen contents in the presence of Titanium 47
IV.3 Performance of LDE crystal as compared to conventional lead-stearate crystal 50
IV.4 Area-Peak Factors for N-Kα relative to Cr_2N 70
IV.5 Emitted intensities for N-Kα radiation as a function of accelerating voltage 70

V DATA REDUCTION 82
V.1 Fundamentals of the Gaussian $\phi(\rho z)$ approach 83
V.2 Latest parameterizations of the PROZA $\phi(\rho z)$ program 84
V.3 Results of the PROZA program on previous data 89
V.3.1 Medium-to-heavy element analysis 89
V.3.2 Boron and Carbon analyses 90
V.4 Results from the present work 92
V.4.1 Analysis of the metal lines in the nitrides 92
V.4.2 Analysis of Nitrogen in the nitrides 93

VI CONCLUSIONS 103

REFERENCES 104

APPENDIX 1 Numerical data on the intensity measurements of metal and nitrogen X-ray lines 106
APPENDIX 2 Graphical representations of variation of k-ratios of metal X-ray lines with accelerating voltage 124
APPENDIX 3 Final data base 133

SUMMARY

Quantitative Electron Probe Microanalysis of Nitrogen has been performed on 18 nitrides at accelerating voltages between 4 and 30 kV, using both a conventional lead stearate crystal as well as a new synthetic multilayer crystal (W/Si, 2d=59.8 Å). A straight-forward comparison of the performances of these crystals has shown that the net peak count rates of the multilayer crystal are approx. 2.8 times higher than those obtained on the lead stearate crystal. In addition, it was found that the multilayer crystal also produced significant improvements in the Peak to Background ratios, which is of extreme importance in difficult nitrides like ZrN, Nb_2N and Mo_2N. A most significant feature of the new crystal, however, is that it is apparently able to suppress higher-order reflections very effectively. As a result, backgrounds are produced which are free of interfering lines and spectral artifacts, which, in turn, makes it much easier to determine the background accurately.

The present work has also resulted in a new procedure for the analysis of Nitrogen in the presence of Titanium. This new procedure is based on the assumption that the Area-Peak Factor (Integral/Peak k-ratio) of the N-Kα peak in Ti-N compounds relative to a Nitrogen standard (Cr_2N) has a fixed value and that, once this value is known, it can be used to separate the Ti-$_{ll}$ peak from the N-Kα peak. After the determination of this APF the new procedure was extensively tested on a number of compositions in the Ti-N system. It was found that using this procedure it is possible to do quantitative analysis of Nitrogen in Ti-N compounds with a relative accuracy of better than 5 % . For very low levels of Nitrogen (below 15 at %) the new method was found unsuitable; in these cases, however, the well-known multiple least squares digital fitting techniques appeared to do an excellent job.

The intensity measurements for Nitrogen in the various nitrides as a function of accelerating voltage were also carried out with both crystals simultaneously. In order to correct for peak shape alterations in the N-Kα peak all Nitrogen spectra were first recorded in an integral fashion and compared to those of the Cr_2N standard. It was found that the peak shape alterations for the N-kα peak were very much smaller than for B-Kα and C-Kα radiations : The observed values for the Area-Peak Factor relative to Cr_2N differed less than 5 % from unity.

The present work has resulted in a final data base containing 144 integral k-ratios for N-Kα and 149 peak k-ratios for the X-ray lines of the metal partners in the nitrides. Our own Gaussian $\phi(\rho z)$ matrix correction procedure "PROZA" yielded excellent results for the Nitrogen data : An average value of k_{calc}/k_{meas} of 1.0051 and a relative root mean square deviation of 3.99 % .

I INTRODUCTION

Contrary to our previous studies on quantitative EPMA of Carbon[1] and Boron[2] which were completed in one year and less than a year, respectively, the present work on Nitrogen has taken considerably more time. As a matter of fact the micro probe measurements were carried out over a period of approx. two and a half years ; not even mentioning the one year period covering most of the year 1984, in which most of the nitrides were prepared in our own laboratory.

The reasons for the appreciable delay in time are the following :

-- The first and most obvious reason is the simple fact that Nitrogen is by far the most difficult ultra-light element to deal with in the microprobe.
The count rates on a conventional Stearate crystal can be extremely low and Peak-to-Background ratios can well be much below 1. On top of that the background can be curved in a number of cases and at the same time it can contain lots of remnants of higher order metal lines (e.g. in ZrN, Nb_2N, Mo_2N) which cannot be completely removed by discrimination techniques. In the end we were, therefore, forced to do all the measurements in a completely integral fashion which took one night per accelerating voltage per nitride ; in short : approx. 2 weeks per nitride for a range of 4-30 kV (in 9 steps).

-- A major improvement in techniques as well as results was achieved by the use of a W/Si multilayer (Ovonics Synthetic Materials Corp. U.S.A) with a 2d spacing of 59.8 Å (LDE crystal). Unfortunately, this crystal only became available in December '85 when the work was well underway. Nevertheless we decided to restart the work from scratch and compare the results of STE and LDE crystals in the same runs.

-- A next major problem was the contamination with Oxygen which was found to take place in certain sensitive nitrides like ZrN, HfN and TaN when an air jet was used in order to prevent a build-up of carbonaceous deposits. Initially, the air jet was used in all cases. Later on, however, it was discovered that a rapid process of in-situ oxidation can set in under electron bombardment on certain nitrides, leading to 30 % or more losses in N-Kα intensity in the time (1.5 hour) required for the accurate integral recording of the N-Kα peak. This in turn forced us to repeat a number of measurements on these sensitive nitrides without an air jet.

-- A lot of time and effort has been spent on deriving a procedure for measuring Nitrogen in Ti-containing specimens. Due to the extreme overlap of the N-Kα and the Ti-ll peaks it is impossible to distinguish the separate contributions under

the combined (N-Kα + Ti-ll)-peaks. This old problem has, in our opinion, never been solved satisfactorily. In the present work a new procedure is proposed and extensively tested.

-- A new problem, hardly encountered so far in the work on Carbon and Boron, turned up in the case of Nitrogen : A number of Nitrides (hex. BN, AlN and Si_3N_4) are electrically insulating materials and as such they present additional problems, hardly discussed so far in the literature on quantitative electron probe microanalysis. Various (time consuming) techniques have been tried in order to deal with these cases, usually without too much success.

-- By far the most difficult and time-consuming problem has been to find the compositions of the available nitrides once the measurements were successfully completed. In a fairly large proportion of cases, especially the more "difficult" nitrides like TiN, ZrN, HfN and TaN, the available chemical analyses were not consistent with the (relatively scarce) literature on phase diagrams. The sum of the reported Nitrogen and Oxygen contents usually exceeded the maximum limit of the homogeneity region by 5 (TiN) up to as much as 20 % relative (HfN). This seems to point to severe systematic errors in the chemical analyses.
As a result of the initial uncertainties on the compositions a very time-consuming iterative procedure was necessary in the final evaluation stage in order to arrive at the concept of the "most probable composition". These compositions are the ones giving the highest possible degree in consistency taking into consideration all available information on phase diagrams, results of the metal analyses, results of the nitrogen analyses, consistency of mass absorption coefficients, known biases of existing correction programs in metals analyses in carbides or borides from previous experiences etc. etc.

All the reasons mentioned so far have led to the result that the present work has taken 2-3 times more time than our previous studies on Carbon and Boron analysis.

II PRACTICAL PROBLEMS IN THE ANALYSIS OF ULTRA-LIGHT ELEMENTS

The practical problems to be encountered in this particular type of work have been discussed extensively in a series of previous publications[1-4] and will only briefly be recalled here.

1. <u>Low yield of X-rays</u>

For N-Kα radiation the situation is particularly bad because this wavelength falls just into the Carbon-K absorption edge and Carbon is abundantly present in the detection system :
- in the conventional lead-stearate crystal.
- on top of that in the counter window (polypropylene). As a result of these excessive absorption effects the count rates for Nitrogen can be one order of magnitude less than in comparable carbides or borides.

Fortunately, the new generation of synthetic multilayer crystals can bring an improvement of a factor of 3 here.

2. <u>Dead time problems</u> for the metal lines in case these have to be measured at the same time as the light element, which will usually be the case in day-to-day practice.

On top of that, one has to be aware of possible pulse shifts in the N-Kα pulse. Such problems may be the direct result of the use of extremely high beam currents (frequently in the order of 300 nA) necessary to arrive at acceptable count levels and the sometimes high differences in count rates between (elemental) standards and the specimen. In the present case of Nitrogen where an elemental standard is out of the question, these dangers[2] are not immediately evident.

3. <u>Interference</u> of higher-order metal lines with the light element line can be quite a nuisance and as a matter of fact it presented one of the biggest problems in the present work as long as the Stearate crystal (STE) was used. Especially the elements Zr, Nb and Mo are usually bothersome in this respect.

Fig. II.1 (lower half) shows a typical example of the background on pure Zr. The presence of remnants of higher-order Zr-lines on a slightly curved background is clearly visible. It is important to note that such interferences cannot be completely removed by the application of narrow discriminator settings. Due to the broad pulse distributions in the counter a part of the tail of the pulses will always penetrate into the window of the discriminator, no matter how narrow the window is.

Apart from this complicated background (typical for nitrides

of Zr, Nb and Mo), which is very difficult to quantify, we have the additional problem of an extremely low peak count rate (see top half of Fig. II.1)

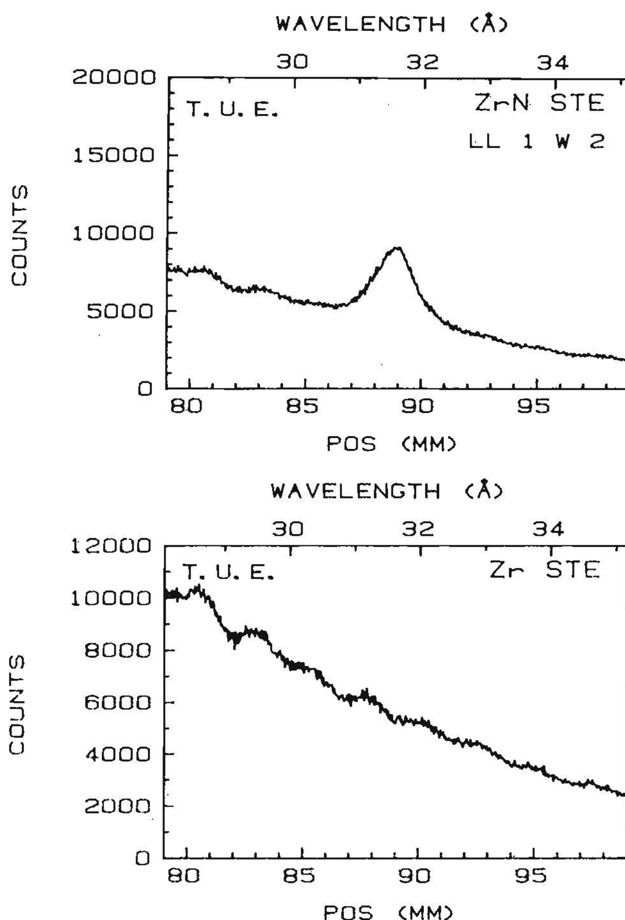

Fig. II.1 Nitrogen-Kα peak (top) in ZrN and corresponding background on pure Zr (bottom) at 10 kV and 300 nA Stearate crystal

Keeping in mind that Fig. II.1 represents the relatively favourable situation at 10 kV, one can imagine that it is difficult indeed to do accurate quantitative analyses of Nitrogen at higher voltages.
Here too, the new multilayer crystals were found to be a major improvement: Not only did they provide an increase in N-Kα count rates of approx. a factor of 3; they also appeared to suppress higher-order reflections very effectively. To give an example: The conventional STE crystal yields an intensity ratio of Fe-Lα (2nd order)/N-Kα in Fe_4N of approx. 6 in favour of the Fe-Lα (2) peak; whereas the LDE crystal (multilayer) produces a ratio of 4 in favour of the N-Kα

peak. Third order reflections can usually safely be neglected all together.

4. Contamination problems which play a major role in the analysis of Carbon[1] can also be a problem in the analysis of Nitrogen. Because the N-Kα X-rays are excessively absorbed in Carbon it is vital to prevent a Carbon build-up on the specimen during electron bombardment. This is especially important in view of the long times (± 1.5 hrs) required on one location for the accurate integral recording of the N-Kα peak. It is, therefore, advisable in most cases to use an anti-contamination device like an air-jet[1]. However, it turned out in the course of the present investigation that certain nitrides, most notably those of Zr, Hf,and Ta, can be oxidized at an incredibly high rate under electron bombardment while using an air-jet. It seems advisable, therefore, always to run a check on the Carbon, Nitrogen and Oxygen signals as a function of measuring time in order to arrive at the best strategy for a particular measurement.
On top of that it is imperative to work under the cleanest possible circumstances. One must keep in mind that the X-ray emission volumes in heavily absorbing nitrides like ZrN, Nb_2N, Mo_2N etc. are extremely shallow and can thus be strongly influenced by the presence of contamination or oxidation layers.

5. The choice of a standard was quite a problem in the present work.
In our opinion a possible Nitrogen standard should meet a number of requirements:
- It should exhibit a reasonable count rate for Nitrogen.
- It should not produce interfering metal lines in the spectral region of interest, in view of the problems mentioned under 3.
- It should be sufficiently electrically conductive. This in order to prevent charging phenomena and corresponding alterations in the interaction of electrons with the target; alterations which have never been taken into account by existing matrix correction programs.
- Preparation of the standard should be possible in reasonable quantities along not too difficult procedures, in order to have sufficient material available for a number of independent chemical analysis.

Considering all these requirements only one binary system appeared to be appropriate and this was the Cr-N system. The best candidate would have been the compound CrN, which is apparently a line-compound. Unfortunately, this could only be prepared in microscopically small quantities. Therefore, the ultimate choice was Cr_2N, which can be prepared in the shape of massive plates (1 mm thick). This particular standard exhibits a clean Nitrogen spectrum as well as a clean background (see Fig. II.2).

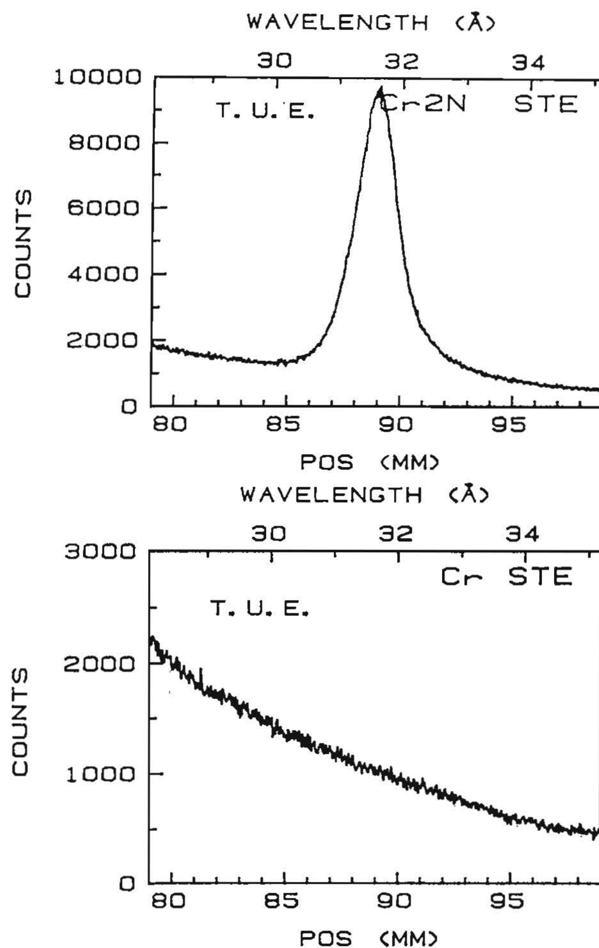

Fig. II.2 N-Kα spectrum (top) of the Cr_2N-standard used in the present investigation and corresponding background (bottom) on pure Cr. Stearate crystal, 10 kV-300 nA

6. An accurate knowledge of the <u>mass absorption coefficients</u> is of extreme importance. On a number of occasions we have argued[1-4] that a 1 % uncertainty in the mac's will in general produce a 1 % uncertainty in the corrected concentrations. Now, it is hardly likely that mac's for ultra-light element radiations will ever be available with such precision; this is not even likely for short-wavelength radiations ! It will, therefore, frequently be necessary to propose new (and possibly) improved values for the mac's, using a series of good measurements on light-element compounds.
   Provided that such measurements are carried out very carefully and over a wide range in accelerating voltages, these data can be used in a number of recent correction programs (PROZA[6], PAP[7,8]) in order to produce more consistent mac's. Due to the very much improved absorption correction schemes in these programs, contrary to the conventional "ZAF" approaches based on e.g. the simplified Philibert model, it has indeed proved possible to obtain sets of mac's which give superior performances for all these programs at the same time.
   Such new sets have been the product of our previous work on

Carbon and Boron and it must be anticipated that the available mac's [9,10] for Nitrogen-Kα X-rays will have to be changed in a number of cases too. Previous experiences showed that this is usually the case for elements like Zr, Nb and Mo, where light-element radiations are very close to the M_5 absorption edges. As a matter of fact the present work has indeed resulted in new mac values for exactly these elements. Table II.1 gives a survey of available mac's for Nitrogen-Kα in the elements investigated in the present work, together with the new values resulting from the present investigation. It must be mentioned that the two sets published by Henke et al are the only independent sets published until now. As far as we know nobody has ever done any systematic microprobe work on Nitrogen so no data on mac's have ever been put forward which were based on actual microprobe measurements.

TABLE II.1

Mass absorption coefficients for N-Kα X-rays according to various sources

Absorber	Henke (1974[9])	Henke (1982[10])	Present work
B	15810	15800	15800
N	1637	1810	1810
Al	13830	13800	13100
Si	17690	16500	17170
Ti	4364	4360	4360
V	4790	4790	4790
Cr	5630	5630	5630
Fe	7121	7190	7190
Zr	25030	20400	24000
Nb	27190	21400	25000
Mo	23220	20200	25000
Hf	12910	12900	14050
Ta	13420	13400	15000

Apart from the changes for Zr, Nb and Mo it was also found necessary to propose much higher values for Hf and Ta.

7. A rather fundamental problem can be <u>systematic differences in X-ray emission</u> from one light element compound to another. The Ni-borides [2] were found to be typical examples of such an effect. In these cases it appears impossible to correct the measured intensity ratios to the nominal (expected) value: The relative root-mean-square value in the ratio between the calculated (k') and the measured k-ratio (k) shows a minimum value with Henke's[10] mac for B-Kα radiation in Ni. This indicates a good performance of the absorption correction with the particular mac as a function of accelerating voltage. However, the average k'/k ratio is approx. 15 % too high which means that the actually emitted intensity is 15 % below the expected level. It is important to realize that

every effort to change the mac in order to obtain a better k'/k ratio will result in a rapid deterioration of the r.m.s. value.
It is possible that such effects also play a role in carbides like TiC and VC where rather large adjustments in the mac's were necessary[1]. The low values of the mac's in these cases, however, do not lead to such a rapid deterioration of the r.m.s. figures; hence, it is not impossible that anomalies in X-ray emission have been overlooked at that time.

By and large, systematic differences in X-ray emission is something to be very much aware of. Such effects can only be traced, however, by systematic measurements over a wide range in accelerating voltages. Most probably these phenomena are related to differences in the chemical bond from one compound to another and as such an investigation of these effects must supply a lot of valuable information on the nature of this bond.

8. The choice of a matrix correction program.
A number of years ago this still appeared to be quite a problem indeed, because it is extremely difficult (if not impossible) to assess the performance of a correction program on light-element work as long as there are so many doubts about the correctness and consistency of the published mac's. Besides, there was a severe lack of reliable and consistent data on which correction programs could be tested. On top of that the conversion of intensity ratios into concentrations was and still is a very complicated process.

-- First the amount of generated intensity in standard and sample has to be calculated (Atomic number effect). This calculation in itself is already rather complex and uses a number of basic assumptions or physical laws which have not always been established beyond any doubt. A typical example of uncertainty is the use of various expressions for the ionisation potential (J) which is used in Bethe's slowing down expression. While the most commonly used expressions[11-14] will yield comparable results for elements with atomic numbers higher than Sodium, the various expressions will produce markedly different results for the ultra-light elements B through O. Unfortunately, the experimental evidence to support either of these expressions is very meagre indeed.
  Another region in the atomic number correction where a number of doubts seem justified is the calculation of backscatter losses. Recent investigations[15] have shown that the backscatter coefficient η is not independent of accelerating voltage as is frequently assumed in the atomic number correction models which are currently in use.

-- The second step concerns the calculation of the emitted intensity by means of applying a correction for absorption within the specimen. Now, it must be clear from the beginning that such a correction can only be properly applied if a detailed knowledge is available about the X-ray pro-

duction as a function of depth in the specimen.
The curve relating the number of X-ray photons produced (ϕ) to the depth z in the specimen, or preferably the mass depth ρz (density times linear depth z) is commonly known as the "$\phi(\rho z)$-curve". Fig. II.3 shows a typical example of such a curve. It is important to point out that such a curve does <u>not</u> give an absolute number of ionisations but rather the ratio relative to a very thin layer of the same material free in space. This stems from the way most $\phi(\rho z)$-curves have been measured in practice using the so-called tracer technique in which a very thin layer of element A (the tracer) is buried under an increasing number of layers of B (the matrix) and the emitted intensity of A-radiation is measured as a function of the mass thickness of B. Besides, this way of representing $\phi(\rho z)$-curves has the obvious advantage of making the curves independent of the particular type of machine they were measured on.

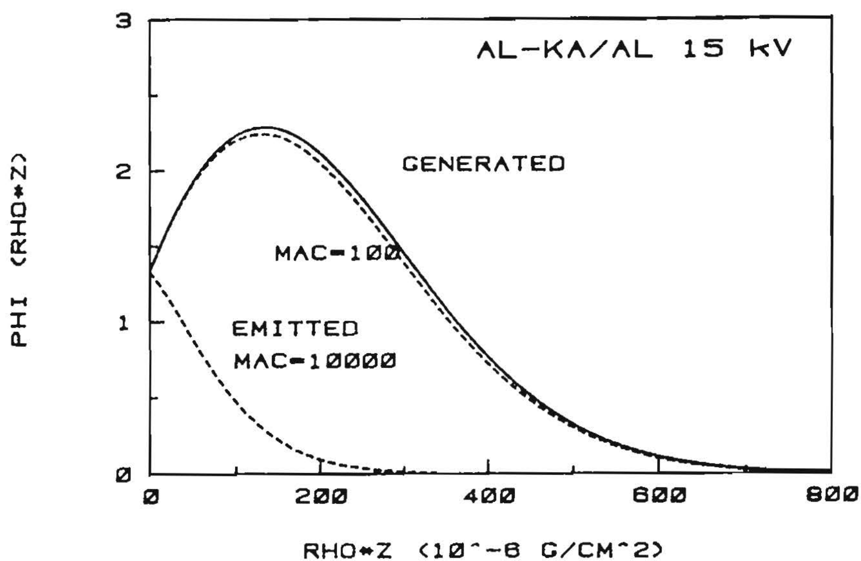

Fig. II.3 Typical example of a $\phi(\rho z)$-curve. Al-Kα-radiation in Al at 15 kV. Solid curve gives the generated intensity, while the dashed curves represent the emitted intensity for a hypothetical mass absorption coefficient of 100 (top) and 10000, respectively.

As Fig. II.3 shows the $\phi(\rho z)$-curve starts at the value of $\phi(0)$, the surface ionisation, which is higher than 1 because the same thin layer on a substrate will always produce more X-rays than without a substrate as a result of an enhanced process of electron back-scattering in the former case. After an initial rise in the $\phi(\rho z)$-curve a saturation level is reached after which the curve finally goes down to zero (no more X-rays produced). This latter part of the curve, from the top on, can usually very efficiently be represented by a Gaussian distribution, thus reflecting the statistical nature of the

X-ray production process. In the (near) surface layers the situation is different; here the electrons are not so efficient yet because of two reasons:

1) The electrons are more or less still collimated in a beam as a result of which the electron trajectories per unit of ρz are short and mostly perpendicular to the successive layers. In deeper layers the electrons will have been scattered many times, resulting in more oblique (and hence more efficient) trajectories.

2) The efficiency in X-ray production is strongly related to the overvoltage ratio (ratio between accelerating voltage and critical excitation voltage). The so-called "ionisation cross-section" has its maximum values at overvoltages of 2-3. The initial high overvoltage in the near-surface layers will therefore produce relatively few ionisations.

-- Finally, a fluorescence correction is sometimes necessary in order to account for the fact that additional, non-electron beam generated, X-rays can be produced by primary X-rays of other elements in the specimen. However, fluorescence effects for ultra-light elements are usually extremely small due to the very low X-ray fluorescence yields and can mostly be safely neglected.

Now, the concentration C of a particular element in a matrix is related to its k-ratio (intensity emitted by the specimen, divided by that emitted by a standard) through the following relationship:

$$C = k \cdot Z \cdot A \cdot F$$

or:

$$C = \frac{I_{spec}}{I_{stand}} \cdot \frac{Z_{stand}}{Z_{spec}} \cdot \frac{F(\chi)_{stand}}{F(\chi)_{spec}} \cdot F$$

in which I stands for the emitted intensity, Z (atomic number effect) for the total integral under the $\phi(\rho z)$ curve (total amount of <u>generated</u> intensity) and $F(\chi)$ for the fraction of the generated intensity which is actually emitted from either the standard or the specimen.
The parameter χ is equal to μ/ρ . cosec ψ in which μ/ρ is the mass absorption coefficient and ψ the X-ray take-off angle.
F stands for the secondary fluorescence correction factor. Due to the straight-forward linear proportionality of the concentration to all three factors Z, A, and F, in which F can be neglected for our present purposes, it would appear that the Z and A factors are of equal importance. The magnitude of the atomic number correction for medium to heavy elements usually differs less than 30 % from unity. The absorption correction, on the other hand, can be an order of magnitude larger: A-factors of more than 10 are not uncommon in heavily absorbing matrices. The latter cases are typical for the analysis of ultra-light elements. In the past the absorption correction has, therefore, always received the most attention. In this correction it is of the utmost

importance to have the correct shape of the $\phi(\rho z)$ curve. Especially the surface ionisation ($\phi(o)$) and the very first part of the $\phi(\rho z)$ curve (see Fig. II.3) play a crucial role in cases of heavy absorption and it is at least remarkable that this is exactly the portion of the $\phi(\rho z)$ curve that has always been neglected in the simplified Philibert absorption correction model, which has been used for many, many years (and is still being used) in the conventional "ZAF" approach. The strong interest for the absorption correction, however, has diverted the attention from the atomic number correction and this is certainly not justified: our experiences with a large number of correction programs on our Boron and Carbon analyses show that the differences in the atomic number correction factors produced by these programs can easily amount to 20 % and these differences in themselves could already account for the discrepancies between calculated and nominal concentrations in a large number of cases !

We have pointed out before[2] that what it all comes down to is that the same product Z.A can be produced by a wide variety of Z and A factors and that it is very difficult to know what the exact distribution over Z and A factors should be. To speak in terms of the $\phi(\rho z)$ approach : The same emitted intensity can be produced by a $\phi(\rho z)$ curve having a relatively small integral of $\phi(\rho z)$ but a peak very close to the surface as by a $\phi(\rho z)$ curve with a larger integral but with its peak deeper in the specimen.
The main problem in quantitative electron probe microanalysis of bulk specimens is that one is usually dicussing the <u>ratios</u> between quantities, rather than the quantities themselves. In many respects it is possible that large errors are present in the calculation for the numerator (i.e. intensity emitted by the specimen) and the denominator (intensity emitted by the standard) and that still the ratio is fairly correct. As a consequence it is very difficult to obtain absolute information on the more fundamental parameters from measured k-ratios in bulk specimens. The situation is completely different in Thin Film analysis; here it is crucial to have both the correct integral of $\phi(\rho z)$ as well as the correct X-ray distribution function.
For bulk analysis under not too difficult conditions, however, it seems that the requirements are not so stringent and this must be the reason that for a period of more than 20 years people have satisfied themselves with the simplified Philibert[16] absorption correction and the relatively simple Duncumb-Reed[14] atomic number correction which together form the basis of the well-known "ZAF" approach.
One glance at Fig. II.3 (lower dashed curve), however, shows that this practice could not possibly be continued in the field of ultra-light element analysis simply because the area from which the intensity is emitted is neglected all together in the simplified Philibert model by assuming a $\phi(o)$ value of zero. Attempts undertaken by Ruste[17] to reinstall the "full" Philibert model with realistic $\phi(o)$ values based on work by Reuter[18] were only partly successful[1,2,3] because the $\phi(\rho z)$ curves were still based on an unrealistic exponential function producing a too long tail into depth which was more or

less compensated by a position of the maximum in the $\phi(\rho z)$ curve too close to the surface.

A completely different approach for the absorption correction was chosen by Love and Scott. Their first matrix correction program, which was also based on a typical "ZAF" approach in the sense that the Z and A factors were calculated separately, contained an atomic number correction of their own[19] and an absorption correction based on Bishop's[20] "square model". In the latter model the X-ray distribution was assumed to have a rectangular shape which is, of course, totally unrealistic. Nevertheless, by an appropriate choice of parameters and especially a suitable parameterization of the latter the model was found to work surprisingly well (for not too difficult cases), at least better than the conventional ZAF approach. The model failed, however, in the analysis of ultra-light elements[1,2].
A further improvement in Love and Scott's program was produced by the introduction of the so-called "quadrilateral" model for the X-ray distribution function[21]. Due to the fact that this (still unrealistic) shape is much closer to the real $\phi(\rho z)$ curve the model was found to perform much better. Still, the performance of this latter program was hardly satisfactory on our Boron and Carbon data bases[1,2] but this was not only due to inadequacies in the parameterization of the quadrilateral model under extreme conditions ; also the atomic number correction broke down at extremely high overvoltages. A new parameterization of the quadrilateral model, in which our Boron and Carbon data bases were used, together with the mac's we proposed, and some alterations in the atomic number correction finally produced a program[6] with a similar performance as our own programs.

In the past decade two completely new and fresh approaches to the field of matrix correction have been introduced by Pouchou and Pichoir[7] and Packwood and Brown[22], respectively. Both approaches can be considered to be based on attempts to describe physical reality as much as possible in the sense that all efforts have been concentrated on producing X-ray distribution functions which are as realistic as possible. Once this goal has been achieved matrix correction becomes a rather straight-forward process. This is not only important for the analysis of ultra-light elements; it also opens the way to analysis under much more extreme conditions of accelerating voltages and X-ray wavelengths in general. Finally, such approaches offer the best possible basis for Thin Film analysis for which an exact knowledge of the $\phi(\rho z)$ curve is crucial. In many respects Thin Film analysis is the ultimate test for any correction program.
A further discussion on this subject will be given in Chapter V where the numerical results obtained on our final data base will be discussed.

9. Peak Shifts and Peak Shape Alterations

We have shown on many previous occasions [1-6] that the intensity measurements for ultra-light element radiations can be seriously influenced by :
-- Peak Shifts and
-- Peak Shape Alterations

The first problem is usually well-known to most microprobe users. Besides, it can easily be dealt with by simply performing a new peak search procedure when moving from standard to specimen and vice versa.
The second problem, however, is much less well-known and, on top of that, much more difficult to deal with.
The direct consequence of peak shape alterations in the light element emission peaks is that the net peak intensity, which is usually measured in day-to-day practice, is no longer a correct measure for the emitted intensity. It is usually not realized that the routine practice of measuring peak intensities is in fact based on the tacit assumption that the peak intensity is proportional to the integral emitted intensity. Now, while this may be correct for the vast majority of K-, L- and M-lines of medium-to-high Z-elements it is definitely no longer correct for ultra-light element radiations. In the latter cases, as a direct result of strong peak shape variations, it is in principle mandatory to perform the intensity measurements in an integral fashion. This is, of course, not a very attractive option for a wavelength-dispersive spectrometer.
We have shown before[1-6], however, that a considerable reduction in time and effort can be obtained if the so-called "Area-Peak Factor" concept is adopted. This concept is based on the consideration that there is a fixed ratio between the correct Integral (or Area) k-ratio and the Peak k-ratio for a specific compound relative to a specific standard and on a specific spectrometer (with its typical spectral resolution, depending on analyzer crystal and dimensions of the Rowland circle). Once an Area-Peak Factor (APF) for a given compound is known, further measurements on the same compound can be performed on the peak again and multiplication of the peak k-ratio with the APF will yield the correct integral k-ratio. In the past few years[1-6] we have shown experimentally that the APF is indeed independent of accelerating voltage which makes it possible to establish APF's under the best possible conditions in order to be used later on under more extreme conditions, like much higher accelerating voltages.
We have also shown that the APF's in borides and carbides show a very typical saw-tooth like variation as a function of atomic number of the alloying partner: extremely low values (narrow peaks relative to the standard) are usually found for combinations with elements like Ti and Zr. Increasingly higher values were always found with increasing atomic number in the same period of the periodic system.
In all cases it has become clear that the effects of peak shape alterations can be very large indeed : APF's of 0.72 were found for C-Kα radiation from TiC relative to an Fe_3C standard. If Glassy Carbon were chosen as a standard the

effects would have been even more serious; in this case an APF of 0.5 would be necessary in order to correct for the extreme variations in peak shapes.
Similar effects were found for B-Kα radiation. In this case, however, additional problems turned up in a sense that the peak shapes for B-Kα appeared to be dependent also on the crystallographic orientation of the specimen with respect to electron beam and position of the analyzer crystal. Needless to say that huge errors in quantitative EPMA of elements like Carbon and certainly Boron are likely to be made if the effects of peak shape alterations are ignored.

In general we can say that Boron is definitely the most difficult element to deal with, followed by Carbon, where at least crystallographic effects were no longer found. Hence, it would be expected that Nitrogen would present less difficulties, at least as far as peak shape alterations are concerned. This turned out to be the case indeed : the highest APF values (for STE) were approx. 1.05 (relative to Cr_2N). These were observed in cubic BN and the (chemically unstable) Mo_2N. The lowest values were approx. 0.96-0.97 and were found in the extremely stable nitrides ZrN and HfN. Fig. II.4 gives 4 spectra of nitrides with APF's covering the full range.

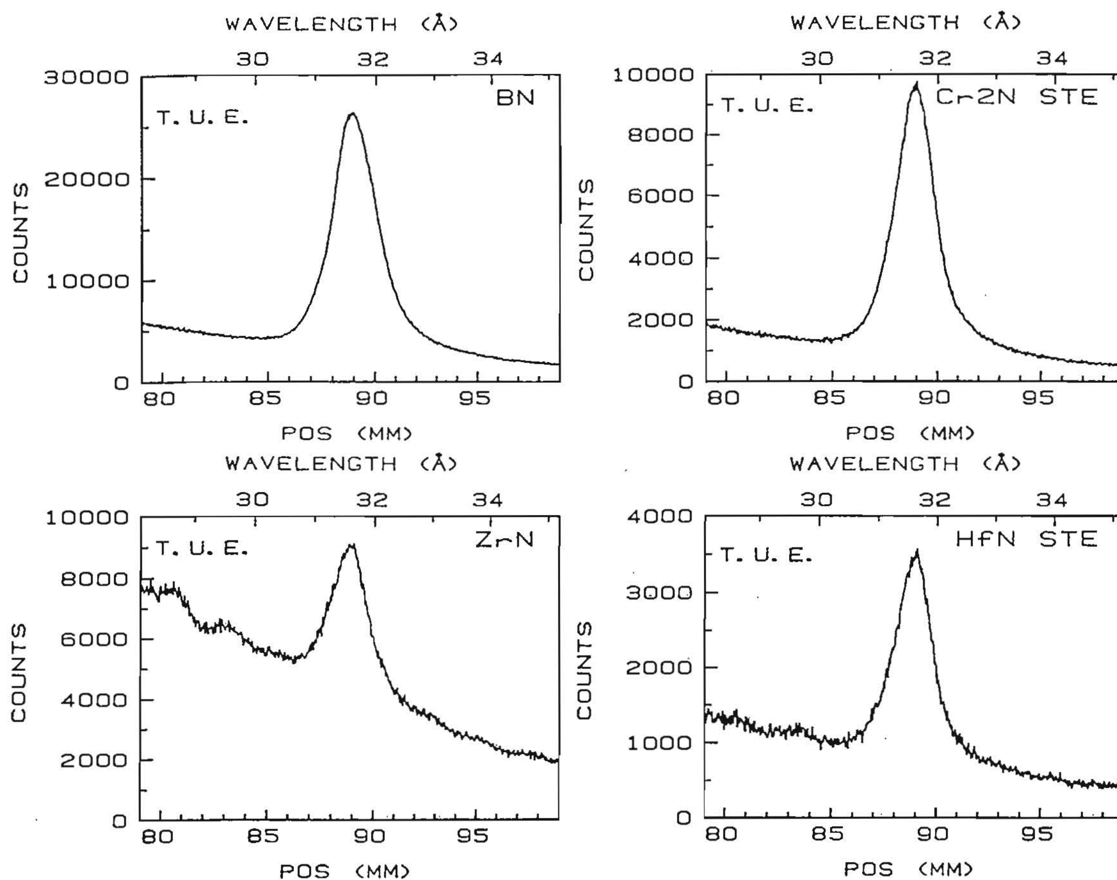

Fig. II.4 Typical N-Kα emission spectra from three nitrides as compared to that of the Cr_2N standard. Lead-stearate crystal; 10 kV, 100 nA

As Fig. II.4 shows the differences in N-Kα peak widths are hardly visible and digital techniques are really necessary in order to extract accurate APF values from these spectra.
However small the effects may be, peak shape alterations of 5 % is still something to be concerned about if one is trying to do accurate quantitative analysis. It must be mentioned here that the determination of APF values turned out to be a very tedious and difficult job for N-Kα because of the desperately low peak count rates in many nitrides, especially in ZrN, Nb_2n, Ta_2N etc. Therefore the actual numbers we will quote further on cannot have the same relative accuracy (± 1 %) as we have given for Boron and Carbon, in spite of the very large number of measurements we performed.

III EXPERIMENTAL PROCEDURES

For the purpose of the present work it is, in principle, required to have fully homogeneous nitride specimens of 100 % density and accurately known compositions. Like it was the case for Carbon and Boron such specimens for Nitrogen can hardly be obtained commercially. It was, therefore, decided to prepare them in our own laboratory. Only 5 out of a total number of 18 Nitride specimens were obtained from external sources. These were the following specimens :

-- Hexagonal BN, produced by Chemical Vapour Deposition, kindly supplied to us by Mr. G. Verspui, C.F.T. Philips, Eindhoven, The Netherlands.
-- Cubic BN, (powder, particle size up to several tens of μm, produced by the "Borazon" process), kindly supplied to us by Mr. R. C. de Vries, General Electric Co, Schenectady, N.Y., U.S.A.
-- Si_3N_4, produced by C. V. D. techniques on a Si substrate, layer thicknesses of 1 and 2.5 μm, respectively. These specimens were supplied to us by Mr. P. v.d. Straten, formerly with C.F.T., Philips, Eindhoven, The Netherlands.
-- TiN, produced by C. V. D. techniques on a Ti substrate, in ± 5 successive steps to yield layer thicknesses up to 2 mm. This specimen was also suppled to us by Mr. G. Verspui, although it presumably stems from a Philips Research Laboratory in Aachen, F. R. G.
-- Fe_4N, produced by low-temperature (560 ^{0}C) nitriding of Fe, resulting in a ± 20 μm thick nitride layer. This specimen was kindly supplied to us by Ir. D. Schalkoord, University of Technology, Delft, The Netherlands.

III.1 Preparation of Nitrides

The preparation of massive, homogeneous nitride specimens turned out to be a major task which took the best part of a year in which the help of many students has been used.
In the majority of cases use has been made of the so-called "Reactive Arc-Melting" technique in which the metal components were melted in a conventional Arc-Melting equipment (Tungsten electrode, water-cooled copper hearth) under Argon-Nitrogen mixtures (10 cm argon, 20 cm Nitrogen).
In general this particular technique led to the production of two-phased alloys : α-Me(N) (solid solution) + MeN for the metals Ti, Zr and Hf; or Me(N) + Me_2N for V, Cr, Nb and Ta.
Subsequent annealing of these starting materials at temperatures between 1100 and 2000 ^{0}C during 12-140 hrs in a 6 kW RF furnace under purified Nitrogen usually yielded homogeneous massive specimens of TiN, VN, ZrN and HfN.
Similar procedures for Cr and Ta led to the formation of the subnitrides Cr_2N and Ta_2N, while in the case of Nb the Nb_4N_3 phase was obtained.
Compounds like Ti_2N, V_2N and Nb_2N could not be produced in the form of massive specimens. In these cases diffusion

layers could be grown by heating the elements in pure Nitrogen at elevated temperatures. Areas close to the Me_2N/MeN (or Me_4N_3 in the case of Nb) interface were selected and marked by microhardness indentations. The compound TaN could be made by heating a massive Ta_2N specimen in Nitrogen at temperatures between 1000 and 1200 ^0C, leading to a ± 10 μm thick TaN layer.
Extremely difficult to produce were the compounds CrN and Mo_2N. The former could be made by low-temperature (900 ^0C) nitriding of a RAM-melted specimen in NH_3, leading to the formation of ± 10 μm thick CrN layers very locally; usually in cracks and crevices only. The latter was made by nitriding Mo sheets at 900 ^0C in NH_3 during approx. 100 hrs. This procedure yielded a ± 30 μm thick Mo_2N layer. In general these turned out to be rather tricky and irreproducible production techniques.
Sufficiently thick (± 30 μm) AlN layers, finally, were produced by C. V. D. techniques on a graphite substrate, using Al shavings and HCl gas, in order to produce gaseous $AlCl_3$, which was then mixed with NH_3 gas and passed over a heated graphite substrate.
Table III.1 gives a quick survey over the production routes used in the preparation of our nitrides.

Table III.1

Survey of the production routes used in the preparation of Nitride specimens for the present investigation

COMPOUND	PRODUCTION ROUTE	PRODUCT
-- BN-Hexagonal	C.V.D.	thin-walled cylinder
-Cubic	Borazon ® process	powder
-- AlN	C.V.D. on graphite	30 μm layer
-- Si_3N_4	C.V.D. on Si	1 and 2.5 μm layers
-- Ti_2N	Diff. couple Ti/N_2, 89 hrs 1400 ^0C	Planparallel section
-- TiN	C.V.D. on Ti	several mm thick layer
-- V_2N	Diff. couple V/N_2, 70 hrs 1300 ^0C	
-- VN	RAM-melted + 70 hrs 1900 ^0C in N_2	
-- Cr_2N- # 1	RAM-melted + 91 hrs 1000 ^0C in N_2	
# 2	RAM-melted + 90 hrs 1400 ^0C in N_2	
-- CrN	Cr/NH_3 45 hrs 910 ^0C	10 μm layer (locally)

Table III.1 (continued)

COMPOUND	PRODUCTION ROUTE	PRODUCT
-- Fe_4N	Fe + red. N_2 pressure 560 ^0C	(± 20 μm layer)
-- ZrN	RAM-melted + 90 hrs 1800-1890 $^0C/N_2$	(RF furnace)
-- Nb_2N	Nb (1 cm)/N_2 70 hrs 1900 ^0C	(RF furnace)
-- Nb_4N_3	Nb (1 mm)/N_2 70 hrs 1900 ^0C	(RF furnace)
-- Mo_2N	Mo/NH_3 100 hrs 900 ^0C	(max. 30μm layer)
-- HfN	RAM-melted 70 hrs 1850 $^0C/N_2$	(RF furnace)
-- Ta_2N	RAM-melted 70 hrs 1600-2000 ^0C	(RF furnace)
-- TaN	Ta/N_2 68 hrs 1500.....1100 ^0C	(RF furnace)

III.2 Characterization of Nitride specimens

Because appreciable amounts of massive Cr_2N, meant to be used as the Nitrogen standard, were needed two batches of this compound have been prepared and a lot of care has been exercised to find the correct composition. Both batches were prepared from RAM-melted starting materials and carefully checked for homogeneity with the electron probe microanalyzer. After that they were subjected to chemical analysis a number of times. Thanks are due to Dr. P. Karduck of the University of Technology in Aachen, F. R. G. for supplying these chemical analyses.
The first batch was prepared by annealing at 1000 ^0C during 91 hrs. The results of the chemical analyses are given in Table III.2.

TABLE III.2

Chemical Analyses of the Cr_2N specimen (Batch # 1) used as the Nitrogen standard throughout this work

	N-content Wt %	O-content Wt %	Cr-content Wt %
	10.5	0.49	89.01
	10.8	0.50	88.70
	10.6	0.46	88.94
	11.2	0.52	88.28
	10.4	0.43	89.17
	----	----	-----
Aver.	10.7 (wt %)	0.48 (wt %)	88.82 (wt %)
	30.53 (at %)	1.20 (at %)	68.27 (at %)

Small pieces of this particular Cr_2N batch have been mounted in combinations with all other nitrides in order to be used as the Nitrogen standard.
The second batch was prepared at 1400 ^{0}C during 90 hrs. The results of the analyses are given in Table III.3.

TABLE III.3

Chemical analyses of the second Cr_2N specimen

	N-content Wt %	O-content Wt %	Cr-content Wt %
	10.2	0.25	89.55
	10.0	0.25	89.75
	10.1	0.22	89.68
	----	----	-----
Aver.	10.1 (wt %)	0.24 (wt %)	89.66 (wt %)
	29.30 (at %)	0.61 (at %)	70.09 (at %)

The results of the chemical analyses were carefully checked against the EPMA analyses of Cr and, most important of all, the available material on the phase diagram Cr-N, the most recent version of which is given in Fig. III.1.

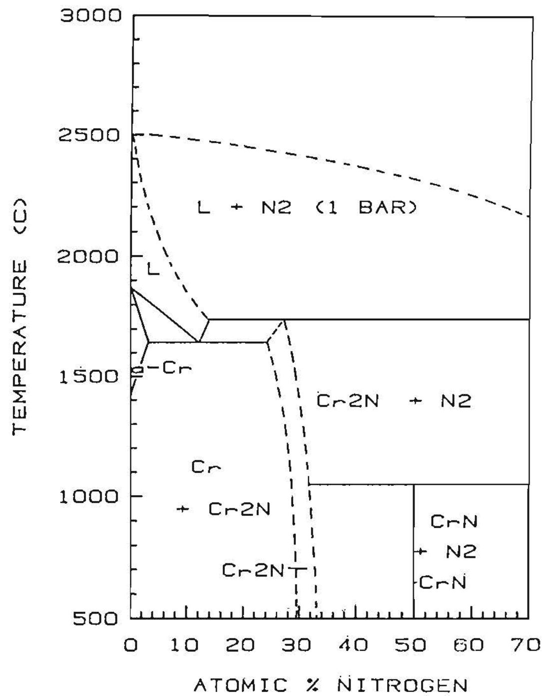

Fig. III.1 Phase diagram of the Cr-N system after Holleck[23]

It can be seen here that the homogeneity range of Cr_2N extends from 30-33 at % N at 500 °C while at higher temperatures it bends back towards lower N-contents. This seems to be in good agreement with the results of the chemical analyses : The specimen produced at 1000 °C (Batch # 1) has a combined N+O content of 31.73 at % which is well in accordance with the phase diagram. For the higher temperature of 1400 °C a correspondingly lower N-content (well under 31 at %) is predicted by the phase diagram and this was indeed found : The combined N+O content was 29.91 at % .
These findings gave us the necessary confidence in these chemical analyses, certainly enough to use these specimens (especially Batch # 1) as the universal Nitrogen standard throughout this work.
Note, by the way, from the phase diagram that the compound CrN, which is apparently a line compound, would have made a much better Nitrogen standard for which an independent chemical analysis would not have been necessary. This compound could, however, only be produced in really too small quantities. It is interesting to point out though that when Cr_2N (Batch # 1) with the reported composition was used as a Nitrogen standard for the analysis of CrN, then indeed stoichiometric CrN was found. This substantiates the correctness of the composition of the Cr_2N standard.

Unfortunately, things turned out to be very much less satisfactory as far as the remaining nitrides were concerned; especially the "difficult" nitrides like TiN, ZrN and HfN. In these cases combined N+O contents were reported which were contradictory to the (sometimes scarce) information on phase diagrams. The maximum limit of the homogeneity region was

exceeded by 5 (in the case of TiN) up to as much as 20 % relative (HfN). This seems to point to severe systematic errors in the chemical analyses of these (highly stable) nitrides. Our own microprobe measurements indicated that especially the oxygen contents were usually highly exaggerated in the chemical analyses; sometimes twice as high as the results from microprobe analysis. The latter would already have to be treated with suspicion because they would probably all come out too high due to the effects of Oxygen contamination (see Chapter IV).

The results for Nitrogen were also usually too high, although less dramatically than for Oxygen : In our opinion the reported values were between 5 % relative (TiN) and 15 % (HfN) too high.

An additional problem was formed by those nitrides that were only available in the form of diffusion layers, like Ti_2N, V_2N, Fe_4N, Nb_2N and Mo_2N : Such specimens cannot be subjected at all to chemical analysis.

For all these reasons we were, therefore, forced in the end to use a different approach in order to find the "Most Probable Composition" of each of the nitride specimens. This approach was based on a tedious and time-consuming process aimed at obtaining the maximum degree of consistency in the results. In this process use was made of every single bit of information that we could lay our hands on : The information on phase diagrams, results of the microprobe analyses of the metals in the nitrides, results of the Nitrogen analyses themselves, consistency in the variation of the mass absorption coefficients (B, C, N, O radiations) in each of the metals, known biases (from earlier work on B and C) of existing correction programs in specific cases, our own experience in solid state chemistry and materials science, thermodynamic considerations, etc. etc. Sometimes features like the typical deep golden color (TiN, ZrN and HfN) can be a good and very sensitive indication for approaching the stoichiometric composition.

In view of all the uncertainties involved it is logical that the whole process of establishing the most probable compositions is iterative in nature. Nevertheless, we finally succeeded in finding a set of compositions which would indeed give a maximum degree of consistency and we sincerely believe that this set is very close to the truth.

Table III.4 gives a survey of these compositions.

TABLE III.4

Most probable compositions of the nitride specimens used in the present investigation (wt %)

Compound	N-content	O-content	Metal content
BN (Hex)	56.45	----	43.55
(Cub)	56.45	----	43.55
AlN	34.18	----	65.82
Si_3N_4	39.24	0.70	60.06
Ti_2N	11.84	----	88.16
TiN	22.50	----	77.50
V_2N	11.99	0.78	87.23
VN	16.04	0.31	83.65
Cr_2N (# 1)	10.70	0.48	88.82
(# 2)	10.10	0.24	89.66
CrN	21.22	----	78.78
Fe_4N	5.60	----	94.40
ZrN	12.70	0.67	86.63
Nb_2N	6.55	0.46	92.99
Nb_4N_3	9.79	0.72	89.49
Mo_2N	5.80	----	94.20
HfN	6.06	0.29	Hf 91.36
			Zr 2.29
Ta_2N	3.47	0.24	96.29
TaN	6.51	0.22	93.27

It is interesting to point out that in the course of the preparation of the nitride specimens we observed that the existing phase diagram of the Ti-N system could not be correct. Hence, we established a new phase diagram[24], the quantitative results of which were essentially confirmed a few months later by a French group[25] using quite different procedures. This can probably also be regarded as substantial support for the correctness of our approach in quantitative respects.

III.3 Mounting, polishing and examination procedures

Each of the nitride specimens, small pieces of the Cr_2N standard (Batch # 1) and pieces of the pure metals were mounted and polished separately. This was done in order to avoid problems in polishing materials exhibiting extreme differences in hardness. The specimens were mounted in copper-filled resin and very carefully polished. Diamond abrasive disks were used for the coarse stages (70, 30 and 15 μm grain size) of polishing; final polishing was done on a nylon cloth with diamond paste (6, 3 and 1 μm). After a satisfactory polish was obtained the specimens were cut out again in small cubes of mounting resin containing the specimen after which all edges of the polished face were carefully rounded off. Next

the specimens were turned upside down onto the bottom of a freshly polished mould in order to be remounted groupwise: the Cr_2N standard in the centre and e.g. specimens like TiN, Ti_2N and Ti grouped around the standard. This procedure was found to guarantee perfectly plane and parallel top and bottom planes of the new mount, which is extremely important in view of the correctness of the take-off angle in light-element work. Superficial contaminants were removed from the polished faces by a brief polishing treatment on a soft cloth using 0.05 μm γ-Alumina. Final cleaning was done ultrasonically using alcohol.

Optical microscopy was used to get a first impression of the quality of the specimens as far as the presence of second (or third) phases, presence of unreacted starting materials, grain size (using polarized light), etc. are concerned.
In some cases (BN, Cr_2N, Mo_2N) standard X-ray diffraction procedures were used to identify the compounds. Microprobe analysis of the metal component as well as the N and O content was used to check vital items like homogeneity, identity of second phases and, sometimes, the compositions of the specimens. Special attention was paid to the consistency of the results obtained in those cases where more than one compound in a particular system was available (Ti, V, Cr, Nb, Ta). This is, by the way, the reason that whenever possible we try to have more than one compound in the same binary system at our disposal. All the examination procedures mentioned here have played a more or less important role in the complicated process aimed at finding the most probable compositions.

III.4 Technical details of the microprobe used

All our measurements were performed on an automated JEOL Superprobe 733, equipped with 4 wavelength-dispersive spectrometers and an energy-dispersive system (TRACOR Northern TN-2000). The automation system was also supplied by TRACOR Northern (TN-1310).
The first spectrometer, specifically designed for light(er) elements, was equipped with a conventional lead-stearate crystal (2d spacing ± 100 Å) for the analysis of B, C, N and O, and a TAP crystal for higher Z-elements. The specially purchased 4th spectrometer was equipped with two new synthetic multilayer crystals. The first one was a W/Si multilayer (200 pairs of layers, 2d spacing 59.8 Å), eminently suited for the analysis of (C), N, O and F. The second one was a Mo/B_4C multilayer (2d spacing 144.8 Å), optimized for the analysis of B and Be. Both crystals were supplied by Ovonic Synthetic Materials Corporation, Troy, Michigan, U.S.A. The other two spectrometers each contained a conventional LiF and a PET crystal. The counters were in all cases of the proportional type: for spectrometers # 1 and # 4 of the Gas-Flow type (Argon- 10 % Methane); for spectrometers # 2 and # 3 of the sealed Xenon type.

On a previous occasion[1] we have already discussed the tests on the operating conditions of the microprobe, such as the correctness of the accelerating voltage, stability of the

beam current, stability of the beam position, etc. Those items were then found highly satisfactory. Besides, our instrument is equipped with an automated beam current detector and count rates are automatically corrected for any drift that might occur during the measurements.

During the present work all Nitrogen measurements were carried out with the lead-stearate (STE) and W/Si multilayer (LDE) crystals simultaneously under identical conditions. This enabled us in the first place to compare the performances of both crystals in a quite straight-forward way. Initially, all measurements were carried out using an air jet[1] in order to prevent build-up of Carbon under the electron beam which could produce a drastic reduction in Nitrogen count rates with time as a result of the strong absorption of N-Kα X-rays in Carbon. In the course of the investigation, however, it was discovered that certain sensitive nitrides such as ZrN, HfN and TaN can be oxidized at an incredibly fast rate under electron bombardment, leading to a rapid decrease of the N-Kα signal with time. The measurements on these materials were, therefore, repeated without the use of the air jet. It is perhaps interesting to point out in this respect that the conventional oil-diffusion pump used in our previous work[1,2] has been replaced by a turbo-molecular pump in an effort to reduce the influence of hydrocarbons in the vacuum system on the carbon-contamination process.

III.5 Measurements of Area-Peak Factors

The Area-Peak Factors (APF's) for N-Kα radiation were determined from integral recordings of the N-Kα peak emitted by the Cr_2N standard and the particular nitride specimen. All these integral measurements were carried out over night and in weekends. The spectrometers (# 1 and # 4) were hereby scanned stepwise over the range of approximately 28-35 Å.
For the multilayer crystal (LDE) this corresponded to the linear range of 130-165 mm in steps of 0.07 mm (0.01495 Å). For the stearate crystal (STE) the range was 79-99 mm in steps of 0.04 mm (0.01426 Å). In each interval counts were accumulated during 10 s and the numbers were subsequently transferred to successive channels of the multi-channel analyzer and displayed on the screen of the C.R.T. of the EDX system. After completion of the spectra they were stored on diskette. One half of the memory of the M.C.A. (Channels 0-512) was for the STE crystal, while the other half (Channels 513-1024) was reserved for the LDE crystal. The beam current was measured before and after the measurement and these values were stored in the channels 511 and 512, the channels 0-500 being reserved for the integral spectrum in 500 steps. A typical sequence in the measurement of e.g. CrN would be: Start on Cr_2N (Nitrogen standard), followed by 3 successive measurements on CrN, after which a spectrum on pure Cr would be recorded. Then the complete cycle would be repeated once more. Because each integral measurement took about 1.5 hrs the complete procedure would take the best part of the night. Far more than 1000 spectra (both for STE as

LDE) have been accumulated in this way.
The vast majority of APF measurements were carried out at 10 kV and a beam current of 300 nA. The Pulse Height Analyzer conditions (Ortec electronics) were chosen such as to produce a N-Kα pulse at 2.0 Volt (Counter high tension 1700 Volt). The threshold was usually fixed at 1.0 Volt and a window of 2.0 Volt was commonly used.

The stored spectra were processed in order to obtain the net Integral (Area) and Peak intensities from standard and specimen. A special computer program was written (in Flextran) to extract the APF values from the integral recordings. The first step in this process was to subtract the background and this turned out to be quite a problem in the case of Nitrogen. This problem was caused by the relatively strong curvature of the background on STE and, to a lesser extent, on LDE, especially on the short-wavelength side of the spectrum. The problem was solved by fitting the background, as recorded on the pure metal element, to the nitride spectrum in a trial and error mode and then subtracting the proper fraction of this background from the spectrum of the unknown. Extensive use was hereby made of the built-in modules of the EDX system. Inspection of the resulting nitride spectrum usually showed a rather flat background on both sides of the N-Kα peak which was then accessible to the normal procedure of linear interpolation. The background on STE was usually taken at ± 5.5-6.5 mm, depending on the curvature of the background; that on LDE at ± 10.5 mm. Another problem with background determination, especially on STE, was associated with the presence of remnants of higher order metal lines in the spectrum, e.g. 4th order Al-Kα in AlN, 4th and 5th order Si-Kα in Si_3N_4. Here too, trial and error procedures were used in which a fraction of the background of the pure element spectrum (Al or Si) was subtracted from the nitride spectrum. The success of the operation was judged from the disappearance of the interfering peak. All these options were available in the special program we made for the extraction of APF values from the raw data.

A major problem was the determination of APF's in compounds like TiN and Ti_2N: due to the extreme overlap of the Ti-ℓℓ and N-kα peaks a straight-forward measurement is out of the question here, In fact, a special procedure has been devised in the course of this work to measure the APF and to extract the Ti-ℓℓ peak from underneath the combined (Ti-ℓℓ + N-Kα) peak. This will be discussed in the next chapter.

Finally, some remarks concerning the accuracies in the APF values seem appropriate. Due to the fact that the net peak count rates on STE can be desperately low, with Peak-to-Background ratios dropping well below 1, the experimental accuracy in APF's as claimed for our Carbon measurements (± 1 % relative), can most certainly not be matched here, in spite of the very large number of measurements performed. Our general feeling is that the accuracies for N-Kα are probably in the order of ± 1.5 % for easy cases like BN, AlN and Si_3N_4 and of 2-3 % for really difficult cases like ZrN, Nb_2N and Mo_2N.

III.6 Measurements of Integral k-ratios between 4 and 30 kV

Although the APF concept has been introduced[1,2] in order to facilitate the conversion of fast (and usually incorrect) peak intensity ratio measurements into correct integral intensity ratio measurements with great savings of time and effort, the concept could only be used in a very limited number of cases in the present work; only for the nitrides of the lighter elements B, Al and Si. The main reason was the sometimes strong curvature in the backgrounds in the heavier nitrides, which made the routine procedure, consisting of background measurements at equal distances on either side of the peak, impossible to use. Therefore, we were forced to perform the vast majority of the intensity measurements in a completely integral fashion, which took 1 night per nitride for each accelerating voltage. The measurements themselves were carried out at 4, 6, 8, 10, 12, 15, 20, 25 and 30 kV. So, almost 2 weeks per nitride specimen were necessary to complete one series on only one compound. Even then, the statistics are bound to be much poorer than in the case of Boron or Carbon because only approx. 6 integral measurements can be carried out per night, which means that only 6 k-ratios (from different locations on the specimen) can be collected per nitride specimen for each accelerating voltage. In all cases the measurements were performed with STE and LDE crystals simultaneously, with a beam current of 300 nA. Since the net peak count rates and Peak-to-Background ratios on LDE were so much better than on STE and also the background on LDE was so much "cleaner" it was decided to average the final integral k-ratios on a 2:1 weight base in favour of LDE. All together 144 k-ratios for N-Kα relative to Cr_2N have been collected in this way and these have served as the final data base on which our matrix correction procedure has been applied.

In all nitrides also the X-ray lines of the metal components have been measured over the full range in voltage. All possible X-ray lines that could be excited (e.g. Ta-Mα, Ta-Lα) in the given range have been measured. The beam current was adjusted to give a maximum count rate of 3000 cps in order to avoid excessive dead time corrections. A total number of 149 k-ratios have finally been collected.

IV RESULTS

Before discussing the actual numerical results of the present work we would like to elaborate on two typical problems which we encountered.

The first (nasty) problem was the contamination with Oxygen which we observed to take place very fast on sensitive nitrides and their constituent pure metals. The second problem was connected with the question how Nitrogen can be measured in Ti-containing compounds. In such compounds the Ti-ıı line and the N-Kα line overlap to such an extent that only one combined peak can be observed. As a matter of fact, we spent quite some time on these two problems, especially the second one, because Ti-N compounds are very frequently used as e.g. wear-resistant coatings on tools and are, therefore, very important in practice. We believe that we have found a solution to this particular problem and we have tested this solution very extensively. The former problem, however, of Oxygen contamination is something we will have to live with because it cannot be alleviated in a simple way. This particular problem will now be discussed first.

IV.1 Oxygen contamination in the microprobe

Contamination problems in the microprobe are commonly discussed in terms of Carbon contamination. This is quite understandable because this phenomenon can be quite a nuisance indeed if one tries to measure carbon contents well below 0.1 wt % in steels. In such cases the carbon build-up under electron bombardment can produce an apparent carbon concentration that can be very much higher than the true content if no special precautions are taken.

In the past two techniques have been proposed to solve this problem. The first one is based on the use of a liquid-nitrogen cooling trap surrounding the point of impact of the electron beam on the specimen. The second one is the use of an air jet in which a fine stream of air is directed towards the point of impact of the electron beam. Usually one of these devices, sometimes both, is part of the standard equipment of commercially available microprobes. For some unknown reason, however, the air jet seems to have lost some of its original popularity. However, according to our experiences[1,3,26] the air jet is definitely the most powerful device in the fight against carbon contamination.

In the present work on Nitrogen analysis it would seem appropriate, therefore, to use the air jet also because N-Kα radiation is extremely heavily absorbed in Carbon: The wavelength of N-Kα falls right into the K-absorption edge of Carbon. On top of that the integral measurements are very time-consuming and the time spent on one location on the specimen can well be in the order of 1.5 hrs. It is thus vital to avoid the build-up of Carbon on the specimen during the measurement. For all these reasons the air jet has initially been used on a routine basis during all our

integral measurements. In the beginning of the work, as long as we were dealing with the lower atomic number nitrides (BN......Fe_4N), no adverse effects of the air jet were noticed. The problems began, however, as soon as we touched on nitrides like ZrN, HfN and TaN. In the case of ZrN we actually measured a variation of k-ratio for Nitrogen with voltage that was completely opposite to the predictions of our matrix correction program: instead of showing a decrease between 4 and 15 kV, followed by a slight increase again between 20 and 30 kV we measured (with air jet) an increase between 4 and 15 kV,followed by a decrease with increasing voltage. Throughout the complete voltage range the k-ratios were dramatically too low, but especially at the lowest voltages: at 4 kV by a factor of 5 too low!

We soon found out that the explanation for these peculiar phenomena had to be sought in the rapid process of in-situ oxidation that sets in on sensitive nitrides like ZrN the moment the electron beam has been positioned on the specimen. This process can apparently be strongly enhanced when an air jet is used which creates a poor vacuum with high partial pressure of Oxygen near the point of impact of the electron beam. The moment we noticed this effect we became, of course, very suspicious about our previous measurements and we decided to investigate the effects of Oxygen contamination in rather more detail. Fortunately, we were in posession of two light-element crystals (STE + LDE) so that we could set up a series of experiments in which we could monitor the variation of the N-Kα signal on STE and the O-Kα signal on LDE simultaneously as a function of time for all nitride specimens both with as without the use of the air jet. Besides, these experiments were run at a number of different accelerating voltages.

The LDE crystal is extremely sensitive to Oxygen as is demonstrated in Fig. IV.1 where an Oxygen peak is visible on pure gold.

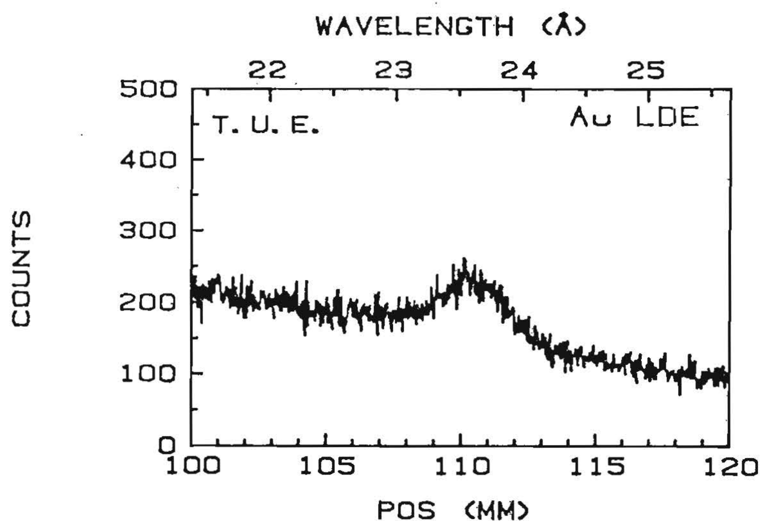

Fig. IV.1 Oxygen peak recorded on pure gold LDE crystal, 10 kV, 50 nA

As the solubility of O in Au is negligible the Oxygen is probably physically absorbed on the specimen surface which, by the way, shows how surface sensitive a microprobe can be. The cases of Oxygen contamination in the present work, however, are definitely not confined to superficially adhering Oxygen. This is demonstrated in Fig. IV.2 for ZrN.

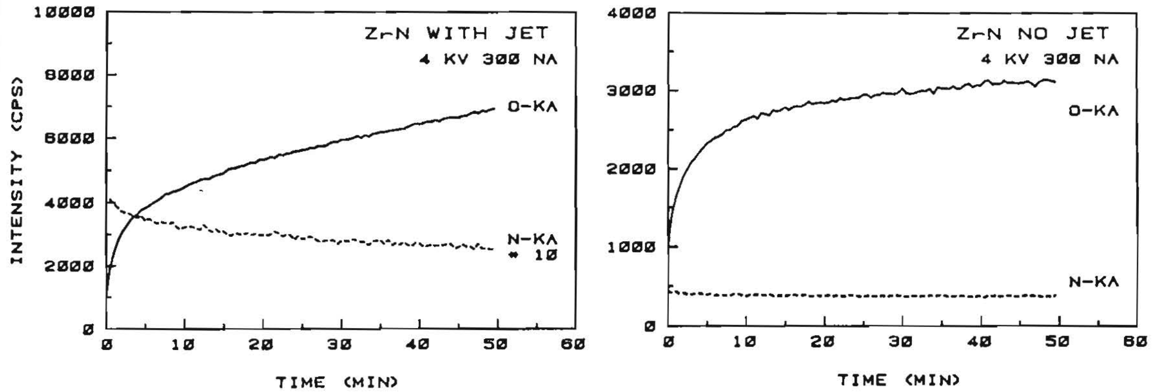

Fig. IV.2 In situ oxidation phenomena on ZrN at 4 kV, 300 nA. Left: With air jet; Right: Without air jet. Note the differences in vertical scales for N-Kα and O-Kα in the left hand figure. Oxygen on LDE; Nitrogen on STE

Fig. IV.2 (left) shows the incredibly high oxidation rate of the ZrN specimen at 4 kV when the air jet is used. Not only does the Oxygen count rate increase very fast but, what is worse, the Nitrogen count rate decreases seriously at the same time leading to a loss in N-Kα counts of more than 50 % after 1 hr. The effects were worst on HfN, ZrN, TaN and Ta_2N (in decreasing order). Fig. IV.3 shows the extremely fast oxidation of a HfN specimen.

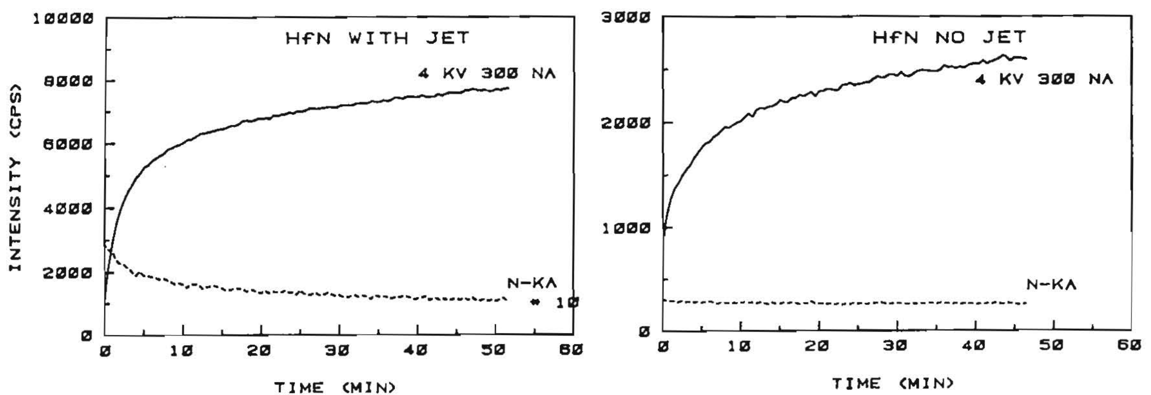

Fig. IV.3 In situ oxidation of HfN at 4 kV, 300 nA
Left: With air jet; Right: Without air jet

The effects we observed were strongly dependent upon voltage and completely explained the erratic behaviour of the k-ratios with voltage for ZrN.

Next, we carried out a number of experiments without the air jet. To our astonishment we found that, in principle, exactly the same phenomena occurred in these sensitive nitrides, although to a lesser extent (See Figs. IV.2 and IV.3). Fortunately, an increase in O-Kα count rate does not necessarily mean a noticeable loss in N-Kα intensity. The stable N-Kα count rates in these cases indicate, by the way, that the self-cleaning action of the well-focused electron beam is apparently sufficient to prevent appreciable build-up of Carbon in a 1 hr period.

In extremely sensitive nitrides we found that a measuring time of 10-30 s can be sufficient to double the Oxygen signal from these materials without necessarily changing the Nitrogen signal. Of course, the effects could be much worse still on the pure elements Ti, V, Zr, Nb, Hf and Ta.

A most peculiar observation was that while the oxidation effects were dramatic on ZrN and HfN, they were almost an order of magnitude less on chemically strongly related nitrides like TiN and VN, in which one would expect a quite similar behaviour. That this is apparently not the case may point to the formation of a closed oxide skin on nitrides like TiN, which prevents to a large extent a further oxidation of the specimen.

From Table IV.1 it becomes clear, though, that literally <u>every</u> nitride specimen is oxidized under the electron beam, even without the air jet. The relatively poor vacuum conditions in commercial microprobes, as compared to typical surface-analytical instruments, are most likely to be blamed for these Oxygen contamination phenomena.

The practical impact of our observations is that it is highly unlikely that realistic measurements of low levels of Oxygen in sensitive materials like Ti, V, Zr, Hf and Ta can ever be made in a straight-forward way. A somewhat sad conclusion seems to be that it will be very difficult to fight these phenomena except by a very expensive improvement in the vacuum conditions, which would make the routine use of the microprobe much more difficult.

We can conclude this paragraph with the remark that it is very difficult to give hard and simple rules about Oxygen (and Carbon) contamination and whether or not it is advisable to use an air jet. In each individual case one should carefully check whether the use of an air jet introduces adverse side-effects for the element to be determined. We still hold the opinion that in the majority of cases there is nothing to be afraid of, with an exception of the cases discussed before. In any case, we repeated our measurements without air jet on all suspect nitride specimens. Moreover, we have verified experimentally that no noticeable losses in N-Kα intensity took place during the time required for the integral recording of our Nitrogen spectra.

TABLE IV.1

Oxygen count rates, related to the initial count rates, on nitride specimens, as a function of time. (+ with air jet; - without air jet). 4 kV 300 nA

Compound		TIME 1 min	5 min	50 min
AlN	+	1.56	1.95	2.03
	-	----	1.12	1.15
Si_3N_4	+	1.39	1.37	1.39
	-	1.23	1.98	2.10
TiN	+	1.18	1.25	1.39
	-	1.12	1.18	1.22
Ti_2N	+	1.13	1.20	1.25
	-	1.08	1.06	1.04
VN	+	1.02	1.02	1.04
	-	1.01	1.02	1.03
V_2N	+	1.05	1.07	1.14
	-	1.00	1.02	1.06
CrN	+	1.12	1.39	2.02
	-	0.99	0.99	1.06
Cr_2N	+	1.02	1.17	1.76
	-	1.08	1.12	1.25
Fe_4N	+	1.18	1.27	1.46
	-	1.04	1.07	1.18
ZrN	+	2.42	3.80	6.84
	-	1.78	2.54	3.39
Nb_4N_3	+	1.19	1.20	1.25
	-	1.02	1.04	1.10
Nb_2N	+	1.00	1.03	1.04
	-	1.00	0.99	1.05
Mo_2N	+	0.94	1.02	1.16
	-	1.04	1.02	1.08
HfN	+	3.05	5.53	8.13
	-	1.56	2.16	3.17
TaN	+	1.80	2.87	4.81
	-	1.65	1.68	1.93
Ta_2N	+	1.18	1.63	3.21
	-	1.06	1.05	1.07

IV.2 New procedures for the analysis of Nitrogen in the presence of Titanium

Quantitative analysis of Nitrogen in Titanium-containing compounds has always been a real problem in the life of many microanalysts. This problem is caused by the severe overlap of the Ti-$\ell\ell$ (wavelength 31.4 Å) and N-Kα (31.6 Å) emission peaks which add up to one single peak in which the separate contributions cannot be discerned with the usual wavelength-dispersive analyzer crystals. However, with the growing interest in Ti-N based materials (e.g., wear-resistant coatings), there is an increasing demand for a procedure capable of separating the Ti-$\ell\ell$ and N-Kα contributions; the final goal is, of course, the accurate quantitative analysis of Nitrogen.

In the past, several methods for peak separation have been proposed[27]. They can be qualified either as ratio methods or as deconvolution techniques. The ratio methods are based on the assumption that there is a fixed ratio between the integral intensities of either Ti-Kα and Ti-$\ell\ell$ or Ti-Lα and Ti-$\ell\ell$ and that these ratios, once they are known from measurements on a pure Ti standard, can also be applied to the Titanium in the Ti-N compound. The deconvolution techniques, on the other hand, do not require the ratios of Ti peaks in the standard, and are, in fact, multiple least squares fitting techniques[28] which are at present quite common in energy-dispersive X-ray microanalysis systems.

In the following sections we first give an analysis of the methods proposed so far in literature and discuss their limitations. Next we discuss the principles of the new method we introduce, followed by a few applications on a number of examples.

IV.2.1 Analysis of existing methods

In the so-called ratio methods the ratio Ti-Lα/Ti-$\ell\ell$ seems to be used with preference because 1) only one spectrometer (with a conventional lead-stearate crystal) has to be used and 2) the intensities of Ti-Lα and Ti-$\ell\ell$ are more or less comparable. Now, one of the prerequisites for this method to work is that the ratio in question is indeed the same in Ti-N specimen and Ti standard and this, in turn, is dependent upon the question wether both wavelengths are equally strongly absorbed in Ti as well as in N. However, as Fig. IV.4 shows, this is evidently not the case.
The presence of the N-K absorption edge causes a pronounced difference in the mac's between Ti-Lα and Ti-$\ell\ell$. Although these values are quite similar (3320 and 4300, respectively) in pure Titanium for a start, the value for Ti-Lα increases to approximately 25000 in pure Nitrogen whereas that for Ti-$\ell\ell$ in Nitrogen is lowered to 1800. This means that a 14-fold increase in the ratios of the mac's occurs. Of course, this is an extreme case for extremely high Nitrogen contents, for which the effects will be worst (assuming that Henke's mac's are correct). Yet it is a good example to

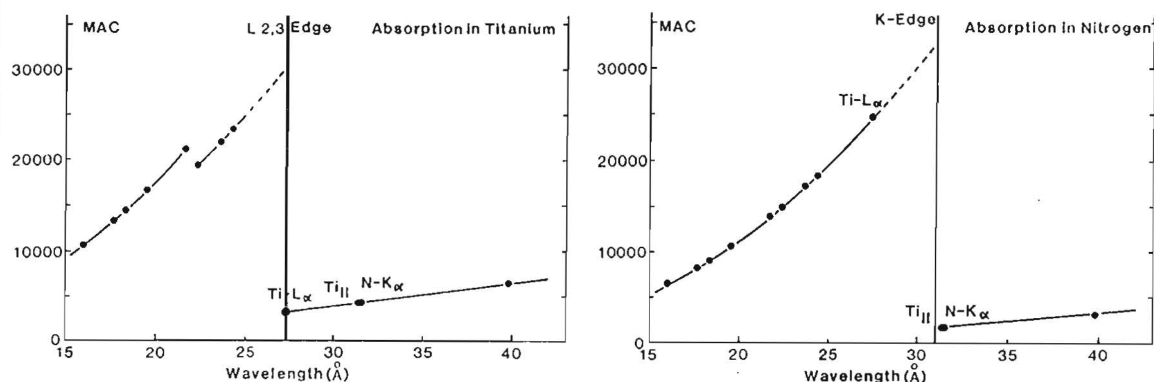

Fig. IV.4 Variation of mass absorption coefficient with wavelength in a) Ti and b) N according to Henke et al[10]. Note that mac and wavelength are plotted on a linear scale.

demonstrate the inherent dangers in the ratio method as long as this ratio is blindly taken for granted. Perhaps the calculation of the Ti-ll contribution from the known Ti content in the sample, derived from the Ti-Kα signal, would provide a better alternative. However, the main problem in these matters is that the Ti-ll peak is so close to the N-K absorption edge (or perhaps even partly in it) that it is simply unlikely that the contribution of the Ti-ll peak can be decribed by a single k-ratio over the complete relevant wavelength range. The extremely strong variation of the mac over the absorption edge is bound to produce a strong variation of k-ratio with wavelength.
The same remarks apply to the variation in the background, which must exhibit a jump more or less, followed at increasing wavelength by a strong variation. The whole picture is not unlike the inverse of Fig. IV.4 (b). The effects discussed so far are also the reason for the strong asymmetry which is usually visible in the combined Ti-ll + N-Kα peak.

For the same reasons it is not a priori clear why the deconvolution techniques should work. These are invariably based on the assumption that the background varies in a smooth and monotonous way with energy or wavelength. The presence of an absorption edge with its typical discontinuity might well invalidate the basic assumptions of these techniques. Moreover, for the reasons discussed above, it is unlikely that a single k-ratio can be applied over a wide region in wavelengths in which a strong and discontinuous variation in mac's and, consequently, in k-ratios occurs. At

best, such an average k-ratio is based on some kind of wavelength-averaged mac and will thus never produce quite satisfactory fits over the complete relevant wavelength range. On top of that these techniques rely on the tacit assumption that no peak shifts and/or peak shape alterations occur between standard and specimen. Since we are dealing here with long-wavelength radiations from the L-shell of Ti which might easily be affected by the nature of the chemical bond it is questionable whether these assumptions are valid.

If the fine structure of the N-K edge were known, one could perhaps model the background and calculate the Ti-ιι contribution as a function of wavelength from the known Ti content, using the Ti-Kα signal. As long as this fine structure is not accurately known, however, it is rather unlikely that such calculations, based on a single wavelength weighted mac for Ti-ιι, can ever be completely successful.

In our opinion, the reason that such methods may have appeared to work satisfactorily in the past is that the homogeneity region of a compound like TiN is extremely wide at high temperatures[24,25], ranging from 11 to approximately 22.6 wt % Nitrogen, with the result that almost any answer between these limits can appear quite acceptable. According to our own experiences in this system and the very similar Ti-C system it is usually extremely difficult to find the true composition. Even when a reliable chemical analysis is available, there is always the danger of discrepancies due to variations in compositions on a micron scale and the ever lasting controversy between bulk analytical techniques like chemical analysis and microanalytical techniques like EPMA.

As a result of the considerations so far it is not impossible that the methods hitherto used lead to systematic errors in the Nitrogen content, which probably go unnoticed because the results are usually not in contradiction with the phase diagram.

IV.2.2 The new method

The method we propose here is mainly based on the consideration that although the Ti-ιι and N-Kα peaks strongly overlap, they do not coincide completely. Hence, the combined peak must inevitably be broader than that of either of the contributors. If we could find access to the true width of the N-Kα peak, or rather the APF, in Ti-N compounds, the problem would be reduced to finding the proper amount of Ti-ιι intensity that has to be stripped (in an integral fashion) from the combined peak in order to produce a residual N-Kα peak with the specified APF. Unfortunately, the APF is not known for Ti-N compounds and cannot be measured directly either for obvious reasons. However, there is a way out of this dilemma : For one thing we know from our experiences in a large number of nitride specimens that the effects of peak shape alterations in the N-Kα peak are very

much smaller than in B-Kα or even C-Kα peaks. Individual APF values (see further on in this Chapter) never differ by more than 10 % from unity. Besides, if the APF values for nitrides of neighbouring elements in the periodic system like V, Cr and Fe are extrapolated toward Ti (like they could be in corresponding boride and carbide systems), then the expected value for Ti-N compounds will most probably be between 0.95 and 1.0. Moreover, we have shown that within the limits of experimental accuracy the APF can be regarded as independent of accelerating voltage.

With these findings in mind and a couple of Ti-N specimens of known compositions it is possible to start an iterative procedure aimed at obtaining the true APF. It goes without saying that in this procedure the necessary attention is paid to the presence of the N-K absorption edge. We have, therefore, decided to treat the wavelength region of interest in two distinct intervals: one interval on the left (short wavelength) side of the edge; the other on the long wavelength side. The k-ratios on the left side will be henceforth denoted by the subscript $_l$, those on the right hand side by $_r$.

The first step in the procedure is, of course, to establish the position of the N-K absorption edge for the STE and LDE crystals. Although this seems to be a very trivial problem, knowing the energy of the edge (400 eV or 30.99 Å) and the 2d-spacings of the crystals, this turned out to be one of the first major problems we encountered. In order to eliminate the effects of mechanical deviations in the spectrometer we decided to calibrate the 2d-spacing of the STE crystal very carefully in the vicinity of the N-Kα peak. To this end we selected a number of accurately known wavelengths and measured their peak positions very carefully. From the known wavelengths and the observed peak positions (in mm in our microprobe) it is then easy to calculate the apparent 2d-spacing for the wavelength in question. To our astonishment we found not only a rather strong variation in apparent 2d-spacing in the linear range between 75 and 85 mm: from 99 to 100.50 Å, but also a pronounced dip between 87 and 88 mm, which exactly corresponds to the anticipated position of the absorption edge (see Fig. IV.5). It is, therefore, not at all clear which apparent 2d-spacing is to be used for the wavelength region of the N-Kα peak: should it be the value of 100.50 Å (dashed line in Fig. IV.5 connecting the measured values for Cu-$_{ll}$ 2nd order and Al-Kα 4th order) or the minimum value in the dip (99.4 Å), or perhaps a value in between? After a few trial and error runs with our new procedure in which the resulting APF value was checked against the anticipated one (between .95 and 1) we finally adopted a value of 99.4 Å for STE and of 59.7 Å for LDE. This guaranteed at least that the N-Kα and Ti-$_{ll}$ peaks came more or less at the expected wavelengths of 31.4 and 31.6 Å, although perfect agreement with the reported wavelengths[10] could never be completely obtained.

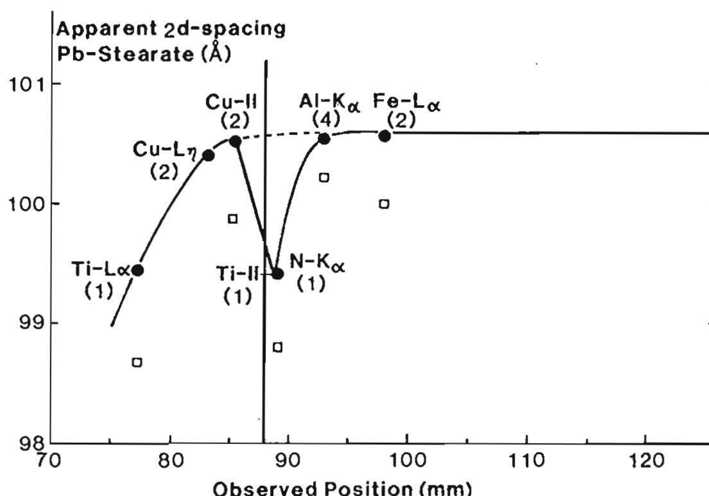

Fig. IV.5 Variation of apparent 2d-spacing of the STE crystal with observed peak position for a number of wavelengths in the range of the N-Kα peak. Solid dots represent our own measurements; open squares those by a collegue on a different microprobe, showing essentially the same peculiar effects in the vicinity of the N-K absorption edge.

Until now we have never been able to explain the peculiar phenomena from Fig. IV.5. However, when the measurements were repeated on a different microprobe at our request (by Ir. D. Schalkoord at Delft University of Technology, The Netherlands) essentially the same results (open squares in Fig. IV.5) were obtained, although at a slightly different numerical level. A conspicuous feature in Fig. IV.5 is that the first order reflections apparently produce the lowest 2d-spacings while the higher-order reflections invariably lead to closely corresponding, but much higher values which agree with the 2d-spacings appropriate for B-Kα and C-Kα radiations. It was not possible to run a similar test for the LDE crystal because of the very effective suppression of higher-order reflections by this crystal. In this case the 2d-spacing was simply obtained from the observed position of the N-Kα peak.

The next step in our procedure is the recording of the Ti-Lα and Ti-ll peaks in a pure (and freshly polished) Titanium standard in an integral fashion. Then exactly the same wavelength region is scanned on the Ti-N specimen under identical conditions. From the known Ti-content the k-ratio (k_1) for Ti-Lα is calculated and the left hand side of the Ti-spectrum up to the N-Kα edge is multiplied by this factor and stripped from the unknown spectrum. Alternatively, if the Ti-content is not known, which will usually be the case, this factor can easily be determined by trial and error: the disappearance of the Ti-Lα peak in the spectrum is an easy measure for success.

Next, the right hand side of the unknown spectrum is processed. The Ti reference spectrum (from the N-K absorption edge on) is multiplied by a factor k_r which is varied in steps of, say, 0.1 between 0 and 1 and after each step a fraction k_r of the reference spectrum is subtracted from the unknown spectrum. The residual peak is subsequently processed in order to find the APF and the Area (or integral) k-ratio AKR, with respect to the particular Nitrogen standard used. Both values are then plotted as a function of k_r.

In the first iteration we assume that the AKR should be equal to the calculated AKR for N-Kα using the mac's of Henke et al[10]. It is then easy to find the corresponding APF value for which this equality occurs. If this procedure is repeated for several accelerating voltages and preferably for at least two different specimens of known compositions, it is possible to establish whether the APF is indeed a constant and, if this is the case, what its exact value is. Once this value is known the procedure can be reversed and from the plots of APF and AKR vs k_r it is easy to find the correct AKR value for a specified APF value. The experimentally obtained k_r values could even be used to make rough estimates about the wavelength-weighted mac for $Ti-_{ll}$ in Nitrogen. It must be admitted that we too were obliged to apply only one (averaged) k_r value for the complete long-wavelength side of the N-K edge and to treat the edge itself as a mathematical step function, which is most probably not correct. Unfortunately, as long as the fine structure of this edge is not known, there seems to be no better way to solve the problem. At least we made a clear distinction between both sides of the edge. It must be anticipated, though, that the idealized step function, representing the edge, will introduce a discontinuity in the resulting N-Kα spectrum, precisely at the location of the edge.

For the spectral measurements two Ti-N compounds were at our disposal :
One specimen was a 0.5 mm thick near-stoichiometric TiN specimen of deep reddish golden colour, prepared by Chemical Vapour Deposition; the other was a Ti_2N specimen prepared out of a diffusion couple $Ti-N_2$, heated for 89 hr at 1400 ^{0}C. The particular Ti_2N composition was exposed by a process of grinding and polishing in a plane perpendicular to the direction of diffusion. Later on, a cross section of the same diffusion couple containing the α-Ti (N) solid solution, Ti_2N and TiN in successive layers, was used in order to test the devised procedure. Such a diffusion couple is of invaluable interest for this particular type of work because it provides the almost unique possibility to find a smooth, consistent and unambiguous variation in the Nitrogen content, contrary to a number of bulk specimens of doubtful homogeneity and with often contradicting chemical analyses.

The compositions of the calibration alloys and the Nitrogen concentration profile in the diffusion couple were determined by measuring the Ti-Kα signal using a near-stoichiometric TiC alloy, in equilibrium with free graphite, as a Ti standard. The Nitrogen measurements themselves were performed relative to a massive Cr_2N standard (Batch # 1).

The Nitrogen spectra for the two calibration alloys were recorded at nine different accelerating voltages between 4 and 30 kV. In a number of cases spectra were recorded simultaneously with the STE and LDE crystals. In each run reference spectra from pure Ti were also taken. The measurements in the diffusion couple were all carried out at 10 kV.

Fig. IV.6 shows the typical variation of APF and AKR with k_r for the near-stoichiometric TiN compound at 10 kV for both STE and LDE crystals. The calculated AKR in this case is 2.386 and the value of k_l used is 0.437. These numbers would lead to an APF value for STE of 0.974 at a k_r value of 0.760. For LDE, in turn, values of 0.980 for the APF and 0.698 for k_r are obtained.

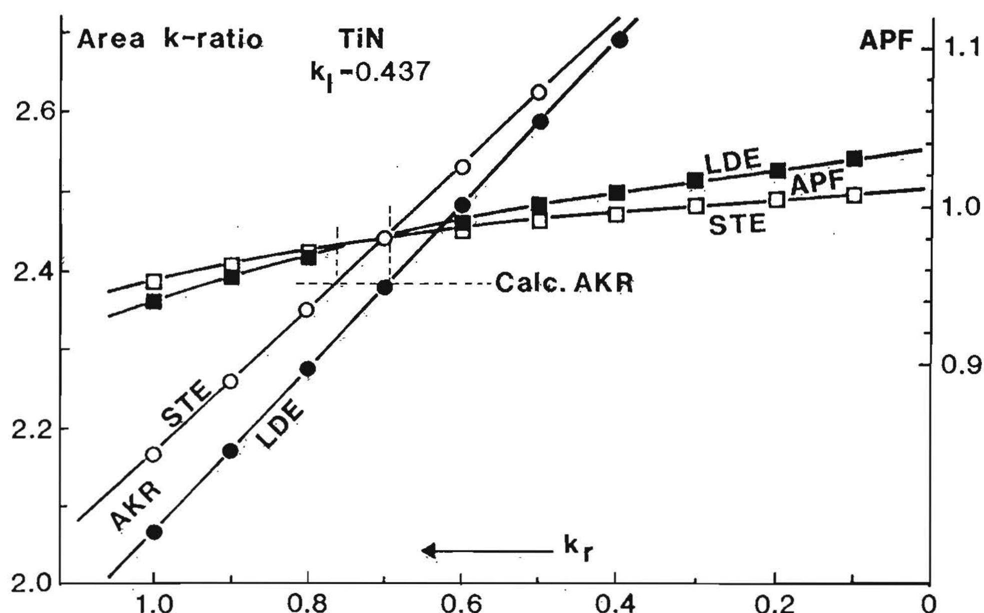

Fig. IV.6 Variation of Area k-ratio (AKR) and Area-Peak factor (APF) with k_r (average k-ratio for Ti-ll for long-wavelength side of N-Kα edge) for Stearate and multilayer (LDE) crystals at 10 kV and a k_l value of 0.437. TiN specimen : 22.50 wt % N. Nitrogen standard: Cr_2N (Batch # 1)

The same procedure has been repeated numerous times at voltages between 4 and 30 kV and it was found that the APF values could indeed be considered as a constant, independent of accelerating voltage. This is demonstrated in Fig. IV.7 (bottom halves).

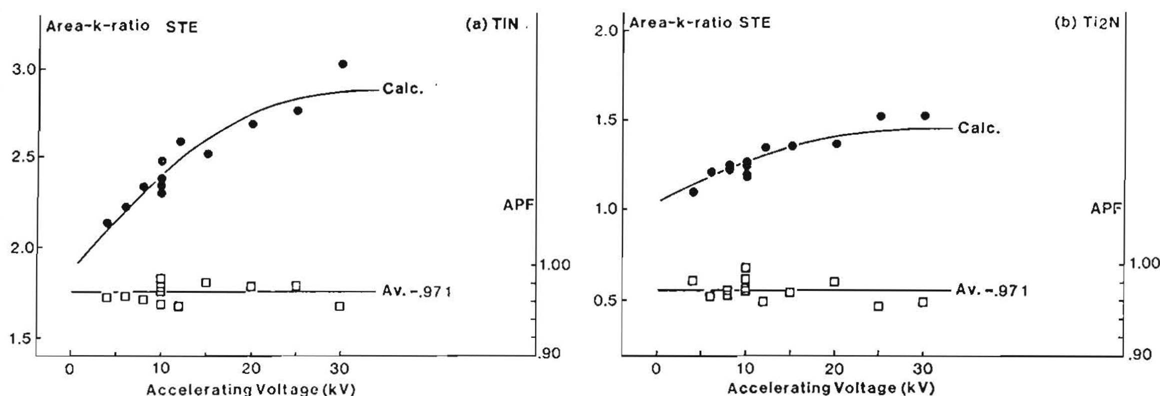

Fig. IV.7 Variation of AKR (relative to Cr_2N) and APF with accelerating voltage for TiN (left, 22.50 wt % N) and Ti_2N (right, 11.84 wt % N). Stearate crystal.

The average APF value for the STE crystal was 0.971 for both calibration alloys. For the LDE crystal, which was obtained only in a much later stage of the work, a number of measurements at 10 kV led to a value of 0.980. This result seems to be in good agreement with many of our observations in Carbon, Nitrogen and Oxygen analyses where the LDE crystal always showed less sensitivity to peak shape alterations as a result of its poorer spectral resolution. Consequently, its APF values are usually closer to unity.

Once the APF values are known, the procedure can be reversed and plots like Fig. IV.6 can be used to find the "measured" AKR starting with the specified APF. As a result the top halves of Fig. IV.7 are obtained, which show the variation of integral k-ratio with accelerating voltage. Each point represents in fact the average for a large number of measurements taken over a period of several months. The excellent agreement between expected and "measured" k-ratios demonstrates that our procedure is obviously successful and that deviations rarely exceed 5 % relative, which is rather surprising in view of the large amount of spectral manipulations involved.

Fig. IV.8 gives a graphical representation of the complete procedure for the LDE crystal at 10 kV applied to the near-stoichiometric TiN specimen. Spectrum # 1 shows the combined Ti-ll + N-Kα peak. Spectrum # 3 is the Ti reference spectrum, which is converted into spectrum # 4 by multiplying the portions on the left and right hand sides of the N-K edge with the appropriate k_l and k_r factors, respectively. Spectrum # 2 represents the resulting N-Kα spectrum after spectrum # 4 has been stripped from spectrum # 1.

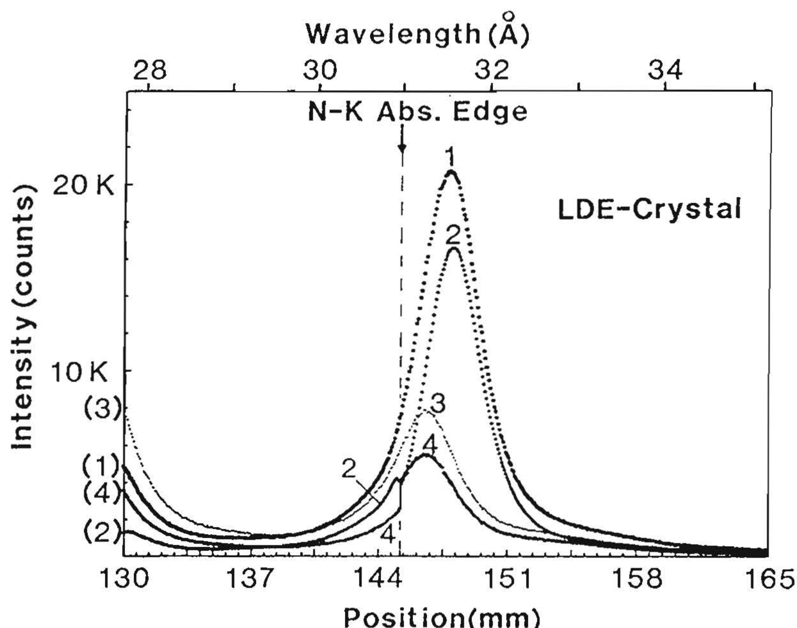

Fig. IV.8 Graphical representation of our procedure for separating the Ti-ll and N-Kα contributions from the combined peak for the LDE crystal on a near-stoichiometric TiN specimen at 10 kV. Spectrum # 3 is the Ti reference spectrum, which is first converted into spectrum # 4 by multiplication with the appropriate k_l and k_r factors and then stripped from spectrum # 1 to yield finally spectrum # 2.

The shift in the peak between spectra # 1 and # 2 corresponds with the shift toward the true peak position of the N-Kα peak after the subtraction of the Ti-ll contribution. It is clear, though, that the final spectrum shows a slight discontinuity at the position of the N-K edge. As we have mentioned before, this is the expected and logical consequence of applying a mathematical step function representing the edge. Beyond any doubt, the true edge will have a much more complex shape. However, as long as its exact shape is not known, there seems to be little point in using several mathematical functions because one procedure would be as arbitrary as another.

The k_r values which are found experimentally (see Fig. IV.9) strongly suggest that the mac for Ti-ll radiation in Nitrogen is somewhat higher than suggested by Henke et al[10],

which in turn means that this particular wavelength is at least partially located in the absorption edge.

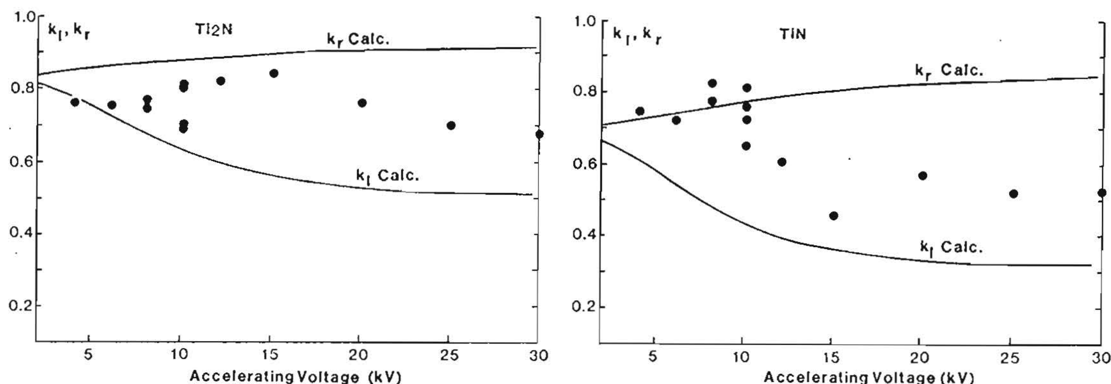

Fig. IV.9 Variation of k_l and k_r with accelerating voltage for Ti_2N (left) and TiN (right). Solid curves are calculations based on Henke et al's[10] mac's for Ti-Lα and Ti-L_l in N; dots represent experimental data. Stearate crystal; beam current at all voltages 300 nA.

The deviations are most pronounced in the case of TiN where, as a result of the higher N-content than in Ti_2N, the presence of the N-K edge becomes more prominent.

A final test of our procedure was carried out at 10 kV on the diffusion couple Ti-N_2 (89 h, 1400 ^{0}C). After diffusion this couple exhibited a more than 500 μm wide diffusion zone consisting of TiN (major part) and Ti_2N covering a remaining nucleus of α-Ti(N) solid solution. From the known concentration profile a number of locations, showing sufficiently significant changes in the Nitrogen content, were selected and integral spectra were recorded on these spots (Run # 1).

After completion the experiment was repeated (Run # 2) with the specimen rotated over 180 deg. with respect to the LDE spectrometer in order to estimate the effect of the strong rounding-off that inevitably takes place due to prolonged polishing at the interface mounting resin/TiN.
The results for both runs for the LDE crystal are shown in Fig. IV.10.

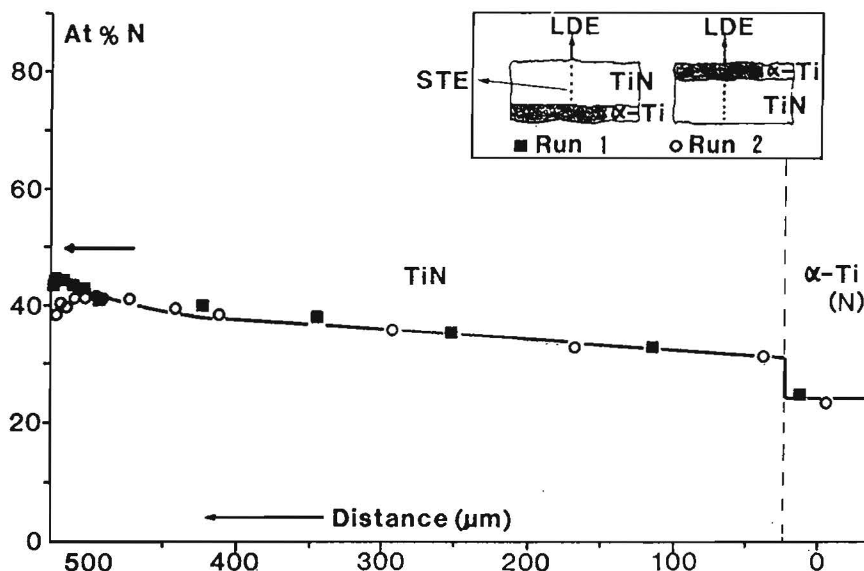

Fig. IV.10 Nitrogen concentration profile in diffusion couple Ti-N_2 (89 h 1400 ^{0}C) as established by Ti-Kα measurements (solid line) and our new procedure for Nitrogen using the LDE crystal. Squares represent results for run # 1; circles those for run # 2. The arrow shows the experimental result for the near-stoichiometric TiN compound in run # 2. Accelerating voltage 10 kV. Beam current 300 nA. Experimental configurations for both runs are shown in the inset.

The strong rounding-off effect is clearly visible in run # 2, where the X-rays leaving for the LDE spectrometer have the poorest chance of escaping close to the mounting resin. Nevertheless, the agreement between Ti and N measurements can be called striking, certainly for locations more than 20 μm away from the mounting resin. In fact, this conclusion holds throughout the complete diffusion zone, including the α-Ti(N) solid solution. At the same time the result for the near-stoichiometric TiN alloy (arrow in Fig. IV.10) agrees closely with the nominal composition, thus demonstrating that the maximum nitrogen content is not yet attained at the outside of the diffusion couple.

The results for the STE crystal were quite acceptable too, although they were generally on the low side, especially for the α-Ti(N) solid solution. In the latter case this may be the result of the tacit assumption that the APF used so far also applies to this particular phase, although strictly speaking it is not really a Ti-N compound but rather a solid solution and as such its APF value may be somewhat different: a value of 1.0 would give results comparable with those of the LDE crystal. Besides, there seems to be some evidence that the APF value for STE at 10 kV is possibly somewhat higher than the average value adopted (Fig. IV.7). In any

case the LDE crystal is definitely less sensitive to peak shape alterations due to its poorer spectral resolution and as such it is not capable of discerning such subtle details.

A few remarks are in order here on the practical aspects of the method we propose. Because the whole method is strongly based on factors such as spectral resolution, it must be clear that all parameters in the microprobe affecting this spectral resolution (Pulse height analyzer conditions, counter slit, etc.) must always be adjusted extremely carefully and reproducibly. In the same way the background limits must always be exactly the same if the highest degree of reproducibility is to be achieved. Furthermore, it is strongly advisable to run a check on a calibration specimen before or after the measurements on an unknown specimen, if only to be warned of sudden changes in the equipment or settings.

We realize very well that the method we propose here will be considered time-consuming and perhaps even complex. Unfortunately, in our opinion, there is little hope that there will ever be an instant solution and a "push-button" operation for the complex problem at hand.

Finally we shall briefly discuss the results of the multiple-least-squares fitting technique[28] when applied to a number of our spectra. In fact, this is the program currently in use in EDX software. In a first effort, the results of which were reported before[29], a very sophisticated version of such a program was used (TRACOR Northern), in which the first and second derivatives of the peaks were used in order to correct for possible peak shifts and peak shape alterations, respectively.
Furthermore, the digital top hat filter[28] was adapted to the better spectral resolution of a WDS spectrometer. As we reported before the results of this procedure were rather disappointing: 10 to 25 % too low Nitrogen contents were found and at that time we judged, therefore, that this particular technique was unsuited to this specific problem.

Quite some time later, however, when we were trying to analyze substantially lower Nitrogen contents than in the diffusion couple of Fig. IV.10, we happened to test a much simpler version of a multiple-least-squares program (TRACOR Northern, "Super ML", version XML-7k'/30) on the spectra of Fig. IV.10, with surprisingly good results. In this particular program the first and second derivatives are not taken into account and the filter width had the standard setting of 150 eV, which corresponds with 0.6 mm (0.2139 Å) for the STE crystal and 1.05 mm (0.2243 Å) for the LDE crystal. The results obtained with this Super ML fitting program on the spectra from the diffusion couple are compared with the results from our new APF procedure in Table IV.2

TABLE IV.2

Results of the Super ML fitting procedure as compared to those of our new APF procedure on the spectra from the Ti/N_2 diffusion couple heated for 89 h at 1400 ^{0}C (See Fig. IV.10). AKR is the Area k-ratio for N-Kα relative to Cr_2N. χ^2 is the statistical measure of success for the digital fit; a value close to 1 indicates an almost ideal fit. Run # 2.

	SUPER ML FIT				APF PROCEDURE	
	STE		LDE		STE	LDE
At % N	χ^2	AKR	χ^2	AKR	AKR	AKR
23.3	2.36	0.848	4.05	0.910	0.774	0.866
31.4	3.62	1.235	5.22	1.258	1.184	1.252
32.7	4.88	1.277	5.51	1.344	1.193	1.318
35.9	4.67	1.420	6.43	1.476	1.394	1.492
38.4	5.61	1.583	7.29	1.650	1.530	1.632
39.5	6.56	1.611	7.25	1.712	1.716	1.696
41.0	5.98	1.742	7.97	1.794	1.710	1.788
41.2	6.82	1.829	8.32	1.843	1.766	1.798
41.8	7.03	1.818	7.71	1.837	1.766	1.836
41.2	6.83	1.834	7.60	1.844	1.772	1.803
41.0	6.39	1.862	7.41	1.849	1.778	1.788
42.2	6.50	1.858	8.65	1.862	1.764	1.860
42.4	6.40	1.908	8.74	1.863	1.874	1.876
41.4	6.27	1.913	8.29	1.823	1.812	1.810
42.7	8.15	1.923	9.88	1.823	1.867	1.896

For higher N-contents the effects of rounding off at the edge became noticeable. The results for the near-stoichiometric TiN calibration specimen were as follows:

At % N	STE χ^2	STE AKR	LDE χ^2	LDE AKR	APF STE AKR	APF LDE AKR
49.6	7.76	2.388	9.87	2.520	2.350	2.368
49.6	7.76	2.457	10.71	2.502	-----	-----
49.6	8.80	2.428	10.83	2.522	-----	-----
49.6	8.39	2.439	10.97	2.539	-----	-----

The general conclusion that can be drawn from Table IV.2 is that the agreement between the results of our new APF procedure for the STE and LDE crystals is quite satisfactory, with an exception perhaps for the lowest Nitrogen contents. A very conspicuous feature is the more or less monotonous increase in the χ^2 value with increasing Nitrogen content for both the STE and the LDE crystals when the Super ML fit procedure is used. It is interesting to point out in this respect that after the subtraction of the Ti-ll and N-Kα peaks in the proper ratios the background on LDE showed negative areas on both sides of the N-Kα peak position while the central area was still positive. This effect was observed

over the whole range in Nitrogen contents. For the STE crystal, on the other hand, this was only found for the higher N-contents. These findings seem to point to peak shape alterations and it is, therefore, all the more surprising that the more sophisticated programs, in which such effects are taken into account, would yield so much poorer results. Perhaps, the continuous increase in χ^2 values with increasing Nitrogen content can be interpreted as a sign of the N-K absorption edge becoming more and more pronounced, as we anticipated before.

The somewhat surprising conclusion of this paragraph can be that it is apparently posssible to do fairly accurate quantitative analysis (within 5 % relative) of Nitrogen in the presence of Titanium with both our new procedure as well as the multiple-least-squares fitting techniques, in spite of the poor χ^2 values that are obtained in the latter cases. Possibly, a process of error compensation takes place in the final fit and the resulting negative areas in the background may be compensated by a central positive area.

IV.2.3 Quantitative analysis of low Nitrogen contents in the presence of Titanium

So far we had not been able to test our new procedure on Nitrogen contents well below 24 at % because this was approximately the lowest level present in the diffusion couple (α-Ti(N) solid solution). Some time in 1988, however, we were asked to analyze two Ti alloys, containing also V and Al, which had been nitrided (by laser- and plasma-nitriding procedures, respectively) to very large depths (more than 300 μm, judging from the changes in microstructure). A preliminary investigation, using the Ti-Kα, V-kα and Al-Kα signals, revealed that only very thin TiN and Ti_2N layers had been produced (in the order of a few μm) and that by far the major part of the extended diffusion zone contained Nitrogen levels well below 10 at % .

We soon found out that our new APF procedure could only be applied to the TiN and Ti_2N layers (with great success) and that when the Nitrogen level dropped below approx. 15 at % the resulting N-Kα peak really became too low for an accurate measurement of the APF. The Super ML fit program, (in its simplest form) however, was indeed able to cope with the problem as Table IV.3 shows. Only the results for the LDE crystal have been given here; those for the STE crystal were much less satisfactory, presumably due to the interference of the 4th order Al-Kα peak and small peak shifts.

TABLE IV.3

Results of the Nitrogen analyses in a laser-nitrided Ti(V, Al) alloy using the Super ML multiple-least-squares digital fitting technique on spectra recorded with the LDE crystal at 10 kV and 300 nA.

Distance from surface (μm)	χ^2	AKR N-Kα	Wt % N	At % N
5	2.98	0.4440	4.17	12.95
5	2.88	0.3961	3.72	11.67
25	2.76	0.2577	2.42	7.81
25	2.40	0.3010	2.82	9.04
50	2.94	0.2713	2.55	8.20
50	2.68	0.3406	3.20	10.15
75	2.47	0.2733	2.56	8.26
75	2.46	0.3420	3.21	10.19
100	2.85	0.2946	2.77	8.86
100	2.42	0.2844	2.67	8.57
150	1.88	0.2302	2.16	7.01
150	2.12	0.2921	2.74	8.79
200	1.79	0.2181	2.00	6.66
200	2.10	0.2910	2.73	8.76
300	1.93	0.0414	0.39	1.32
300	1.85	0.0000	0.00	0.00
400	1.81	0.0160	0.15	0.51
475	1.86	0.0146	0.14	0.47
550	1.86	0.0194	0.18	0.62
760	2.02	0.0137	0.13	0.44

It is obvious from Table IV.3 that the Super ML program is able to detect very low levels of Nitrogen indeed, down to less than 0.2 wt %, which can be called really impressive. Also the fact that at long distances from the surface sometimes zero values are found gives a lot of confidence in the technique. It is interesting to point out, though, that the same trend is present here as in Table IV.2 : there is a definite correlation between the magnitude of the χ^2 value and the nitrogen concentration. The surprisingly good quality of the fits for low Nitrogen levels is not only expressed in very low χ^2 values in Table IV.3 but can also be judged visually from Fig. IV.11 where all steps of the fitting procedure are graphically represented for a composition of 1.37 wt % N in the other (plasma-nitrided) alloy.
It can be seen that after the subtraction of the Ti-ll peak in the proper ratio a remaining N-Kα peak is visible with its top at the correct position. After the subtraction of this N-Kα peak an almost ideally smooth background is obtained which shows only extremely weak signs of forming small dips on both sides of the N-Kα peak. These dips become much more pronounced at much higher Nitrogen levels, as we mentioned before. This is demonstrated in Fig. IV.12 for the case of the near-stoichiometric TiN calibration specimen.

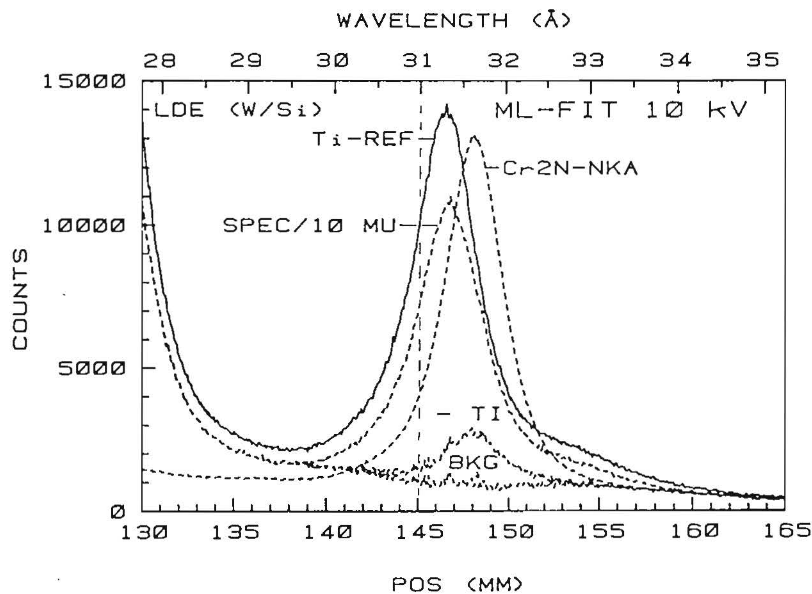

Fig. IV.11 Graphical representation of the Super ML fitting procedure applied to the spectra recorded from a location 10 μm away from the surface in a plasma-nitrided Ti(V,Al) alloy. LDE crystal; 10 kV, 300 nA, 500 steps, counting time 3 s/step. Area k-ratio N-Kα relative to Cr_2N 0.1458, corresponding to 1.37 wt % Nitrogen (4.52 at %); χ^2= 1.89

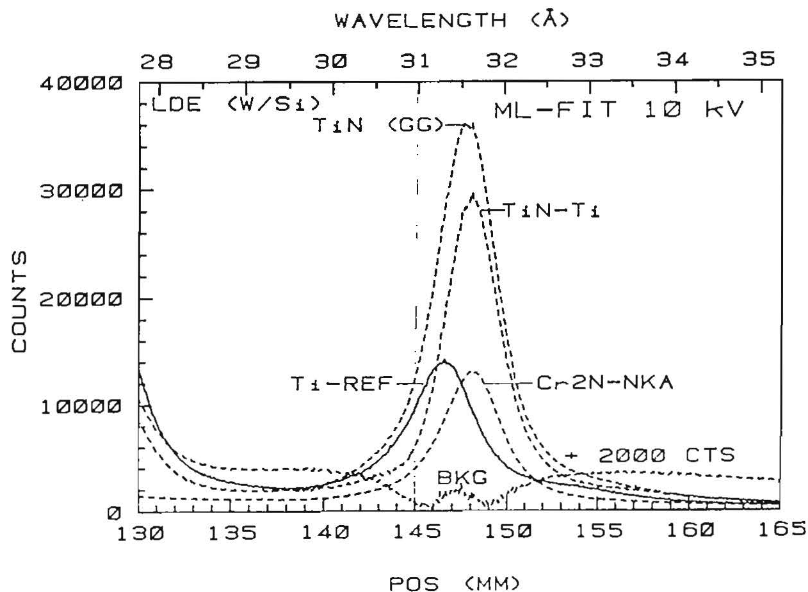

Fig. IV.12 Graphical representation of the Super ML fitting procedure applied to the spectra recorded with the LDE crystal on the near-stoichiometric TiN calibration specimen. Experimental conditions as in Fig. IV.11. Area k-ratio N-Kα relative to Cr_2N 2.4567; χ^2 = 9.75. Note that the resulting background after the removal of the components has been increased by 2000 counts.

The two negative areas on both sides of the small positive central peak in the background are clearly visible. In spite of the relatively poor χ^2 value, however, the resulting Area k-ratio for N-Kα , although slightly high (see Table IV.2), is quite reasonable. As mentioned before the resulting background seems to point to peak shape alterations between standards and specimen. A similar procedure for the STE crystal led to even a much poorer χ^2 value of 16.75 and an Area k-ratio for N-Kα of 2.3156. Again, this is a reasonable but this time slightly low answer. The resulting background in this case showed a remaining positive peak left of the N-Kα peak position, followed by a dip almost touching the base line on the right side of the N-Kα peak position. These phenomena seem to point to small shifts in the peaks between standards and specimen. Due to the better spectral resolution of the STE crystal, as compared to the LDE crystal, one could expect the former to be more sensitive to these effects.

Summarizing the last two paragraphs we can say that the quantitative analysis of Nitrogen in Ti-containing compounds is definitely possible with a relative accuracy of better than 5 % (for not too low levels). For Nitrogen levels between 0 and 15 at % there is little choice between the two procedures discussed here : the Super ML fitting procedure is the only option in this case and the simplest form of this program, in which no use is made of first and second derivatives, seems to give the best answers. For higher Nitrogen levels there is a choice between the Super ML fitting technique and our new APF procedure. The former is the fastest technique although we have a slight preference for the APF procedure which gives slightly better and more consistent answers for the highest Nitrogen contents. In all cases, however, the use of the LDE crystal has to be preferred; not in the last place because of its much higher peak intensities, but also because of its strong suppression of higher-order reflections and poorer spectral resolution. The latter property makes it less sensitive to peak shape alterations.

IV.3 Performance of LDE crystal as compared to conventional lead stearate crystal

As we have mentioned in the introduction already the element Nitrogen is by far the most difficult to deal with in the sequence of the ultra-light elements Boron, Carbon, Nitrogen and Oxygen. There are two reasons for this :

- -- In the first place the wavelength of N-Kα falls right into the K-absorption edge of Carbon and the emitted radiation has to travel through lots of Carbon (Stearate crystal, detector window) on its way to the detector.
- -- In the second place interference of higher-order metal lines frequently takes place; notorious examples are the elements Zr and Nb.

As a result we have to deal with extremely low Peak to Background ratios (frequently below 1) for a conventional lead-stearate crystal, in conjunction with backgrounds which are very difficult to determine in many cases.

Fortunately, since a number of years a new generation of analyzer crystals have become available : the new synthetic multilayers. The first crystal of this kind (code name LDE) that came to our possession was the W/Si multilayer (2d-spacing 59.8 Å, supplied by Ovonic Synthetic Materials Corp., Troy, Michigan, U.S.A.), the results of which have been mentioned before already on a number of occasions. Since we were at that time heavily involved in Nitrogen analysis and had a fairly large number of nitride specimens available it seemed a good opportunity to compare the performances of LDE and STE crystals on all these nitrides. Some preliminary results of these tests have been published before[5]. At that time, however,we reported some problems with the LDE crystal when it was used at accelerating voltages beyond 20 kV. In those cases two broad unidentified extra peaks turned up in the immediate vicinity of the N-Kα peak with intensities comparable to the latter. We thought then that these peaks might be caused by Laue reflections from the (100)-Si single crystal substrate produced by components of the "white" spectrum generated in the specimen, thus giving rise to the presence of non-characteristic and, therefore, unidentifiable wavelengths in the spectrum. That reflections from the substrate are indeed possible was shown by the presence of strong characteristic K$\alpha_{1,2}$ and Kβ reflections from a Copper specimen at 40 kV : the observed peak positions correspond to a d-spacing of 1.357 Å, which in turn corresponds with the (400) reflection of Si. Later on it was discovered that these unidentified peaks were produced by backscattered electrons which were reflected by the LDE crystal rather efficiently. After the installation (by JEOL) of a simple extra electron trap near the objective lens these contributions could be suppressed very effectively.

In the following pages (Fig. IV.12 a-q) the performances of both crystals are compared on all our nitride specimens. The Pulse Height Analyzer conditions (counter high tension and gain) were chosen such as to produce an N-Kα pulse at exactly 2.0 V and the lower level and window were set at 1.0 and 2.0 V, respectively. The accelerating voltage in all cases was 10 kV and a beam current of 300 nA has been used. In view of our bad experiences with oxidation phenomena under electron bombardment the air jet was not employed. For technical reasons (differences in 2d-spacings of both crystals and limitations in the choice of the step size) it was not possible to scan exactly the same wavelength regions with both crystals. All spectra contain 500 channels with step sizes of 0.04 mm (STE) and 0.07 mm (LDE) between them. The counting time in each channel was 10 s.

All figures are composed of 4 spectra, the top couple of which are always the N-Kα spectra from the nitride specimen in question (left side for STE; right side for LDE). The bottom couple are the spectra recorded from the pure metal partner in the nitride (left side again STE; right side LDE).

The latter spectra give a good survey over features like presence of interfering metal lines, curvatures or other peculiar effects of backgrounds, etc.

A number of conclusions can be drawn from Fig. IV.12 :

-- It is obvious that the LDE crystal brings an important improvement of the net count rates by approximately a factor of 2.8.
-- The Peak-to-Background ratio is significantly improved by a factor of 2-4.
-- The spectral resolution of the LDE crystal is slightly worse than that of the STE crystal, which may turn out to be an improvement in terms of the effects of Peak Shape alterations.
-- The LDE crystal is apparently able to produce a strong suppression of higher order reflections. One of the best examples of this effect is shown in Fig. IV.12.j for the case of Fe_4N. The STE crystal produces a very strong 2nd order $L\alpha_{1,2}$ and $L\beta$ peak, much stronger than the N-Kα peak itself. The corresponding LDE spectrum shows the reverse effect : the second order lines are effectively suppressed and the N-Kα peak has become much stronger than the metal lines. This makes an accurate determination of the background much easier.

It is important to note here that the strong suppression of higher order lines by the LDE crystal is not a universal feature of this crystal. According to our experiences with C, N and O it only takes place in the wavelength regions of the N-Kα and O-Kα peaks ; in the region of the C-Kα peak no sign of such an effect is noticeable. In the latter case too, however, it can still be advantageous to use the LDE crystal in spite of its lower peak count rates for Carbon than STE : in a number of cases, notably the lighter carbides like B_4C and SiC, the LDE crystal produces a smooth and horizontal background as compared to the kinked (B_4C) or strongly curved (SiC) background on STE.

The excellent qualities of the LDE crystal are best shown off in the most difficult cases, which are the nitrides of the elements Zr, Nb and Mo. The wavelength of N-Kα is very close to the M_5 edge in these elements which leads to mac's for N-Kα in the order of 20000; among the highest values that can be encountered for N-Kα. This fact, in combination with the low weight fraction of Nitrogen in these compounds, leads to extremely low net count rates on STE (Fig. IV.12.k-n) and P/B ratios well below 1. In addition to this, quantitative analysis of Nitrogen with a STE crystal is severely hampered by the presence of numerous interfering lines (Zr, Nb) and/or peculiarities in the background (e.g. for Mo at 90 mm or 32 Å). The significant improvements produced by the LDE crystal are obvious in these cases. Apart from the higher peak intensities there is a conspicuous improvement in the backgrounds : they are completely free from interferences and spectral artifacts and can thus be determined with much higher accuracy.

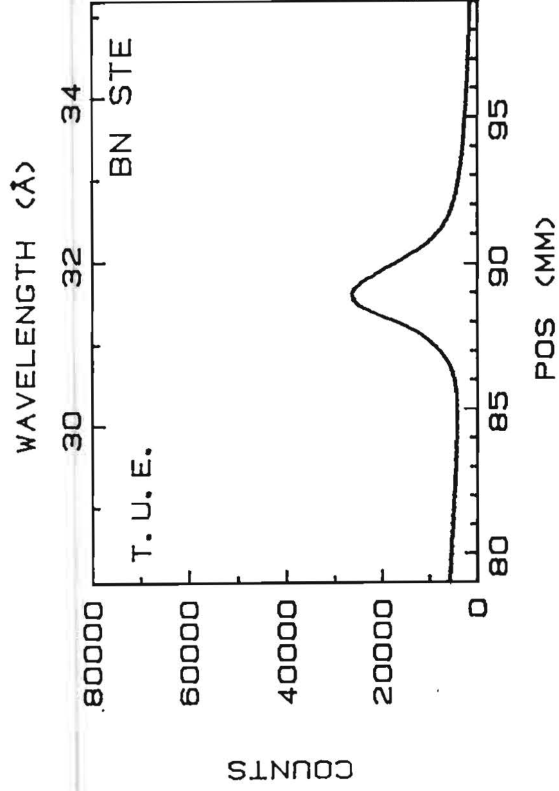

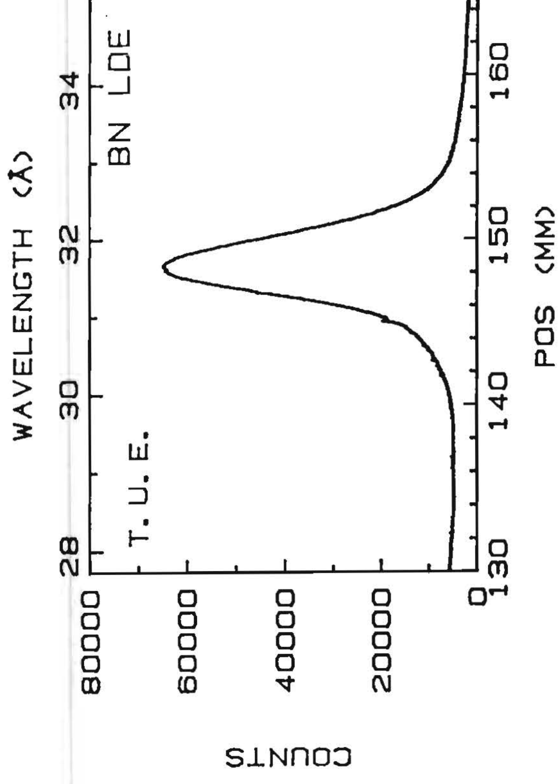

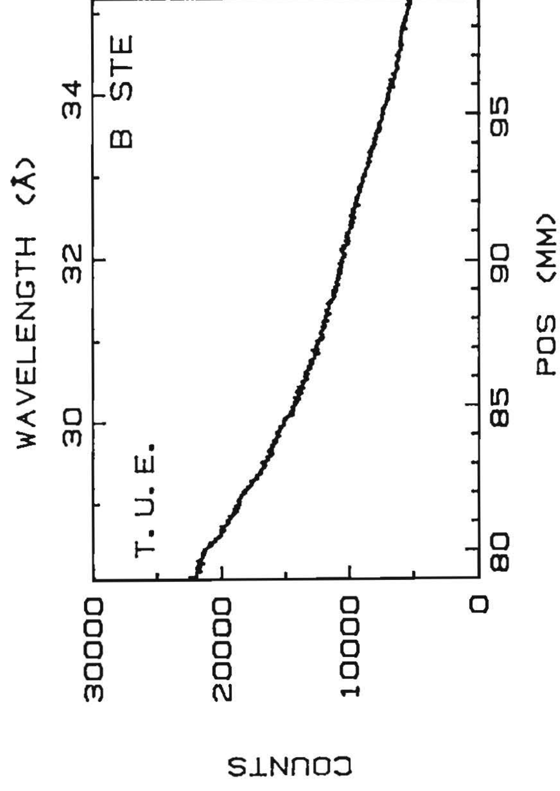

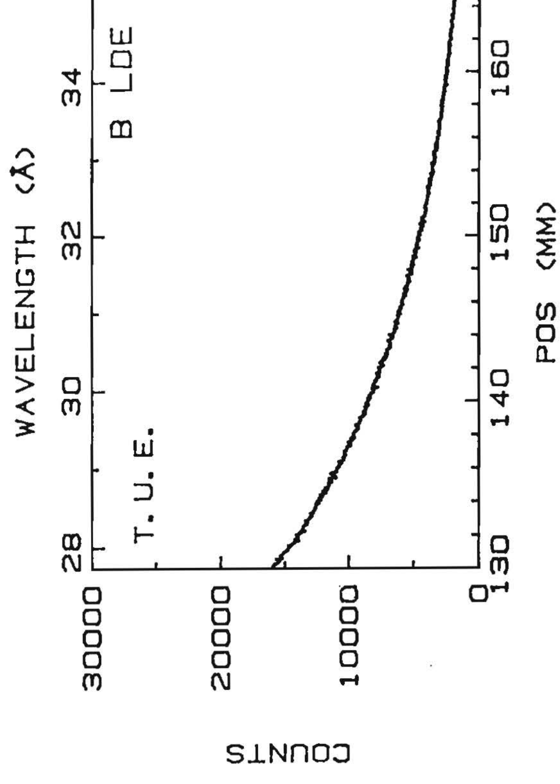

Fig. IV.12.a Nitrogen spectra and backgrounds for BN

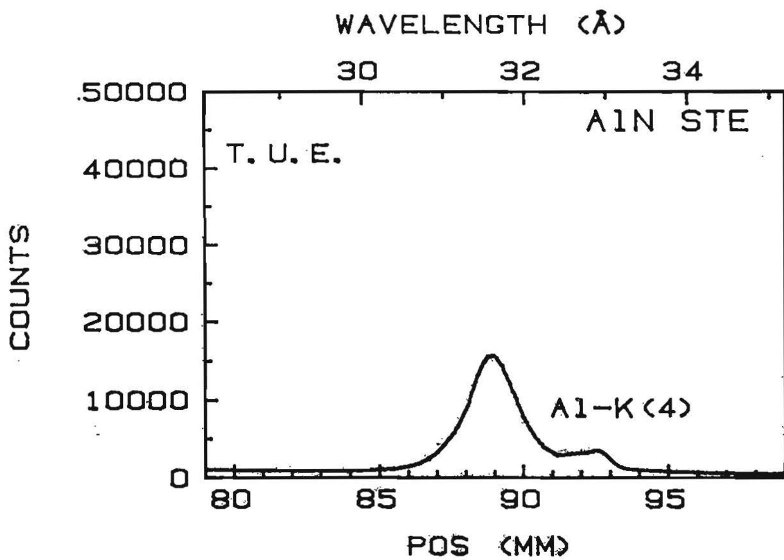

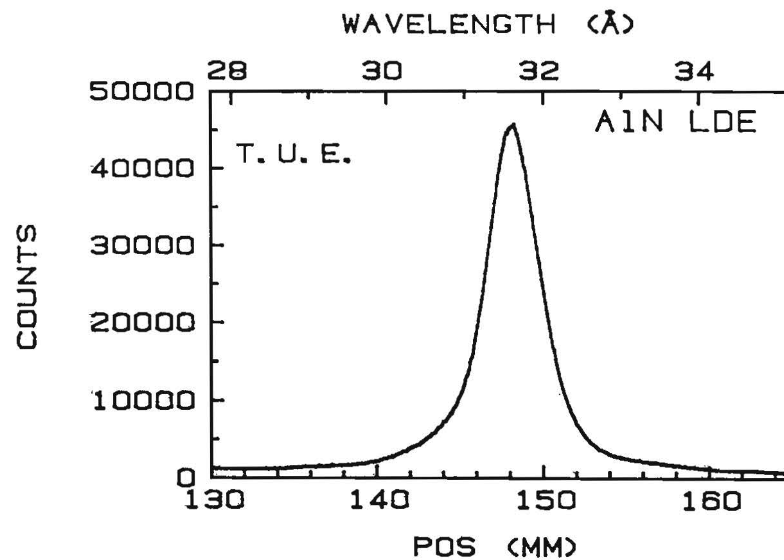

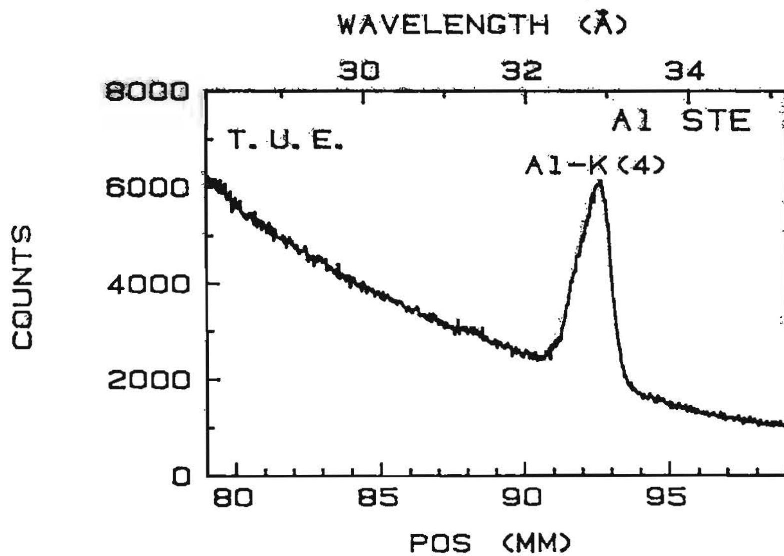

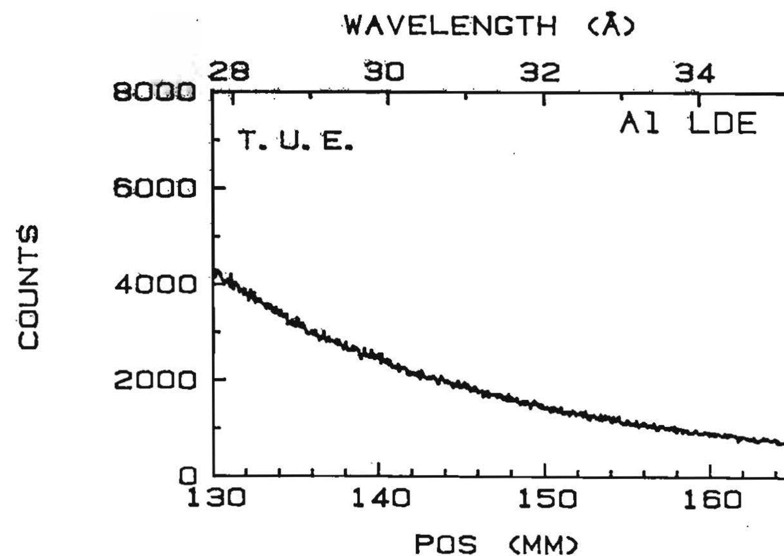

Fig. IV.12.b Nitrogen spectra and backgrounds for AlN

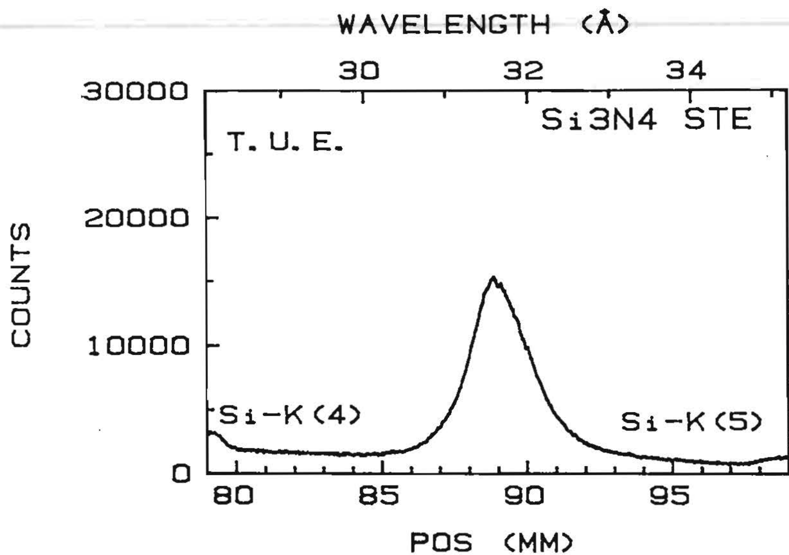

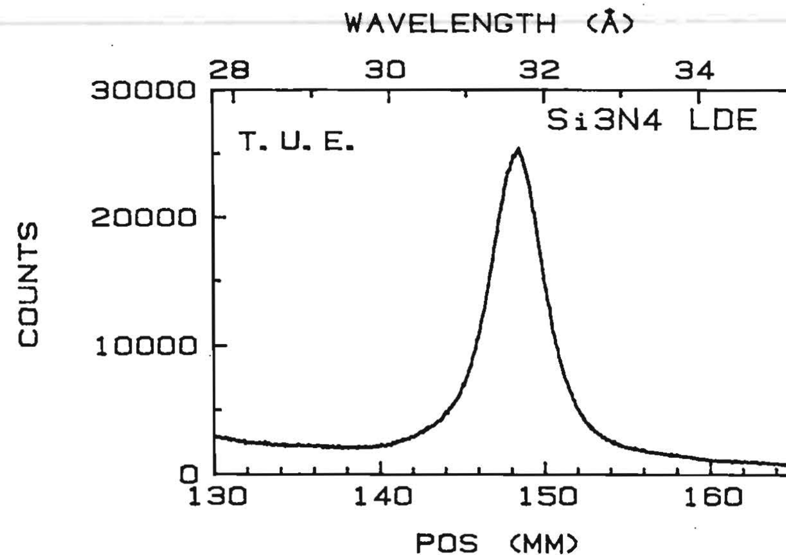

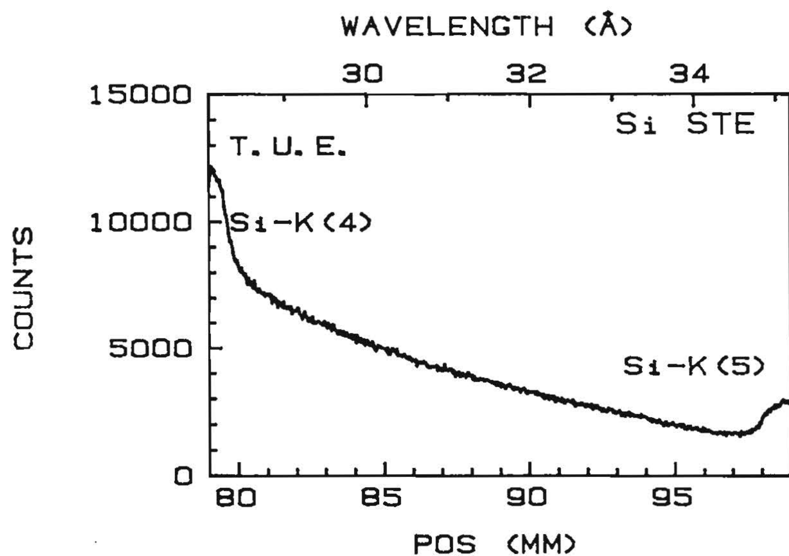

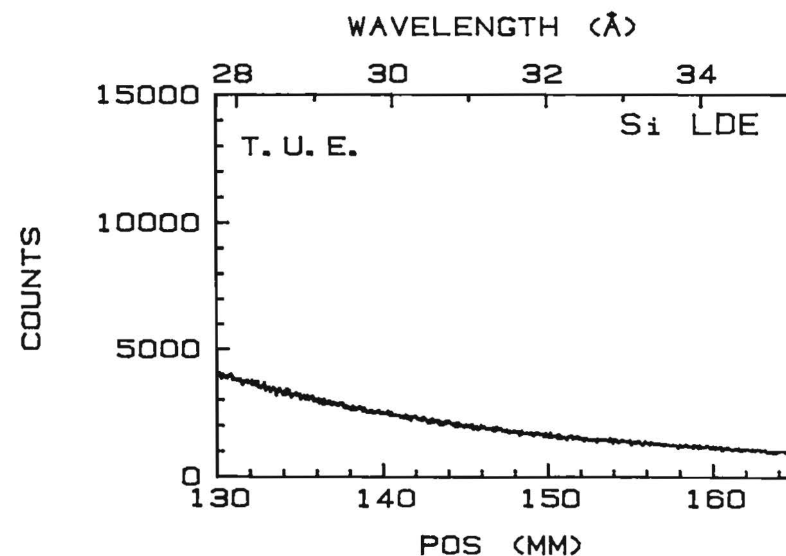

Fig. IV.12.c Nitrogen spectra and backgrounds for Si_3N_4

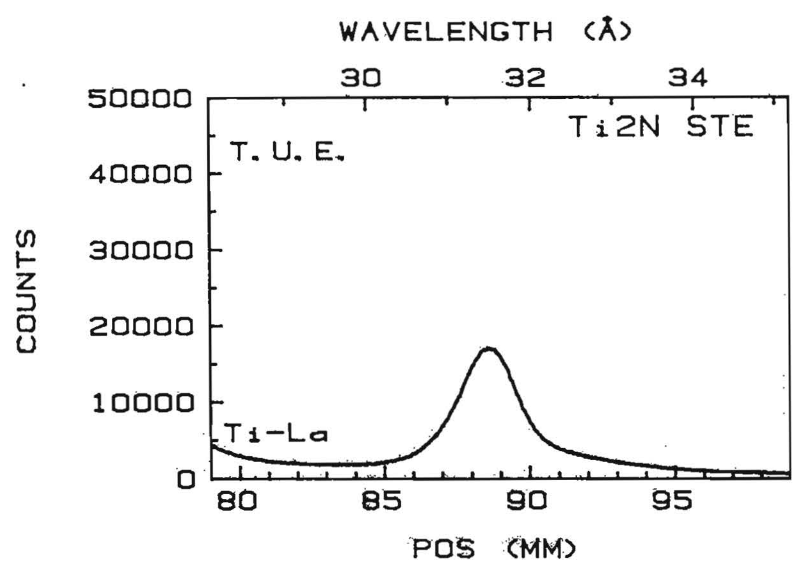

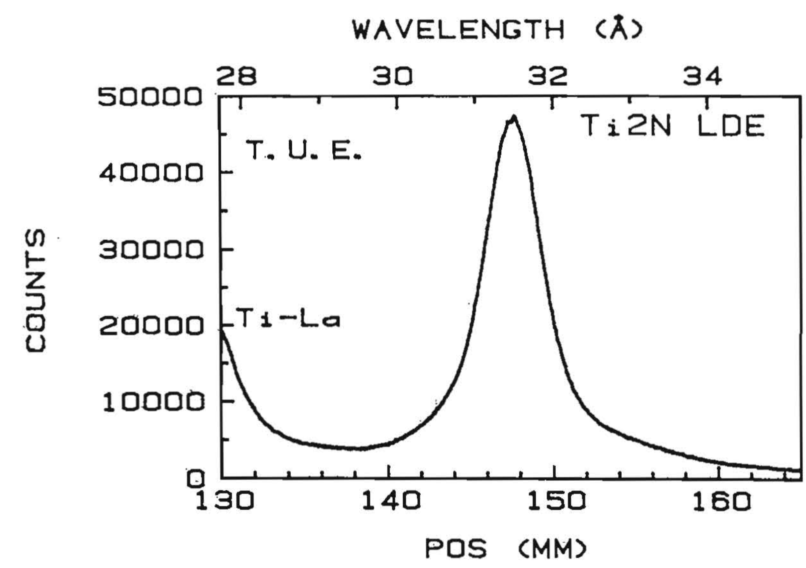

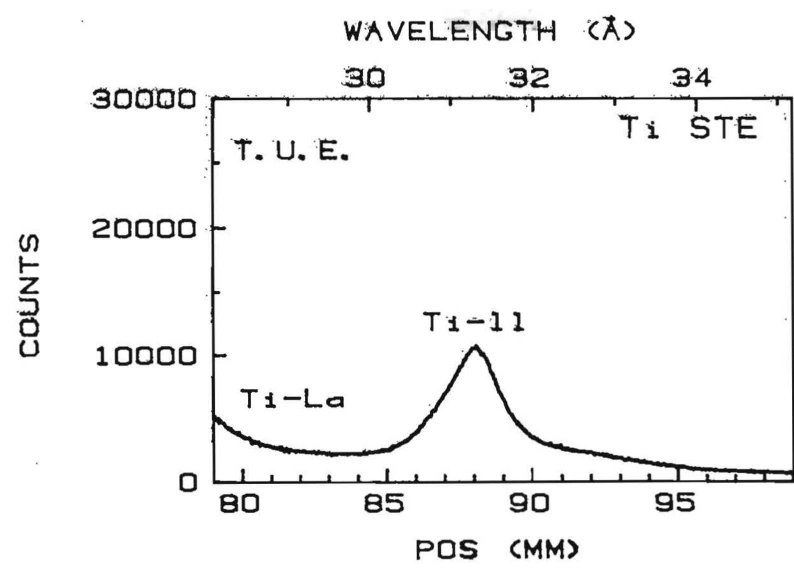

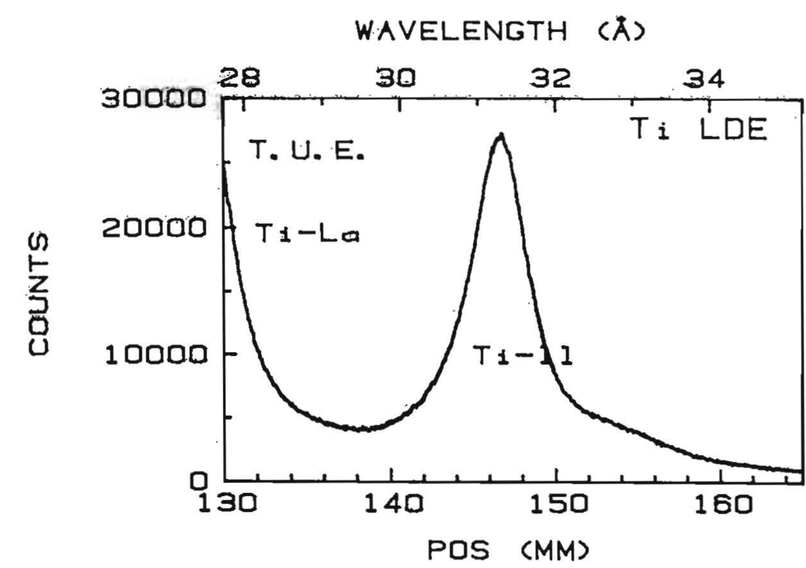

Fig. IV.12.d Nitrogen spectra and backgrounds for Ti_2N

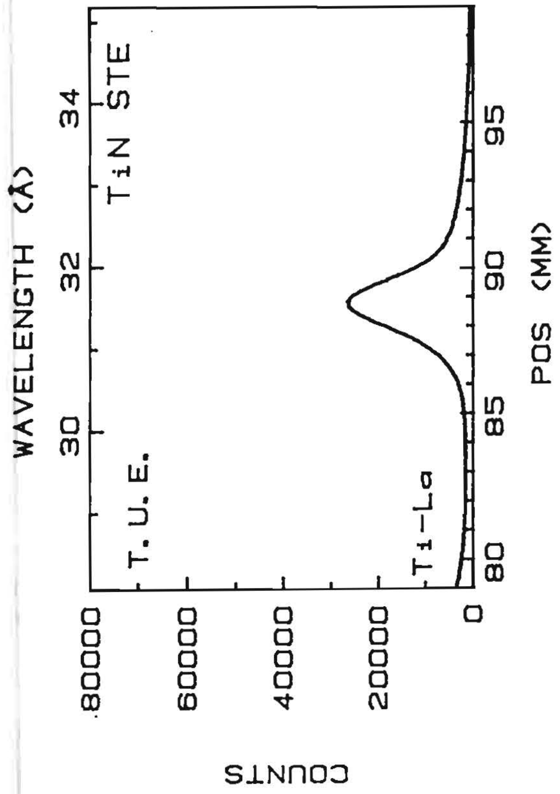

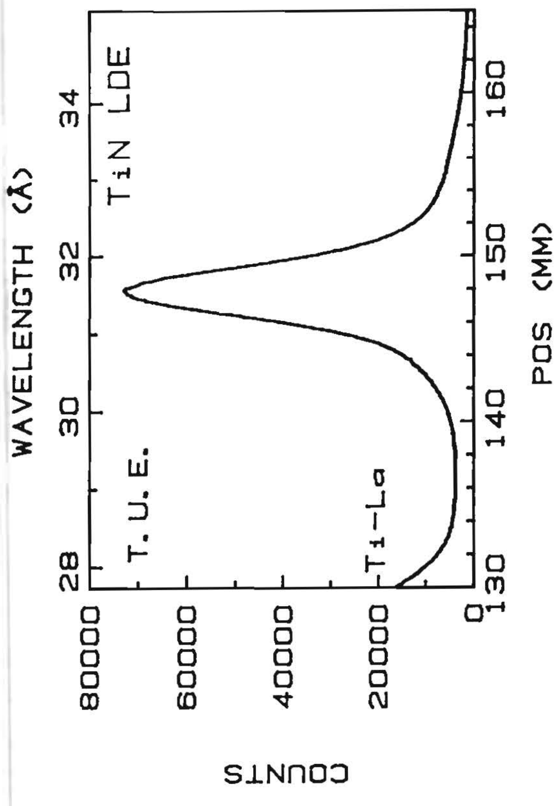

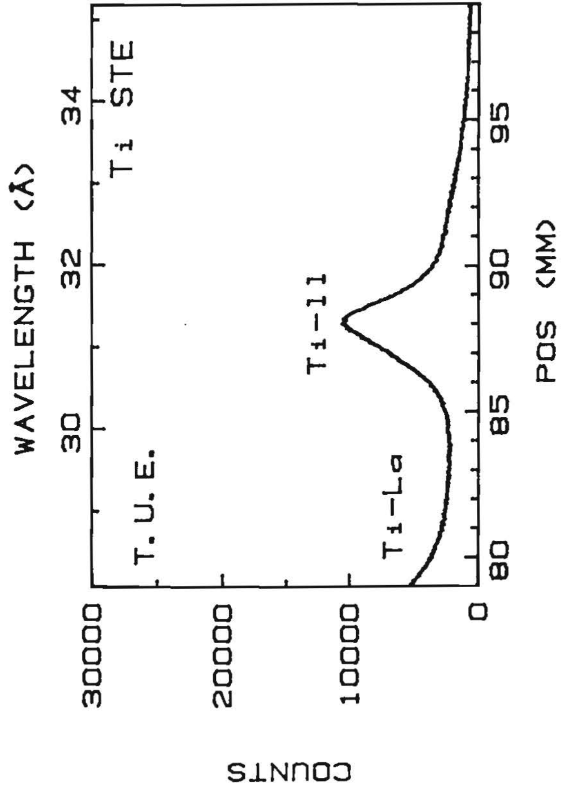

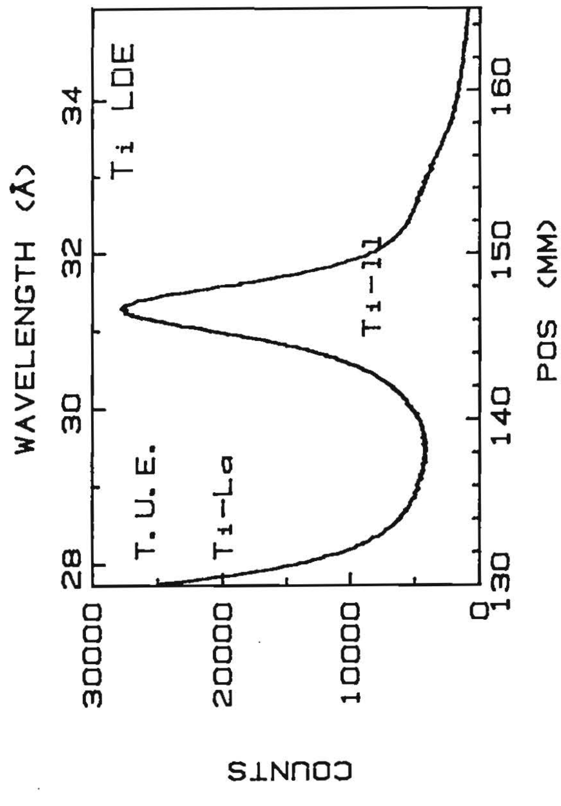

Fig. IV.12.e Nitrogen spectra and backgrounds for TiN

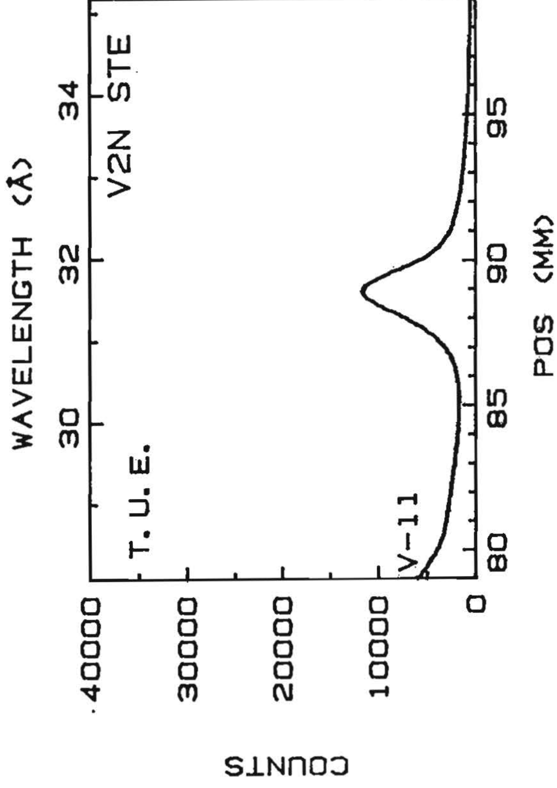

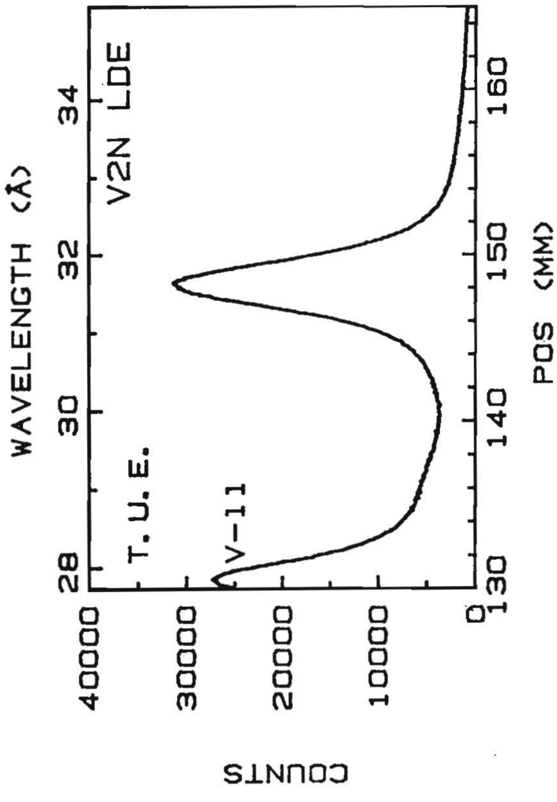

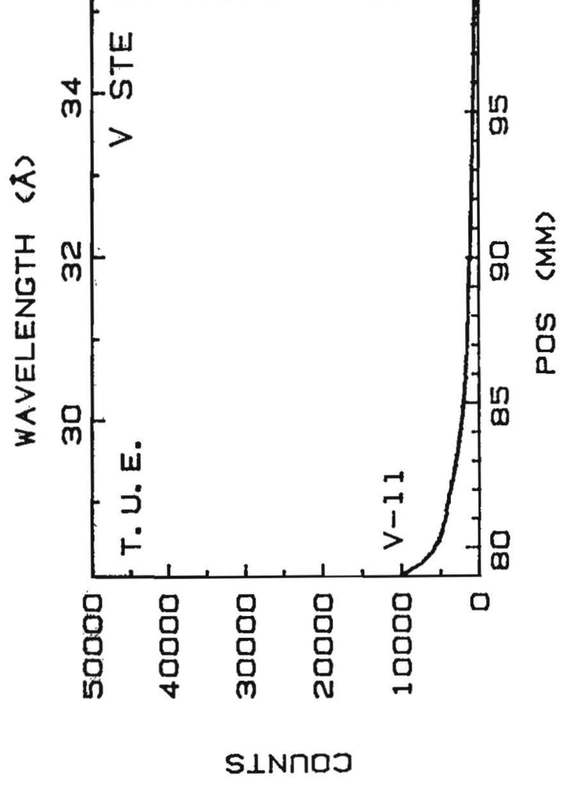

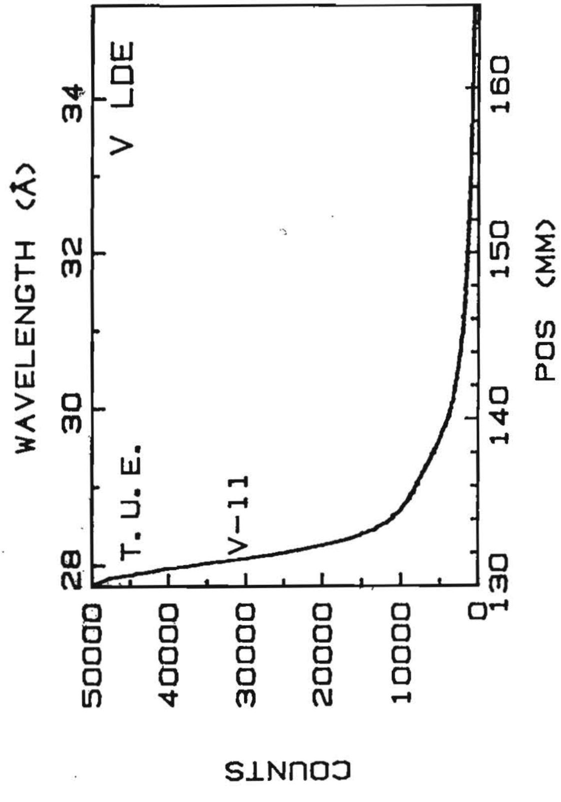

Fig. IV.12.f Nitrogen spectra and backgrounds for V_2N

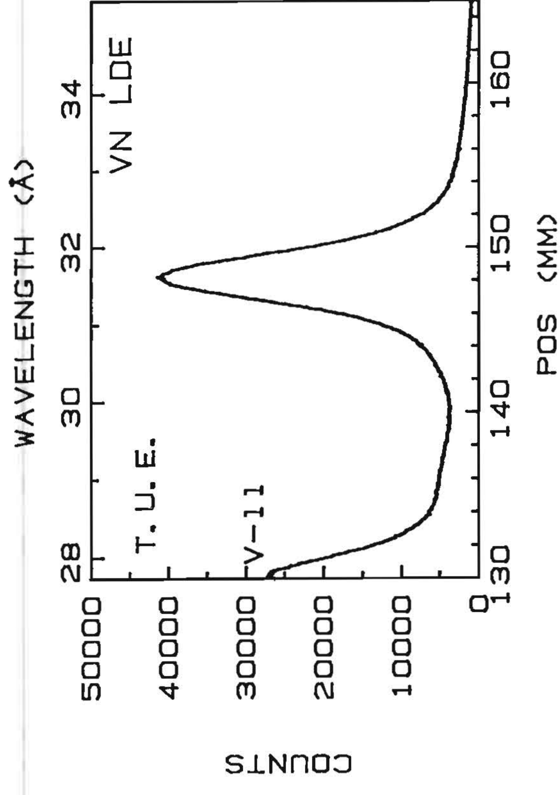

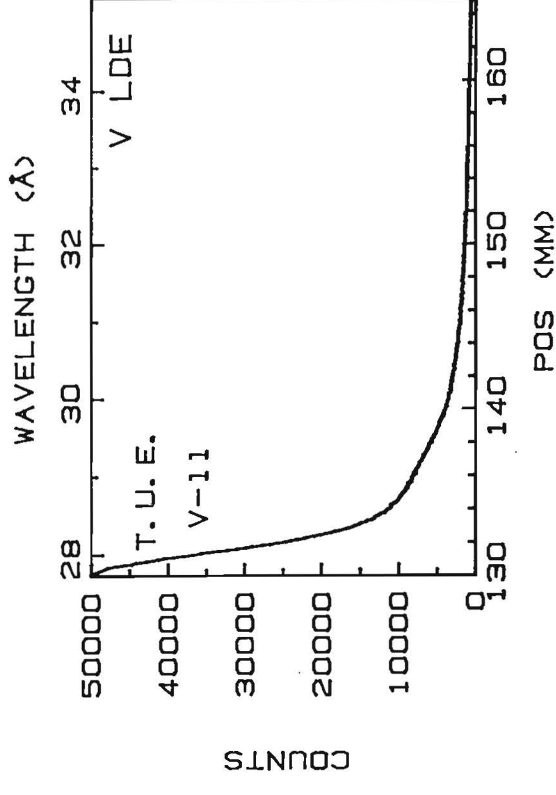

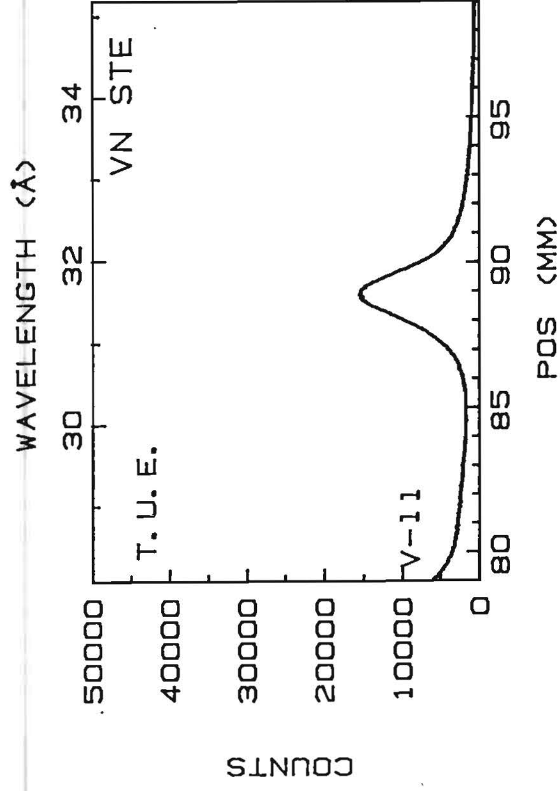

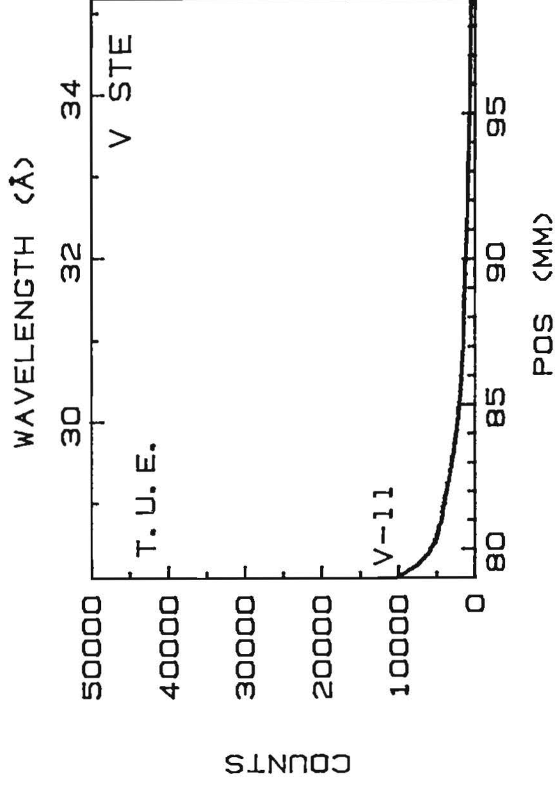

Fig. IV.12.g Nitrogen spectra and backgrounds for VN

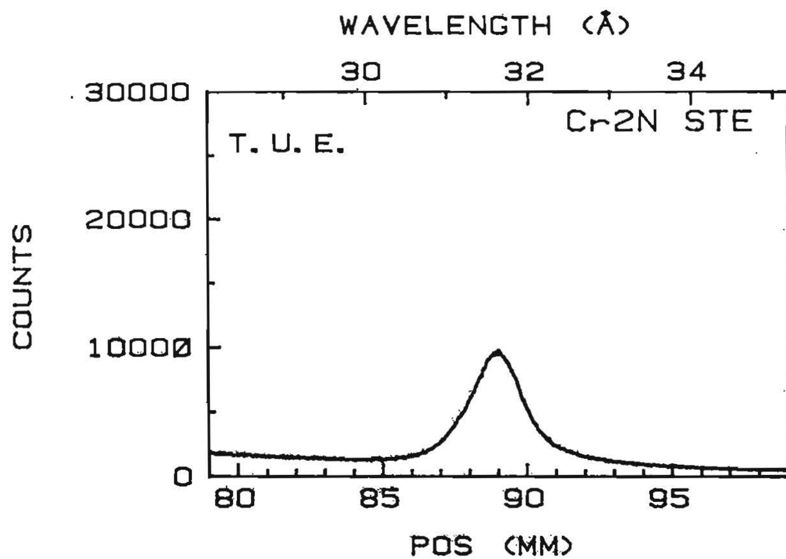

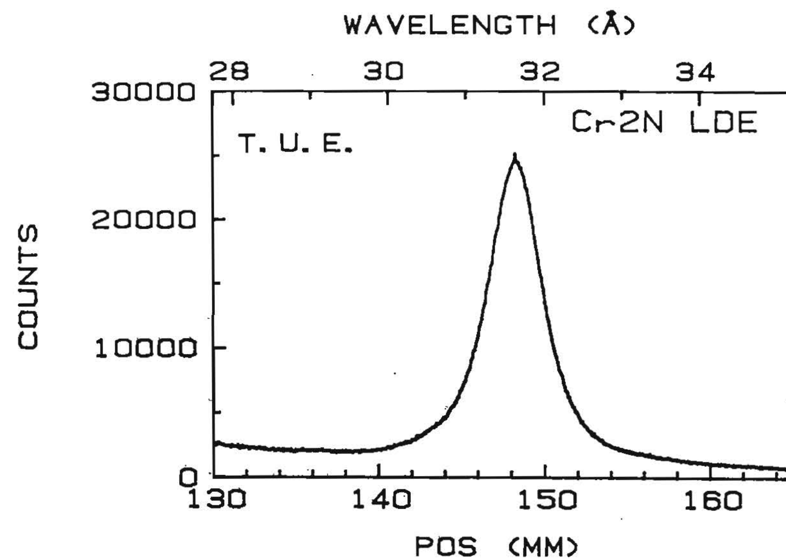

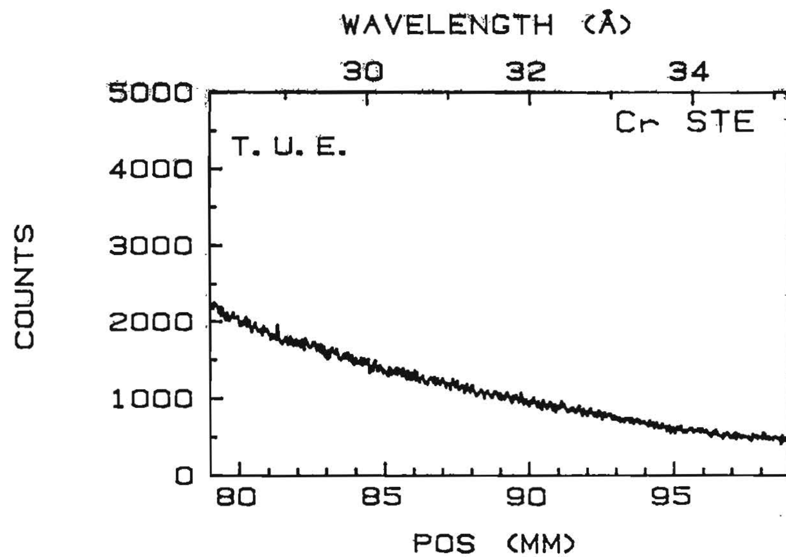

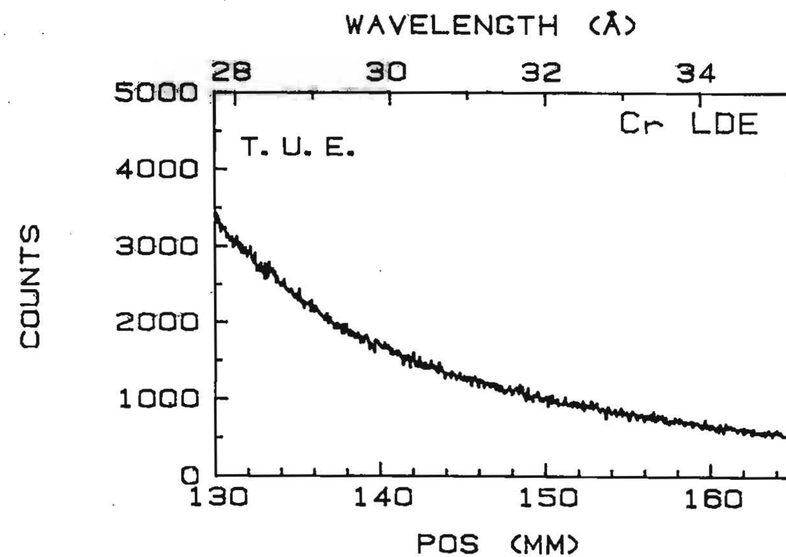

Fig. IV.12.h Nitrogen spectra and backgrounds for Cr_2N

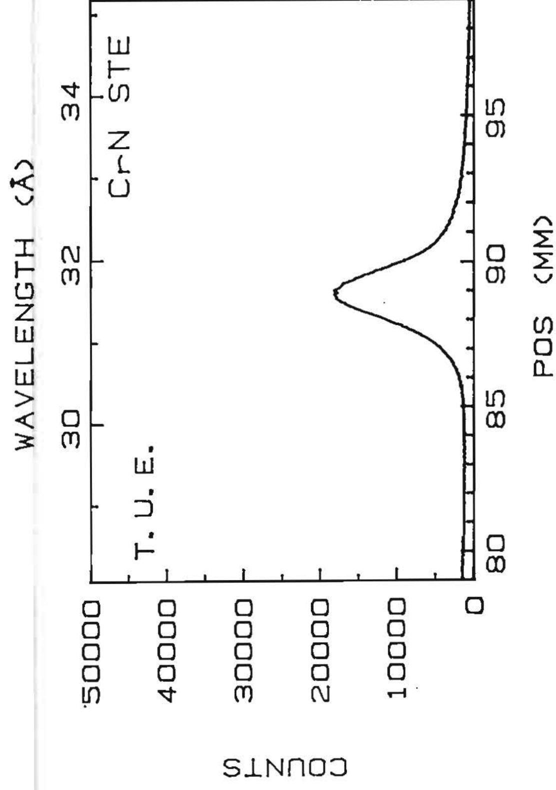

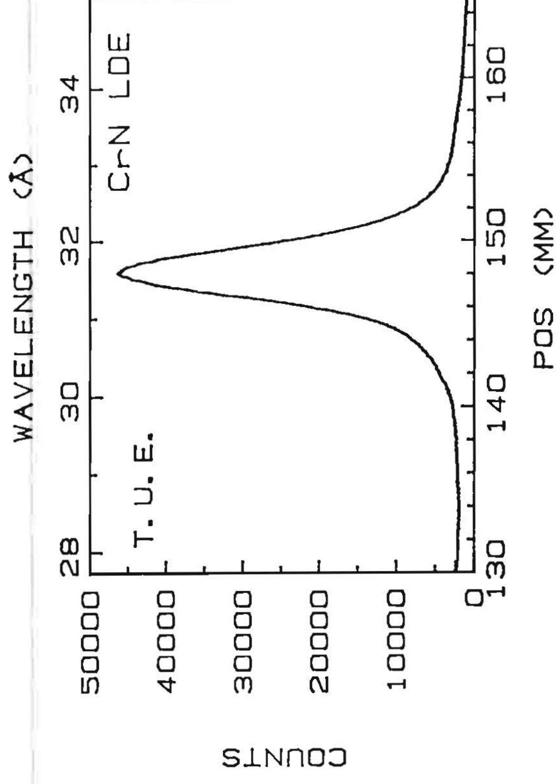

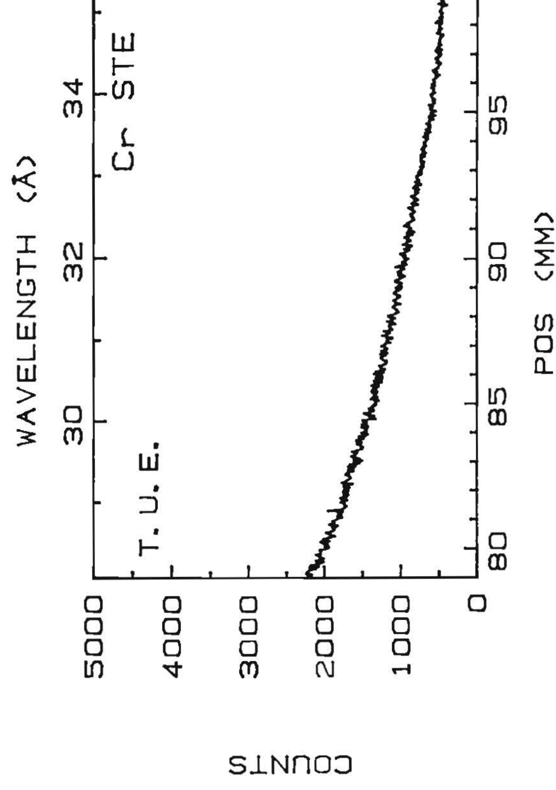

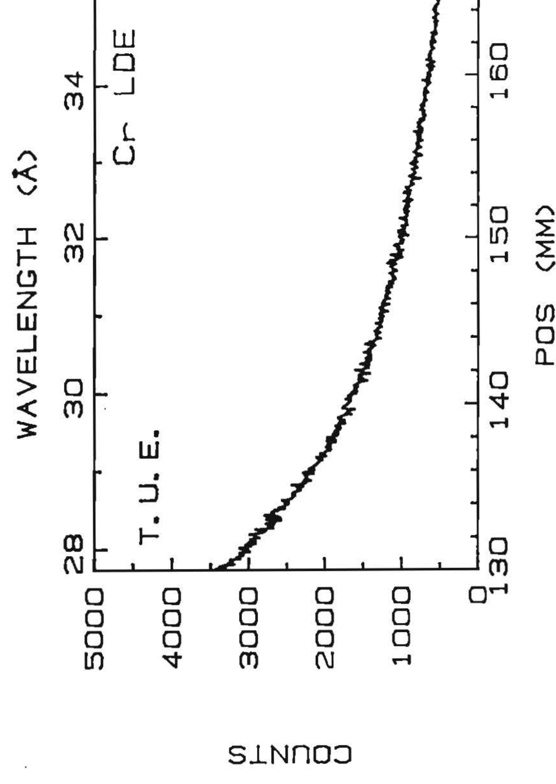

Fig. IV.12.i Nitrogen spectra and backgrounds for CrN

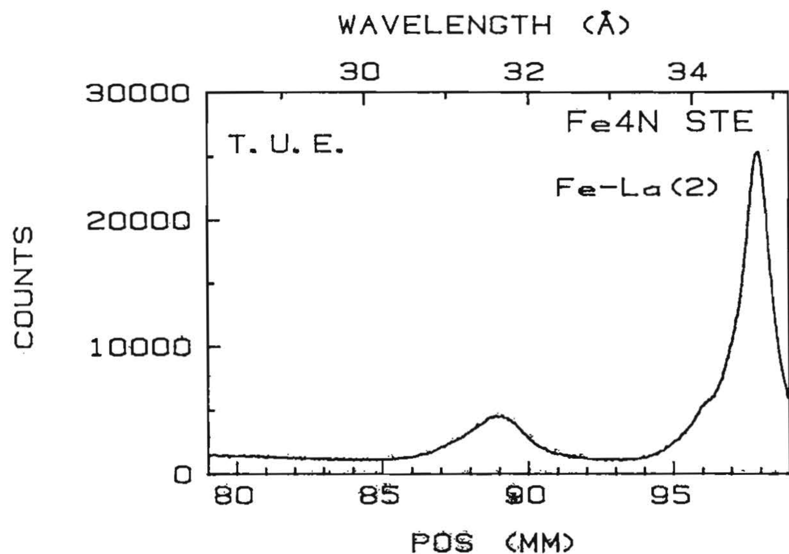

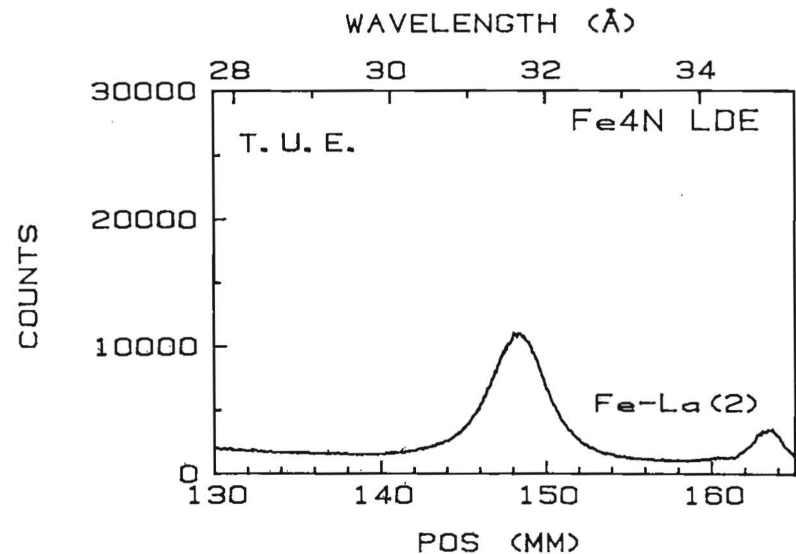

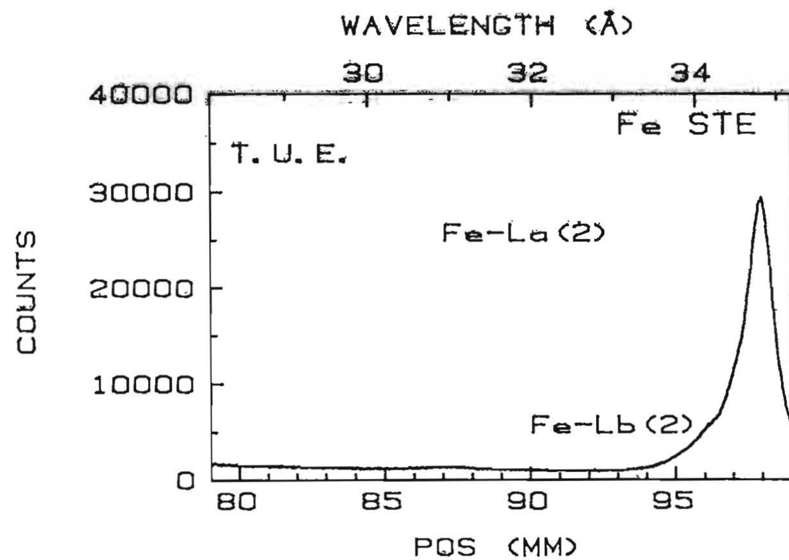

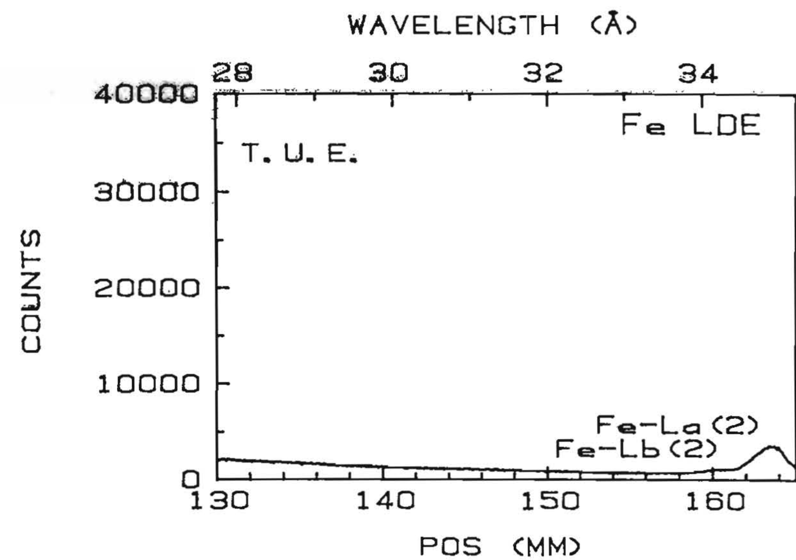

Fig. IV.12.j Nitrogen spectra and backgrounds for Fe_4N

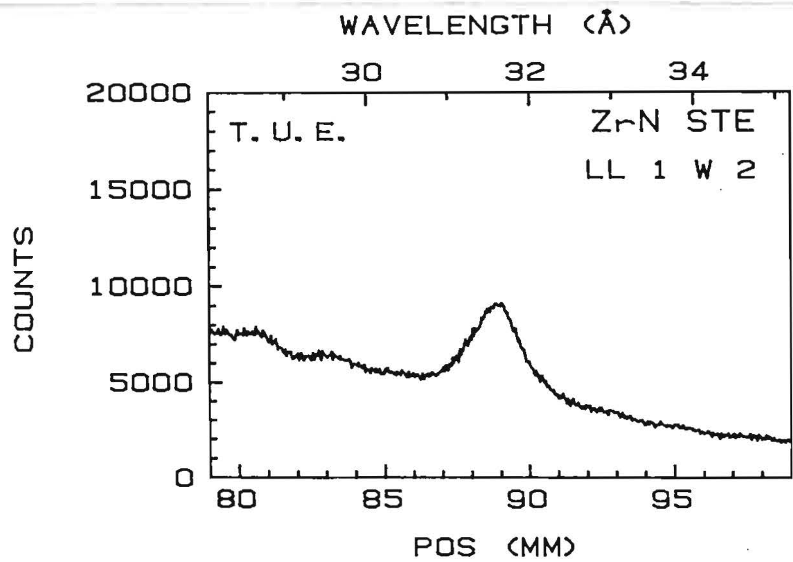

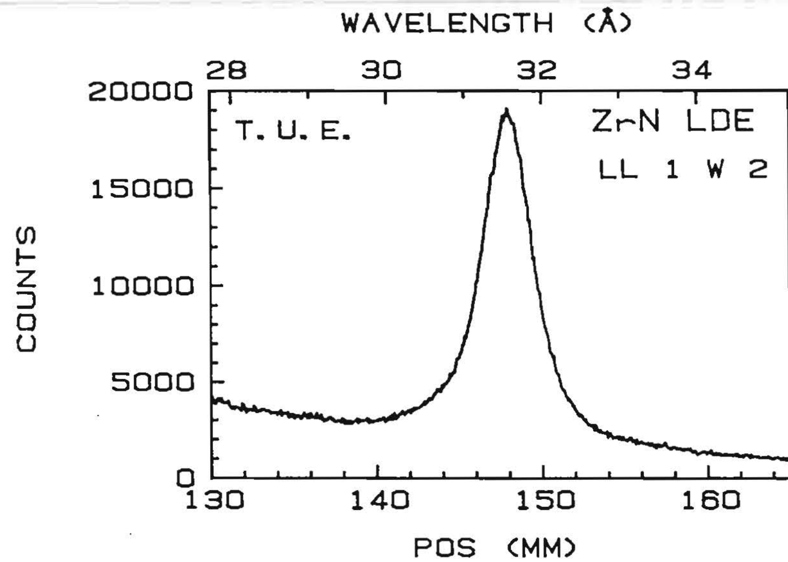

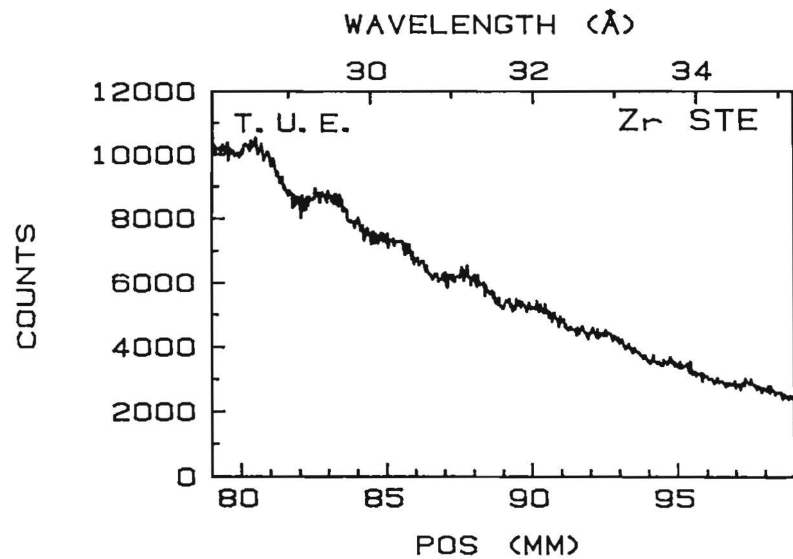

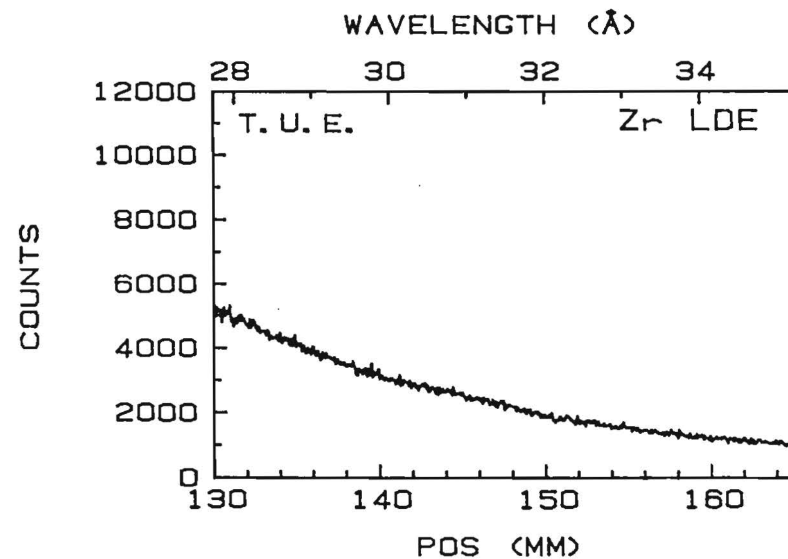

Fig. IV.12.k Nitrogen spectra and backgrounds for ZrN

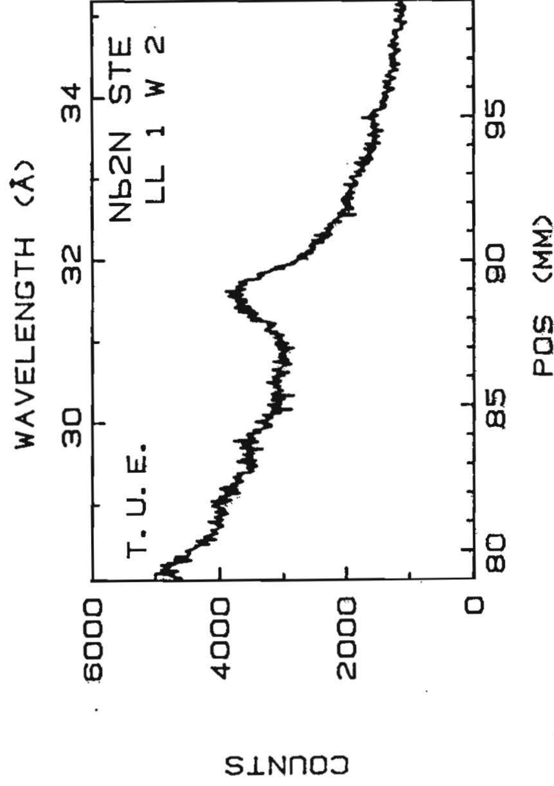

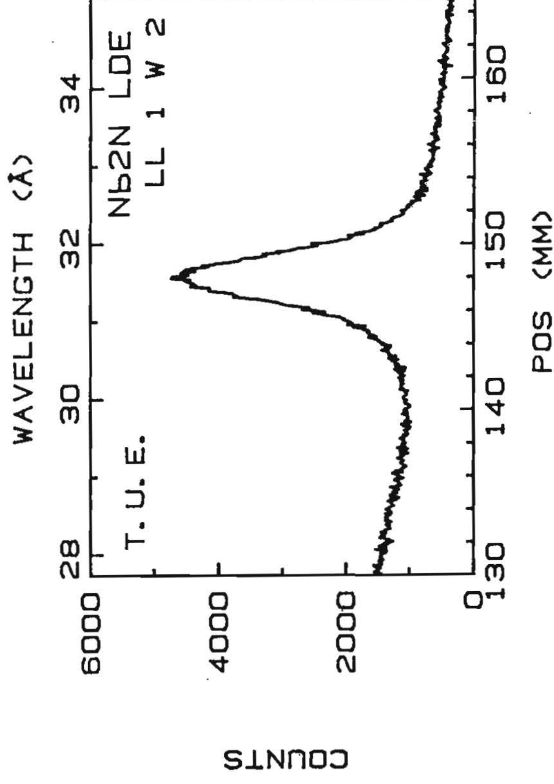

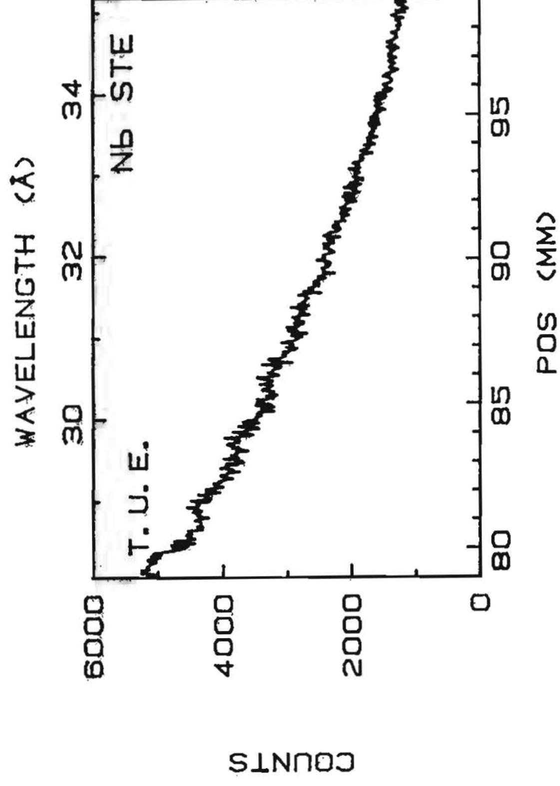

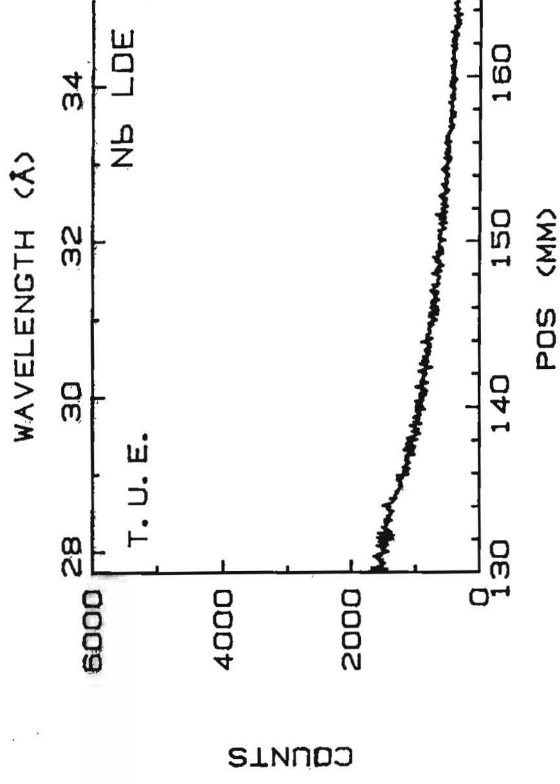

Fig. IV.12.1 Nitrogen spectra and backgrounds for Nb_2N

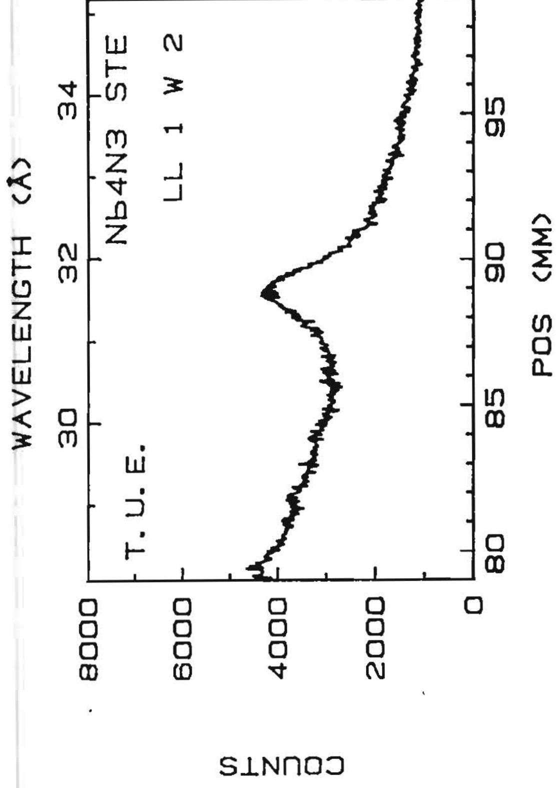

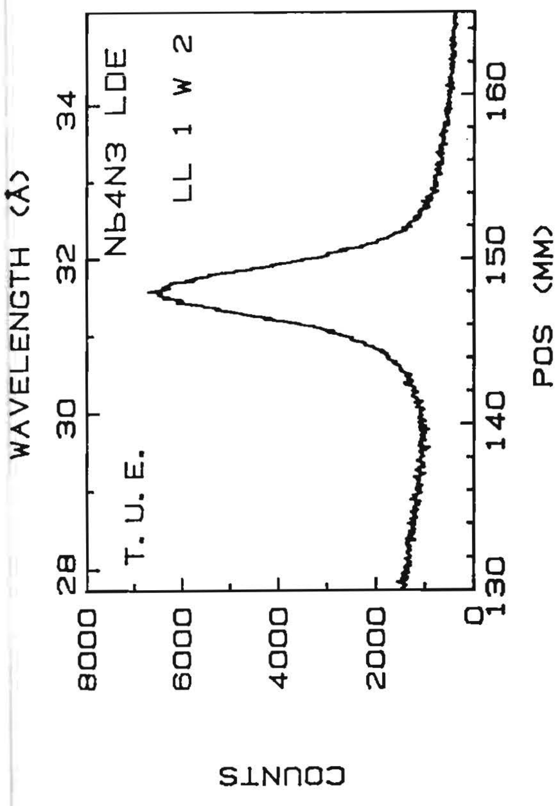

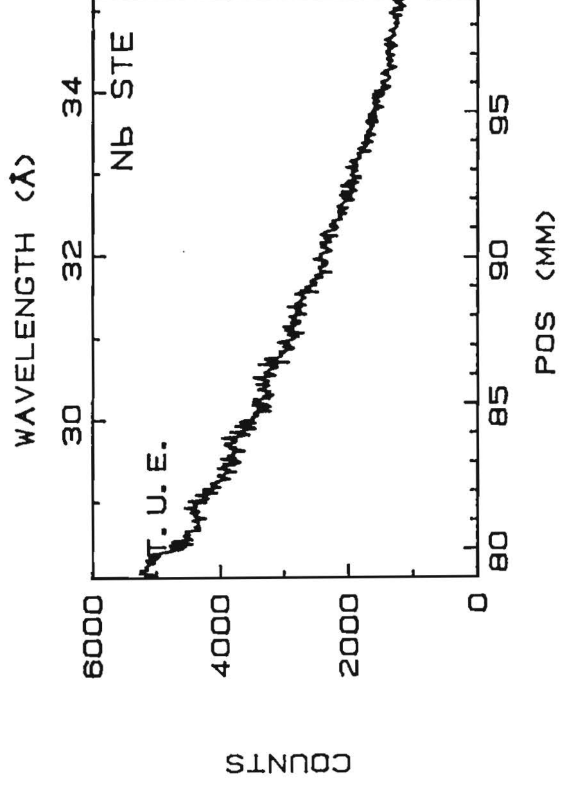

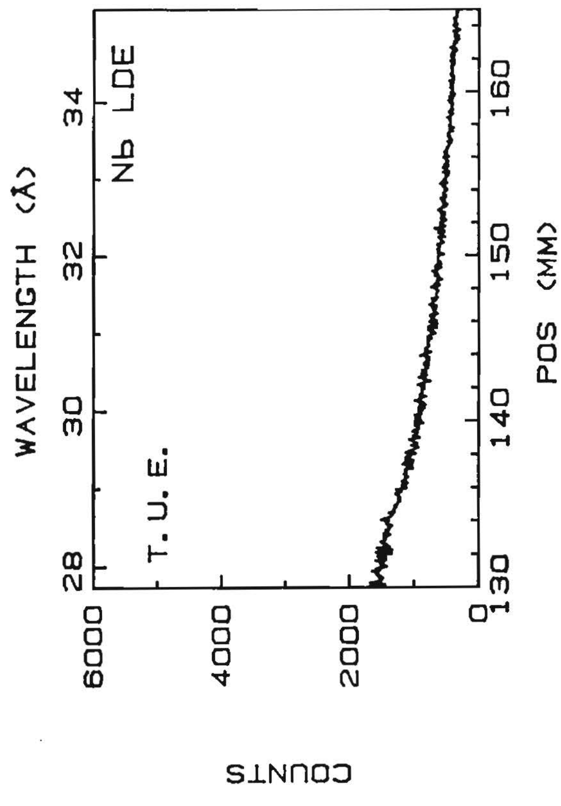

Fig. IV.12.m Nitrogen spectra and backgrounds for Nb_4N_3

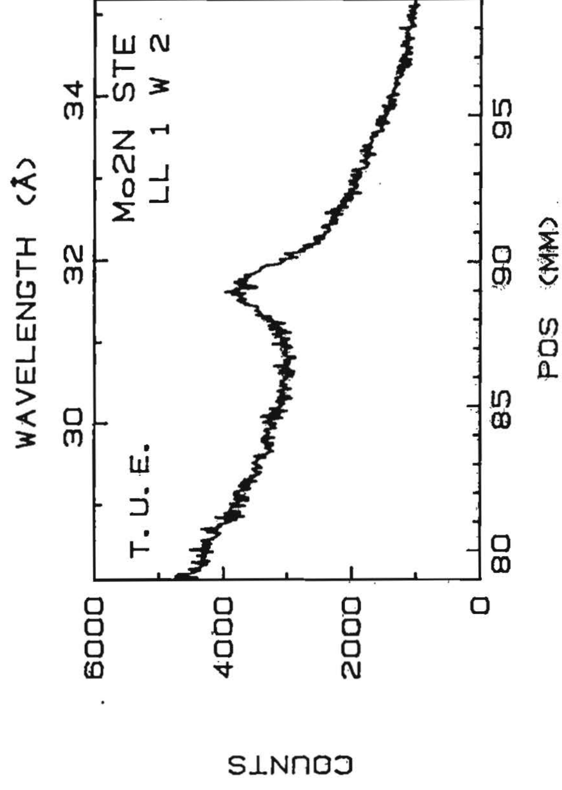

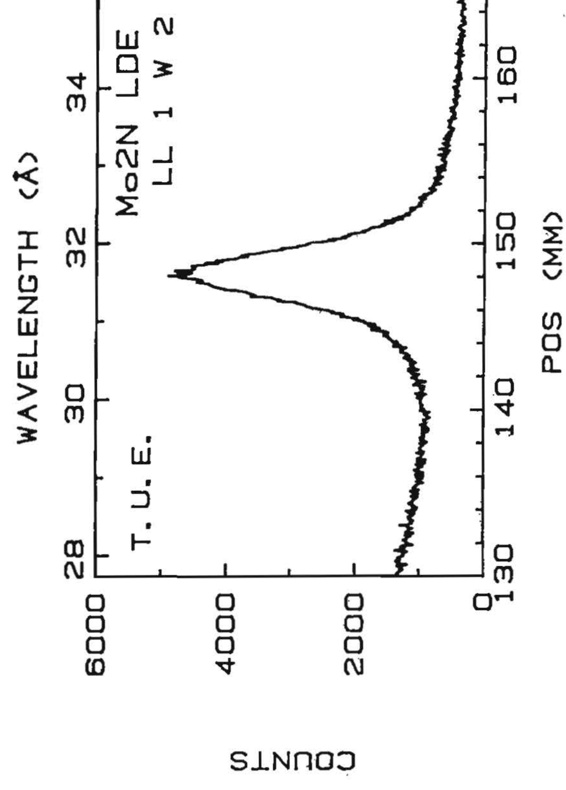

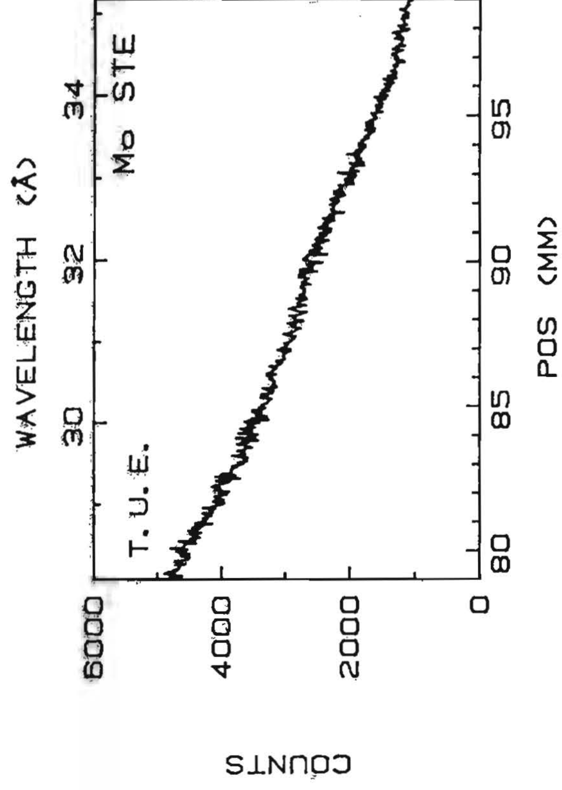

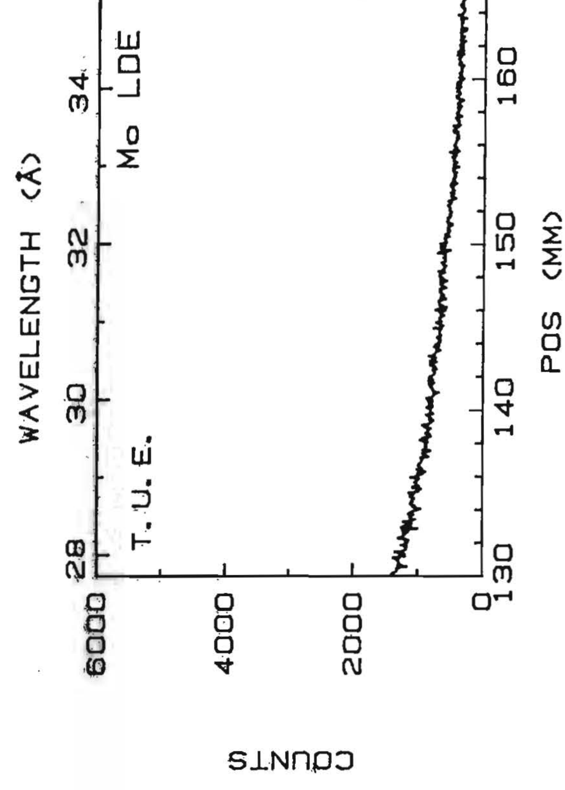

Fig. IV.12.n Nitrogen spectra and backgrounds for Mo2N

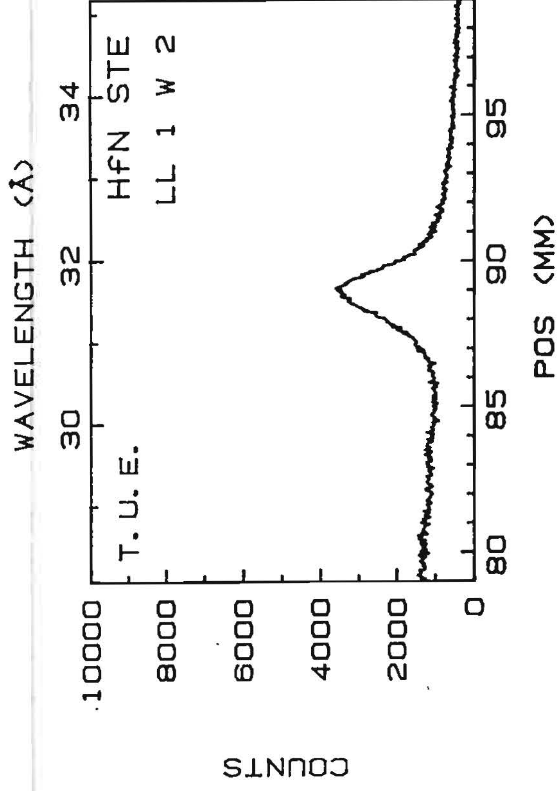

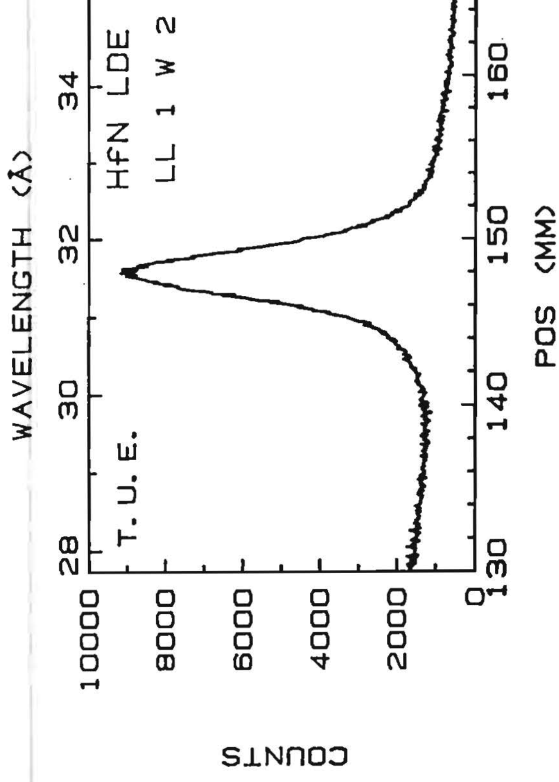

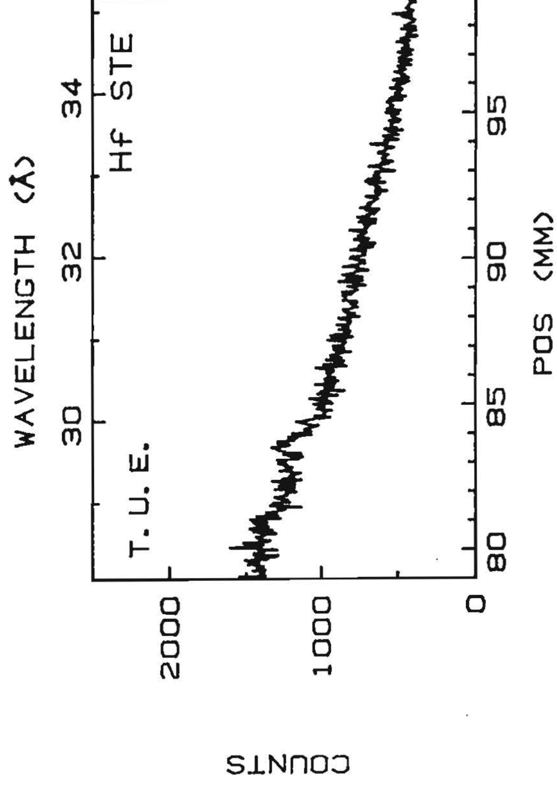

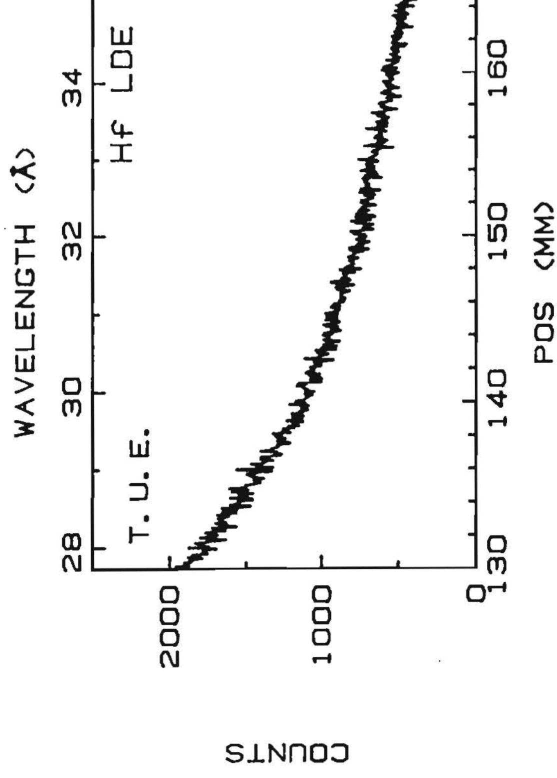

Fig. IV.12.o Nitrogen spectra and backgrounds for HfN

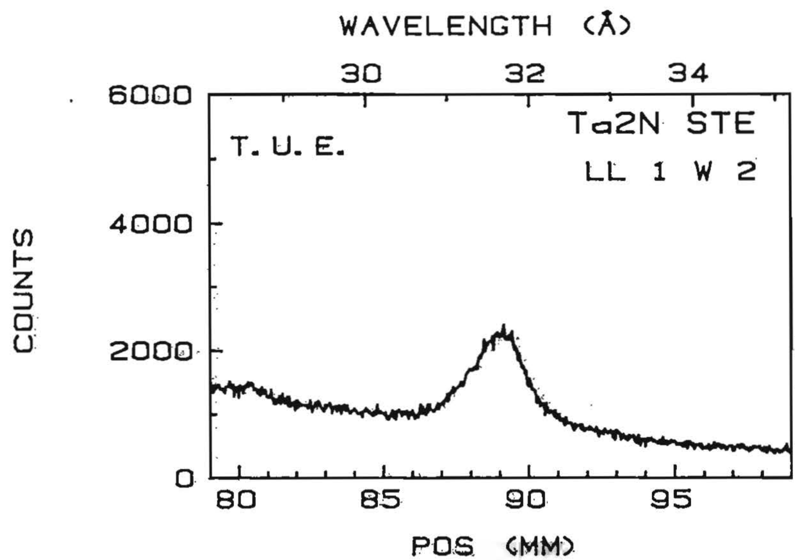

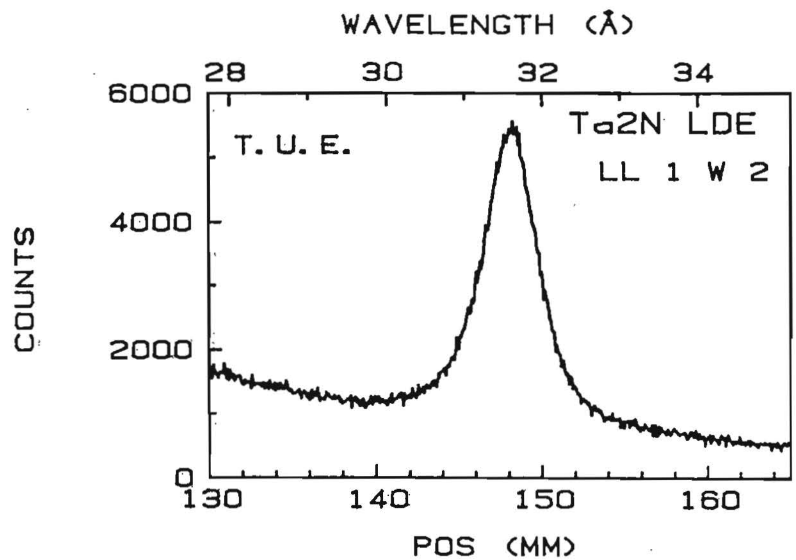

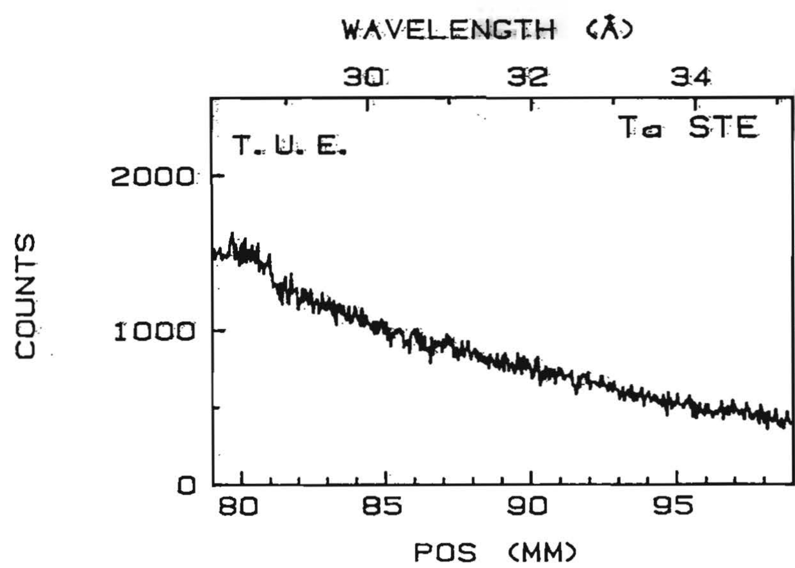

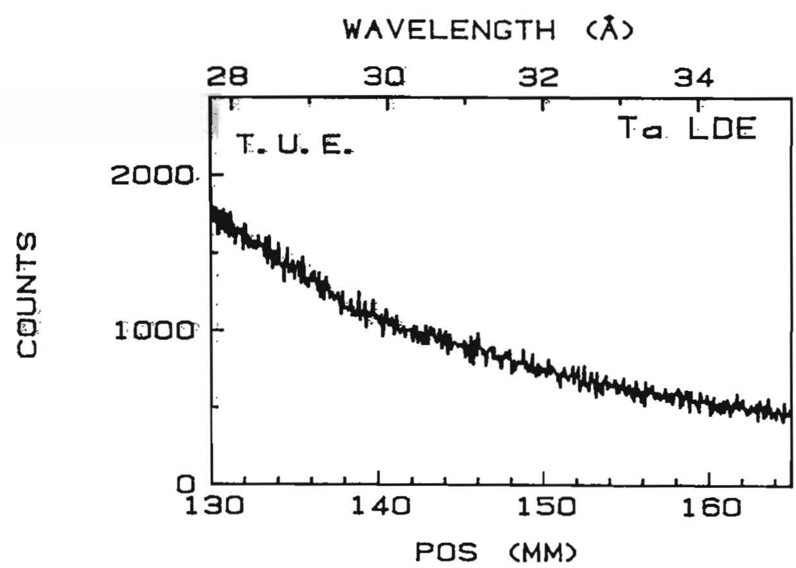

Fig. IV.12.p Nitrogen spectra and backgrounds for Ta_2N

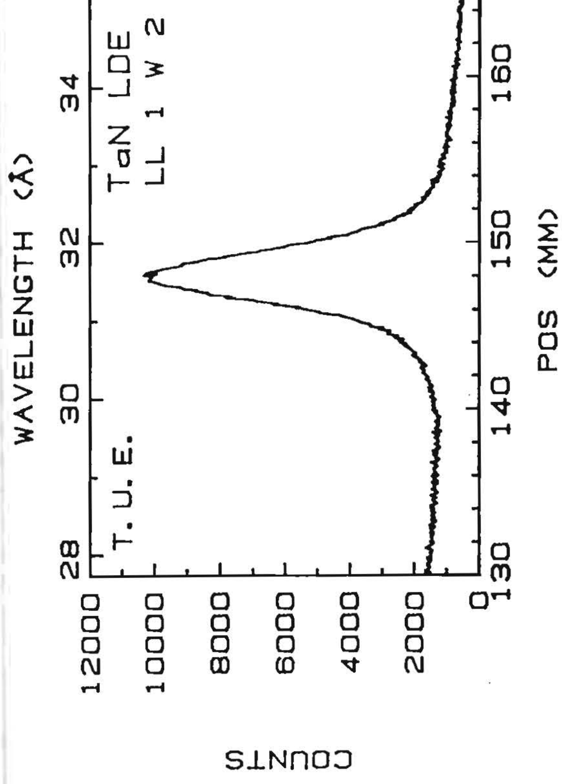

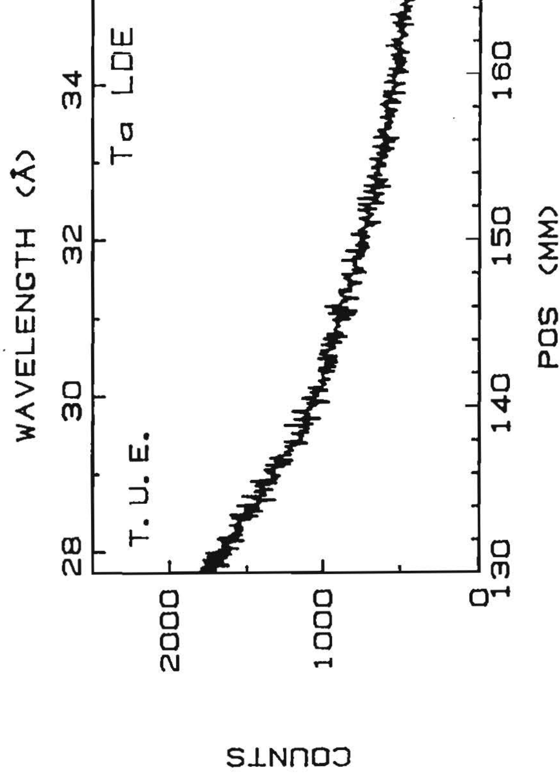

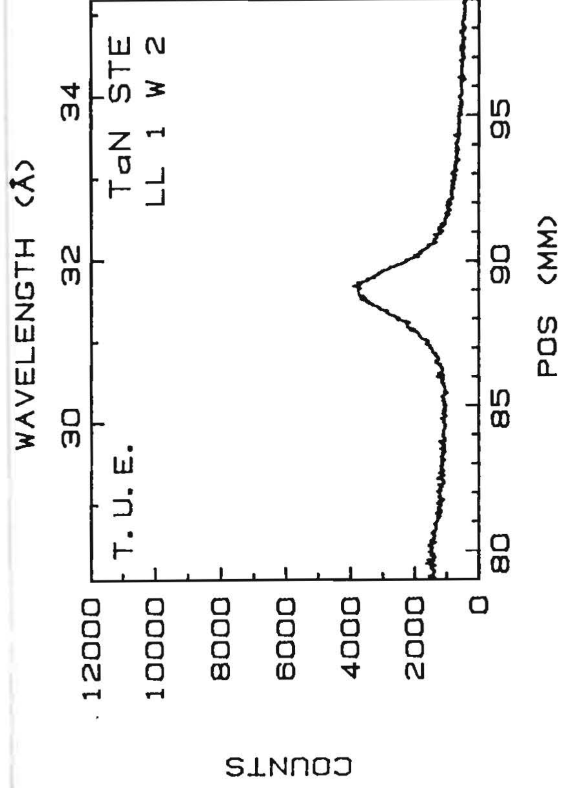

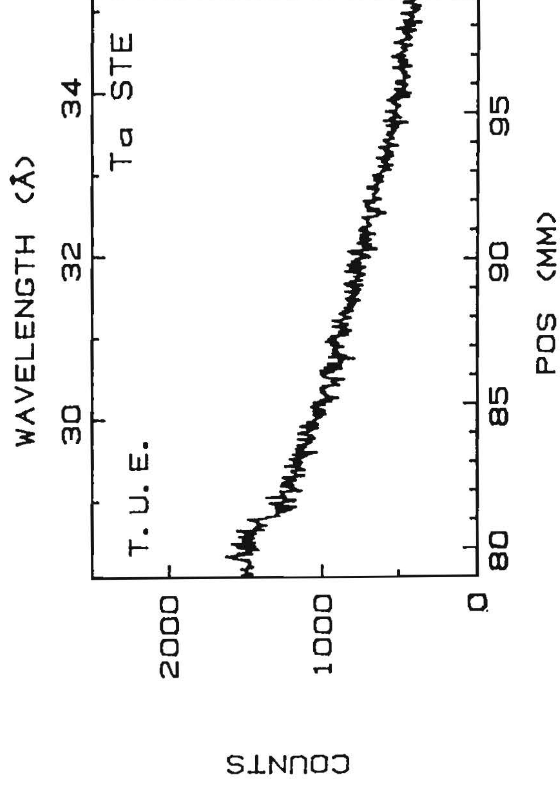

Fig. IV.12.q Nitrogen spectra and backgrounds for TaN

As a general conclusion of this comparison it can be stated that, although the LDE crystal brings significant improvements over the whole range of nitrides, both in terms of count rates as well as Peak-to-Background ratios, it definitely brings the largest improvements in those cases where it is most needed : i e. the nitrides of Zr, Nb and Mo.

IV.4 Area-Peak Factors for N-Kα relative to Cr_2N

Although we have stated before (section III.6) that the APF concept could only be used in a limited number of cases for fast routine measurements in the present work, due to the problems associated with background determination (curvatures, interfering lines, etc.) it is nevertheless interesting to report the values we found ; if only to make a comparison possible between the present results and those on Boron, Carbon and (in the future) Oxygen. We must emphasize again that in spite of the large number of measurements we cannot claim the same relative accuracy (± 1 %) which we claimed for our Carbon measurements. Our feeling is that for the "easy" cases (BN, AlN, Si_3N_4) the accuracy is at the ± 1.5 % level ; for the "difficult" cases (ZrN, Nb_2N, Mo_2N) it is probably ± 2-3 % . Table IV.4 gives a survey of the observed values for both crystals.
It will be clear from Table IV.4 that the effects of Peak Shape Alterations are very much less pronounced than for Boron or even Carbon. Nevertheless, shape alterations of + 8 % (BN on LDE) or - 4 % (Nb_2N on STE) is still something to be concerned about if one is interested in quantitative analysis. Furthermore, it is interesting to point out that in spite of the small effects still something of a saw-tooth like variation of APF with atomic number of the metal partner is visible, similar to the observations in borides and carbides. Again, very stable compounds like TiN and ZrN hold absolute minimum values while highly unstable nitrides like Mo_2N have among the highest values.

IV.5 Emitted intensities for N-Kα radiation as a function of accelerating voltage

During our efforts to measure the integral k-ratios for N-Kα radiation of the various nitride specimens relative to Cr_2N as a function of accelerating voltage we had an excellent opportunity to measure at the same time the absolute N-Kα intensities as a function of voltage. Such measurements can be extremely useful in the process of testing the correctness and consistency of the mac for N-Kα in a particular nitride specimen, provided that a set of high quality intensity measurements is available over a sufficiently wide range in accelerating voltage. The two most stringent requirements for such measurements are :
1) The beam current must be accurately known. In our equipment this is not such a big problem because the beam current is automatically measured before and after each

TABLE IV.4

Area-Peak Factors for N-Kα relative to Cr_2N (Batch # 1) for the nitrides of the present investigation. The numbers in parentheses refer to the number of measurements involved.

Compound	Area-Peak Factor STE	Area-Peak Factor LDE
BN (Hex)	1.0522 (77)	1.1010 (5)
(Cub)	------	1.0820 (7)
AlN	0.9829 (36)	0.9825 (7)
Si_3N_4	1.0707 (78)	1.0838 (6)
Ti_2N	0.9710 (*)	0.9800 (*)
TiN	0.9710 (*)	0.9800 (*)
V_2N	0.9948 (80)	0.9960 (70)
VN	1.0048 (81)	1.0048 (71)
Cr_2N	1.0000 Def.	1.0000 Def.
CrN	1.0180 (75)	1.0180 (62)
Fe_4N	1.0318 (33)	0.9941 (12)
ZrN	0.9644 (88)	0.9778 (68)
Nb_2N	0.9599 (101)	0.9969 (84)
Nb_4N_3	1.0135 (112)	1.0207 (94)
Mo_2N	1.0572 (139)	1.0334 (96)
HfN	0.9732 (90)	0.9841 (77)
Ta_2N	0.9695 (90)	0.9806 (77)
TaN	0.9751 (90)	0.9863 (76)

* *These results have been obtained from numerous spectra involved in the development of our new procedure for analysis of Nitrogen in Ti-N compounds (Section IV.2)*

measurement.
2) The absolute intensities must exhibit an extremely smooth and consistent variation with accelerating voltage.

The latter requirement presented us with a big problem indeed, because with the exception of the lighter nitrides BN, AlN and Si_3N_4, where the intensity measurements could be performed on the peak within one day over the full range in voltage, the vast majority of the nitrides had to be measured in an integral fashion, which took one night per accelerating voltage per specimen. Hence, approximately two weeks were necessary to complete the measurements on only one nitride specimen. The direct consequence of such a long period in time is that the absolute intensities can exhibit a rather large scatter due to changes in the atmospheric conditions (open gas-flow counter !). It is, therefore, hardly likely that such measurements could lead to the necessary smoothness and consistency required.

In order to arrive at sets of absolute emitted intensities which are as smooth and consistent as possible we have,

therefore, chosen a different approach. One good set of measurements on Cr_2N, performed during the continuous (one day) measurements on cubic BN was selected as the basic reference set and all other emitted intensities were calculated from the integral k-ratios relative to Cr_2N, measured over the 2-week period. These k-ratios would not be expected to show the scatter in the absolute intensities because they are relative rather than absolute quantities. In this way we managed to arrive at the best possible results under these (difficult) circumstances. Fig. IV.13 gives an example of these measurements for BN. All numerical data are given in Appendix 1, not only for Nitrogen but also for all the metal X-ray lines that could be excited in the voltage range.

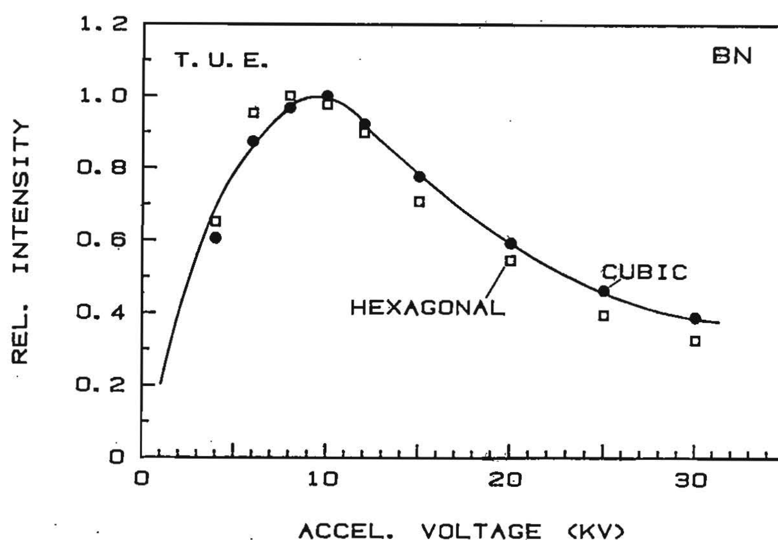

Fig. IV.13 Relative N-Kα intensity emitted from Hexagonal (open squares) and Cubic (full circles) BN as a function of accelerating voltage.

Fig. IV.13 reflects another problem, hardly discussed until now : The problem of a lack of electrical conductivity in some of the nitride specimens. Hexagonal BN (open squares) was the most notorious example we encountered so far in this respect, although we had some problems too with AlN and Si_3N_4. The influence of a lack of electrical conductivity on the quantitative results of EPMA has been discussed in detail in one of our recent publications[32]. It has been shown that the application of a conductive (Carbon) coating will not necessarily lead to meaningful results, not even when a hole is burned in the conductive coating using an air jet, like we have done for hexagonal BN in Fig. IV.13. It is obvious that the conductive cubic form of BN shows a different variation of emitted intensity with voltage than the hexagonal one, suggesting at first sight a different mac of N-Kα in BN. Fig. IV.14 a-h gives the results for all other nitride specimens.

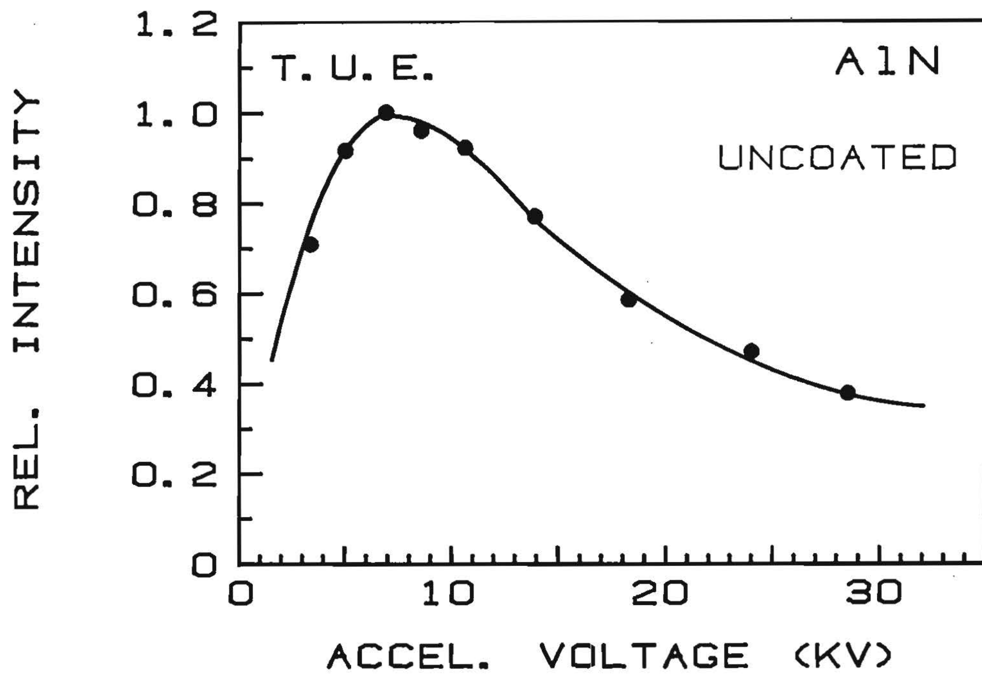

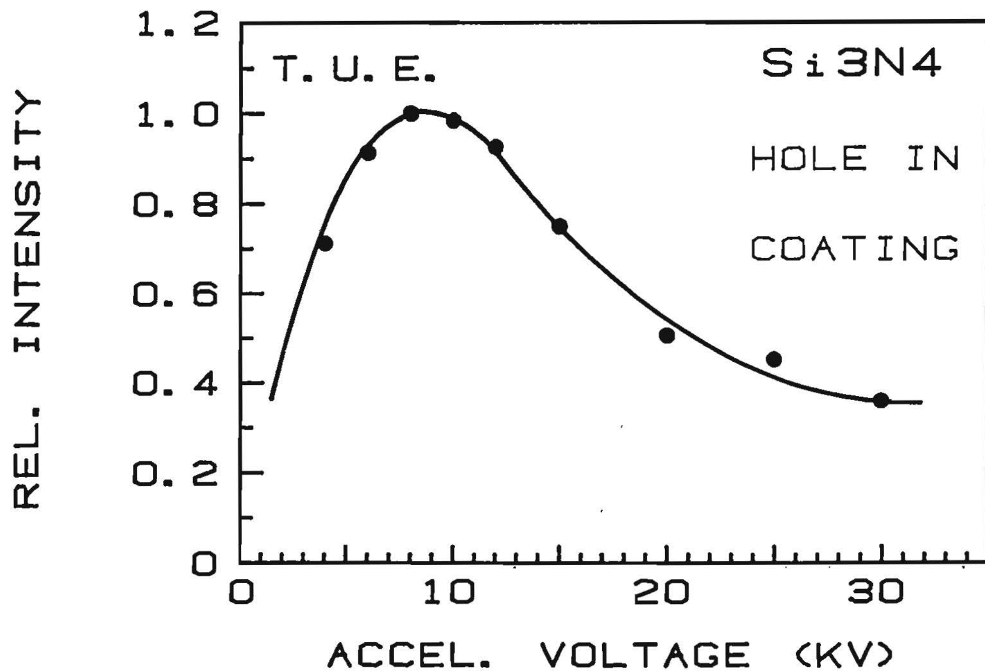

Fig. IV.14.a. Relative emitted N-Kα intensities from AlN (top) and Si_3N_4 (bottom) as a function of accelerating voltage. Note the slight voltage drop in the uncoated AlN due to surface charging. Si_3N_4 was measured through a hole burned in a Carbon coating. For numerical details see Appendix 1

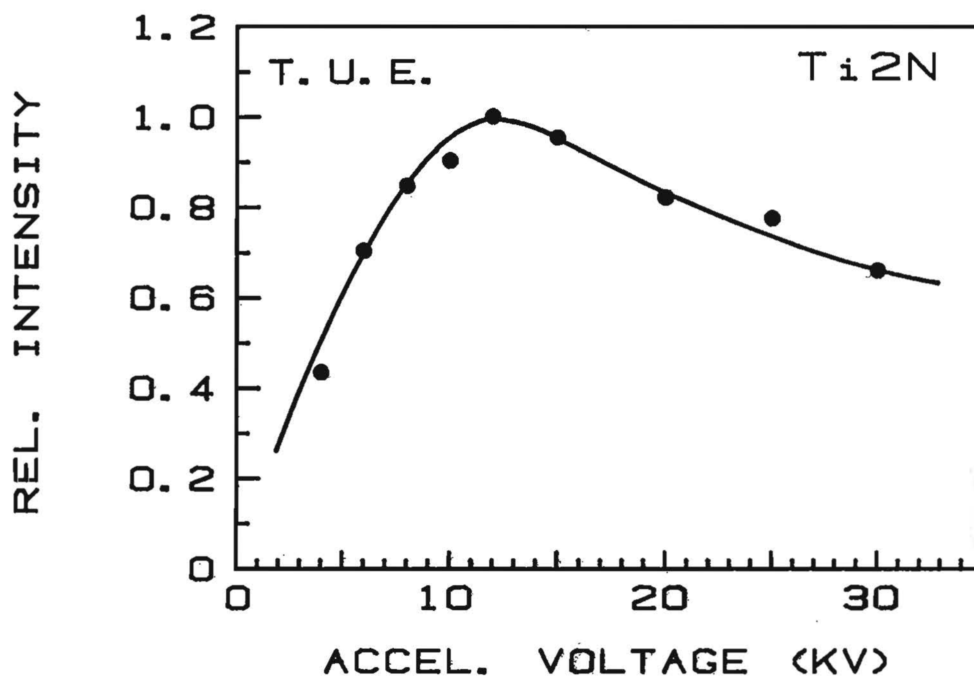

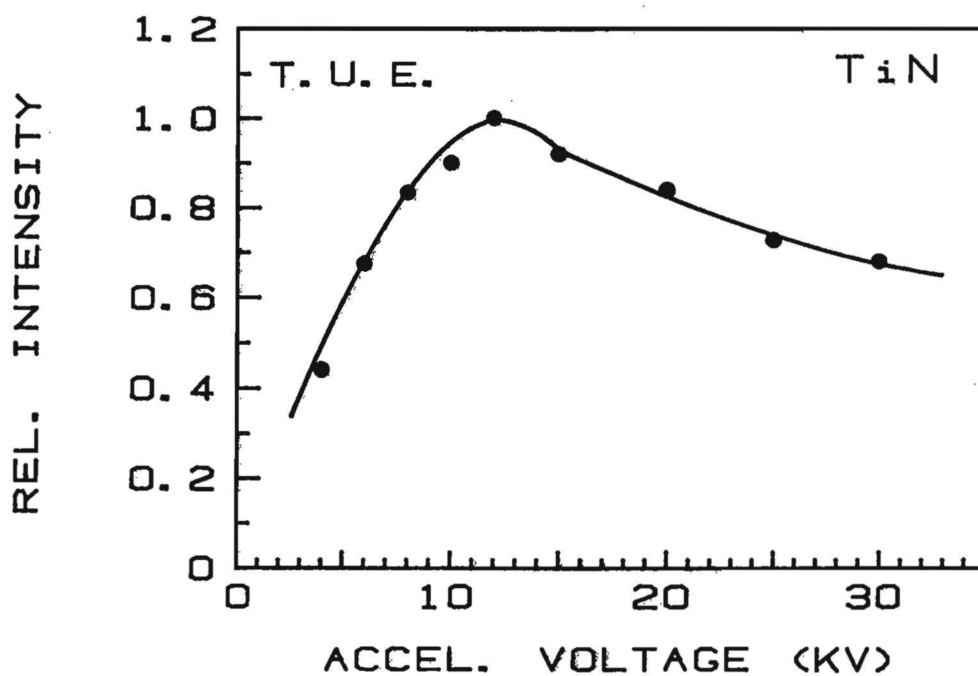

Fig. IV.14. b. Relative emitted N-Kα intensities from Ti_2N (top) and TiN (bottom) as a function of accelerating voltage. No coating used. For numerical details see Appendix 1

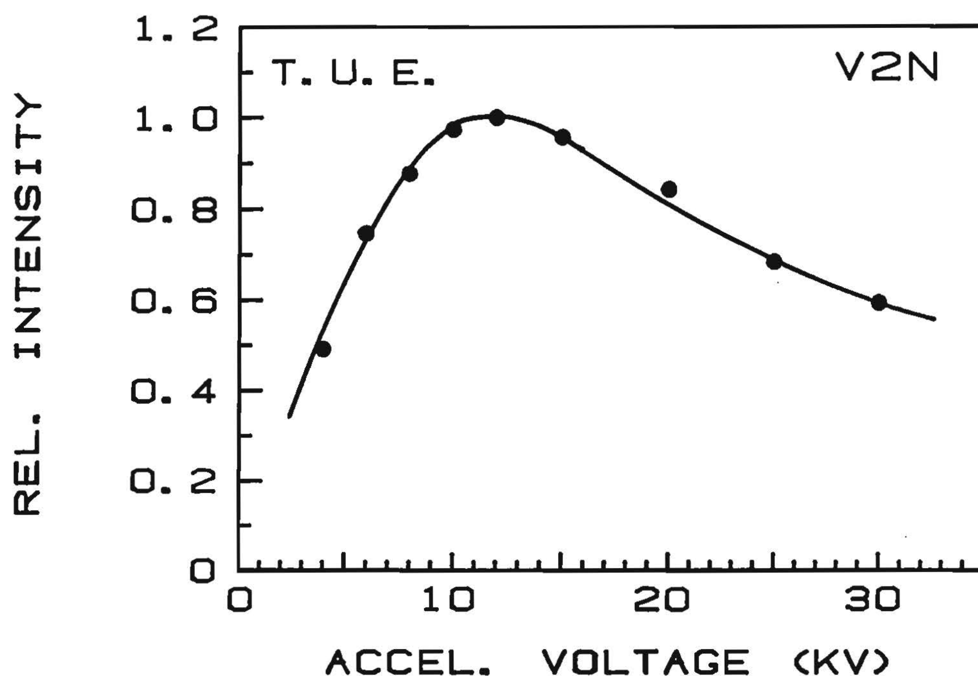

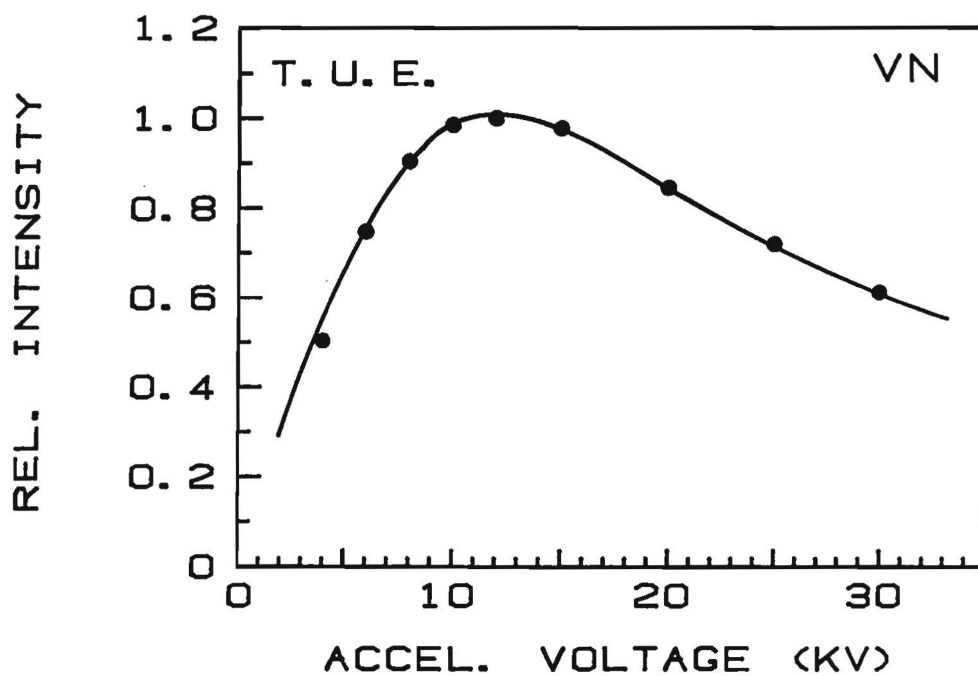

Fig. IV.14.c. Relative emitted N-Kα intensities from V_2N (top) and VN (bottom) as a function of accelerating voltage. No coating used. For numerical details see Appendix 1

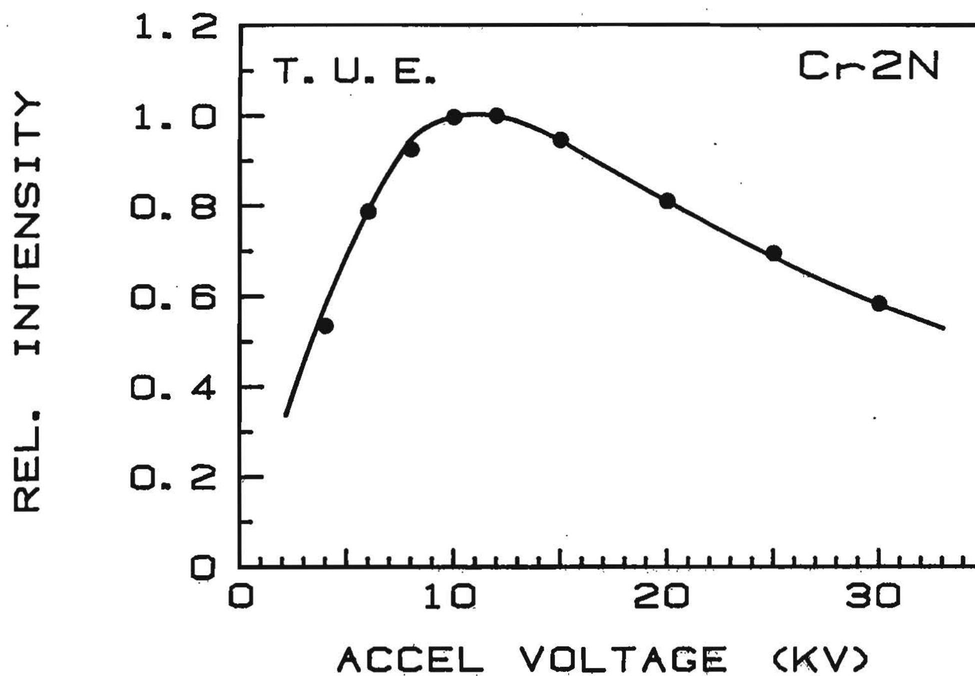

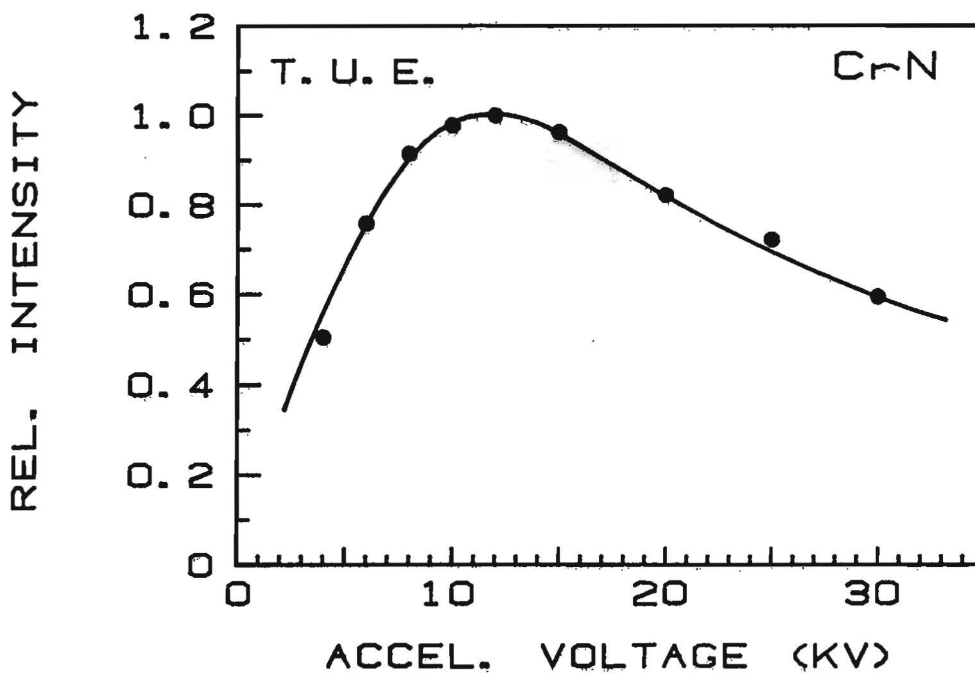

Fig. IV.14. d. Relative emitted N-Kα intensities from Cr_2N (top) and CrN (bottom) as a function of accelerating voltage. No coating used. For numerical details see Appendix 1

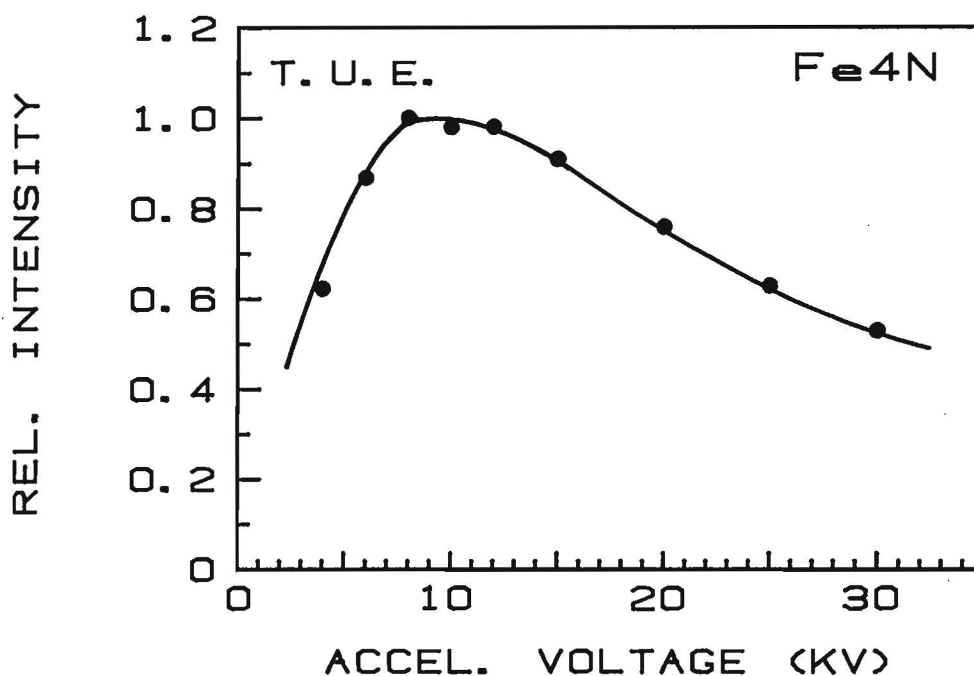

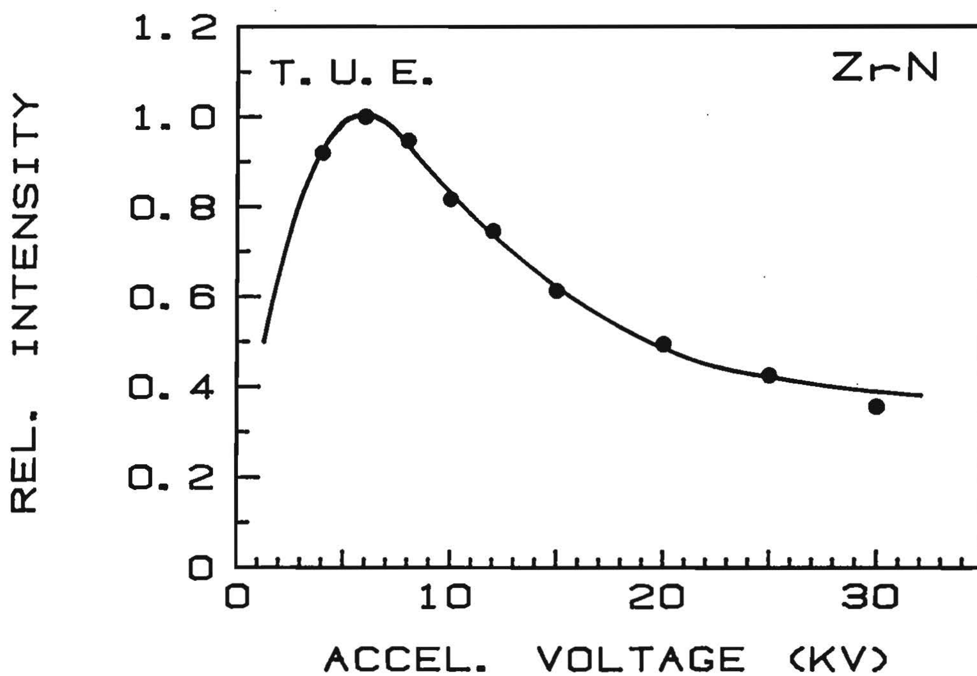

Fig. IV.14. e. Relative emitted N-Kα intensities from Fe_4N (top) and ZrN (bottom) as a function of accelerating voltage. No coating used. For numerical details see Appendix 1

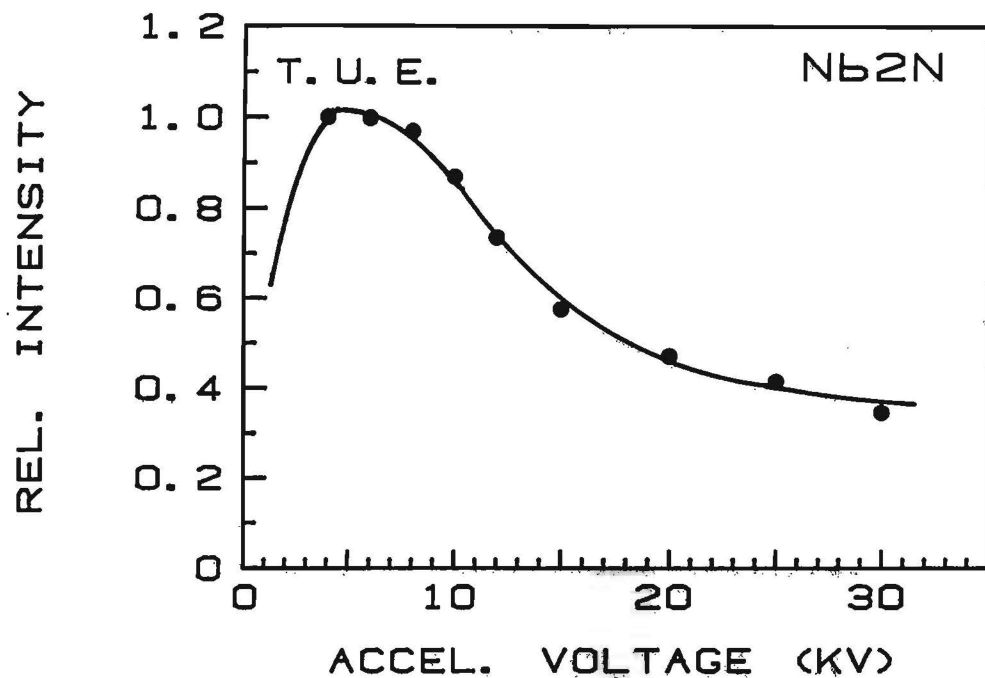

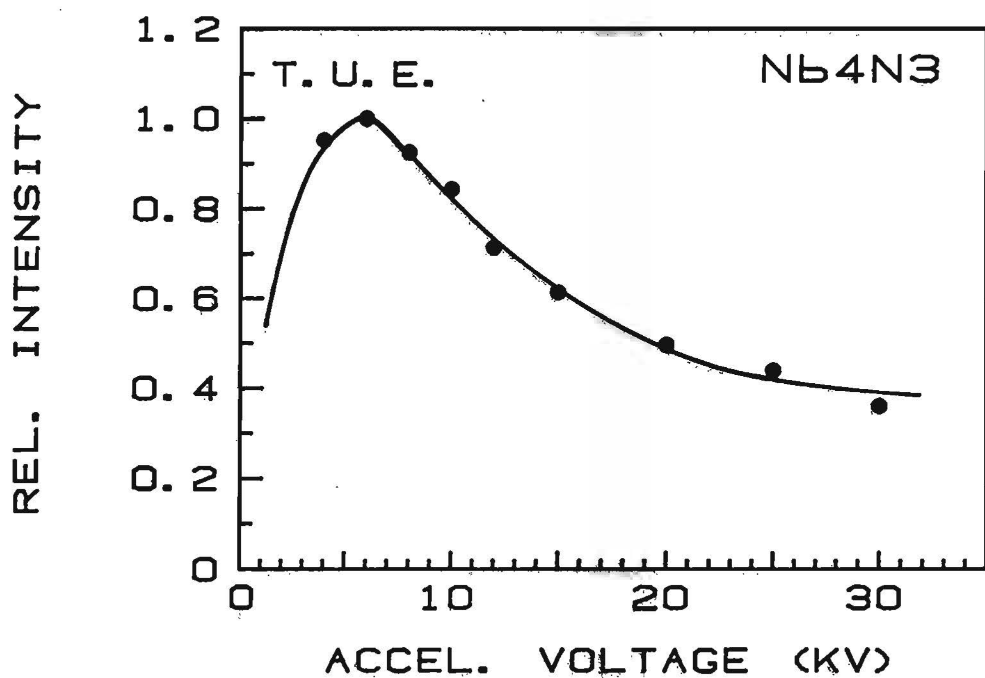

Fig. IV.14. f. Relative emitted N-Kα intensities from Nb_2N (top) and Nb_4N_3 (bottom) as a function of accelerating voltage. No coating used. For numerical details see Appendix 1

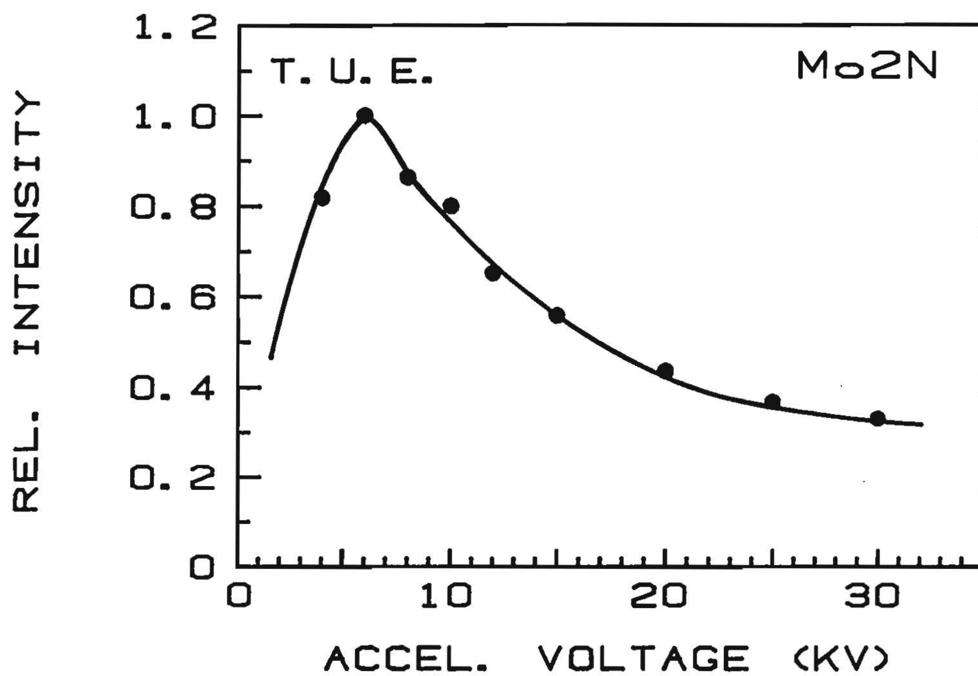

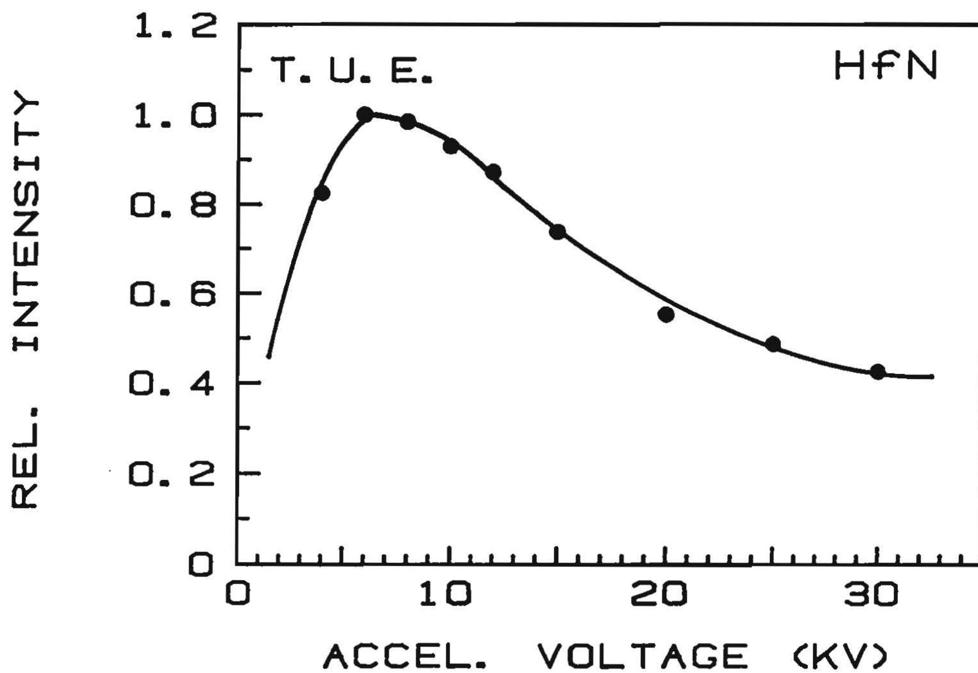

Fig. IV.14. g. Relative emitted N-Kα intensities from Mo_2N (top) and HfN (bottom) as a function of accelerating voltage. No coating used. For numerical details see Appendix 1

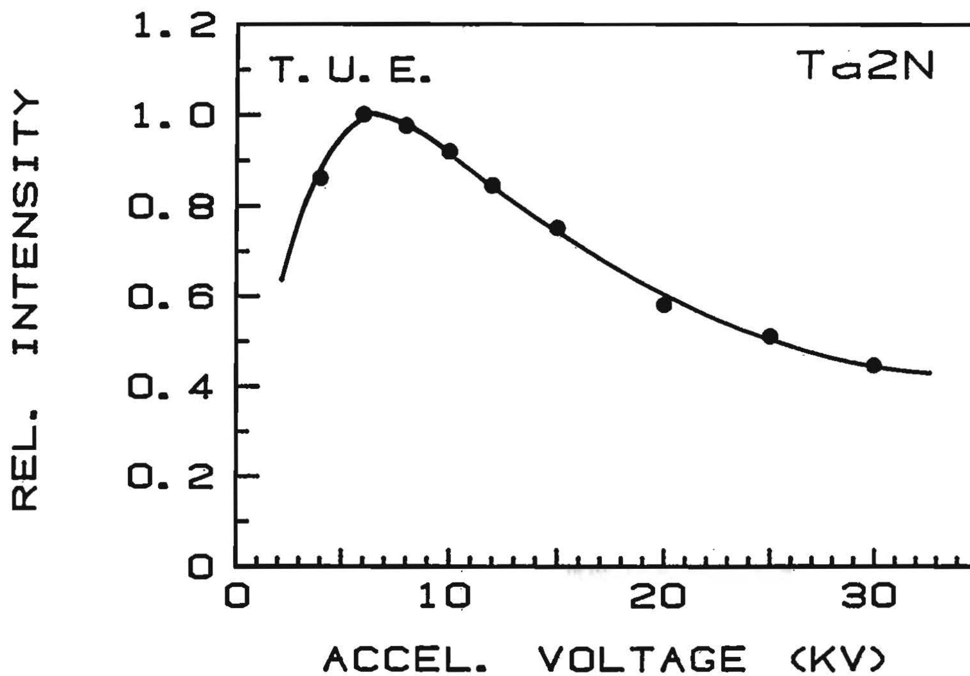

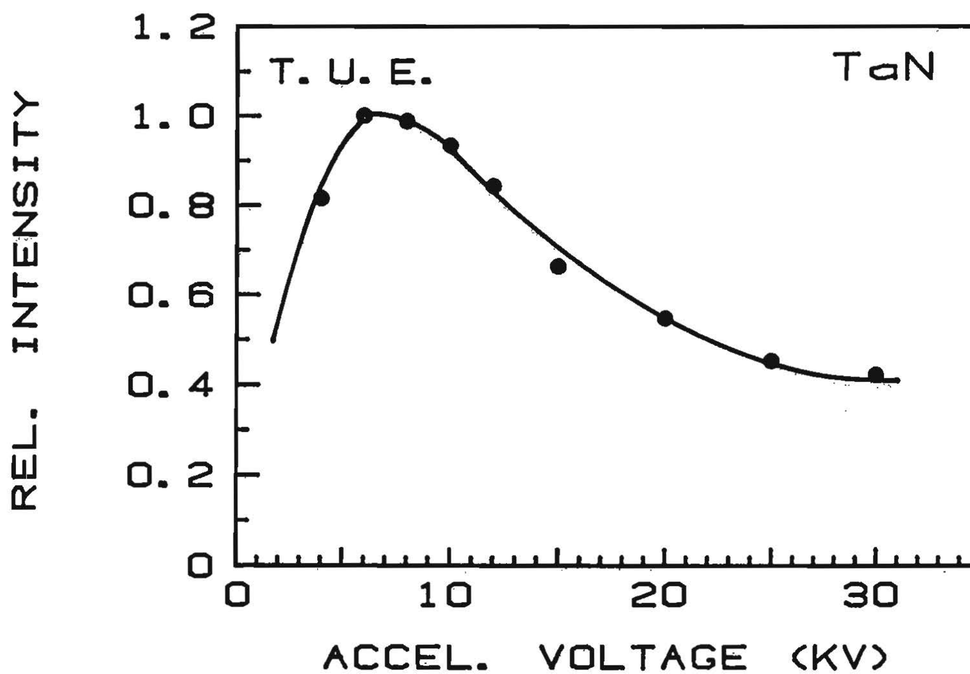

Fig. IV.14. h. Relative emitted N-Kα intensities from Ta_2N (top) and TaN (bottom) as a function of accelerating voltage. No coating used. For numerical details see Appendix 1

The problems with the non-conducting hexagonal form of BN not only manifested themselves in a deviating behaviour of the emitted intensity with varying voltage but also in an abnormal variation of k-ratio with accelerating voltage : It proved virtually impossible to obtain agreement between the observed k-ratios and the predictions made by our correction program (see Chapter V), not only for N-Kα but also for B-Kα. Attempts to perform the measurements on carbon-coated samples (standard, as well as specimen) were only partly successful : only the voltage range around 10 kV yielded anywhere near acceptable results. Outside this range, however, large deviations were usually observed. Also all efforts to perform the measurements through a hole burned in the carbon coating using an air jet failed to produce tolerable results.

As soon as the measurements could be carried out on cubic BN, however, which exhibits a much better electrical conductivity, everything was back to normal again and good agreement was found between predictions and observations, without the use of any coating.

The measurements on Si_3N_4 could be performed quite successfully through holes burned in a carbon coating. Apparently the presence of a well-conducting Si-substrate underneath the 2.5 μm Si_3N_4 layer provides sufficient relief to the incoming electrons as to prevent serious charging effects inside the specimen. Possible slight surface charging effects are obviously alleviated by the presence of the remaining carbon coating surrounding the hole.

The measurements on AlN could be carried out without any coating at all. However, small voltage drops did occur at the specimen surface, due to charging. This was established by recording the short-wavelength cut-off at the CRT of the EDX system. Table IV.5 gives a survey of the observed apparent beam voltage as compared to the nominal accelerating voltage.

TABLE IV.5

Relationship between the apparent beam voltage, measured from the short-wavelength cut-off on the CRT of the EDX system, and the nominal accelerating voltage for uncoated AlN

Nominal Voltage (kV)	Apparent Voltage (kV)
4	3.38
6	5.02
8	6.92
10	8.56
12	10.64
15	13.92
20	18.28
25	24.00
30	28.50

The apparent voltages have been used in the voltage scale of Fig. IV. 14 a (AlN) and in the final data base.

V DATA REDUCTION

After the accurate measurements of absolute and relative emitted intensities in all the nitride specimens the last step in the procedure is the conversion of measured k-ratios into concentration units. Ever since we started our work on ultra-light element analysis in 1983 we have been very much in favour of the surface-centred Gaussian $\phi(\rho z)$ approach for matrix correction, which was introduced by Packwood and Brown[22] in 1981. Our special appeal to this particular approach in bulk matrix correction and certainly for thin film applications stems from the consideration that this method is based on realistic X-ray distribution functions with depth, the so-called $\phi(\rho z)$ functions. The particular advantage of these $\phi(\rho z)$ functions is that they enable the calculation of the generated as well as the emitted X-ray intensities at any depth in the specimen, contrary to the so-called "ZAF" approaches which allow only the calculation of the total amounts of generated and emitted intensities. As we have pointed out already in Chapter II these $\phi(\rho z)$ approaches provide the best possible starting position for the analysis of thin films and in-depth profiling. However, they are of the utmost importance also for the analysis of ultra-light elements. In cases of extreme absorption the absorption correction depends almost entirely upon the $\phi(0)$ value and the very first (curved) part of the $\phi(\rho z)$ curve (see e.g. Fig. II.3), an area which is ignored in the absorption correction schemes of many "ZAF" correction models.

Since the time when we adopted the Gaussian Packwood and Brown model for matrix correction we have continuously tried to improve the original equations on which it was based, mainly by using the data bases which we collected during our work on light element analysis; starting with Carbon[1], followed by Boron[2], and at present Nitrogen. In the meantime the work on Oxygen has also been completed. As a result an extensive data base is now available for testing and improving correction programs and sets of mac's. When more and more data became available we have been able to produce better and better programs in the course of the last six years, not only for light element analysis but also for the analysis of medium-to-high Z elements. Our ultimate goal has always been to arrive at a correction program which can be applied universally.

We shall now give a brief description of the fundamentals of the Gaussian $\phi(\rho z)$ approach, followed by the details of our latest correction program. Finally we shall discuss the results that could be achieved in the present work.

V.1 Fundamentals of the Gaussian $\phi(\rho z)$ approach

The $\phi(\rho z)$ approach of Packwood and Brown[22] is based on the observation that most measured $\phi(\rho z)$ curves can be fitted with an equation of the type :

$$\phi(\rho z) = \gamma \cdot [1 - \frac{\gamma - \phi(o)}{\gamma} \cdot \exp - (\beta \rho z)] \cdot \exp - (\alpha^2 \cdot (\rho z)^2)$$

In this equation the ionisation ϕ as a function of mass-depth ρz is basically given by the Gaussian expression :

$$\gamma \cdot \exp - (\alpha^2 \cdot (\rho z)^2)$$

in which γ can be regarded as a scaling factor or starting point for the basic surface-centred Gaussian and α represents the decay rate in the Gaussian. The functional behaviour of all parameters involved is best demonstrated with the help of Fig. V. 1.

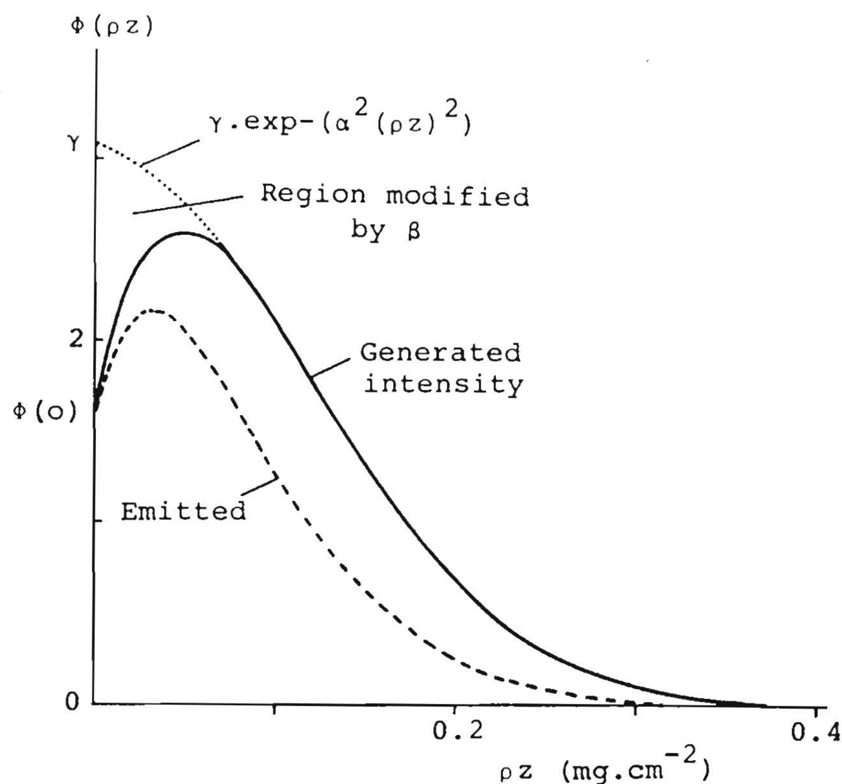

Fig. V.1 Example of a $\phi(\rho z)$ curve showing the functional behaviour of the four Gaussian parameters α, β, γ and $\phi(o)$. Solid curve represents the generated intensity while the lower broken curve corresponds to the actually emitted intensity.

The basic surface-centred Gaussian function is modified in the near-surface regions by a transient function :

$$(\gamma - \phi(o)) \cdot \exp - (\beta \rho z)$$

This transient function has been introduced in order to deal with the rate at which the originally collimated electron beam becomes randomized (see Chapter II).

Straight-forward integration of the generated $\phi(\rho z)$ curve between $\rho z=0$ and infinity gives the **generated** intensity within the specimen. Multiplication of each point in the generated $\phi(\rho z)$ curve with the absorption factor $\exp - (\chi \rho z)$, in which χ stands for $\mu/\rho \cdot \text{cosec}\ \psi$ (ψ is take-off angle), gives the **emitted** intensity as a function of mass depth (lower broken curve in Fig. V.1). This emitted intensity can also be integrated between the ρz limits of zero and infinity in order to yield the total amount of **emitted** intensity from either standard or specimen. Now, the k-ratio is linearly proportional to the ratio in the calculated integrals of the emitted intensities from specimen and standard and the proportionality constant is simply the concentration of the element in question in the specimen .

The performance of the Gaussian $\phi(\rho z)$ approach for matrix correction is, of course, largely dependent upon the successful parameterization of the parameters α, β, γ and $\phi(o)$ on which the model is based. In the course of the years we have produced a number of different versions[1,2,3,6,31] of our correction program, based on parameterizations obtained from the latest experimental data available at each time. After the completion of our data files for the ultra-light elements Boron, Carbon, Nitrogen and (in the meantime) Oxygen and the final establishment of an acceptable data file of 877 measurements on medium-to-high Z elements[31] we made a new parameterization which produces optimum results for all cases at hand. The new program, which has been called "PROZA", must be considered as more or less "final", although, of course, there will always be room for further improvements. However, it is our expectation that future improvements will be of a minor nature. The same PROZA program has been used in the meantime for the development of a Thin Film Analysis program ("TFA", 1 layer) and a Multilayer Analysis program ("MLA", up to 5 layers). We shall now give the details on our PROZA program.

V.2 Latest parameterizations of the PROZA $\phi(\rho z)$ program

In this new program a drastic change has been made compared to previous versions[1,2,3,30,31] in which the $\phi(\rho z)$ parameterizations were based on independent equations for the Gaussian parameters α, β, γ and $\phi(o)$ in the Packwood-Brown model[22].

The value of the parameter β is now no longer calculated using an independent equation but through a procedure based on the atomic number correction of Pouchou and Pichoir[8].
This atomic number correction provides the value of the integral of $\phi(\rho z)$ (i.e. the generated intensity in the

specimen) which will be called F.
Using the F-value and new expressions for α and γ the value of β is mathematically adapted in such a way as to ensure that the integral equals F and to ensure at the same time that the peak of the $\phi(\rho z)$ curve has both the "correct" position as well as the correct height.
This means that the parameters α, β, γ and $\phi(o)$ are now forced to cooperate in a consistent way in order to provide a specified value for the total generated intensity in the specimen.
The main reason why this procedure has been adopted is that now a better and more consistent performance of the correction program must be expected at low overvoltage ratios; an area which has always caused problems in previous versions.

PROCEDURE

STEP #1 Calculation of Primary (Generated) Intensity (P.I.) and integral of $\phi(\rho z)$ (≡ F) according to Pouchou and Pichoir[8].

The Primary Intensity (P.I.) can be expressed as the product of R * 1/S, in which R stands for the backscatter factor and S is the so-called "stopping power" of the matrix:

$$1/S = \int_{E_o}^{E_c} Q_i(E)/(dE/d\rho s)\ .dE \qquad (1)$$

E_o and E_c are accelerating voltage and critical excitation voltage of the X-ray line in question. The parameter $Q_i(E)$ is the ionisation cross-section at voltage E of the same X-ray line and $dE/d\rho s$ is the energy loss rate for the electrons along a small increment $d\rho s$ in path (ρ is density, s is linear length).
The electron energy loss rate itself can be expressed by:

$$dE/d\rho s = (-1/\overline{J})\ .\ (\sum C_i\ .\ Z_i/A_i)\ .\ (1/f(V)) \qquad (2)$$

C_i, Z_i and A_i are concentration, atomic number and atomic weight of the matrix element in question and V is defined by $E/\overline{J}$, in which $\overline{J}$ stands for the mean ionization potential. The latter, in turn, is defined by:

$$\ln \overline{J} = (\sum C_i\ .\ Z_i/A_i\ .\ \ln J_i)/M$$

J_i is calculated according to Zeller[12]:

$$J_i = Z_i\ .\ [10.04 + 8.25\ .\ \exp(-Z_i/11.22)] \quad (J_i \text{ in eV})$$

$$M = \sum C_i\ .\ Z_i/A_i$$

In equation (2) the usual Bethe expression has been replaced by a semi-empirical expression in terms of f(V), mainly in order to ensure a more reliable performance below 15 kV[8]. The parameter f(V) is the sum of three terms :

$$f(V) = \sum_{k=1}^{3} D_k \cdot V^{P_k} \quad \text{, with:}$$

$D_1 = 6.6 * 10^{-6}$ $\qquad P_1 = 0.78$

$D_2 = 1.12 * 10^{-5} \cdot (1.35 - 0.45 \cdot \overline{J}^2)$ $\qquad P_2 = 0.1$

$D_3 = 2.2 * 10^{-6} / \overline{J}$ $\qquad P_3 = -(0.5 - 0.25 \cdot \overline{J})$

The ionisation cross-section $Q_i(U)$ of the i-shell is proportional to:

$$\ln(U)/(E_c^2 \cdot U^m)$$

in which $U = E/E_c$ and:

$m = 0.86 + 0.12 \cdot \exp[-(Z_A/5)^2]$ for K-shell excitations
$m = 0.82$ for L-shell excitations
$m = 0.78$ for M-shell excitations

Z_A is the atomic number of the excited atom.
The use of these particular expressions for the ionisation cross-sections, which seem to be in better agreement[8] with experimental data, makes it possible to calculate the integral in equation (1) analytically. After introducing a new parameter T_k $(=1 + P_k - m)$ it can be shown that the Primary Intensity P.I. can be written as:

$$P.I. = R.(U_o/V_o/M) \cdot \sum_{k=1}^{3} D_k \cdot (V_o/U_o)^{P_k} \cdot (T_k \cdot U_o^{T_k} \cdot \ln U_o - U_o^{T_k} + 1)/T_k^2$$

The backscatter factor R can be calculated according to:

$$R = 1 - \overline{\eta} \cdot \overline{W} \cdot [1 - G(U_o)]$$

in which the mean electron backscatter coefficient $\overline{\eta}$ and the average reduced energy $\overline{W}$ of the backscattered electrons can be written as:

$$\overline{\eta} = 1.75 * 10^{-3} \cdot \overline{Z_p} + 0.37 \cdot [1 - \exp(-0.015 \cdot \overline{Z_p}^{1.3})]$$

$$\overline{Z_p} = (\sum C_i \cdot Z_i^{0.5})^2$$

$$\overline{W} = \overline{E}/E_o = 0.595 + \overline{\eta}/3.7 + \overline{\eta}^{\,4.55}$$

$G(U_o)$ is de Coulon-Zeller expression[12]:

$$G(U_o) = [U_o - 1 - (1 - 1/U_o^{\alpha+1})/(1+\alpha)]/(2+\alpha)/J(U_o)$$

with : $J(U_o) = 1 + U_o \cdot (\ln U_o - 1)$ and $\alpha = (2\overline{W} - 1)/(1 - \overline{W})$

Once the Primary Intensity is known, the integral of $\phi(\rho z)$ ($\equiv$ F) can be calculated by dividing the Primary Intensity by the ionisation cross-section:

$$F = P.I./\ Q_i(E_o)$$

STEP #2 Parameterization of Gaussian $\phi(\rho z)$ curves.

The object of this step is to find the α, β, γ and $\phi(o)$ parameters which will provide the correct integral of $\phi(\rho z)$ ($\equiv$ F).

- The equation for $\phi(o)$ is that used by Pouchou and Pichoir[8] :

$$\phi(o) = 1 + 3.3 \cdot (1 - 1/U_o^{\gamma}) \cdot \overline{\eta}^{\,1.2}$$

$$\text{with :} \qquad \gamma = 2 - 2.3 \cdot \overline{\eta}$$

- Our latest equation for α is:

$$\alpha = \frac{2.1614.10^5 .\ Z^{1.163}}{(U_o-1)^{.5} \cdot E_o^{1.25} \cdot A} \cdot \left[\frac{\ln(1.166\ E_o\ /\ J)}{E_c}\right]^{.5}$$

in which Z, A, and J are atomic number, atomic weight and ionisation potential of the matrix element. E_o, E_c and U_o are accelerating voltage, critical excitation voltage and overvoltage for the X-ray line in question. For a compound target a matrix of $\alpha_{i,j}$ values (α for element i-radiation in interaction with element j of the matrix) is calculated and the α_i-value in the compound target is composed as follows :

$$(1/\alpha_i)_{comp.} = \sum_j C_j \cdot \frac{Z_j}{A_j} \cdot 1/\alpha_{i,j} \Big/ \sum_j C_j \cdot \frac{Z_j}{A_j}$$

- The equation for γ is:

for $U_o \leq 6$:

$$\gamma = 3.98352 \cdot U_o^{-0.0516861} \cdot \left(1.276233 - U_o^{-1.25558 \cdot Z^{-0.1424549}}\right)$$

for $U_o > 6$:

$$\gamma = 2.814333 \cdot U_o^{0.262702 \cdot Z^{-0.1614454}}$$

In order to accommodate the change in ionisation cross-section with atomic number for ultra-light element radiations, proposed by Pouchou and Pichoir, it is necessary in these cases to multiply γ further by the equation:

$$E_c / (-4.1878.10^{-2} + 1.05975 \cdot E_c)$$

This is only necessary if $E_c < 0.7$ keV.
For a compound target the weight-fraction averaged atomic number is substituted for Z.

- The calculation of β proceeds in the following way:
We have shown before[30] that the total intensity generated in a specimen ($\equiv$ F) can be expressed by:

$$F = \frac{[\gamma-(\gamma-\phi(o)) \cdot R(\beta/2\alpha)] \cdot \sqrt{\pi}}{2\alpha}$$

in which $R(\beta/2\alpha)$ is the fifth degree polynomial used in the approximation of the erfc $(\beta/2\alpha)$ function. In fact, the latter equation is the formal solution of the Gaussian integral of $\phi(\rho z)$ between 0 and infinity in closed form. After rearranging it follows that:

$$R(\beta/2\alpha) = [\gamma - 2\alpha \cdot F/\sqrt{\pi}]/[\gamma - \phi(o)]$$

Contrary to our previous versions this time F is known first and the problem is now to find the value of β using the known values of α, γ and $\phi(o)$ through the latter equation. This means that the function $R(\beta/2\alpha)$ has to be used backward: i.e. the function value is known and the argument $(\beta/2\alpha)$ has to be determined.

The simplest way to solve this problem was to cut the function into 9 different regions and to fit these regions with much simpler geometric functions. If for a moment we substitute x for $R(\beta/2\alpha)$ we obtained as the best fits:

$.9 \le x < 1$	$\beta/2\alpha = .9628832 - .9642440.x$
$.8 < x < .9$	$\beta/2\alpha = 1.122405 - 1.141942.x$
$.7 < x \le .8$	$\beta/2\alpha = 13.43810.exp(-5.180503.x)$
$.57 < x \le .7$	$\beta/2\alpha = 5.909606.exp(-4.015891.x)$
$.306 < x \le .57$	$\beta/2\alpha = 4.852357.exp(-3.680818.x)$
$.102 < x \le .306$	$\beta/2\alpha = (1-.5379956.x)/(1.685638.x)$
$.056 < x \le .102$	$\beta/2\alpha = (1-1.043744.x)/(1.604820.x)$
$.03165 < x \le .056$	$\beta/2\alpha = (1-2.749786.x)/(1.447465.x)$
$0 < x \le .03165$	$\beta/2\alpha = (1-4.894396.x)/(1.341313.x)$

As a result of the fitting procedure the value of $R(\beta/2\alpha)$ thus obtained will never be exactly the same as the one calculated before, especially near the transition points of one function to another. In an extra loop in the program the approximated value of $R(\beta/2\alpha)$ is compared to the formal one and β is adjusted in an iterative procedure in order to produce a specified relative precision (at the moment 0.1 %) in the approximated value of $R(\beta/2\alpha)$ as compared to the formal one.

Once α, β, γ and $\phi(o)$ are known the usual procedure[30] can again be followed.
A special precaution had to be taken at extremely low overvoltages. In such cases it is virtually impossible to ensure a correct parameterization of $\phi(\rho z)$ curves due to the extreme delicacy involved in the balance of parameters which are still expected to produce the specified F-value. Thus it can happen occasionally that $R(\beta/2\alpha)$ values are calculated which are negative or larger than one.
It is obvious though, that $R(\beta/2\alpha)$ can only have values between 0 and 1, which means that β is between infinity and zero. When $R(\beta/2\alpha)$ is outside these limits then the normal parameterization route cannot be used and an auxiliary procedure has to be followed.
In these (rare) cases the calculated value of α is dropped and for a start it is assumed that the $\phi(\rho z)$ curve starts halfway the value of $\phi(o)$ and γ. Using the known value for F a new (and usually higher) value for α is calculated through:

$$\alpha = \frac{[\phi(o) + \gamma] \cdot \sqrt{\pi}}{4\ F}$$

The value of $R(\beta/2\alpha)$ is thereby set at exactly 0.5. Although the $\phi(\rho z)$ curves in such cases may not be 100 % realistic, the answers returned by the program are still very good because the atomic number correction is still consistent and the effects of (slight) shifts in the peak of the $\phi(\rho z)$ curves have a negligible influence on the magnitude of the absorption correction under these circumstances.
The advantage of the new program is that it can now be used down to the lowest possible overvoltages (if one insists on working under these difficult conditions).

V.3 Results of the PROZA program on previous data

V.3.1 Medium-to-heavy element analyses

The composition of this data base and the origin of the measurements contained in it have been discussed in detail before[31]. The original 627 analyses have been supplemented with the analyses of metal lines in carbides[1] and borides[2] totaling now 877 entries. This particular data base is the result of a time-consuming process of careful selection and check on internal consistency of all the entries involved.

Only highly consistent series of measurements have been admitted : These can be either measurements on a fixed (binary) composition but taken over a wide range in accelerating voltages or measurements at a fixed voltage but taken over a wide range in compositions inside the binary system. All isolated measurements were deleted from our file. The accelerating voltages in our file range from as low as 4 kV up to as high as 48.5 kV while the atomic numbers involved vary between 5 (B) and 92 (U).

The usual procedure to test a correction program on such a data file is to calculate for each entry the k-ratio (k') for the given composition and to compare it to the measured k-ratio. A convenient way to present the results is to display them in a histogram showing the number of analyses versus the ratio k'/k. The narrowness of the obtained distribution, in terms of the relative root-mean-square value (r.m.s. in %) and the average k'/k value are then used as a measure of success for the program in question. Of course, with the presence in our data file of cases of extreme absorption, e.g. Al-Kα measurements in Mg-9.1 wt % Al alloys up to 40 kV and a take-off angle as low as 20 deg., it is imperative to have the best possible parameterizations for the calculation of the mac's. It appears to us that the recent parameterization by Heinrich[33] gives the best results as far as can be judged with our data base. Therefore, we have used (and still use) this particular parameterization in our calculations. Fig. V.2 shows the histogram we obtained with our PROZA program under these conditions. It must be emphasized that the resulting excellent r.m.s. value of 2.44 % is not due to the program alone but still contains the sum of three errors :

1) The uncertainties in the nominal compositions.
2) The remaining errors in the intensity measurements, which will be appreciable in the cases of heavy absorption.
3) Possible errors and biases in the correction program itself in combination with remaining uncertainties in the mac's used.

Considering the fact that the experimental error is likely to be of the order of 1-2 % relative and probably much larger even in the cases of heavy absorption and/or low take-off angles, it is unlikely that significant further improvements in the program can be expected from future measurements.

V.3.2 Boron and Carbon analyses

The results obtained with PROZA on our Boron and Carbon data files are given in Table V.1. Please note that in this case the ratios between the calculated and the nominal concentration of the light element have been used. It is further important to note that significantly better results for Boron could be achieved when the results for the three Ni-borides would have been eliminated. These cases exhibit a 15 % too low emission of B-Kα radiation, which must be concluded from the fact that the averages in c'/c for all three sets of measurements come out at 0.84-0.87, in spite of the fact that the r.m.s. values range between 2 and 3.7 %, which means that the mac of B-Kα in Ni is satisfactory.

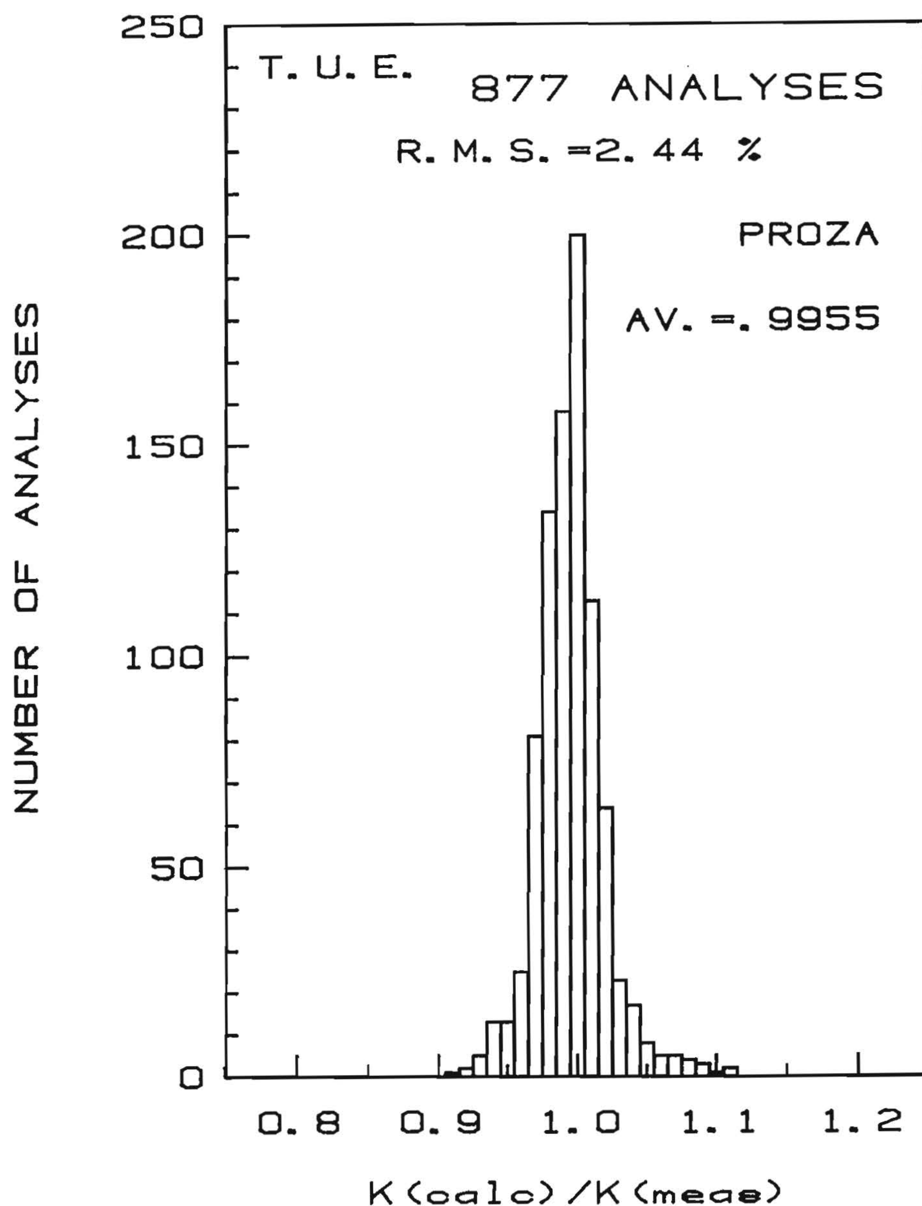

Fig. V.2 Histogram showing the results of the PROZA correction program on a data file of 877 analyses on medium-to-high Z elements.

Table V.1

Results obtained with PROZA on our Boron[2] and Carbon[1] data

Element	No. of meas. ts	Accel. Voltage (kV)	c'/c	r.m.s %
B	180	4-15 (30)	0.977	6-7
C	117	4-30	0.983	4

The results obtained with our new program on our previous data indicate an excellent performance of PROZA both for the ultra-light elements as for the heavier elements. In the latter case the performance at very low overvoltage ratios has greatly been improved.

V.4 Results from the present work

V.4.1 Analysis of the metal lines in the nitrides

The numerical details of the measurements are given in Appendix 1. All possible X-ray lines that could be excited between 4 and 30 kV have been measured. Appendix 2 gives the graphical displays. The (smoothed) k-ratios were finally entered into our data base (Appendix 3). Fig. V.2 gives the histogram obtained with PROZA on this data set of 149 entries.

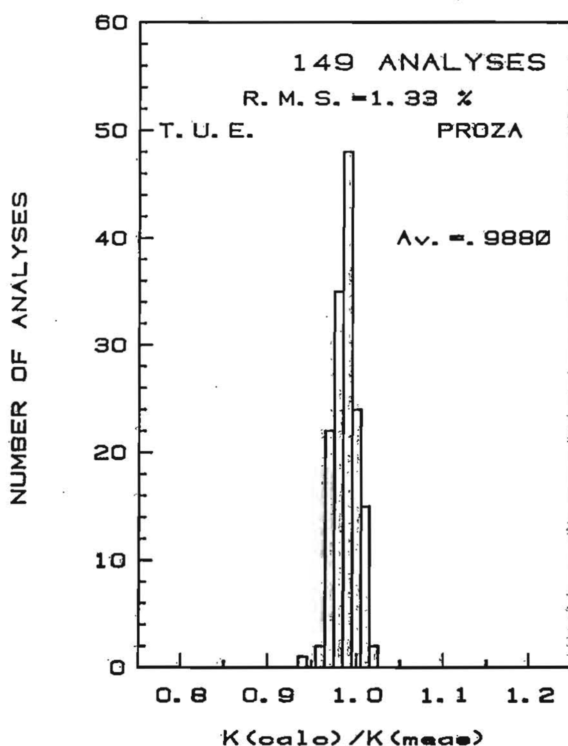

Fig. V.2 Histogram obtained with our PROZA program on a data file of 149 analyses of the X-ray lines of the metals in our nitride specimens between 4 and 30 kV.

The results of the individual sets of measurements are given in Table V.2. As the average overall k'/k ratio of 0.9880 and the r.m.s. figure of 1.3259 % indicate the program performs highly satisfactorily for this type of analysis.

V.4.2 Analysis of Nitrogen in the nitrides

The numerical details of all our Nitrogen measurements are given in Appendix 1., together with some special remarks on the procedures where appropriate. For the lighter Nitrides (BN up to TiN) the measurements were exclusively performed with the STE crystal. From V_2N on both STE and LDE crystals were used simultaneously. In the latter cases the final k-ratios for N-Kα were obtained by weighting the results in a 2:1 ratio in favour of LDE. Fig. V.3 shows the histogram obtained with PROZA on this data base of 144 (unsmoothed) k-ratios for N-Kα using the mac's of Table II.1.

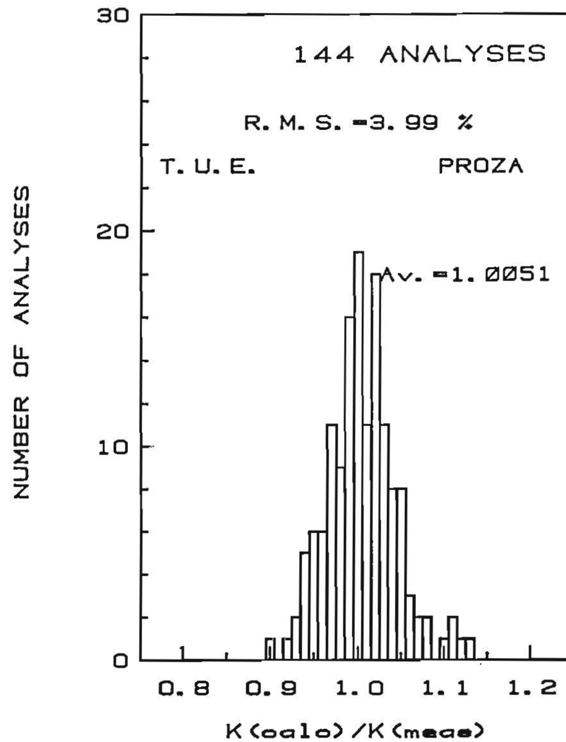

Fig. V.3 Histogram obtained with our PROZA program on a data base of 144 Nitrogen analyses between 4 and 30 kV. Mass absorption coefficients of Table II.1 were used.

The numerical results of the individual sets of measurements for Nitrogen are given in Table V.2, while the graphical representations are shown in Fig. V.4. a-h, together with the predictions of our program (solid curves). It is obvious that the program performs remarkably well up to accelerating voltages as high as 30 kV. The discrepancies between the predicted and the experimentally obtained k-ratios rarely exceed 5 % relative, even in the most difficult cases like ZrN, Nb_2N and Mo_2N. This is all the more remarkable because the measurements were obtained over a 2-week period in most cases and as a result one would expect a somewhat larger scatter than from a continuous (1-day) measurement.

Table V.2

Numerical results obtained in the individual sets of intensity measurements of the X-ray lines of the metals and Nitrogen in the Nitride specimens of the present investigation between 4 and 30 kV.

		Metal Analysis		Nitrogen Analysis	
Compound	**Line**	**Av. k'/k**	**R.M.S. %**	**Av. k'/k**	**R.M.S. %**
BN (cub)	B-Kα	0.9722	1.3966	0.9989	5.9150
AlN	Al-Kα	0.9867	0.6667	0.9867	3.4641
Si_3N_4	Si-Kα	0.9900	0.0000	1.0033	6.9121
Ti_2N	Ti-Kα	0.9725	0.4330	0.9856	3.2356
TiN	Ti-Kα	0.9725	0.4330	0.9922	2.8588
V_2N	V-Kα	0.9800	0.0000	1.0089	2.0245
VN	V-Kα	0.9800	0.0000	1.0056	1.7069
Cr_2N	Cr-Kα	0.9914	0.3499	------	------
CrN	Cr-Kα	0.9871	0.6999	0.9911	1.0999
Fe_4N	Fe-Kα	1.0100	0.0000	1.0322	1.4741
ZrN	Zr-Lα	0.9689	0.3143	1.0244	2.6713
Nb_2N	Nb-Lα	0.9911	0.5666	1.0367	4.4222
Nb_4N_3	Nb-Lα	0.9878	0.4157	0.9922	2.8197
Mo_2N	Mo-Lα	1.0011	0.8749	1.0267	5.0990
HfN	M/L-α	1.0022	0.6285	1.0022	1.9309
Ta_2N	Ta-Mα	0.9878	0.4157	0.9956	4.4500
"	Ta-Lα	1.0000	0.0000	------	------
TaN	Ta-Mα	0.9944	0.6849	1.0000	2.7487
"	Ta-Lα	1.0100	0.8944	------	------

OVERALL RESULTS :

METALS ANALYSES (149 entries) :
k'/k = 0.9880 R.M.S. = 1.3259 %

NITROGEN ANALYSES (144 entries) :
k'/k = 1.0051 R.M.S. = 3.9965 %

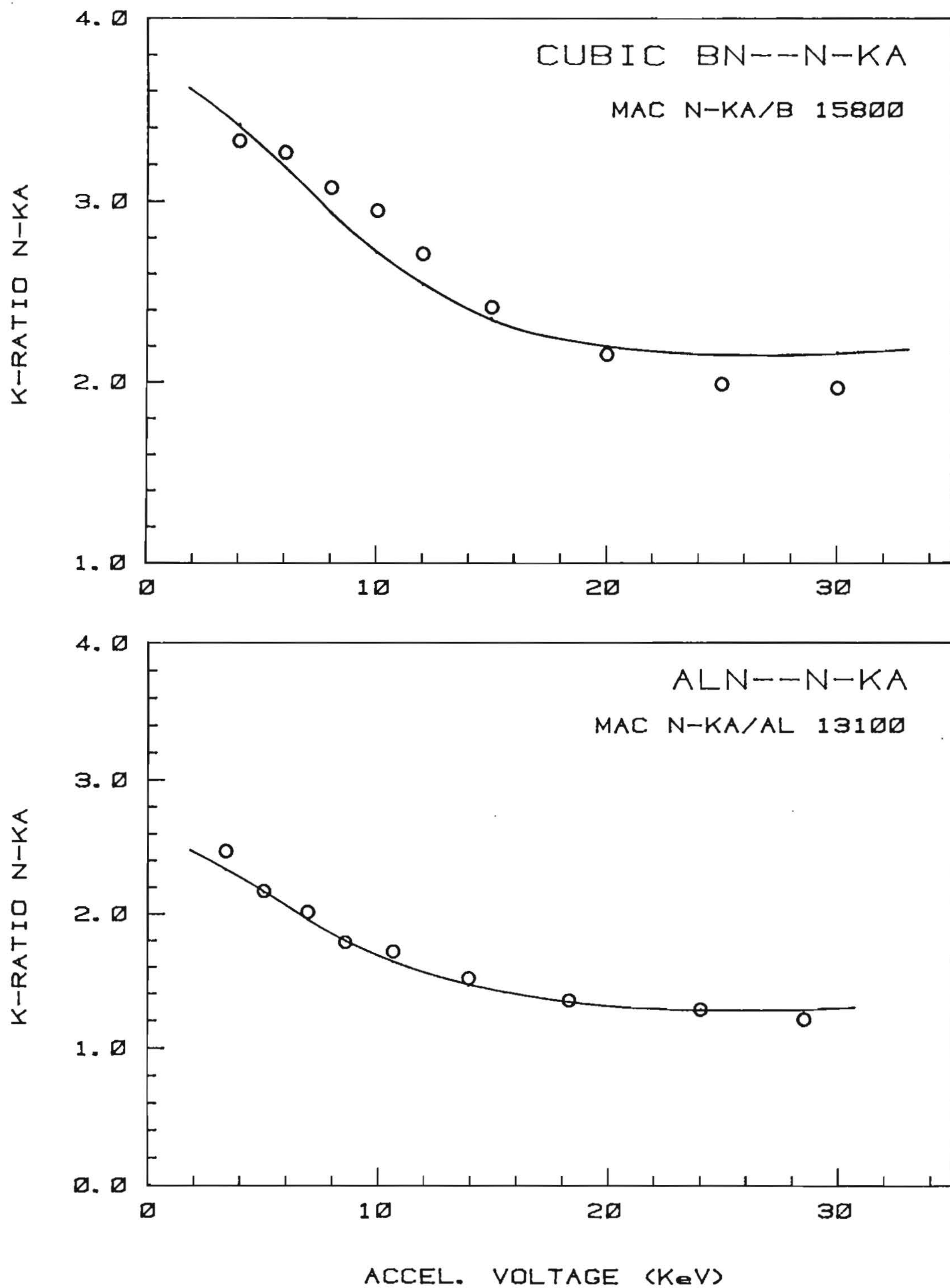

Fig. V.4.a. Comparison between the experimental integral k-ratios for N-Kα relative to Cr_2N (circles) and the predictions of our PROZA program (solid curve). Top : uncoated Cubic BN; bottom : uncoated AlN. Note the shift in the voltage for AlN due to slight surface charging effects. Stearate crystal only.

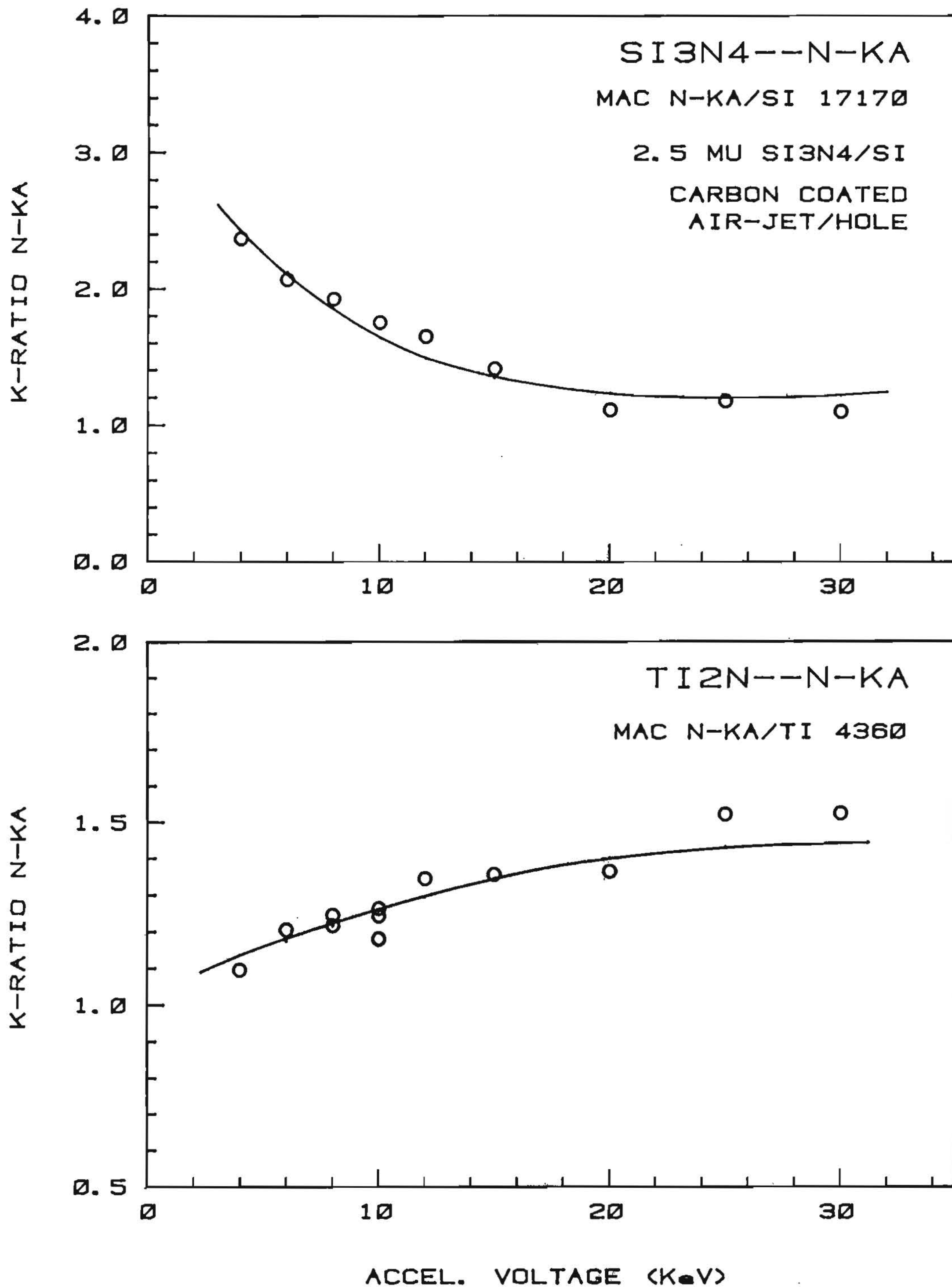

Fig. V.4.b. Comparison between the experimental integral k-ratios for N-Kα relative to Cr_2N (circles) and the predictions of our PROZA program (solid curve). Top : Si_3N_4 ; bottom : uncoated Ti_2N. Measurements on Si_3N_4 through holes burned in a carbon coating using an air jet. Stearate crystal only.

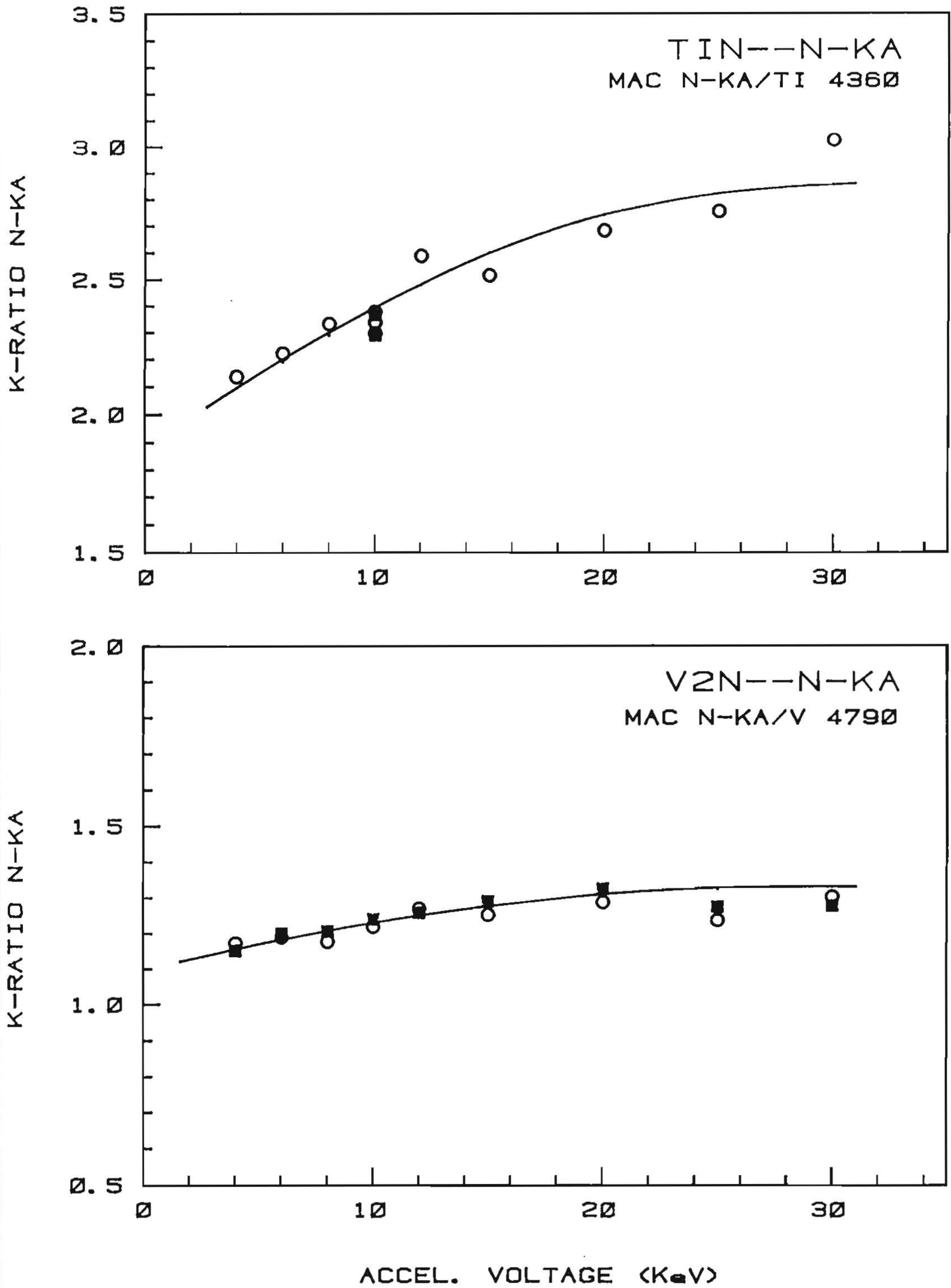

Fig. V.4.c. Comparison between the experimental integral k-ratios for N-Kα relative to Cr_2N and the predictions of our PROZA program (solid curve). Top : uncoated TiN ; bottom : uncoated V_2N. Circles indicate the results of the Stearate ; solid squares those of the LDE crystal.

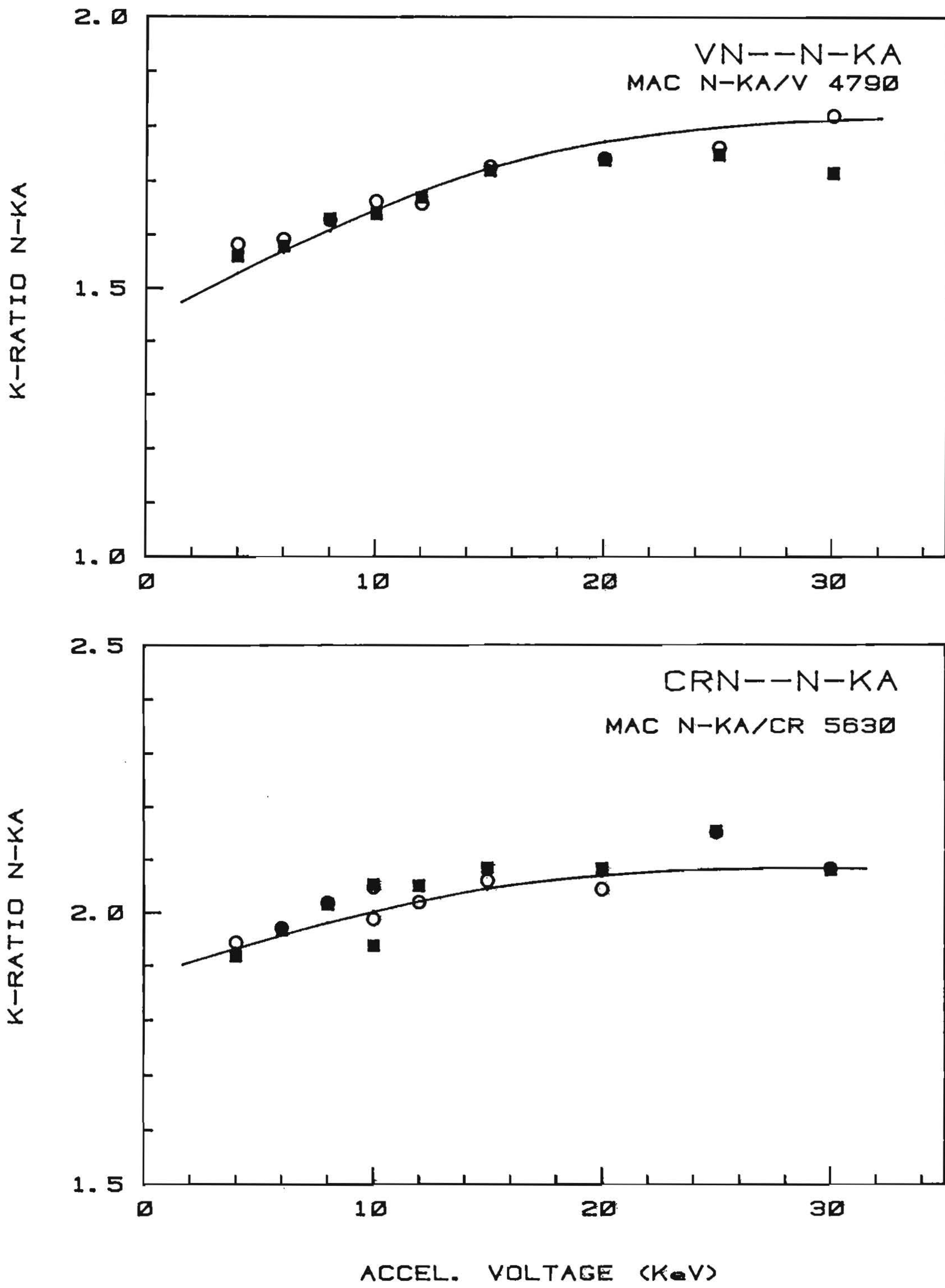

Fig. V.4.d. Comparison between the experimental integral k-ratios for N-Kα relative to Cr_2N and the predictions of our PROZA program (solid curve). Top : uncoated VN ; bottom : uncoated CrN. Circles indicate the results of the Stearate ; solid squares those of the LDE crystal.

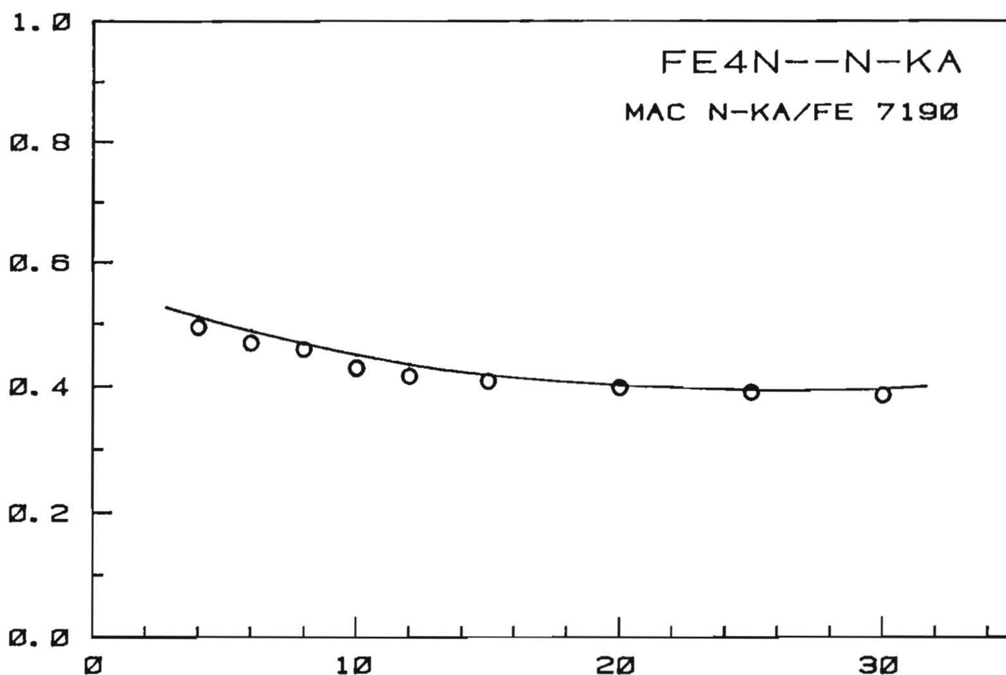

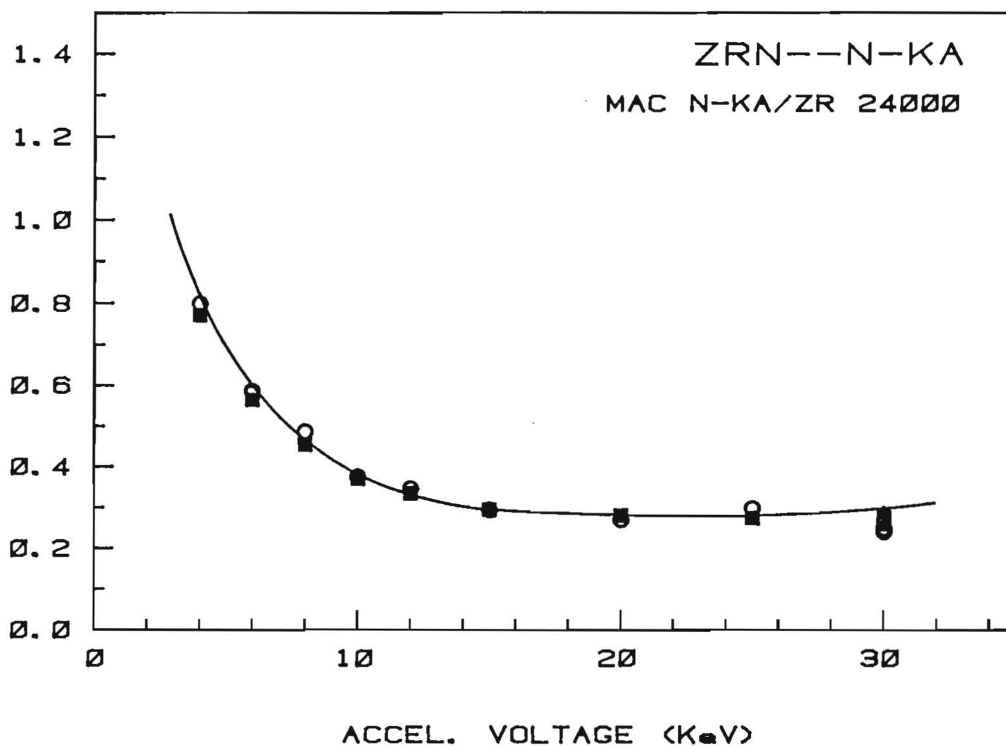

Fig. V.4.e. Comparison between the experimental integral k-ratios for N-Kα relative to Cr_2N and the predictions of our PROZA program (solid curve). Top : uncoated Fe_4N ; bottom : uncoated ZrN. Circles indicate the results of the Stearate ; solid squares those of the LDE crystal.

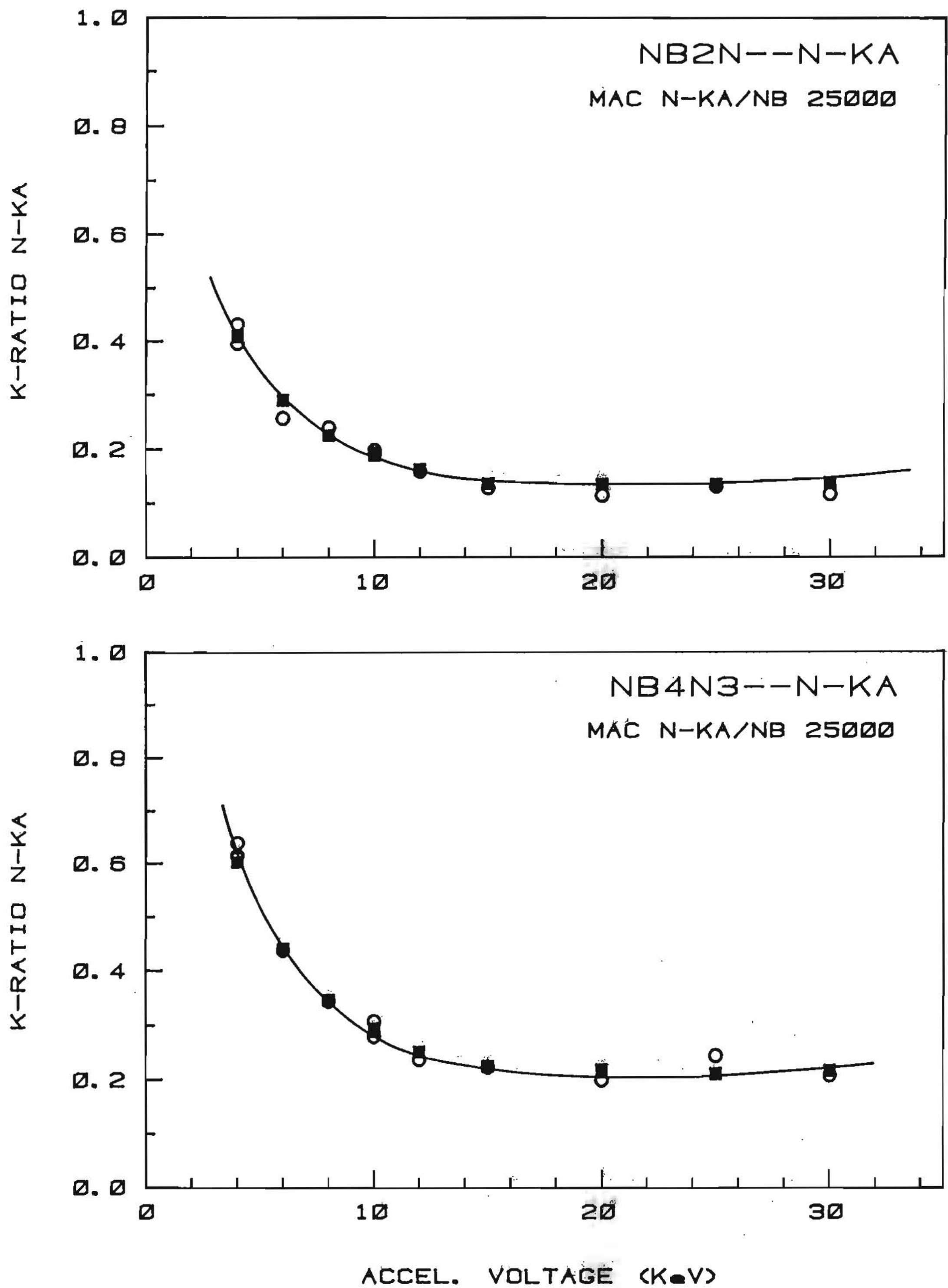

Fig. V.4.f. Comparison between the experimental integral k-ratios for N-Kα relative to Cr_2N and the predictions of our PROZA program (solid curve). Top : uncoated Nb_2N ; bottom : uncoated Nb_4N_3. Circles indicate the results of the Stearate ; solid squares those of the LDE crystal.

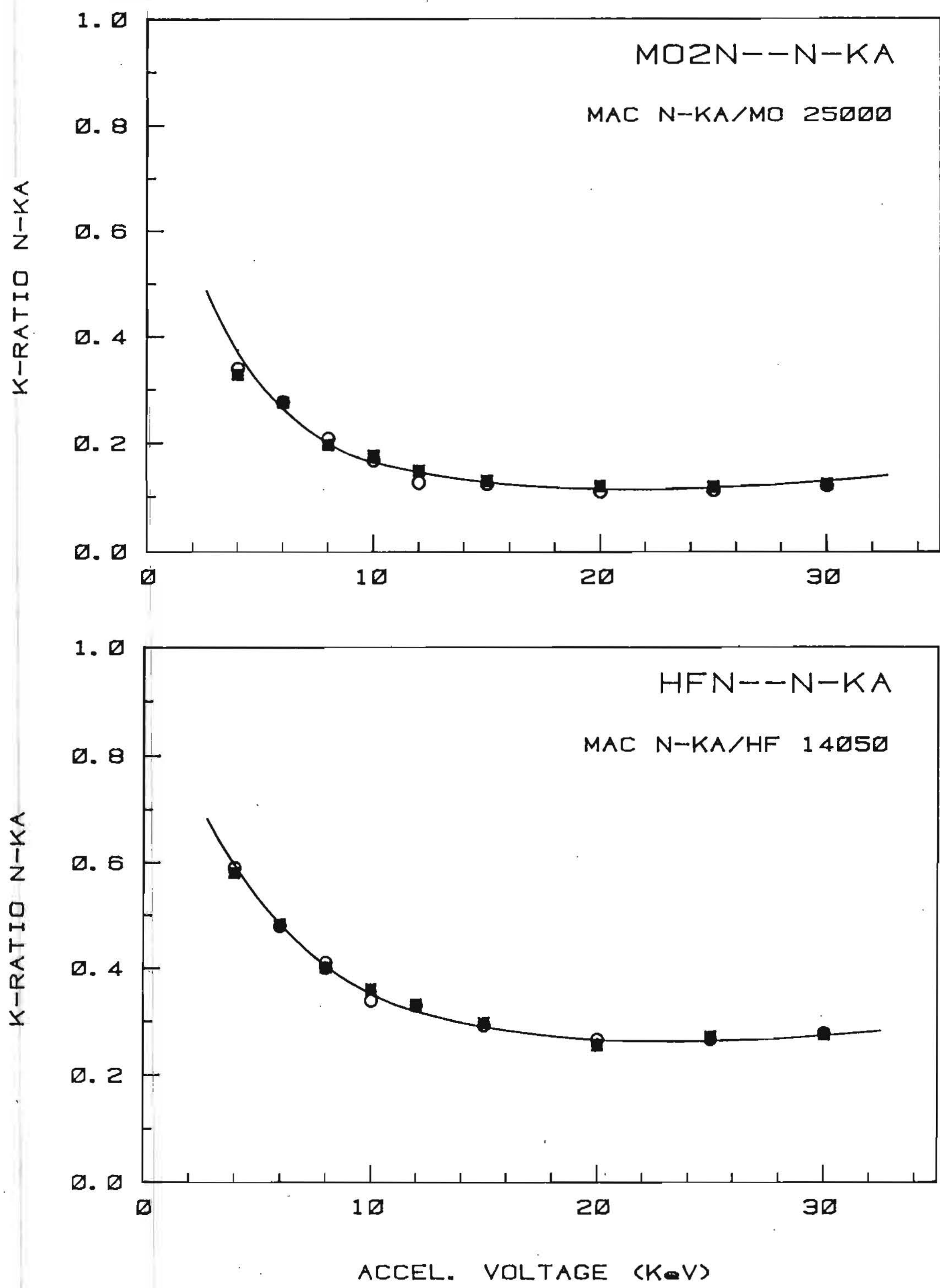

Fig. V.4.g. Comparison between the experimental integral k-ratios for N-Kα relative to Cr_2N and the predictions of our PROZA program (solid curve). Top : uncoated Mo_2N ; bottom : uncoated HfN. Circles indicate the results of the Stearate ; solid squares those of the LDE crystal.

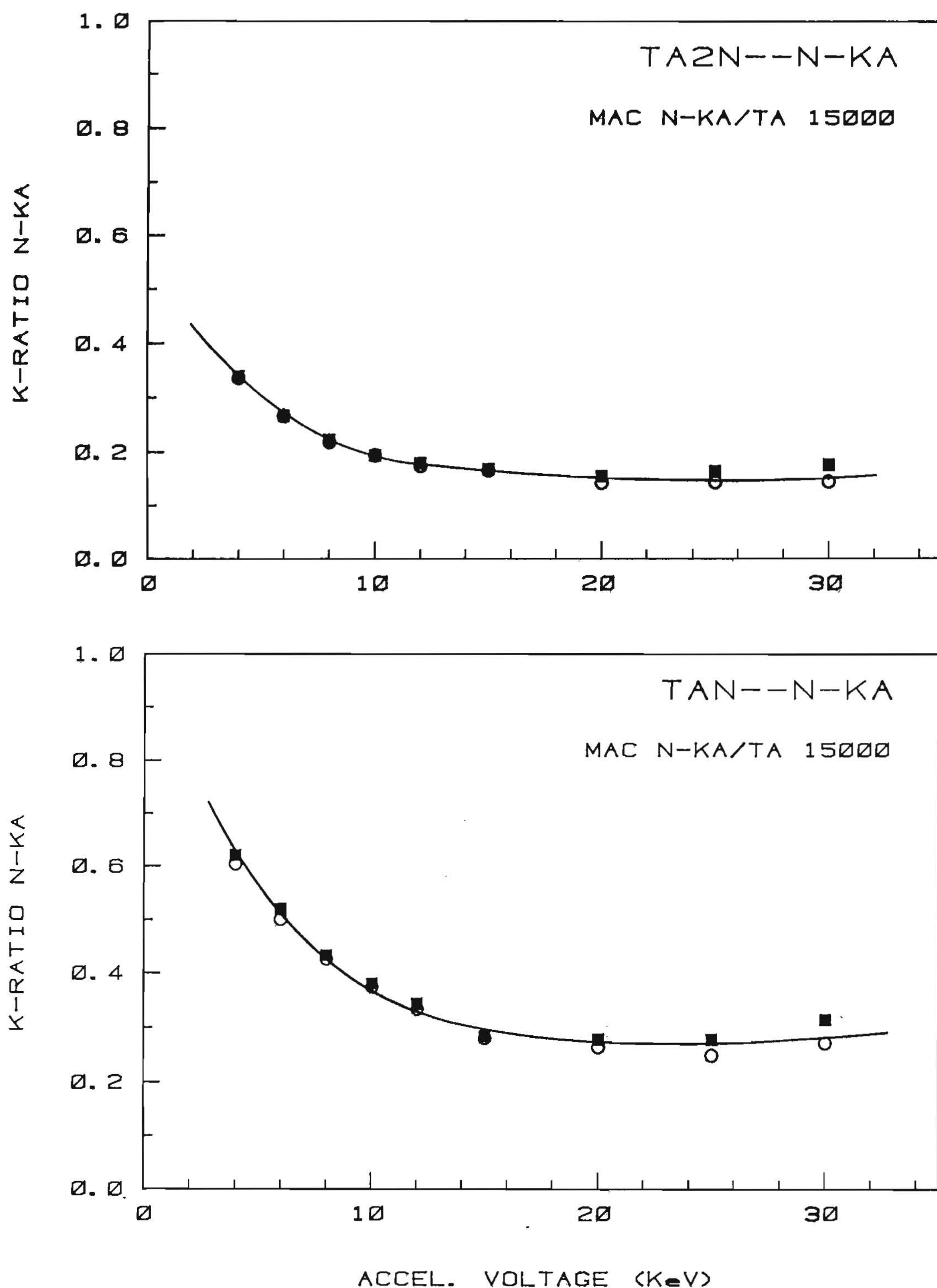

Fig. V.4.h. Comparison between the experimental integral k-ratios for N-Kα relative to Cr_2N and the predictions of our PROZA program (solid curve). Top : uncoated Ta_2N ; bottom : uncoated TaN. Circles indicate the results of the Stearate ; solid squares those of the LDE crystal.

VI CONCLUSIONS

A number of general conclusions can be drawn from the present work :

1) Accurate intensity measurements are possible for N-Kα radiation over a wide range in accelerating voltages, in spite of the fact that this particular element is by far the most difficult to deal with in the sequence of the ultra-light elements B, C, N and O.
The use of a modern synthetic multilayer crystal (W/Si, 2d=59.8 Å) gives a major improvement in this respect, since it can provide 2.8 times higher net peak intensities. At the same time, however, it can produce a strong suppression of higher-order reflections which is extremely beneficial for the accurate determination of the backgrounds.

2) Reasonably accurate (better than 5 % relative) analysis of Nitrogen appears to be possible even in Ti-containing compounds, in spite of the severe overlap of the Ti-ll and the N-Kα peaks. In this respect too the application of the W/Si multilayer crystal leads to major improvements in the results.

3) Peak shape alterations in the N-Kα peak, relative to a Cr_2N standard, are much smaller than those observed for B-Kα and C-Kα radiations : The APF-values (Area-Peak Factors) were found to differ less than 5 % from unity. Nevertheless, for accurate quantitative analysis these effects have to be taken into account.

4) Our latest Gaussian $\phi(\rho z)$ correction program "PROZA", which is based on new parameterizations for the Gaussian α, β, γ and $\phi(0)$ parameters, produces excellent results on the newly collected data base of 144 N-Kα measurements between 4 and 30 kV. However, the results are equally satisfactory on previous[1,2] ultra-light element data as well as on medium-to-high Z element data. The conclusion seems, therefore, justified that this latest program is a genuine step forward towards the ultimate goal of a "universal" correction program. At all times, however, it is imperative to use a set of the most consistent mass absorption coefficients.

The overall conclusion of the present work can be that accurate quantitative analysis of Nitrogen is definitely possible, provided that the measurements are performed carefully, a good correction program is used and, not in the last place, a consistent set of mass absorption coefficients is used.

REFERENCES

1. G.F. Bastin and H.J.M. Heijligers, "Quantitative Electron Probe Microanalysis of Carbon in binary Carbides", Internal Report, University of Technology, Eindhoven, The Netherlands (1984), ISBN 90-6819-002-4.

2. G.F. Bastin and H.J.M. Heijligers, "Quantitative Electron Probe Microanalysis of Boron in binary Borides", Internal Report, University of Technology, Eindhoven, The Netherlands (1986), ISBN 90-6819-006-7.

3. G.F. Bastin and H.J.M. Heijligers, X-ray Spec., **15**, 135-150 (1986).

4. G.F. Bastin and H.J.M. Heijligers, J. Microsc. Spectr. Electron., **11**, 215-228 (1986).

5. G.F. Bastin and H.J.M. Heijligers, Proc. 11th ICXOM, London, Canada (1986), Eds. J.D. Brown and R.H. Packwood, Univ. of Western Ontario Press, 257-261 (1987).

6. G.F. Bastin and H.J.M. Heijligers, Workshop at the Nat. Bureau of Standards, Paper # 1, August 1988, Gaithersburg, Md, USA., N.B.S. Spec. Publ. (in press).

7. J.L. Pouchou and F. Pichoir, Rech. Aerospat., **3**, 13 (1984).

8. J.L. Pouchou and F. Pichoir, Proc. 11th ICXOM, London, Canada (1986), Eds. J.D. Brown and R.H. Packwood, Univ. of Western Ontario Press, 249-253 (1987).

9. B.L. Henke and E.S. Ebisu, Adv. in X-ray Analysis, **17**, 150 (1974).

10. B.L. Henke et al., Atomic Data and Nuclear Data Tables, **27**, 1 (1982).

11. M.J. Berger and S.M. Seltzer, Nat. Acad. of Sc.- Nat. Res. Council, Publications, NASRA, **1133**, 205 (1964).

12. J.Coulon and C. Zeller, C.R. Acad. Sc. Paris, **276 B**, 215 (1973).

13. J. Ruste and C. Zeller, C.R. Acad. Sc. Paris, **284 B**, 507 (1977).

14. P. Duncumb and S.J.B. Reed, N.B.S. Spec. Publ., No. 298, 133 (1968).

15. H.J. Hunger and L. Küchler, Phys. Stat. Sol. (a), **56**, K 45 - K 48 (1979).

16. J. Philibert, J. Métaux, **465**, 157 (1964).

17. J. Ruste and M. Gantois, J. Phys. D: Appl. Phys., **8**, 872 (1975).

18. W. Reuter, Proc. 6th ICXOM, Osaka (1971), Univ. of Tokyo Press, 121 (1972).

19. G. Love, M.G. Cox and V.D. Scott, J. Phys. D: Appl. Phys., **11**, 7 (1978).

20. H.E. Bishop, J. Phys. D: Appl. Phys., **7**, 2009 (1974).

21. D.A. Sewell, G. Love and V.D. Scott, J. Phys. D. : Appl. Phys., **18**, 1233, (1985).

22. R.H. Packwood and J.D. Brown, X-ray Spec., **10**, 138 (1981).

23. H. Holleck, "Binäre und ternäre Carbid- und Nitridsysteme der Übergangsmetalle", Gebrüder Borntraeger Berlin - Stuttgart (FRG) 1984.

24. L. Wolff, G. Bastin and H. Heijligers, Solid State Ionics, **16**, 105 (1985).

25. E. Etchessahar, J.P. Bars and J. Debuigne, J. Less-Common Met., **134**, 123 (1987).

26. G. F. Bastin and H.J.M. Heijligers, Microbeam Analysis, D.E. Newbury, Ed., 325 (1988).

27. A. Armigliato, L. Dori, A Garulli and P. Venturi, J. Microsc. Spectr. Electron., **7**, 593 (1982).

28. J.J. McCarthy and F.H. Schamber, N.B.S. Spec. Publ., No. 604, 273 (1981).

29. G.F. Bastin and H.J.M. Heijligers, Microbeam Analysis, D.E. Newbury, Ed., 290 (1988).

30. G.F. Bastin, H.J.M. Heijligers and F.J.J. van Loo, Scanning, **6**, 58 (1984).

31. G.F. Bastin, H.J.M. Heijligers and F.J.J. van Loo, Scanning, **8**, 45 (1986).

32. G.F. Bastin and H.J.M. Heijligers, Workshop at the Nat. Bureau of Standards, Paper # 2, August 1988, Gaithersburg, Md, USA., N.B.S. Spec. Publ. (in press).

33. K.F.J. Heinrich, Proc. 11th ICXOM, London, Canada (1986), Eds. J.D. Brown and R.H. Packwood, Univ. of Western Ontario Press, 67-119 (1987).

Appendix 1...a

Nitride: BN (cubic)

Date: B-Kα 8-9-10 July 1987
N-Kα 8-9-10 July 1987

Compo: 56.45 wt% N
----- wt% O
43.55 wt% B

kV	Beam current (nA)		Net.intensities (cps/nA)				k-ratios		
			B-Kα integral		N-Kα integr		AKR	AKR N-Kα	
	B-Kα	N -Kα	B	BN	Cr_2N	BN	B-Kα	STE	LDE
4	300	300	9.15	3.428	4.55	15.141	0.3747	----	3.3278
6	300	300	13.47	4.468	6.69	21.840	0.3317	----	3.2646
8	300	300	16.21	4.629	7.87	24.197	0.2856	----	3.0746
10	300	300	17.19	4.364	8.48	25.019	0.2539	----	2.9503
12	300	300	16.80	3.887	8.51	23.071	0.2316	----	2.7111
15	300	300	15.99	3.278	8.05	19.427	0.2049	----	2.4133
20	300	300	13.35	2.434	6.89	14.827	0.1823	----	2.1520
25	300	300	10.64	1.916	5.82	11.574	0.1800	----	1.9887
30	300	300	8.54	1.566	4.96	9.753	0.1834	----	1.9663

Remarks: BN Cubic (black crystals); not coated!

Backgrounds: B-Kα: ± 25 mm on either side of the peak and interpolated
N-Kα: ± 11.2 mm (LDE)

PHA settings:	counter HT	Lower level	Window	Gain	Pulse	
B-Kα:	1700 volt	0.5 volt	3.0 V	64*5.5	2.0 V	AS STE
N-Kα:	1700 volt	0.5 volt	3.0 V	100*1.0	2.0 V	DS LDE

Appendix 1...b

Nitride: BN (Hex)

conductivity problems

Date: B-Kα February 1986
N-Kα March 1985

Compo: 56.45 wt% N
----- wt% O
43.55 wt% B

kV	Beam current (nA)		Net.intensities (cps/nA)				k-ratios			
			B-Kα integral		N-Kα integral		AKR B-Kα		AKR N-Kα hole in carb.	
	B-Kα	N-Kα	B	BN	Cr_2N	BN	no hole in carbon	hole in carbon	STE	LDE
4	300	300	12.41	3.825	4.55	15.022		0.3082	3.3016	----
6	300	300	18.33	5.131	6.69	21.961		0.2799	3.2827	----
8	300	300	21.93	5.513	7.87	23.074	*	0.2514	2.9319	----
10	300	300	23.65	5.366	8.48	22.529	0.2199	0.2269	2.6567	----
12	300	300	23.93	4.925	8.51	20.722	0.2255	0.2058	2.4350	----
15	300	300	22.27	4.104	8.05	16.331	0.2139	0.1843	2.0287	----
20	300	300	17.94	2.878	6.89	12.596	0.1915	0.1604	1.8282	----
25	300	300	14.32	2.165	5.82	9.117	0.1724	0.1512	1.5665	----
30	300	300	11.85	1.747	4.96	7.559	0.1573	0.1474	1.5240	----

<u>Remarks:</u> N-Kα: BN Carbon coated; Airjet, 20 minutes ⟶ hole in carbon
Cr_2N standard <u>NOT</u> coated

*Carbon coating (B & BN) without hole!
Conductivity problems below 10 kV
For Boron 10 holes burned in carbon coating 30 kV 300 nA 1 hour

Backgrounds: B-Kα: ± 25 mm on either side of the peak and interpolated
N-Kα: ± 6.7 mm (STE)

PHA settings:	counter HT	Lower level	Window	Gain	Pulse	
B-Kα:	1700 volt	0.5 volt	3.5 V	64*5.5	2.0 V	STE AS
N-Kα:	1700 volt	1.5 volt	1.0 V	32*8.0	2.0 V	STE AS

Appendix 1...c

Nitride: AlN

Date: Al-Kα 11-12 March 1985
N-Kα September 1985

Compo: 34.18 wt% N
----- wt% O
65.82 wt% Al

kV	Beam current (nA)		Net.intensities (cps/nA)				k-ratios		
			Al-Kα peak		N-Kα integral		PKR	AKR N-Kα	
	Al-Kα	N-Kα	Al	AlN	Cr2N	AlN	Al-Kα	STE	LDE
4	30	300	165.27	101.79	4.55	11.242	0.6159	2.4707	----
6	10	300	429.38	270.76	6.69	14.529	0.6306	2.1717	----
8	3	300	760.41	475.79	7.87	15.854	0.6257	2.0145	----
10	3	300	1102.55	672.84	8.48	15.220	0.6103	1.7948	1.7636
12	3	300	1459.38	902.42	8.51	14.612	0.6184	1.7170	----
15	1	300	1987.78	1182.51	8.05	12.209	0.5949	1.5166	----
20	1	300	2728.99	1586.83	6.89	9.303	0.5815	1.3502	----
25	1	300	3368.76	1863.90	5.82	7.467	0.5533	1.2830	----
30	1	300	3835.05	2040.82	4.96	6.002	0.5322	1.2100	----

Remarks: AlN not coated

Backgrounds: Al-Kα: ± 5 mm on either side of the peak and interpolated
N-Kα: ± 7 mm (STE)

PHA settings:	counter HT	Lower level	Window	Gain	Pulse	
Al-Kα:	1600 volt	0.6 volt	open	32*5.5	2.0 V	AS TAP
N-Kα:	1700 volt	1.5 volt	1.0 V	32*8.0	2.0 V	AS STE

Appendix 1...d

Nitride: Si_3N_4
2.5 μm /Si

Date: Si-Kα 13 March 1985
N-Kα March 1985

Compo: 39.24 wt% N
0.70 wt% O
60.06 wt% Si

kV	Beam current (nA)		Net.intensities (cps/nA)				k-ratios		
			Si-Kα peak		N-K-α integral		PKR	AKR	N-Kα
	Si-Kα	N-Kα	Si	Si_3N_4	Cr_2N	Si_3N_4	Si-Kα	STE	LDE
4	30	300	106.26	56.55	4.55	10.781	0.5322	2.3694	----
6	10	300	356.66	199.79	6.69	13.832	0.5602	2.0676	----
8	3	300	679.13	383.61	7.87	15.147	0.5649	1.9246	----
10	3	300	1020.70	579.78	8.48	14.904	0.5680	1.7575	1.7381
12	3	300	1393.84	785.39	8.51	14.013	0.5635	1.6467	----
15	1	300	1955.36	1081.84	8.05	11.350	0.5533	1.4099	----
20	1	300	2797.77	1524.90	6.89	7.646	0.5450	1.1097	----
25	--	300	----	----	5.82	6.832	----	1.1738	----
30	--	300	----	----	4.96	5.433	----	1.0954	----

Remarks: For Si-Kα: 1) Si3N4 + Si carbon coated.
Beyond 20 kV conductivity sufficient without carb
2) Si-Kα measurements were stopped at 20 kV; layer n
thick enough
For N-Kα: Holes burned in carbon coating

Backgrounds: Si-Kα: ± 5 mm on either side of the peak and interpolated
N -Kα: ± 6.7 mm (STE)

PHA settings:	Counter HT	Lower level	Window	Gain	Pulse	
Si-Kα:	1600 volt	0.6 volt	open	32*4.4	2.0 V	AS TAP
N-Kα:	1700 volt	1.5 volt	1.0 V	32*8.0	2.0 V	AS STE

Appendix 1...e

Nitride: TiN

Date: Ti-Kα 31 January 1986
N-Kα May 1985-March 1987

Compo: 22.50 wt% N
----- wt% O
77.50 wt% Ti

kV	Beam current (nA)		Net.intensities (cps/nA)				k-ratios		
			Ti-Kα peak		N-Kα integral		PKR	AKR N-Kα	
	Ti-Kα	N-Kα	Ti	TiN	Cr2N	TiN	Ti-Kα	STE	LDE
4	---	300	---	---	4.55	9.719	---	2.136	----
6	100	300	22.27	16.24	6.69	14.858	0.7293	2.221	----
8	30	300	132.72	97.46	7.87	18.353	0.7343	2.332	----
10	15	300	292.50	214.43	8.48	19.821	0.7331	2.337	2.329
12	10	300	493.96	366.77	8.51	22.024	0.7425	2.588	----
15	10	300	862.52	645.85	8.05	20.254	0.7488	2.516	----
20	3	300	1542.73	1161.37	6.89	18.479	0.7528	2.682	----
25	3	300	2279.12	1725.29	5.82	16.028	0.7570	2.754	----
30	2	300	3057.72	2320.20	4.96	14.994	0.7588	3.023	----

Backgrounds: Ti-Kα: ± 5 mm on either side of the peak and interpolated
N-Kα: ± 11.2 mm (LDE) or ± 6.7 mm (STE)

PHA settings:	counter HT	Lower level	Window	Gain	Pulse	
Ti-Kα:	1700 volt	0.5 volt	open	128*6.5	2.0 V	PET CS
N-Kα:	1700 volt	1.0 volt	2.0 V	32*8.0	2.0 V	STE AS

Appendix 1...f

Nitride: Ti_2N

Date: Ti-Kα 31 January 1986
N-Kα May 1985-March 1987

Compo: 11.84 wt% N
----- wt% O
88.16 wt% Ti

kV	Beam current (nA)		Net.intensities (cps/nA)				k-ratios		
			Ti-Kα peak		N-Kα integral		PKR	AKR N-Kα	
	Ti-Kα	N-Kα	Ti	Ti_2N	Cr_2N	Ti_2N	Ti-Kα	STE	LDE
4	---	300	---	---	4.55	4.987	---	1.096	----
6	100	300	22.27	19.23	6.69	8.068	0.8636	1.206	----
8	30	300	132.72	114.95	7.87	9.696	0.8661	1.232	----
10	15	300	292.50	252.80	8.48	10.329	0.8643	1.218	1.321
12	10	300	493.96	429.24	8.51	11.446	0.8690	1.345	----
15	10	300	862.52	754.45	8.05	10.916	0.8747	1.356	----
20	3	300	1542.73	1351.82	6.89	9.398	0.8763	1.364	----
25	3	300	2279.12	2013.15	5.82	8.858	0.8833	1.522	----
30	2	300	3057.72	2683.94	4.96	7.559	0.8778	1.524	----

Backgrounds: Ti-Kα: ± 5 mm on either side of the peak and interpolated
N-Kα: ± 11.2 mm (LDE) or ± 6.7 mm (STE)

PHA settings:	counter HT	Lower level	Window	Gain	Pulse	
Ti-Kα:	1700 volt	0.5 volt	open	128*6.5	2.0 V	PET CS
N-Kα:	1700 volt	1.0 volt	2.0 V	32*8.0	2.0 V	STE AS

Appendix 1...g

Nitride: VN

Date: V-Kα 28 March-2 April 1985
N-Kα February/March 1987

Compo: 16.04 wt% N
0.31 wt% O
83.65 wt% V

kV	Beam current (nA)		Net.intensities (cps/nA)				k-ratios			Wt Av
			V-Kα peak		N-Kα integral		PKR	AKR N-Kα		AKR
	V-Kα	N-Kα	V	VN	Cr_2N	VN	V-Kα	STE	LDE	N-Kα
4	---	300	---	---	4.55	7.130	---	1.5819	1.5597	1.5671
6	100	300	10.30	8.39	6.69	10.590	0.8149	1.5912	1.5789	1.5830
8	30	300	135.39	109.16	7.87	12.817	0.8063	1.6273	1.6293	1.6286
10	15	300	337.74	268.44	8.48	13.965	0.7948	1.6623	1.6391	1.6468
12	10	300	610.63	490.34	8.51	14.179	0.8030	1.6583	1.6702	1.6662
15	10	300	1121.91	905.16	8.05	13.860	0.8068	1.7258	1.7196	1.7217
20	3	300	2117.72	1722.98	6.89	11.986	0.8136	1.7407	1.7391	1.7396
25	3	300	3238.35	2669.70	5.82	10.201	0.8244	1.7611	1.7487	1.7528
30	3	300	4431.64	3617.99	4.96	8.678	0.8164	1.8193	1.7148	1.7496

Remarks: N-Kα spectra stripped with V background (VII peak)

Backgrounds: V-Kα: ± 5 mm on either side of the peak and interpolated
N-Kα: ± 11.2 mm (LDE) or ± 6.7 mm (STE)

PHA settings:	counter HT	Lower level	Window	Gain	Pulse	
V-Kα:	1600 volt	0.6 volt	open	64*6.5	2.0 V	PET CS
N-Kα:	1700 volt	0.5 volt	3.0 V	32*5.2	2.0 V	STE AS
N-Kα:	1700 volt	1.0 volt	4.0 V	100*1.0	2.0 V	LDE DS

Appendix 1...h

Nitride: V_2N

Date: V-Kα 28 March-2 April 1985
N-Kα February/March 1987

Compo: 11.99 wt% N
0.78 wt% O
87.23 wt% V

kV	Beam current (nA)		Net.intensities (cps/nA)				k-ratios			Wt A
			V-Kα peak		N-Kα integral		PKR	AKR N-Kα		AKR
	V-Kα	N-Kα	V	V_2N	Cr_2N	V_2N	V-Kα	STE	LDE	N-Kα
4	---	300	---	---	4.55	5.273	---	1.1724	1.1520	1.158
6	100	300	10.30	7.83	6.69	8.005	0.7603	1.1893	1.2001	1.196
8	30	300	135.39	114.61	7.87	9.413	0.8465	1.1765	1.2058	1.196
10	15	300	337.74	283.06	8.48	10.455	0.8381	1.2188	1.2399	1.232
12	10	300	610.63	516.65	8.51	10.740	0.8461	1.2691	1.2584	1.262
15	10	300	1121.91	961.36	8.05	10.283	0.8569	1.2523	1.2900	1.277
20	3	300	2117.72	1849.83	6.89	9.047	0.8735	1.2875	1.3257	1.313
25	3	300	3238.35	2831.29	5.82	7.344	0.8743	1.2370	1.2744	1.261
30	3	300	4431.64	3810.32	4.96	6.379	0.8598	1.3027	1.2778	1.286

Remarks: N-Kα spectra stripped with V background (V_{II} peak)

Backgrounds: V-Kα: ± 5 mm on either side of the peak and interpolated
N-Kα: ± 11.2 mm (LDE) or ± 6.7 mm (STE)

PHA settings:	counter HT	Lower level	Window	Gain	Pulse	
V-Kα:	1600 volt	0.6 volt	open	64*6.5	2.0 V	PET CS
N-Kα:	1700 volt	0.5 volt	3.0 V	32*5.2	2.0 V	STE AS
N-Kα:	1700 volt	1.0 volt	4.0 V	100*1.0	2.0 V	LDE DS

Appendix 1...i

Nitride: CrN

Date: Cr-Kα 14/15 March 1985
N-Kα February 1987

Compo: 21.22 wt% N
----- wt% O
78.78 wt% Cr

kV	Beam current (nA)		Net.intensities (cps/nA)				k-ratios			Wt
			Cr-Kα peak		N-Kα integral		PKR	AKR N-Kα		AKR
	Cr-Kα	N-Kα	Cr	CrN	Cr_2N	CrN	Cr-Kα	STE	LDE	N-K
4	---	300	---	---	4.55	8.764	---	1.9430	1.9176	1.92
6	---	300	---	---	6.69	13.165	---	1.9703	1.9667	1.96
8	30	300	104.52	74.52	7.87	15.875	0.7130	2.0180	2.0167	2.01
10	30	300	308.33	226.35	8.48	16.983	0.7341	2.0179	1.9951	2.00
12	10	300	581.52	441.84	8.51	17.366	0.7598	2.0199	2.0509	2.04
15	5	300	1140.07	855.96	8.05	16.716	0.7508	2.0604	2.0845	2.07
20	1	300	2254.25	1686.86	6.89	14.264	0.7483	2.0442	2.0832	2.07
25	1	300	3426.00	2620.20	5.82	12.529	0.7648	2.1517	2.1534	2.15
30	1	300	4695.11	3616.17	4.96	10.320	0.7702	2.0824	2.0797	2.08

Backgrounds: Cr-Kα: ± 5 mm on either side of the peak and interpolated
N-Kα: ± 11.2 mm (LDE) or ± 6.7 mm (STE)

PHA settings:	counter HT	Lower level	Window	Gain	Pulse	
Cr-Kα:	1600 volt	0.6 volt	open	64*5.5	2.0 V	CS PET
N-Kα:	1700 volt	0.5 volt	3.0 V	32*5.4	2.0 V	AS STE
N-Kα:	1700 volt	1.0 volt	4.0 V	100*1.0	2.0 V	DS LDE

Appendix 1...j

Nitride: Cr_2N
Standard (Batch # 1)

Date: Cr-Kα 14/15 March 1985
N-Kα February 1987

Compo: 10.70 wt% N
0.48 wt% O
88.82 wt% Cr

kV	Beam current (nA)		Net.intensities (cps/nA)				k-ratios		
			Cr-Kα peak		N-Kα integral		PKR	AKR N-Kα	
	Cr-Kα	N-Kα	Cr	Cr_2N	Cr_2N		Cr-Kα	STE	LDE
4	---	300	---	---	4.55	----	----	----	----
6	---	300	---	---	6.69	----	----	----	----
8	30	300	104.52	87.77	7.87	----	0.8397	----	----
10	30	300	308.33	264.82	8.48	----	0.8589	----	----
12	10	300	581.52	508.71	8.51	----	0.8748	----	----
15	5	300	1140.07	985.13	8.05	----	0.8641	----	----
20	1	300	2254.25	1962.78	6.89	----	0.8707	----	----
25	1	300	3426.00	3016.59	5.82	----	0.8805	----	----
30	1	300	4695.11	4161.75	4.96	----	0.8864	----	----

Backgrounds: Cr-Kα: ± 5 mm on either side of the peak and interpolated
N-Kα: ± 11.2 mm (LDE) or ± 6.7 mm (STE)

PHA settings:	counter HT	Lower level	Window	Gain	Pulse	
Cr-Kα:	1600 volt	0.6 volt	open	64*4.5	2.0 V	CS PET
N-Kα:	1700 volt	0.5 volt	3.0 V	32*5.4	2.0 V	AS STE
N-Kα:	1700 volt	1.0 volt	4.0 V	100*1.0	2.0 V	DS LDE

Nitride: Fe_4N

Date: Fe-Kα 7/8 March 1985
N-Kα November 1985

Compo: 5.60 wt% N
---- wt% O
94.40 wt% Fe

kV	Beam current (nA)		Net.intensities (cps/nA)				k-ratios			Wt Av
			Fe-Kα peak		N-Kα integral		PKR	AKR N-Kα		AKR
	Fe-Kα	N-Kα	Fe	Fe_4N	Cr_2N	Fe_4N	Fe-Kα	STE	LDE	N-Kα
4	---	300	---	---	4.55	2.248	---	0.4941	----	----
6	---	300	---	---	6.69	3.136	---	0.4688	----	----
8	300	300	6.16	5.56	7.87	3.610	0.9024	0.4587	----	----
10	100	300	37.69	34.33	8.48	3.533	0.9109	0.4285	0.4107	0.4166
12	50	300	90.36	83.40	8.51	3.535	0.9230	0.4154	----	----
15	30	300	202.30	184.38	8.05	3.280	0.9114	0.4075	----	----
20	15	300	437.24	407.03	6.89	2.739	0.9309	0.3975	----	----
25	15	300	717.74	666.85	5.82	2.269	0.9291	0.3898	----	----
30	10	300	1001.54	922.12	4.96	1.911	0.9207	0.3853	----	----

Remarks: N-Kα spectrum (STE) stripped with background
pure Fe (Fe-L$\alpha_{1,2}$ (2nd order))

Backgrounds: Fe-Kα: ± 5 mm on either side of the peak and interpolated
N-Kα: ± 11.2 mm (LDE) or ± 6.7 mm (STE)

PHA settings:	counter HT	Lower level	Window	Gain	Pulse	
Fe-Kα:	1600 volt	0.6 volt	open	32*7.0	2.0 V	BS LIF
N-Kα:	1700 volt	1.5 volt	1.0 V	32*8.0	2.0 V	AS STE

Appendix 1...1

Nitride: ZrN

Date: Zr-Lα 11 February 1986
N-Kα March/April 1987

Compo: 12.70 wt% N
0.67 wt% O
86.63 wt% Zr

kV	Beam current (nA)		Net.intensities (cps/nA)				k-ratios			Wt A
			Zr-Lα peak		N-Kα integral		PKR	AKR N-Kα		AKR
	Zr-Lα	N-Kα	Zr	ZrN	Cr_2N	ZrN	Zr-Lα	STE	LDE	N-Kα
4	100	300	7.26	6.02	4.55	3.549	0.8291	0.7975	0.7711	0.7799
6	100	300	22.20	17.97	6.69	3.861	0.8095	0.5864	0.5640	0.5771
8	100	300	39.21	32.93	7.87	3.653	0.8399	0.4854	0.4536	0.4642
10	100	300	56.02	47.08	8.48	3.149	0.8404	0.3741	0.3699	0.3713
12	100	300	74.05	62.24	8.51	2.875	0.8405	0.3447	0.3344	0.3378
15	30	300	97.44	83.79	8.05	2.362	0.8599	0.2932	0.2935	0.2934
20	30	300	131.71	111.87	6.89	1.905	0.8494	0.2694	0.2801	0.2765
25	30	300	157.52	135.42	5.82	1.639	0.8597	0.2967	0.2741	0.2816
30	30	300	172.15	148.75	4.96	1.373	0.8641	0.2441	0.2677	0.2768

Remarks: Backgrounds on STE and LDE stripped with reference spectra from pure Zr

Backgrounds: Zr-Lα: ± 5 mm on either side of the peak and interpolated
N-Kα: ± 11.2 mm (LDE) or ± 6.7 mm (STE)

PHA settings:	counter HT	Lower level	Window	Gain	Pulse
Zr-Lα:	1600 volt	0.7 volt	open	128*9.0	2.0 V CS PET
N-Kα:	1700 volt	1.0 volt	2.0 V	32*5.5	2.0 V AS STE
N-Kα:	1700 volt	1.0 volt	2.0 V	100*0.9	2.0 V DS LDE

Appendix 1...m

Nitride: Nb_4N_3

Date: Nb-Lα 13 February 1986
N-Kα April/May 1987

Compo: 9.79 wt% N
0.72 wt% O
89.49 wt% Nb

kV	Beam current (nA)		Net.intensities (cps/nA)				k-ratios			Wt Av
			Nb-Lα peak		N-Kα integral		PKR	AKR N-Kα		AKR
	Nb-Lα	N-Kα	Nb	Nb_4N_3	Cr_2N	Nb_4N_3	Nb-Lα	STE	LDE	N-Kα
4	150	300	7.80	6.71	4.55	2.789	0.8601	0.6262	0.6062	0.6129
6	200	300	25.69	21.91	6.69	2.931	0.8529	0.4365	0.4389	0.4381
8	150	300	47.10	41.06	7.87	2.710	0.8717	0.3436	0.3448	0.3444
10	100	300	67.89	58.70	8.48	2.470	0.8646	0.2927	0.2906	0.2913
12	50	300	90.25	78.27	8.51	2.091	0.8673	0.2365	0.2503	0.2457
15	50	300	121.52	105.47	8.05	1.798	0.8679	0.2225	0.2239	0.2234
20	30	300	166.15	145.28	6.89	1.454	0.8744	0.1988	0.2172	0.2111
25	20	300	199.41	174.88	5.82	1.286	0.8770	0.2432	0.2099	0.2210
30	20	300	222.80	194.08	4.96	1.056	0.8711	0.2073	0.2157	0.2129

Remarks: Backgrounds on STE and LDE stripped with reference spectra from pure Nb

Backgrounds: Nb-Lα: ± 5 mm on either side of the peak and interpolated
N-Kα: ± 11.2 mm (LDE) or ± 6.7 mm (STE)

PHA settings:	counter HT	Lower level	Window	Gain	Pulse	
Nb-Lα:	1700 volt	0.7 volt	open	128*4.5	2.0 V	BS PET
N-Kα:	1700 volt	1.0 volt	2.0 V	32*5.5	2.0 V	AS STE
N-Kα:	1700 volt	1.0 volt	2.0 V	100*0.9	2.0 V	DS LDE

Appendix 1...n

Nitride: Nb_2N

Date: Nb-Lα 13 February 1986
N-Kα April, May 1987

Compo: 6.55 wt% N
0.46 wt% O
92.99 wt% Nb

kV	Beam current (nA)		Net.intensities (cps/nA)				k-ratios			Wt Av.
			Nb-Lα peak		N-Kα integral		PKR	AKR N-Kα		AKR
	Nb-Lα	N-Kα	Nb	Nb_2N	Cr_2N	Nb_2N	Nb-Lα	STE	LDE	NKA
4	150	300	7.80	7.12	4.55	1.867	0.9130	0.4134	0.4089	0.4104
6	200	300	25.69	23.10	6.69	1.863	0.8991	0.2563	0.2896	0.2785
8	150	300	47.10	43.14	7.87	1.809	0.9160	0.2389	0.2252	0.2298
10	100	300	67.89	61.73	8.48	1.623	0.9092	0.1939	0.1901	0.1914
12	50	300	90.25	82.22	8.51	1.372	0.9110	0.1592	0.1622	0.1612
15	50	300	121.52	110.64	8.05	1.074	0.9105	0.1283	0.1359	0.1334
20	30	300	166.15	151.35	6.89	0.878	0.9109	0.1141	0.1342	0.1275
25	20	300	199.41	182.22	5.82	0.772	0.9138	0.1306	0.1337	0.1327
30	20	300	222.80	202.12	4.96	0.645	0.9072	0.1159	0.1370	0.1300

Remarks: Backgrounds on STE and LDE stripped with reference spectra from pure Nb

Backgrounds: Nb-Lα: ± 5 mm on either side of the peak and interpolated
N-Kα: ± 11.2 mm (LDE) or ± 6.7 mm (STE)

PHA settings:	counter HT	Lower level	Window	Gain	Pulse	
Nb-Lα:	1700 volt	0.7 volt	open	128*4.5	2.0 V	BS PET
N-Kα:	1700 volt	1.0 volt	2.0 V	32*5.5	2.0 V	AS STE
N-Kα:	1700 volt	1.0 volt	2.0 V	100*0.9	2.0 V	DS LDE

Appendix 1...o

Nitride: Mo_2N

Date: Mo-Lα 14 March 1985
N-Kα May 1987

Compo: 5.80 wt% N
---- wt% O
94.20 wt% Mo

kV	Beam current (nA)		Net.intensities (cps/nA)				k-ratios			Wt Av.
			Mo-Lα peak		N-Kα integral		PKR	AKR N-Kα		AKR
	Mo-Lα	N-Kα	Mo	Mo_2N	Cr_2N	Mo_2N	Mo-Lα	STE	LDE	N-Kα
4	150	300	7.40	6.62	4.55	1.508	0.8943	0.3389	0.3278	0.3315
6	150	300	25.98	23.43	6.69	1.842	0.9018	0.2761	0.2751	0.2754
8	30	300	48.39	43.68	7.87	1.590	0.9026	0.2078	0.1970	0.2020
10	30	300	71.25	64.37	8.48	1.473	0.9077	0.1680	0.1766	0.1737
12	10	300	94.63	86.71	8.51	1.201	0.9163	0.1264	0.1485	0.1411
15	5	300	126.77	116.65	8.05	1.029	0.9202	0.1241	0.1296	0.1278
20	5	300	175.50	163.32	6.89	0.803	0.9306	0.1100	0.1199	0.1166
25	5	300	211.00	197.75	5.82	0.678	0.9372	0.1126	0.1185	0.1165
30	5	300	238.96	225.51	4.96	0.609	0.9437	0.1213	0.1234	0.1227

Remarks: Backgrounds on STE and LDE stripped with reference spectra from pure Mo

Backgrounds: Mo-Lα: ± 5 mm on either side of the peak and interpolated
N-Kα: ± 11.2 mm (LDE) or ± 6.7 mm (STE)

PHA settings:	counter HT	Lower level	Window	Gain	Pulse	
Mo-Lα:	1600 volt	0.5 volt	open	128*5.0	2.0 V	CS PET
N-Kα:	1700 volt	1.0 volt	2.0 V	32*5.5	2.0 V	AS STE
N-Kα:	1700 volt	1.0 volt	2.0 V	100*1.0	2.0 V	DS LDE

Appendix 1...p

Nitride: HfN
Hf contains 2.45 wt% Zr

Date: Hf-Mα,Lα 30 June 1987 — N-Kα May 1987

Compo: 6.06 wt% N
0.29 wt% O
91.36 wt% Hf
2.29 wt% Zr

kV	Beam current (nA)		Net.intensities (cps/nA)				k-ratios			Wt A
			Hf-Mα peak		N-Kα (integral)		PKR	AKR N-Kα		AKR
	Hf-Mα	N-Kα	Hf*	HfN	Cr_2N	HfN	Hf-Mα	STE	LDE	N-Kα
4	300	300	3.49	2.98	4.55	2.655	0.8537	0.5894	0.5805	0.5835
6	300	300	7.92	6.85	6.69	3.220	0.8655	0.4791	0.4824	0.4813
8	300	300	12.72	11.10	7.87	3.170	0.8728	0.4049	0.4007	0.4028
10	150	300	16.97	14.90	8.48	2.992	0.8783	0.3381	0.3601	0.3528
	Hf-Lα		Hf-Lα	Hf-Lα			Hf-Lα			
12	100	300	26.41	22.67	8.51	2.808	0.8584	0.3287	0.3306	0.3300
15	50	300	93.12	80.96	8.05	2.376	0.8694	0.2922	0.2965	0.2951
20	10	300	237.15	208.50	6.89	1.782	0.8792	0.2651	0.2553	0.2586
25	10	300	401.40	354.07	5.82	1.568	0.8821	0.2667	0.2708	0.2694
30	5	300	568.52	505.02	4.96	1.370	0.8883	0.2777	0.2756	0.2763

Remarks: Backgrounds on STE and LDE stripped with reference spectra from pure Hf

*Corrected for presence of 2.45 wt% Zr in Hf standard

Backgrounds: Hf-Mα: ± 5 mm on either side of the peak and interpolated
Hf-Lα: ± 5 mm on either side of the peak and interpolated
N-Kα: ± 11.2 mm (LDE) or ± 6.7 mm (STE)

PHA settings:	Counter HT	Lower level	Window	Gain	Pulse	
Hf-Mα:	1600 volt	1.0 volt	2.0 V	64*8.6	2.0 V	CS PET
Hf-Lα:	1600 volt	1.0 volt	open	32*4.25	2.0 V	BS LIF
N-Kα:	1700 volt	1.0 volt	2.0 V	32*5.5	2.0 V	AS STE
N-Kα:	1700 volt	1.0 volt	2.0 V	100*1.0	2.0 V	DS LDE

Appendix 1...q

Nitride: TaN

Date: Ta-Mα/Lα 14 February 1986   Compo: 6.51 wt% N
N-Kα May 1987   0.22 wt% O
93.27 wt% Ta

kV	Beam current (nA)		Net.intensities (cps/nA)				k-ratios			Wt Av
			Ta-Mα peak		N-Kα integral		PKR	AKR N-Kα		AKR
	Ta-Mα	N-Kα	Ta	TaN	Cr_2N	TaN	Ta-Mα	STE	LDE	N-Kα
4	300	300	5.01	4.42	4.55	2.798	0.8830	0.6037	0.6205	0.6149
6	300	300	12.20	10.91	6.69	3.432	0.8945	0.4997	0.5197	0.5130
8	200	300	19.92	17.67	7.87	3.390	0.8869	0.4258	0.4331	0.4307
10	100	300	26.55	23.75	8.48	3.204	0.8946	0.3738	0.3798	0.3778
12	100	300	32.20	29.06	8.51	2.892	0.9026	0.3335	0.3430	0.3398
15	50	300	40.83	36.97	8.05	2.273	0.9054	0.2796	0.2837	0.2823
20	20	300	50.46	45.94	6.89	1.878	0.9105	0.2628	0.2774	0.2725
25	30	300	55.58	51.22	5.82	1.553	0.9216	0.2475	0.2765	0.2668
30	30	300	57.87	53.36	4.96	1.447	0.9220	0.2699	0.3135	0.2917
	Ta-Lα		Ta-Lα	Ta-Lα			Ta-Lα			
12	100	----	22.06	18.35			0.8319			
15	50	----	89.13	77.38			0.8682			
20	20	----	246.70	218.30			0.8849			
25	30	----	430.24	382.70			0.8895			
30	30	----	622.81	558.72			0.8971			

Backgrounds: Ta-Mα: ± 5 mm on either side of the peak and interpolated
Ta-Lα: ± 5 mm on either side of the peak and interpolated
N-Kα: ± 11.2 mm (LDE) or ± 6.7 mm (STE)

PHA settings:	counter HT	Lower level	Window	Gain	Pulse	
Ta-Mα:	1600 volt	0.6 volt	open	64*10.0	2.0 V	CS PET
Ta-Lα:	1600 volt	0.6 volt	open	64*5.5	2.0 V	BS LIF
N-Kα:	1700 volt	1.0 volt	2.0 V	32*5.5	2.0 V	AS STE
N-Kα:	1700 volt	1.0 volt	2.0 V	100*1.0	2.0 V	DS LDE

Appendix 1...r

Nitride: Ta_2N

Date: Ta-Mα,Lα 14 February 1986   Compo: 3.47 wt% N
N-Kα May 1987   0.24 wt% O
96.29 wt% Ta

kV	Beam current (nA)		Net.intensities (cps/nA)				k-ratios			Wt A
			Ta-Mα peak		N-Kα integral		PKR	AKR N-Kα		AKR
	Ta-Mα	N-Kα	Ta	Ta_2N	Cr_2N	Ta_2N	Ta-Mα	STE	LDE	N-Kα
4	300	300	5.01	4.80	4.55	1.533	0.9584	0.3358	0.3390	0.337
6	300	300	12.20	11.81	6.69	1.780	0.9678	0.2657	0.2661	0.266
8	200	300	19.92	18.80	7.87	1.737	0.9438	0.2180	0.2221	0.220
10	100	300	26.55	25.30	8.48	1.637	0.9530	0.1934	0.1928	0.193
12	100	300	32.20	30.69	8.51	1.504	0.9532	0.1734	0.1783	0.176
15	50	300	40.83	38.85	8.05	1.338	0.9515	0.1649	0.1668	0.166
20	20	300	50.46	48.02	6.89	1.034	0.9517	0.1419	0.1542	0.150
25	30	300	55.58	53.48	5.82	0.909	0.9622	0.1429	0.1621	0.156
30	30	300	57.87	55.58	4.96	0.794	0.9604	0.1437	0.1747	0.160
	Ta-Lα		Ta-Lα	Ta-Lα			Ta-Lα			
12	100		22.06	20.76			0.9411			
15	50		89.13	83.02			0.9315			
20	20		246.70	231.48			0.9383			
25	30		430.24	404.47			0.9401			
30	30		622.81	588.18			0.9444			

Backgrounds: Ta-Mα: ± 5 mm on either side of the peak and interpolated
Ta-Lα: ± 5 mm on either side of the peak and interpolated
N-Kα: ± 11.2 mm (LDE) or ± 6.7 mm (STE)

PHA settings:	counter HT	Lower level	Window	Gain	Pulse	
Ta-Mα:	1600 volt	0.6 volt	open	64*10.0	2.0 V	CS PET
Ta-Lα:	1600 volt	0.6 volt	open	64* 5.5	2.0 V	BS LIF
N-Kα:	1700 volt	1.0 volt	2.0 V	32*5.5	2.0 V	AS STE
N-Kα:	1700 volt	1.0 volt	2.0 V	100*1.0	2.0 V	DS LDE

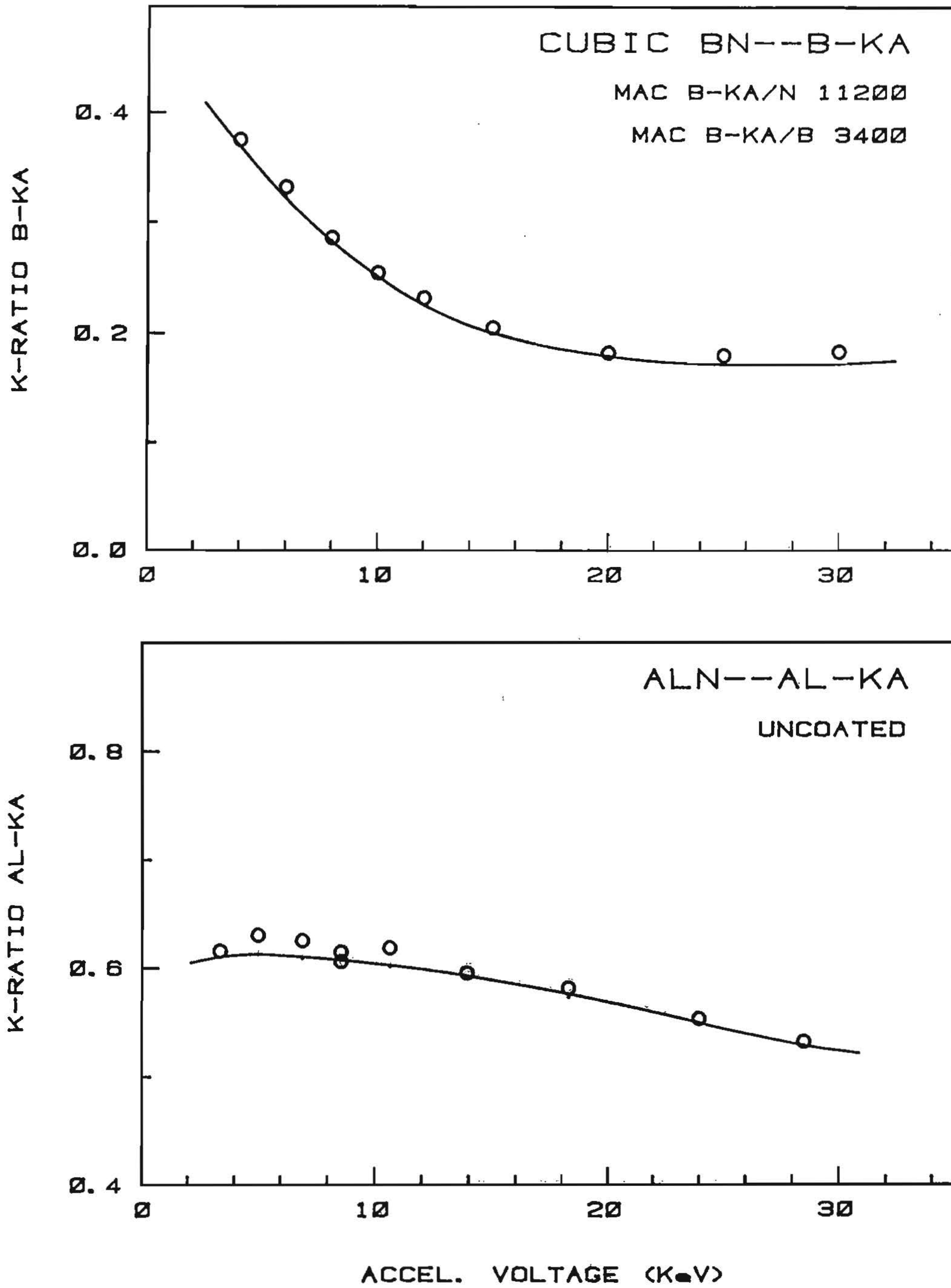

Comparison between the experimental k-ratios (relative to elemental standards) of the X-ray lines of the metal components (circles) and the predictions of our PROZA program (solid curves). Top : uncoated Cubic BN (integral k-ratios B-Kα); bottom : uncoated AlN. Note the shift in the voltage for AlN due to slight surface charging effects.

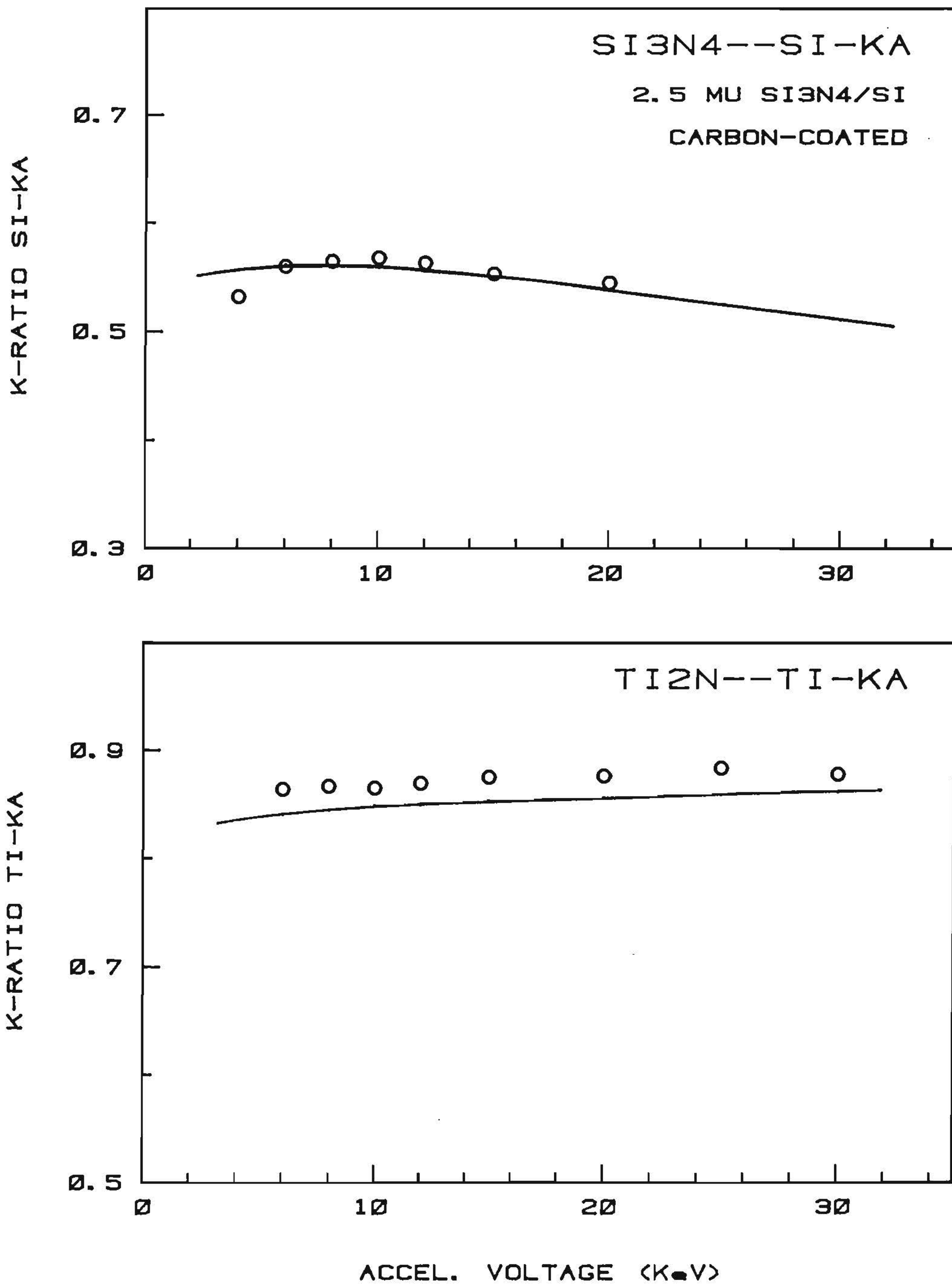

Comparison between the experimental k-ratios (relative to elemental standards) of the X-ray lines of the metal components (circles) and the predictions of our PROZA program (solid curves). Top : Si_3N_4 (Si-standard + Si_3N_4 carbon coated); bottom : uncoated Ti_2N.

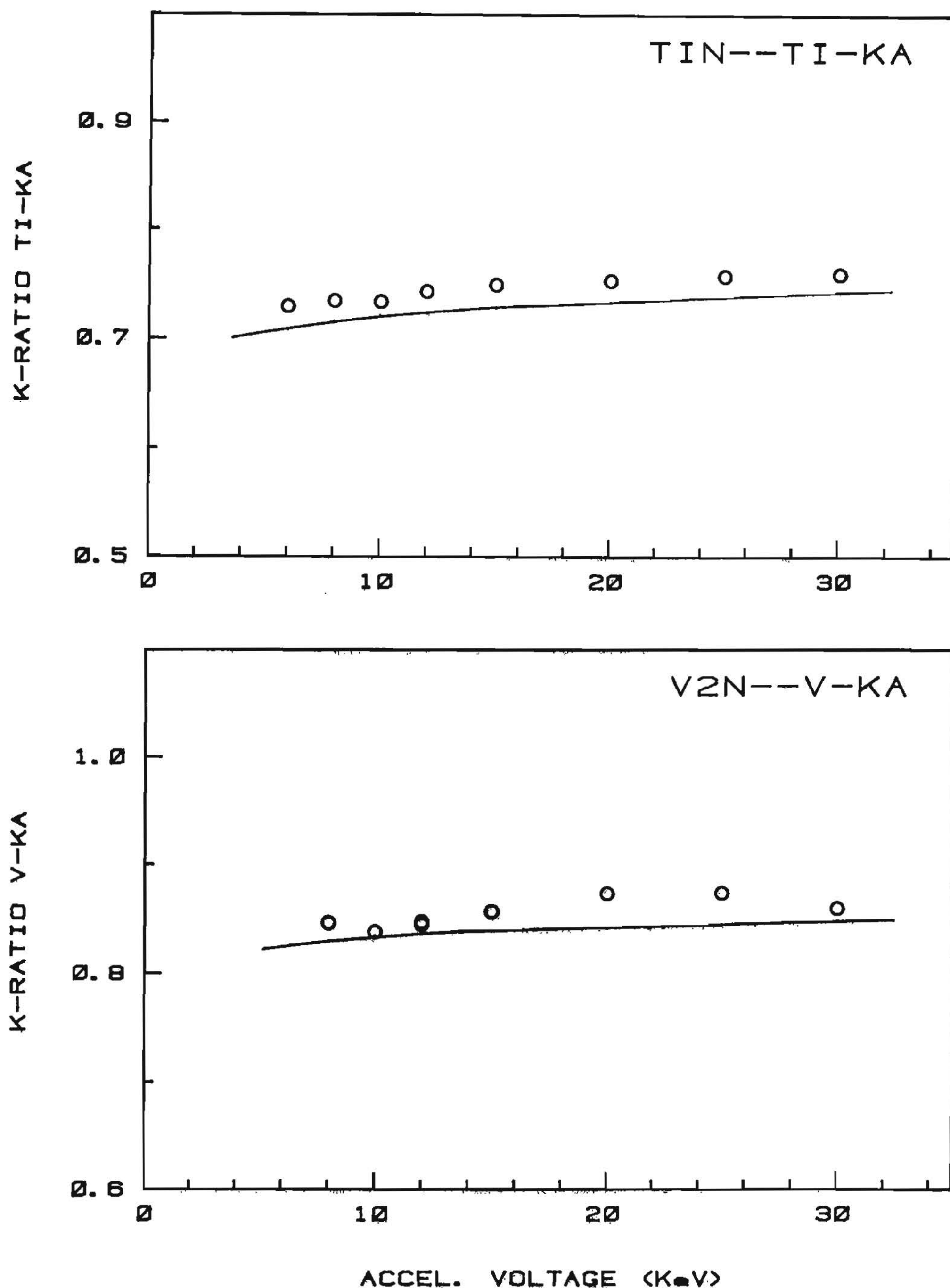

Comparison between the experimental k-ratios (relative to elemental standards) of the X-ray lines of the metal components (circles) and the predictions of our PROZA program (solid curves). Top : uncoated TiN; bottom : uncoated V_2N.

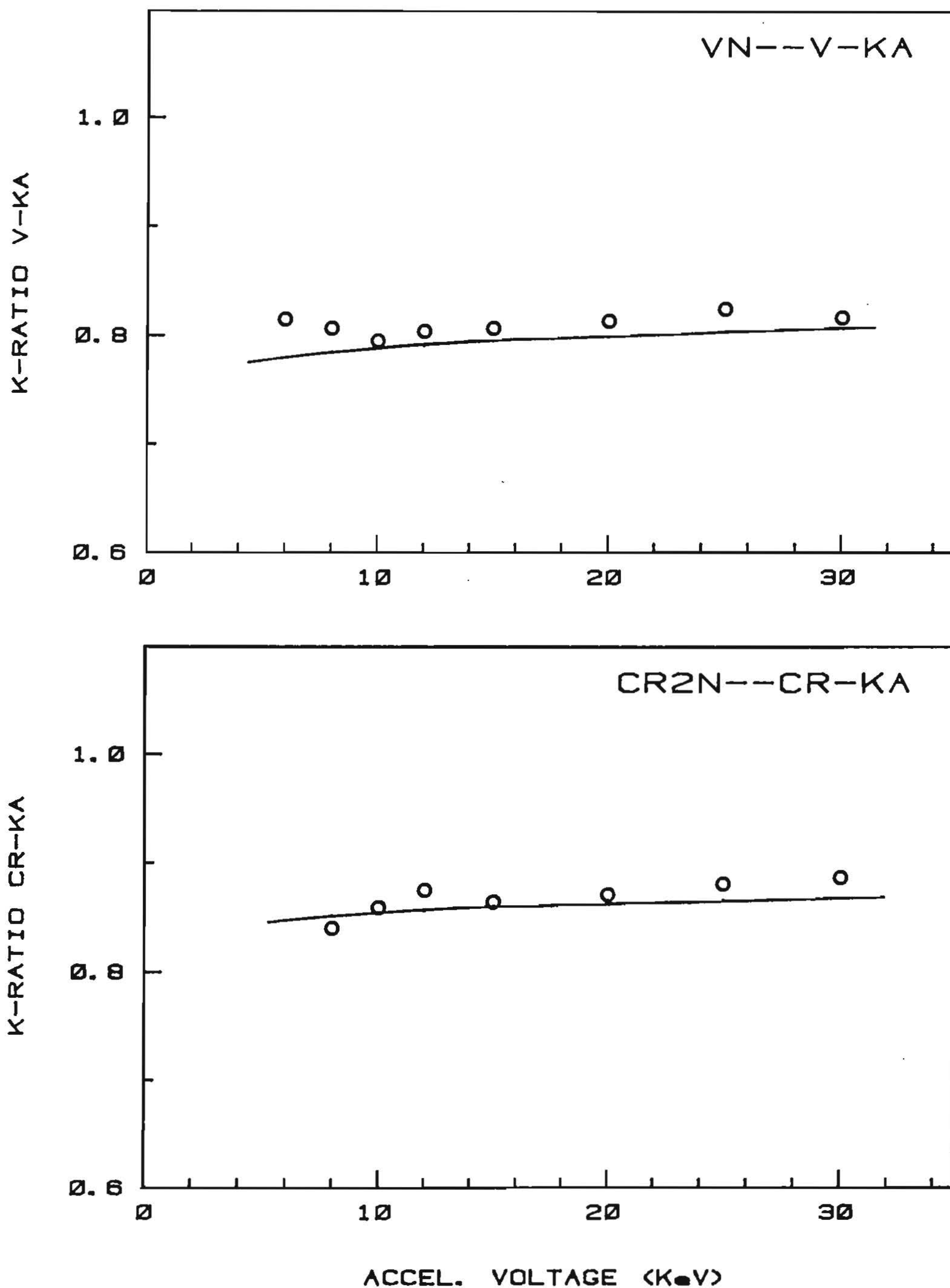

Comparison between the experimental k-ratios (relative to elemental standards) of the X-ray lines of the metal components (circles) and the predictions of our PROZA program (solid curves). Top : uncoated VN; bottom : uncoated Cr_2N.

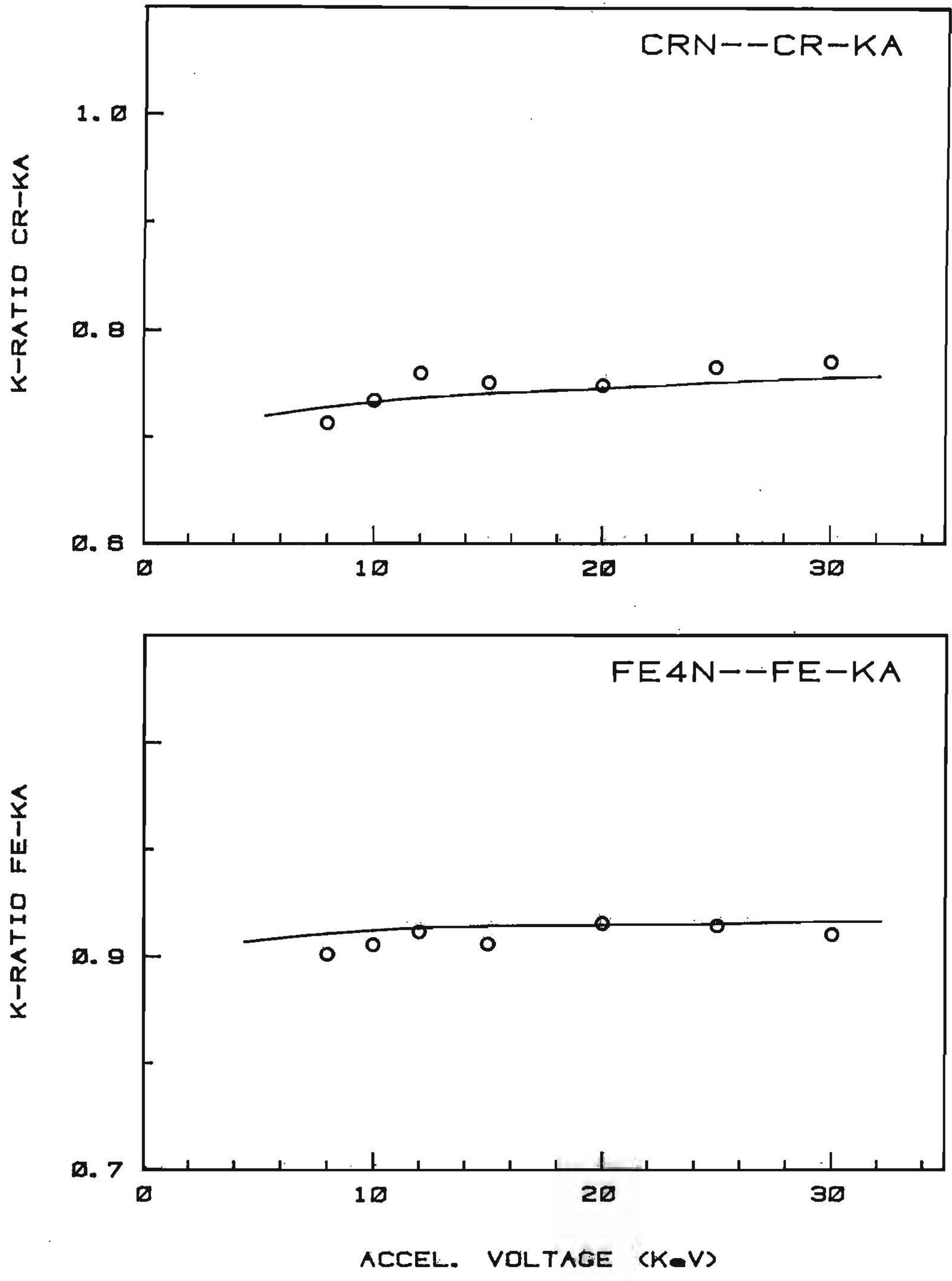

Comparison between the experimental k-ratios (relative to elemental standards) of the X-ray lines of the metal components (circles) and the predictions of our PROZA program (solid curves). Top : uncoated CrN; bottom : uncoated Fe_4N.

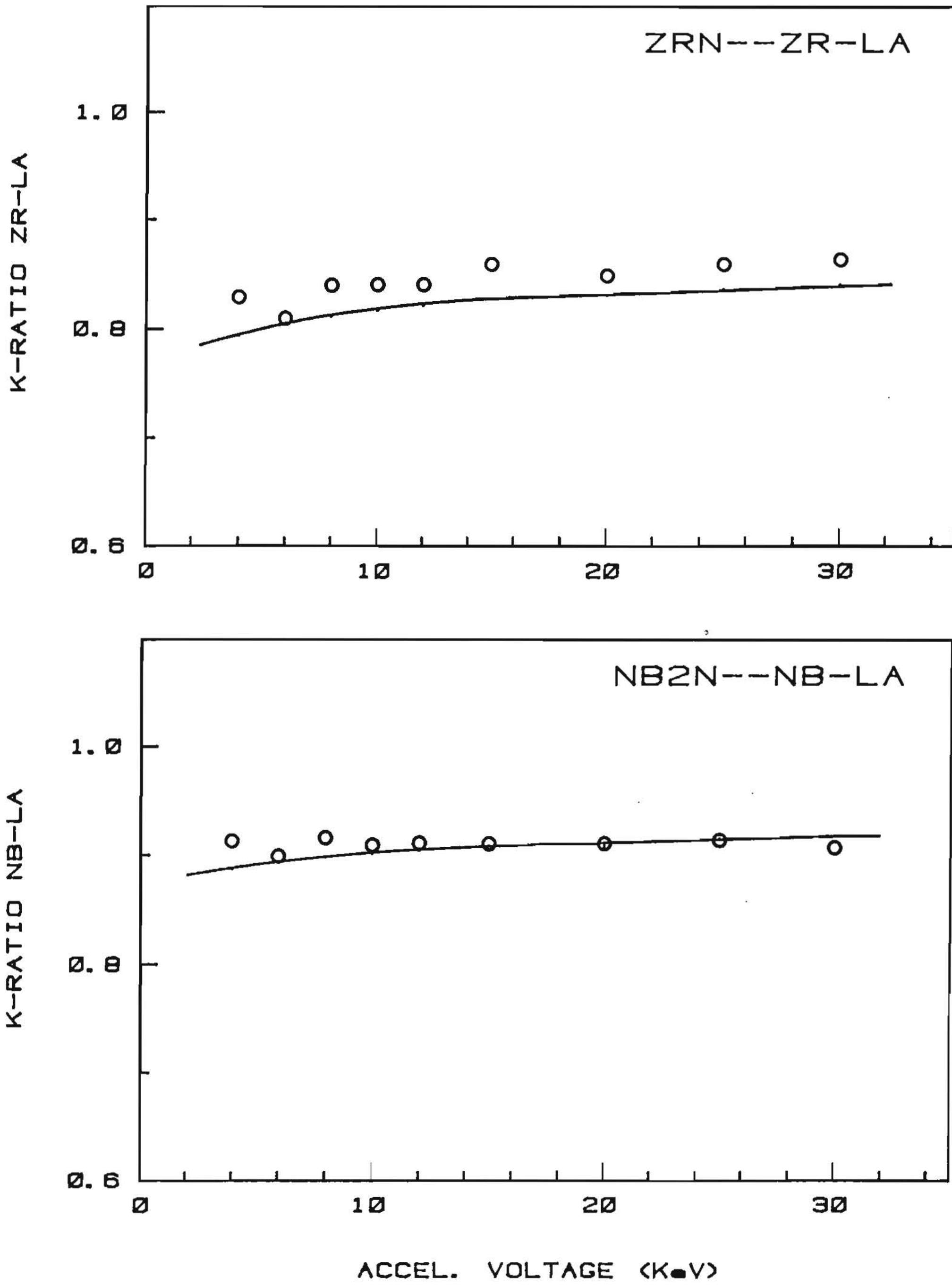

Comparison between the experimental k-ratios (relative to elemental standards) of the X-ray lines of the metal components (circles) and the predictions of our PROZA program (solid curves). Top : uncoated ZrN; bottom : uncoated Nb_2N.

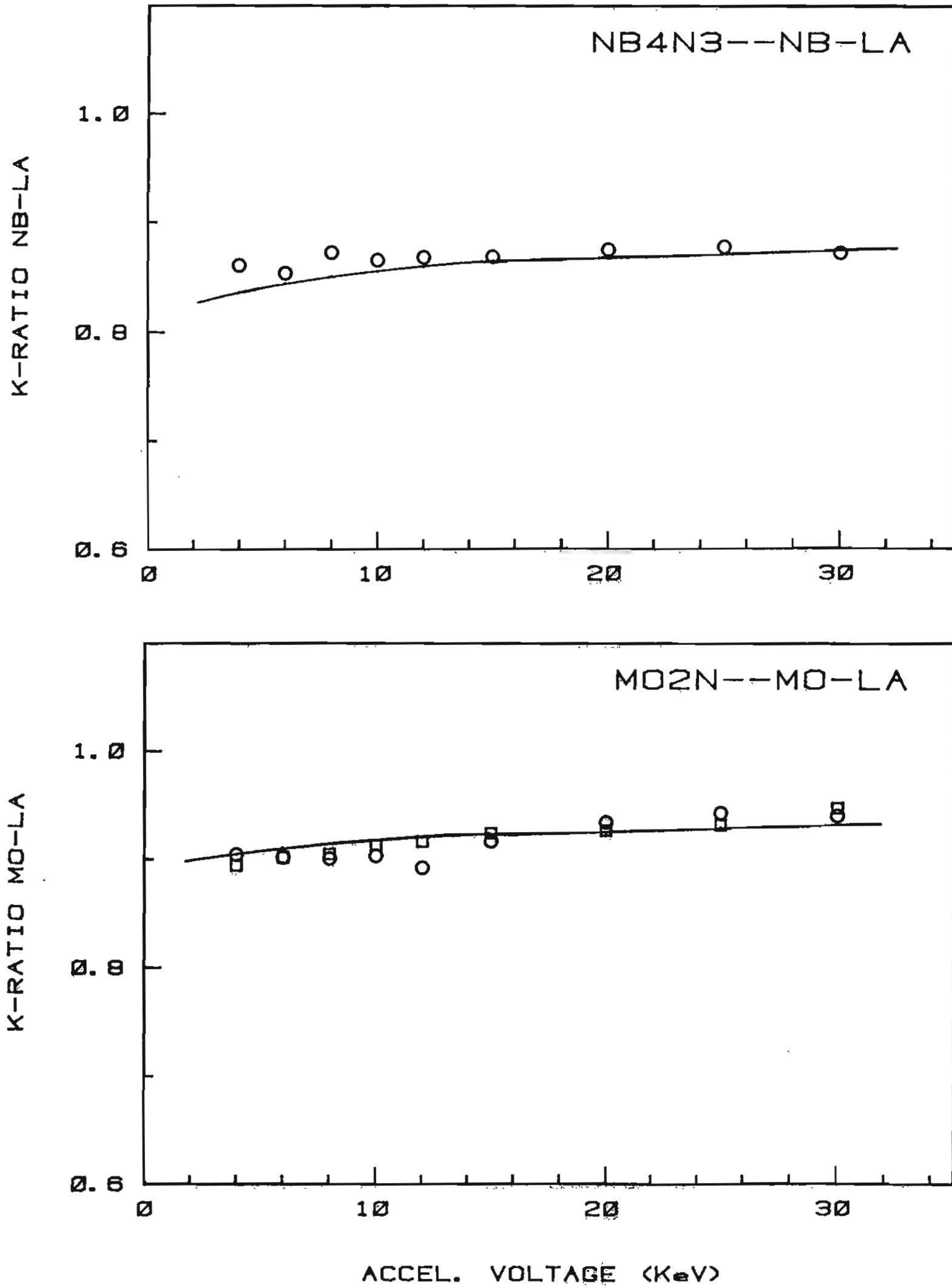

Comparison between the experimental k-ratios (relative to elemental standards) of the X-ray lines of the metal components (circles and squares) and the predictions of our PROZA program (solid curves). Top : uncoated Nb_4N_3; bottom : uncoated Mo_2N.

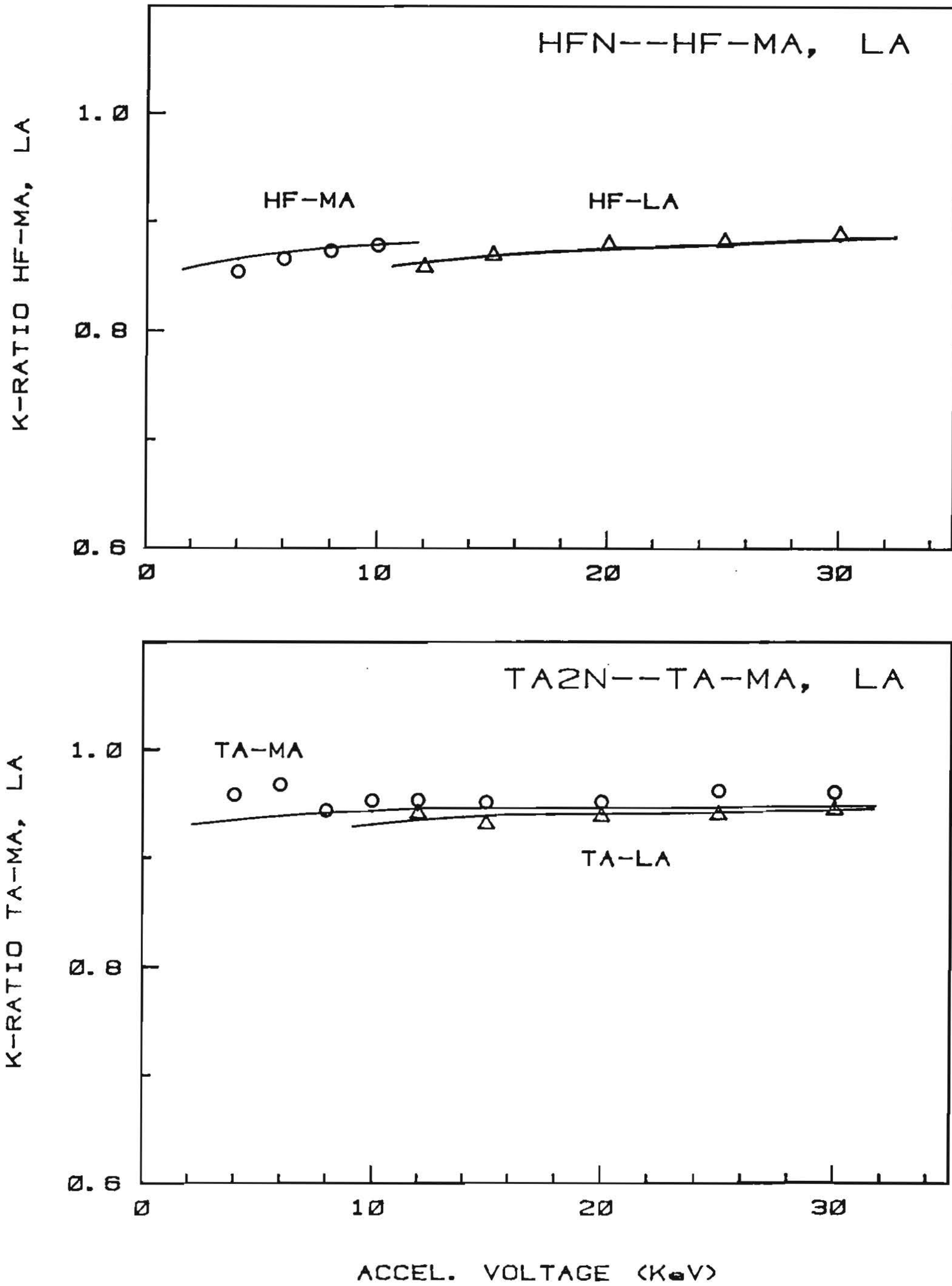

Comparison between the experimental k-ratios (relative to elemental standards) of the X-ray lines of the metal components (circles for the M-α and triangles for the L-α lines) and the predictions of our PROZA program (solid curves). Top : uncoated HfN; bottom : uncoated Ta_2N.

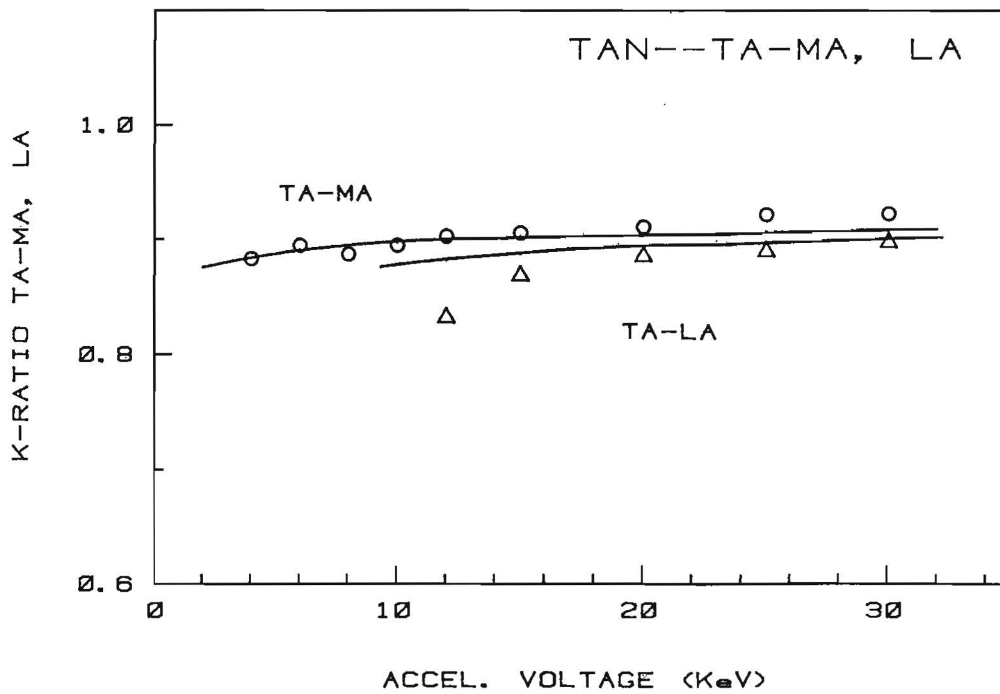

Comparison between the experimental k-ratios (relative to elemental standards) of the X-ray lines of the metal components (circles for the M-α and triangles for the L-α line) and the predictions of our PROZA program (solid curves). Uncoated TaN.

Appendix 3

Numerical details of the final data base containing the unsmoothed Integral k-ratios for N-Kα relative to Cr_2N (Batch # 1) and the smoothed peak k-ratios for the metal X-ray lines relative to elemental standards.

LEGEND :
- 1st column...*Number of elements - 1.*
- 2nd column...*Atomic number of chief metal component.*
- 3rd column...*Atomic number of second metal component.*
- 4th column...*Weight fraction of chief metal component.*
- 5th column...*Weight fraction of Nitrogen.*
- 6th column...*Weight fraction of second metal component. Note that the weight fraction of Oxygen is obtained as 1 - the sum of columns 4-6.*
- 7th column...*k-ratio of chief metal component X-ray line.*
- 8th column...*k-ratio of N-Kα relative to Cr_2N.*
- 9th column...*Accelerating Voltage (kV).*
- 10th column...*Type of X-ray line of chief metal component (K=0, L=1, M=2).*
- 11th column...*Type of X-ray line of second metal component (K=0, L=1, M=2).*

1	5	0	0.4355	0.5645	0.0000	0.3747	3.3278	4.00	0	0
1	5	0	0.4355	0.5645	0.0000	0.3317	3.2646	6.00	0	0
1	5	0	0.4355	0.5645	0.0000	0.2856	3.0746	8.00	0	0
1	5	0	0.4355	0.5645	0.0000	0.2539	2.9503	10.00	0	0
1	5	0	0.4355	0.5645	0.0000	0.2316	2.7111	12.00	0	0
1	5	0	0.4355	0.5645	0.0000	0.2049	2.4133	15.00	0	0
1	5	0	0.4355	0.5645	0.0000	0.1823	2.1520	20.00	0	0
1	5	0	0.4355	0.5645	0.0000	0.1800	1.9887	25.00	0	0
1	5	0	0.4355	0.5645	0.0000	0.1834	1.9663	30.00	0	0
1	13	0	0.6582	0.3418	0.0000	0.6220	2.4707	3.38	0	0
1	13	0	0.6582	0.3418	0.0000	0.6218	2.1717	5.01	0	0
1	13	0	0.6582	0.3418	0.0000	0.6195	2.0145	6.92	0	0
1	13	0	0.6582	0.3418	0.0000	0.6160	1.7870	8.56	0	0
1	13	0	0.6582	0.3418	0.0000	0.6100	1.7170	10.64	0	0
1	13	0	0.6582	0.3418	0.0000	0.6010	1.5166	13.92	0	0
1	13	0	0.6582	0.3418	0.0000	0.5800	1.3502	18.28	0	0
1	13	0	0.6582	0.3418	0.0000	0.5560	1.2830	24.00	0	0
1	13	0	0.6582	0.3418	0.0000	0.5275	1.2100	28.50	0	0

1	13	0	0.6582	0.3418	0.0000	0.5275	1.2100	28.50	0	0
2	14	0	0.6006	0.3924	0.0000	0.5640	2.3694	4.00	0	0
2	14	0	0.6006	0.3924	0.0000	0.5655	2.0676	6.00	0	0
2	14	0	0.6006	0.3924	0.0000	0.5660	1.9246	8.00	0	0
2	14	0	0.6006	0.3924	0.0000	0.5640	1.7510	10.00	0	0
2	14	0	0.6006	0.3924	0.0000	0.5625	1.6467	12.00	0	0
2	14	0	0.6006	0.3924	0.0000	0.5570	1.4099	15.00	0	0
2	14	0	0.6006	0.3924	0.0000	0.5450	1.1097	20.00	0	0
2	14	0	0.6006	0.3924	0.0000	0.0000	1.1738	25.00	0	0
2	14	0	0.6006	0.3924	0.0000	0.0000	1.0954	30.00	0	0
1	22	0	0.8816	0.1184	0.0000	0.0000	1.0960	4.00	1	0
1	22	0	0.8816	0.1184	0.0000	0.8630	1.2060	6.00	0	0
1	22	0	0.8816	0.1184	0.0000	0.8662	1.2320	8.00	0	0
1	22	0	0.8816	0.1184	0.0000	0.8695	1.2520	10.00	0	0
1	22	0	0.8816	0.1184	0.0000	0.8719	1.3450	12.00	0	0
1	22	0	0.8816	0.1184	0.0000	0.8750	1.3560	15.00	0	0
1	22	0	0.8816	0.1184	0.0000	0.8792	1.3640	20.00	0	0
1	22	0	0.8816	0.1184	0.0000	0.8816	1.5220	25.00	0	0
1	22	0	0.8816	0.1184	0.0000	0.8820	1.5240	30.00	0	0
1	22	0	0.7750	0.2250	0.0000	0.0000	2.1360	4.00	1	0
1	22	0	0.7750	0.2250	0.0000	0.7300	2.2210	6.00	0	0
1	22	0	0.7750	0.2250	0.0000	0.7345	2.3320	8.00	0	0
1	22	0	0.7750	0.2250	0.0000	0.7390	2.3575	10.00	0	0
1	22	0	0.7750	0.2250	0.0000	0.7425	2.5880	12.00	0	0
1	22	0	0.7750	0.2250	0.0000	0.7480	2.5160	15.00	0	0
1	22	0	0.7750	0.2250	0.0000	0.7538	2.6820	20.00	0	0
1	22	0	0.7750	0.2250	0.0000	0.7582	2.7540	25.00	0	0
1	22	0	0.7750	0.2250	0.0000	0.7605	3.0230	30.00	0	0
2	23	0	0.8723	0.1199	0.0000	0.0000	1.1588	4.00	1	0
2	23	0	0.8723	0.1199	0.0000	0.0000	1.1965	6.00	1	0
2	23	0	0.8723	0.1199	0.0000	0.8460	1.1960	8.00	0	0
2	23	0	0.8723	0.1199	0.0000	0.8500	1.2329	10.00	0	0
2	23	0	0.8723	0.1199	0.0000	0.8530	1.2620	12.00	0	0
2	23	0	0.8723	0.1199	0.0000	0.8560	1.2774	15.00	0	0
2	23	0	0.8723	0.1199	0.0000	0.8618	1.3130	20.00	0	0
2	23	0	0.8723	0.1199	0.0000	0.8640	1.2619	25.00	0	0
2	23	0	0.8723	0.1199	0.0000	0.8650	1.2861	30.00	0	0
2	23	0	0.8365	0.1604	0.0000	0.0000	1.5671	4.00	1	0
2	23	0	0.8365	0.1604	0.0000	0.0000	1.5830	6.00	1	0
2	23	0	0.8365	0.1604	0.0000	0.8000	1.6286	8.00	0	0
2	23	0	0.8365	0.1604	0.0000	0.8038	1.6468	10.00	0	0
2	23	0	0.8365	0.1604	0.0000	0.8068	1.6662	12.00	0	0
2	23	0	0.8365	0.1604	0.0000	0.8110	1.7217	15.00	0	0
2	23	0	0.8365	0.1604	0.0000	0.8162	1.7396	20.00	0	0
2	23	0	0.8365	0.1604	0.0000	0.8200	1.7528	25.00	0	0
2	23	0	0.8365	0.1604	0.0000	0.8215	1.7496	30.00	0	0
2	24	0	0.8882	0.1070	0.0000	0.8518	0.0000	8.00	0	0
2	24	0	0.8882	0.1070	0.0000	0.8595	0.0000	10.00	0	0
2	24	0	0.8882	0.1070	0.0000	0.8635	0.0000	12.00	0	0
2	24	0	0.8882	0.1070	0.0000	0.8680	0.0000	15.00	0	0
2	24	0	0.8882	0.1070	0.0000	0.8740	0.0000	20.00	0	0
2	24	0	0.8882	0.1070	0.0000	0.8783	0.0000	25.00	0	0
2	24	0	0.8882	0.1070	0.0000	0.8805	0.0000	30.00	0	0

Appendix 3 (Continued)

1	24	0	0.7878	0.2122	0.0000	0.0000	1.9261	4.00	1	0
1	24	0	0.7878	0.2122	0.0000	0.0000	1.9679	6.00	1	0
1	24	0	0.7878	0.2122	0.0000	0.7290	2.0171	8.00	0	0
1	24	0	0.7878	0.2122	0.0000	0.7365	2.0027	10.00	0	0
1	24	0	0.7878	0.2122	0.0000	0.7433	2.0406	12.00	0	0
1	24	0	0.7878	0.2122	0.0000	0.7505	2.0765	15.00	0	0
1	24	0	0.7878	0.2122	0.0000	0.7595	2.0702	20.00	0	0
1	24	0	0.7878	0.2122	0.0000	0.7650	2.1528	25.00	0	0
1	24	0	0.7878	0.2122	0.0000	0.7685	2.0806	30.00	0	0
1	26	0	0.9440	0.0560	0.0000	0.0000	0.4941	4.00	1	0
1	26	0	0.9440	0.0560	0.0000	0.0000	0.4688	6.00	1	0
1	26	0	0.9440	0.0560	0.0000	0.9118	0.4587	8.00	0	0
1	26	0	0.9440	0.0560	0.0000	0.9140	0.4226	10.00	0	0
1	26	0	0.9440	0.0560	0.0000	0.9173	0.4154	12.00	0	0
1	26	0	0.9440	0.0560	0.0000	0.9202	0.4075	15.00	0	0
1	26	0	0.9440	0.0560	0.0000	0.9240	0.3975	20.00	0	0
1	26	0	0.9440	0.0560	0.0000	0.9260	0.3898	25.00	0	0
1	26	0	0.9440	0.0560	0.0000	0.9270	0.3853	30.00	0	0
2	40	0	0.8663	0.1270	0.0000	0.8235	0.7799	4.00	1	0
2	40	0	0.8663	0.1270	0.0000	0.8308	0.5771	6.00	1	0
2	40	0	0.8663	0.1270	0.0000	0.8365	0.4642	8.00	1	0
2	40	0	0.8663	0.1270	0.0000	0.8420	0.3713	10.00	1	0
2	40	0	0.8663	0.1270	0.0000	0.8465	0.3378	12.00	1	0
2	40	0	0.8663	0.1270	0.0000	0.8518	0.2934	15.00	1	0
2	40	0	0.8663	0.1270	0.0000	0.8583	0.2765	20.00	1	0
2	40	0	0.8663	0.1270	0.0000	0.8637	0.2816	25.00	1	0
2	40	0	0.8663	0.1270	0.0000	0.8660	0.2768	30.00	1	0
2	41	0	0.9299	0.0655	0.0000	0.9042	0.4104	4.00	1	0
2	41	0	0.9299	0.0655	0.0000	0.9068	0.2785	6.00	1	0
2	41	0	0.9299	0.0655	0.0000	0.9097	0.2298	8.00	1	0
2	41	0	0.9299	0.0655	0.0000	0.9120	0.1914	10.00	1	0
2	41	0	0.9299	0.0655	0.0000	0.9130	0.1612	12.00	1	0
2	41	0	0.9299	0.0655	0.0000	0.9140	0.1334	15.00	1	0
2	41	0	0.9299	0.0655	0.0000	0.9158	0.1275	20.00	1	0
2	41	0	0.9299	0.0655	0.0000	0.9162	0.1327	25.00	1	0
2	41	0	0.9299	0.0655	0.0000	0.9165	0.1300	30.00	1	0
2	41	0	0.8949	0.0979	0.0000	0.8520	0.6129	4.00	1	0
2	41	0	0.8949	0.0979	0.0000	0.8578	0.4381	6.00	1	0
2	41	0	0.8949	0.0979	0.0000	0.8618	0.3444	8.00	1	0
2	41	0	0.8949	0.0979	0.0000	0.8650	0.2913	10.00	1	0
2	41	0	0.8949	0.0979	0.0000	0.8682	0.2457	12.00	1	0
2	41	0	0.8949	0.0979	0.0000	0.8722	0.2234	15.00	1	0
2	41	0	0.8949	0.0979	0.0000	0.8763	0.2111	20.00	1	0
2	41	0	0.8949	0.0979	0.0000	0.8793	0.2210	25.00	1	0
2	41	0	0.8949	0.0979	0.0000	0.8800	0.2129	30.00	1	0
1	42	0	0.9420	0.0580	0.0000	0.8964	0.3315	4.00	1	0
1	42	0	0.9420	0.0580	0.0000	0.9023	0.2754	6.00	1	0
1	42	0	0.9420	0.0580	0.0000	0.9078	0.1899	8.00	1	0
1	42	0	0.9420	0.0580	0.0000	0.9122	0.1737	10.00	1	0
1	42	0	0.9420	0.0580	0.0000	0.9163	0.1411	12.00	1	0
1	42	0	0.9420	0.0580	0.0000	0.9220	0.1278	15.00	1	0
1	42	0	0.9420	0.0580	0.0000	0.9298	0.1166	20.00	1	0
1	42	0	0.9420	0.0580	0.0000	0.9360	0.1165	25.00	1	0

Appendix 3 (Continued)

1	42	0	0.9420	0.0580	0.0000	0.9399	0.1227	30.00	1	0
3	72	40	0.9136	0.0606	0.0229	0.8537	0.5835	4.00	2	1
3	72	40	0.9136	0.0606	0.0229	0.8655	0.4813	6.00	2	1
3	72	40	0.9136	0.0606	0.0229	0.8728	0.4028	8.00	2	1
3	72	40	0.9136	0.0606	0.0229	0.8783	0.3528	10.00	2	1
3	72	40	0.9136	0.0606	0.0229	0.8584	0.3300	12.00	1	1
3	72	40	0.9136	0.0606	0.0229	0.8694	0.2951	15.00	1	1
3	72	40	0.9136	0.0606	0.0229	0.8792	0.2586	20.00	1	1
3	72	40	0.9136	0.0606	0.0229	0.8821	0.2694	25.00	1	1
3	72	40	0.9136	0.0606	0.0229	0.8883	0.2763	30.00	1	1
2	73	0	0.9629	0.0347	0.0000	0.9505	0.3379	4.00	2	0
2	73	0	0.9629	0.0347	0.0000	0.9518	0.2660	6.00	2	0
2	73	0	0.9629	0.0347	0.0000	0.9522	0.2207	8.00	2	0
2	73	0	0.9629	0.0347	0.0000	0.9534	0.1930	10.00	2	0
2	73	0	0.9629	0.0347	0.0000	0.9540	0.1767	12.00	2	0
2	73	0	0.9629	0.0347	0.0000	0.9558	0.1662	15.00	2	0
2	73	0	0.9629	0.0347	0.0000	0.9580	0.1501	20.00	2	0
2	73	0	0.9629	0.0347	0.0000	0.9600	0.1562	25.00	2	0
2	73	0	0.9629	0.0347	0.0000	0.9620	0.1600	30.00	2	0
2	73	0	0.9629	0.0347	0.0000	0.9343	0.0000	12.00	1	0
2	73	0	0.9629	0.0347	0.0000	0.9375	0.0000	15.00	1	0
2	73	0	0.9629	0.0347	0.0000	0.9400	0.0000	20.00	1	0
2	73	0	0.9629	0.0347	0.0000	0.9422	0.0000	25.00	1	0
2	73	0	0.9629	0.0347	0.0000	0.9440	0.0000	30.00	1	0
2	73	0	0.9327	0.0651	0.0000	0.8843	0.6149	4.00	2	0
2	73	0	0.9327	0.0651	0.0000	0.8900	0.5130	6.00	2	0
2	73	0	0.9327	0.0651	0.0000	0.8942	0.4307	8.00	2	0
2	73	0	0.9327	0.0651	0.0000	0.8983	0.3778	10.00	2	0
2	73	0	0.9327	0.0651	0.0000	0.9022	0.3398	12.00	2	0
2	73	0	0.9327	0.0651	0.0000	0.9071	0.2823	15.00	2	0
2	73	0	0.9327	0.0651	0.0000	0.9142	0.2725	20.00	2	0
2	73	0	0.9327	0.0651	0.0000	0.9190	0.2668	25.00	2	0
2	73	0	0.9327	0.0651	0.0000	0.9220	0.2917	30.00	2	0
2	73	0	0.9327	0.0651	0.0000	0.8640	0.0000	12.00	1	0
2	73	0	0.9327	0.0651	0.0000	0.8740	0.0000	15.00	1	0
2	73	0	0.9327	0.0651	0.0000	0.8860	0.0000	20.00	1	0
2	73	0	0.9327	0.0651	0.0000	0.8940	0.0000	25.00	1	0
2	73	0	0.9327	0.0651	0.0000	0.8980	0.0000	30.00	1	0

Bibliotheek Technische Universiteit Eindhoven
Postbus 513
5600 MB
Eindhoven
Telefoon (040) 47 22 24

9000718

1192

University of Technology
Laboratory of Solid State Chemistry and Materials Science
P.O. Box 513, NL-5600 MB Eindhoven
The Netherlands